Elucidating the molecular mechanism of TRIB2-mediated degradation of C/EBPα in AML

A thesis presented for the Title of Doctor of Philosophy

To the University of Glasgow

By

Fíona Lohan, MSc

College of Medical Veterinary and Life Sciences

University of Glasgow

Date submitted: 08/10/2014

Supervisor: Dr. Karen Keeshan

Abstract

The pseudokinase TRIB2 is a potent AML oncogene, capable of inducing transplantable AML with a relatively short latency in murine models. Functionally, the oncogenicity of TRIB2 has been linked to its degradation of C/EBPα, a transcription factor necessary for regulation of HSCs, myeloid differentiation and is identified mutated in ~10-15 % of cytogenetically normal AMLs. Previously, we have demonstrated that elevated *TRIB2* mRNA expression is associated with a subset of C/EBPα dysregulated AML patients.

Here, using in vivo ubiquitination assays I determined TRIB2 exerts its effect through K48 specific ubiquitin-dependent proteasomal degradation of C/EBPαp42. Peptide array analysis identified the specific amino acids involved in the direct binding of these two proteins. Site-directed mutagenesis of these amino acids demonstrated that the direct binding of TRIB2 and C/EBPα was required for TRIB2-mediated C/EBPαp42 ubiquitination. C/EBPαp42 may exist as a dimer or a monomer; however differential dimerisation perturbs terminal myeloid differentiation. TRIB2 binds both monomeric and dimeric C/EBPαp42 but ubiquitination assays revealed it preferentially mediates ubiquitin-dependent degradation of dimeric C/EBPαp42, suggesting dimeric C/EBPαp42 provides a structurally preferential confirmation for TRIB2-mediated ubiquitination of C/EBPαp42. In order to determine if a post-translational modification of C/EBPαp42 was a trigger for TRIB2-mediated binding and degradation, I assessed the phosphorylation status of C/EBPα, often a modification involved in C/EBPα ubiquitination. I determined TRIB2 decreased the levels of phosphorylated Serine 21 (S21) C/EBPα through preferential binding to the phosphorylated S21 form of C/EBPαp42 and mediating increased ubiquitination. Further molecular elucidation of the TRIB2:C/EBPαp42 proteolytic relationship identified C/EBPαp42-K313 as the site of ubiquitin conjugation on C/EBPα and subsequent annotation of this region revealed it is mutated in ~10 % of C/EBPα mutAMLs.

Using the clinically available proteasome inhibitor Bortezomib I investigated the targeted inhibition of the TRIB2 degradation function to induce cell death in AML cells. In TRIB2 overexpressing AML cell lines, and in AML patient samples identified to have elevated levels of TRIB2, I have demonstrated that high TRIB2 expressing samples are more sensitive than low TRIB2 expressing samples to cell death induced by proteasomal inhibition.

I propose TRIB2 mediates is leukaemogenic effects through functioning as an adaptor protein, facilitating the formation of a multiprotein complex COP1:TRIB2:C/EBPα resulting in ubiquitin-

dependent C/EBPαp42 degradation. Dimeric P-Ser21-C/EBPαp42 provides a structurally favourable confirmation for enhanced TRIB2-mediated ubiquitination. As C/EBPαp42 plays a key role in both stem cell function and myeloid differentiation in AML, the targeted inhibition of TRIB2-mediated C/EBPαp42 degradation may provide therapeutic avenues in AML.

Table of Contents

Acknowledgements

“In memory of Mary Lohan”

I would like to greatly thank my supervisor Dr. Karen Keeshan and everyone in Paul O’Gorman Leukaemia Research Centre for their friendship and support; Caitriona, Maura, Joana, Sheela, Leena, Mara, Loveena and Kai. Not only were you lab colleagues you were great friends.

Declaration

This thesis has not been previously submitted, in part or in whole, to this or any other University for any degree and is, unless otherwise stated, the original work of the author.

Signed 

Fiona Mary Lohan

Abbreviations

ABL	Abelson
AGM	Aorta-gonad mesonephros
AL	Acute leukaemia
ALL	Acute lymphoid leukaemia
AMP	Ampicillin
AP-1	Activator protein 1
APL	Acute promyelocytic leukaemia
ASA	Solvent-accessible surface area amino acids
ATP	Adenosine triphosphate
ATRA	All-trans retinoic acid
B-ALL	B-cell acute lymphoid leukaemia
BCR	Break point cluster region
BLAST	Basic local alignment search tool
BM	Bone marrow
BMT	Bone marrow transplantation
Brtz	Bortezomib
BSA	Bovine serum albumin
CaCl2	Calcium chloride
CA-MKK3	Constitutively active Mitogen-activated protein kinase kinase 4
CA-PKB	Constitutively active protein kinase B
CBFβ	Core binding factor β
CDK2/4	Cyclin dependent kinase 2/4
CEBP	CCAAAT/enhancer binding proteins
CHOP	C/EBP homologs protein
CHX	Cycloheximide
CL	Chronic leukaemia
CLL	Chronic lymphoid leukaemia
CLP	Common lymphoid progenitor
CML	Chronic myeloid leukaemia

CMPS	Committed myeloid progenitors
CO-IP	Co immunoprecipitation
COP1	Constitutively photomorphogenic 1
Dapi	4',6-diamidino-2-phenylindole
DMEM	Dulbecco modified eagle medium
dmin	double minute
DMSO	Dimethyl sulfoxide
DNA	Deoxyribonucleic acid
DNM3Ta	DNA methyltransferase 3a
dUBs	deubiquitination enzymes
E/N	Endogenous
E1	Ubiquitin-activating enzymes
E2	Ubiquitin-conjugation enzymes
E3	Ubiquitin ligases
E6AP	E6 associated protein
ECL	Enhanced chemiluminescence
EDTA	Ethylendiaminotetraacetic acid
eIF-2α	Eukaryotic translation initiation factor 2
ER	Endoplasmic reticulum
ERK1/2	Extracellular kinase 1/2
FAB	French and British
FACS	Fluorescent activated cell sorting
FBS	Foetal bovine serum
FBXW7	F-box/WD repeat-containing protein 7
FDA	Food and drug administration
FLT3	Fms like tyrosine
FLT3-ITD	Fms like tyrosine-internal tandem duplication
Fmoc	9-fluorenylmethyloxycarbonyl
FOG1	Friend of GATA 1
GATA1/2	Globin transcription factor ½
G-CSFR	Granulocyte stimulating factor receptor
GFI1	Growth-factor independent 1

GFP	Green fluorescent protein
GM-CSFR	Granulocyte/ macrophage stimulating factor receptor
GMPS	Granulocyte macrophage progenitors
GSK3	Glycogen synthase kinase-3
GST	Glutathione Sepharose transferase
HA	Haemagluttin
HBSS	Hanks buffered saline solution
HCL	Hydrochloric acid
HECT	Homologous to the E6-AP Carboxyl Terminus
HEK	Human embryonic kidney
HeLa	Henrietta Lacks cells
hr(s)	Hour(s)
HRP	Horse radish peroxidise
HSC	Haematopoietic stem cell
IDH1/2	Isocitrate dehydrogenase 1/2
IL-3/6/10	Interleukin 3/6/10
IRF8	Interferon-regulatory factor 8
JAK	Janus kinase
JNK1	c-Jun N-Terminal kinase 1
LGA	Leukaemia genome atlas
LIC	Leukaemia initiating cell
LiCL	Lithium chloride
LSC	Leukaemic stem cell
LSK	$Lin^-/Sca1^+/Ckit^+$
LT-HSC	Long term haematopoietic stem cell
MAPK	Mitogen-activated protein kinase
M-CSFR	Macrophage colony stimulating factor receptor
MDS	Myelodysplastic disorder
MEK	Mitogen/extracellular signal-regulated kinase

MEP	Megakaryocyte erythroid progenitor
MG-132	Z-Leu-Leu-Leu-al
MgSO4	Magnesium sulphate
microRNA	miR
min(s)	minute(s)
MKK3/4	Mitogen-activated protein kinase kinase 3/4
MPN	Myeloproliferative disorder
MPP	Multipotential progenitor
mRNA	Messenger ribonucleic acid
mutC/EBPα	C/EBPα mutant
mutFLT3	Mutant FLT3
MYC	Myelocytomatosis
MYH11	Muscle myosin heavy chain 11 gene
myr-PKB	Dominant negative protein kinase B
Na2HP04	Sodium phosphate
Na3V04	Sodium pyruvate
NaCl	Sodium chloride
NAF	Sodium fluoride
NDC	No drug control
NEM	N-ethylmaleimide
NES	Nuclear exportation sequence
NFκB	Nuclear factor kappa
NK	Natural killer
NLS	Nuclear localisation sequence
NSCLC	Non small cell lung cancer
O/E	Over expression
p38MAPK	p38 Mitogen activated pathway kinase
PAGE	Polyacrylamide gel electrophoresis
PAX5	Paired box protein 5
PBS	Phosphate-buffered saline
PEST	Glutamic acid (Glu-E), Serine (Ser-S) and Threonine (Thr-T) rich
pIpC	Poly (I-C)

PIPE	Protein interaction and properties explorer
PKB	Protein Kinase B
PKC	Protein kinase C
PKCδ-CF	Protein Kinase C delta- catalytic fragment
PMA	Phorbol 12-myristate 13-acetate
PML-RARα	Promyelocytic leukaemia-retinoic acid receptor
PMSF	Phenylmethanesulfonyl fluoride
PP1/PP2A	Phosphatases 1 and 2A
PS	Phosphatidylserine
P-Ser21	Phosphorylated serine 21
P-Thr222/226	Phosphorylated threonine 222/226
RA	Retinoic acid
RING	Really interesting new gene
RIPA	Radioimmunoprecipitation assay buffer
RXR	Retinoid X receptors
SASSA	Specific alanine scanning substitution arrays
SCL	Stem cell leukaemic factor
SDS	Sodium dodecyl sulphate
sec(s)	Seconds
Slbo	Slow border cell
ST-HSC	Short term haematopoietic stem cell
SUMO	Small Ubiquitin like MOdifier
TAD1	Transactivation domain 1
T-ALL	T-cell acute lymphoid leukaemia
TBST	Tris-buffered saline-T
TKI	Tyrosine kinase inhibitor
TLR	Toll like receptor
TPA	2-O-tetradecanoyl-phorbol-13-acetate
TRIB1	Tribbles 1
TRIB2	Tribbles 2
TRIB3	Tribbles 3
TTS	C/EBPα T222A/T226A/S23A mutant

UB	Ubiquitin
Ubc9	Ubiquitin conjugating enzyme 9
UK	United kingdom
UPS	Ubiquitin proteasome system
USA	United states of America
UTR	Untranslated region
WHO	World health organisation
WT	Wild type

Amino Acid	**3-Letter**	**1-Letter**
Alanine	Ala	A
Arginine	Arg	R
Asparagine	Asn	N
Aspartic acid	Asp	D
Cysteine	Cys	C
Glutamic acid	Glu	E
Glutamine	Gln	Q
Glycines	Gly	G
Hisitidine	His	H
Isoleucine	Ile	I
Leucine	Leu	L
Lysine	Lys	K
Methionine	Met	M
Phenylalanine	Phe	F
Proline	Pro	P
Serine	Ser	S
Threonine	Thr	T
Tryptophan	Trp	W
Tyrosine	Tyr	Y
Valine	Val	V

Chapter 1: Introduction

1.1.1 The early stages of haematopoiesis and the production of the haematopoietic stem cell.

Haematopoiesis and the origins of leukaemic disease are developmentally intertwined (Orkin and Zon, 2008). Haematopoiesis describes the process of developing and maintaining an unlimited blood supply from embryogenesis throughout adult life. Dysregulation of this process results in haematopoietic malignancies termed leukaemia (from the ancient Greek *leukos* "white", and αἷμα *haima* "blood"), with leukaemic subtypes defined by the blood lineage affected. Haematopoiesis is highly evolutionary conserved in all vertebrates; studies of murine models have taught us much of what we know of the human haematopoietic system. The lifelong ability to homeostatically produce blood is dependent on the self-renewal and differentiation capacity of haematopoietic stem cells (HSCs). HSCs sit atop of the hierarchy of blood lineage. A pool of HSCs are formed early in embryogenesis and migrate to different anatomical niches under temporal control which support the intrinsic characteristics and properties of the HSC. During organogenesis simultaneous de novo generation of HSCs and stockpiling to create a pool for post-natal life is required. The sequential sites of human haematopoiesis during embryogenesis are the embryonic yolk sac, the aorta-gonad-mesonephros (AGM), the placenta, the foetal liver and the bone marrow (summarised in **Fig1.1**).

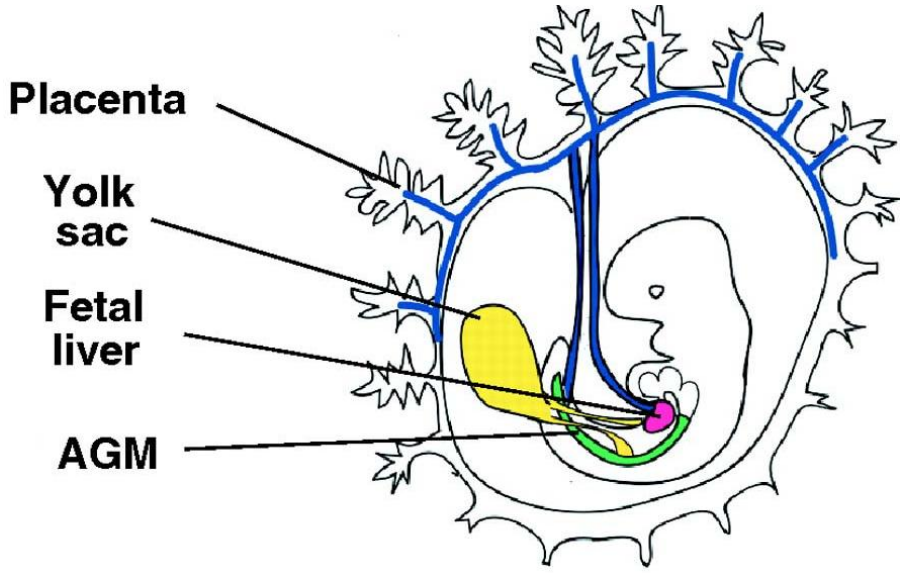

Fig 1.1 Anatomical localisation of embryonic haematopoiesis. The embryonic yolk sac, the AGM, the foetal liver and placenta are the sites of haematopoiesis during embryogenesis adapted from (Mikkola and Orkin, 2006).

Early in embryogenesis post gastrulation, mesodermal precursor cells become the early haematopoietic precursor cells in the embryonic yolk sac. It was been long proposed that these early precursor cells termed ”hemangio-blast” cells have the ability to form either the blood cells or the vascular endothelial cells (Sabin, 1917). Differential transcription factor expression controls this early stage of haematopoiesis termed the “primitive stage”. The embryonic yolk sac produces immature erythroid cells which migrate to the foetal liver and mature into differentiated erythroid cells necessary to oxygenate tissues required to support rapid embryogenesis (Li et al., 2003, Ferkowicz et al., 2003, McGrath and Palis, 2005). The yolk sac also forms a foetal-maternal transport system prior to development of the placenta (McGrath and Palis, 2005). There is as of yet no definitive answer regarding the role of the yolk sac in HSC production (reviewed by (Mikkola and Orkin, 2006, Orkin and Zon, 2008)). It is suggested that the AGM is the sole site of HSC production (Muller et al., 1994, Cumano et al., 1996, Medvinsky and Dzierzak, 1996, Cumano et al., 2001). Alternatively it is also reported that HSC production by the AGM alone is not sufficient to maintain the pool of HSCs but later in embryogenesis the yolk sac forms a supportive niche for HSC expansion (Moore et al., 1970, Kumaravelu et al., 2002). The AGM is formed by the median migration of the lateral mesoderm to the endoderm. HSCs accumulate within the ventral wall. From here the HSCs migrate to the foetal liver for expansion and differentiation (Ema and Nakauchi, 2000). Once the bone marrow is established HSCs migrate to the bone marrow where they remain in a quiescent state for post-natal life. The placenta is not categorised as a haematopoietic organ however haematopoietic activity has also been detected within the placenta (Ottersbach and Dzierzak, 2005, Gekas et al., 2005). Accumulation of HSCs have been identified within the placenta, suggesting the placenta either acts as a de novo site of HSC production or it provides a niche for HSC storage and expansion just upstream of the foetal liver blood supply (Orkin and Zon, 2008). Schematic of sequential haematopoiesis summarised in **Fig 1.2** (adapted from (Mikkola and Orkin, 2006)).

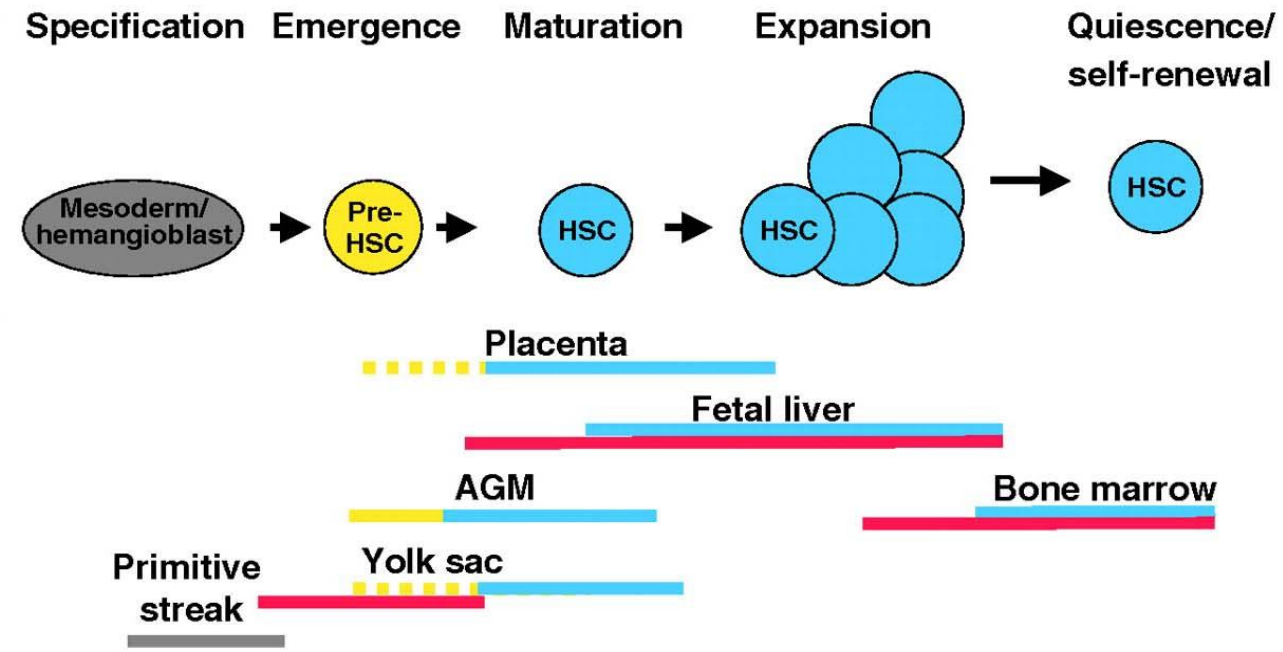

Fig 1.2 Schematic of sequential haematopoiesis. Haematopoiesis initiates as a hemangio-blast which generates vascular and blood cells. Primitive red blood cells are produced in the yolk sac. De novo HSC genesis occurs in AGM, HSCs are circulated to the placenta, foetal liver and yolk sac for expansion. Expanded HSCs migrate to established bone marrow for post-natal life adapted from (Mikkola and Orkin, 2006).

1.1.2 HSCs and haematopoietic lineage commitment

There are intrinsic differences between the HSC within the foetal liver and those located within the bone marrow. During embryogenesis foetal liver HSCs are cycling quite frequently and rapidly in order to generate a HSCs pool (Bowie et al., 2006). This is contrary to adult HSCs within the bone marrow which are normally found in G0, a metabolically inactive quiescent state (Cheshier et al., 1999). Adult HSCs cycle very rarely, this is proposed to reduce the chances of acquiring deoxyribonucleic acid (DNA) replication errors promoting the longevity of the cell and reducing the production of cytotoxic metabolic side products (reviewed by (Mikkola and Orkin, 2006)). HSCs preside over a haematopoietic hierarchy which results in at least 8 distinct functional effector cell types (Weismann model **Fig 1.3** adapted from (Bryder et al., 2006)). Differentiation of HSCs arises through either asymmetrical division of HSCs or asymmetrical environmental exposures (Wilson and Trumpp, 2006). The former occurring through unequal distribution of cell fate governing factors and the latter due to differential environmental exposures, i.e. a daughter cell leaves the self-renewal supportive niche.

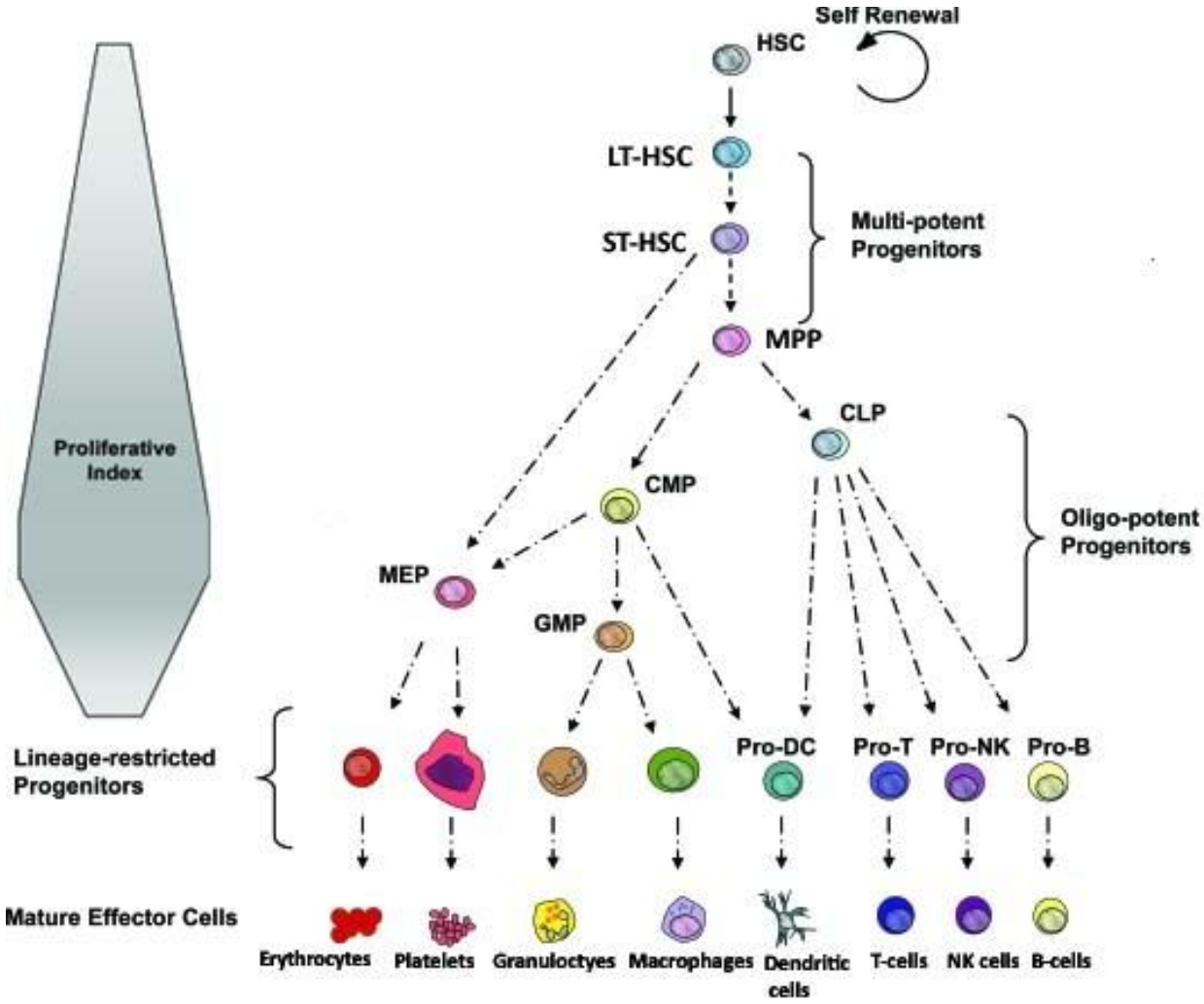

Fig 1.3 Weismann model of haematopoietic differentiation adapted from (Bryder et al., 2006). Consecutive rounds of differentiation with resultant decrease in self-renewal potential from LT-HSC to ST-HSC resulting in the generation of MPP, oligopotential CLP and CMP resulting in 8 terminally differentiated mature effector cell types.

HSCs can be subdivided into two distinct types based on their functionality, long term (LT) and short term (ST). LT-HSCs are relatively infrequent in the bone marrow and possess lifelong self-renewal ability and multilineage potential (Christensen and Weissman, 2001). LT-HSCs give rise to ST-HSCs which retain multilineage potential but have decreased self-renewal abilities (Weissman et al., 2001). The progressive stages of differentiation from HSC to multipotential progenitor (MPP) generate a cell which retains multilineage potential with a decrease in self-renewal capacity. The next round of differentiation generates oligo-potential progenitors which form lineage restrictions toward the lymphoid (common lymphoid progenitor-CLP) or myeloerythroid progenitors (common myeloid progenitor-CMP and megakaryocyte erythroid progenitor-MEP). Commitment toward a

specific lineage is simultaneously associated with de-selection for other possible lineages. These cells have lost self-renewal capabilities but have a high proliferative index. Terminal differentiation of the lymphoid lineage gives rise to B-Cells, T-Cells, Natural killer (NK) cells and dendritic cells. Terminal differentiation of GMPs produces granulocytes and macrophages while terminal differentiation of MEP produces erythrocytes and platelets **(Fig 1.3** adapted from (Bryder et al., 2006)). It is widely thought under normal physiological conditions differentiation is an irreversible state. In vitro experimentation has shown that overexpression of transcription factors governing one form of lineage commitment can reprogramme a cell already committed to another lineage (Xie et al., 2004, Laiosa et al., 2006b). Several well-defined transcription factors have been identified to govern terminal differentiation. Expression of these transcription factors has also been detected within the HSC, whereby they are thought to prime a HSC for its eventual fate. It is hypothesised that the invested chromatin remains in an open configuration allowing transcription of these cell fate determinants with successive rounds of differentiation extinguishing other potential pathways as opposed to applying a cell fate transcriptional signature on a blank cell (Orkin and Zon, 2008).

1.1.3 Disruption of haematopoiesis

Haematopoietic homeostasis is governed by HSC intrinsic factors and micro-environmental extrinsic factors. Disruption of the cell processes which tightly regulate stem cell self-renewal, proliferation or differentiation result in haematopoietic malignancy and leukaemic disease. These aberrant processes result in the generation of a leukaemic stem cell (LSC) with accompanying unregulated self-renewal and differentiation capabilities. The different haematopoietic cell type which acquires these malignant transformations governs the phenotypic manifestation of the haematopoietic disease. Intrinsic factors which may be disrupted include cell signalling cascades, cell cycle regulation and transcription factor functionality often due to chromosomal translocations and genetic aberrations. Extrinsically, developmental pathways have been found dysregulated and components of the extracellular HSC niche resulting in disruption of haematopoiesis.

1.2. Leukaemia

Leukaemia is the 11th most common cancer in the United States, the 12th most common cancer in Europe and 6th leading cause of cancer related deaths (Ferlay et al., 2012). Five year survival rates have dramatically increased from 14 % in the 1960s however they have stalled at 56 % in the last decade (statistics from SEER cancer statistics review (Howlader et al., 2012). There is no staging associated with leukaemia presentation, patients are classified as untreated, in remission or relapsed. While socially leukaemia is largely associated with paediatric patients, leukaemia is more common in adults with median age of diagnosis 66 years. Leukaemia is categorised as acute or

chronic and further subdivided based on whether the blood lineage affected is myeloid or lymphoid. Chronic leukaemia (CL) progresses slowly over a course of months and years, resulting in the excessive accumulation of mature yet abnormal haematopoietic cells. Acute leukaemia (AL) progresses rapidly over weeks and months effecting haematopoietic progenitor cells resulting in accumulation of immature blast like cells and bone marrow failure.

1.2.1 Chronic Leukaemias

CL encompasses two disease entities; chronic myeloid leukaemia (CML) and chronic lymphoid leukaemia (CLL), determined by the identity of the originating LSC. Patients with CL do not usually develop bone marrow failure unlike AL patients. CL evolves slowly over 4-5 years; patients present with abnormal white blood cell counts, lymphadenopathy and splenomegaly with CL disease often entering an acute phase. CLL is currently incurable, all patients are anticipated to relapse with CLL disease (Gibson et al., 2013). CLL is characterised by the expansion of $CD5^+$ $CD23^+$ B lymphocytes in blood, bone marrow and lymphoid tissues. No single recurrent genetic mutation is associated with CLL but deletions in chromosomes 11q22-23, 13q14 and 17p13 and trisomy of chromosome 12 have been identified (reviewed by (Zhang and Kipps, 2013)). 17p13 (TP53 gene) and 13q14 (ATM gene) deletions are associated with a poor prognosis as functional p53 is required for cellular response to most current chemotherapies (Döhner et al., 2000). CLL was initially regarded as a disease manifesting through inhibition of apoptosis resulting in the accumulation of leukaemic cells. Circulating CLL cells were identified to be in G0 or G1 phase of cell cycle and to overexpress anti-apoptotic BCL2 (Dighiero et al., 1991, Kitada et al., 1998). However a distinct subset of patients have been identified with CLL cells with rapid cell cycle kinetics and increase their CLL cell population by 1 % in 1 day but yet have stable disease owing to simultaneous apoptosis (Messmer et al., 2005). Variability in CLL disease progression is reflective of huge heterogeneity in genetic lesions identified in patients. Studies of the CLL subclone populations prior to, during and post treatment identified huge heterogeneity in subclone populations complicating identification of initiating, maintenance and relapse associated genetic lesions (Schuh et al., 2012). Mutations in *NOTCH1, SF3B1, BIRC3, MyD88,* dysregulated Wnt signalling and NF-κB activation have all been identified in CLL patients reviewed by (Zhang and Kipps, 2013). Additionally the CLL microenvironment supports the CLL cell viability releasing prosurvival signals (Burger et al., 2009). The current standard treatment regime for CLL patients is combination of fludarabine, monoclonal CD20 antibody rituximab and cyclophosphamide (Hallek et al., 2010). Allogeneic stem cell transplants offer specific patients with a potential cure.

CML was the first malignancy identified to be associated with a recurrent cytogenetic abnormality, the Philadelphia chromosome (Nowell and Hungerford, 1960). The Philadelphia chromosome arises as a result of reciprocal translocation between chromosome 9 and 22 (t(9;22)(q34;q11)) producing breakpoint cluster region-Abelson leukaemia-virus (BCR)-(ABL) fusion protein which has constitutive receptor tyrosine kinase activity (de Klein et al., 1982, Lugo et al., 1990). CML is a clonal bone marrow stem cell disease resulting in the excessive expansion of granulocytes and is treated with a targeted therapy imatinib, a potent selective tyrosine kinase inhibitor (TKI). Imatinib competes for the adenosine triphosphate (ATP) binding site on BCR-ABL fusion oncoprotein, quenching tyrosine kinase activity resulting in cell death for pathway addicted leukaemic cells. Unfortunately 30 % of patients are required to discontinue imatinib treatment due to drug related toxicities and emergence of imatinib resistant disease. Imatinib resistance has been attributed to generation of mutations within the BCR-ABL kinase domain and the imatinib binding site T315I. Second generation TKIs nilotinib, dastainib, bosutinib and ponatinib offer reduced cytotoxicities with varying improvements to overall survival. Ponatinib has demonstrated efficacy against BCR-ABL T315I imatinib resistant disease.

1.2.2 Acute Leukaemias

AL progresses more rapidly that CL and requires immediate treatment upon diagnosis. ALs are classified as lymphoid or myeloid depending on the cell lineage affected. ALL is a malignant haematopoietic disorder of pre B (80-85 %) and T (15-20 %) lymphocytes. The exact mechanisms resulting in transformation are unknown however many chromosomal translocations, regions of hyper/hypodiploidy and genetic lesions have been associated with ALL. The most common chromosomal translocation identified in B-cell precursor ALL (B-ALL) is the Philadelphia chromosome t(9;22)(q34;q11) (Moorman et al., 2010). Mixed lineage leukaemia (MLL) gene rearrangements and subsequent oncogenic fusions with various gene partners (t(v;11q23)) are frequent and indicative of an aggressive disease with a young age of onset. Further translocations identified include t(12;21) ETV6-RUNX1 which is associated with a favourable outcome, t(5;14), t(1;19) TCF3-PBX1 and rearrangement of MYC antigen (Inaba et al., 2013). Additional genetic lesions often accompany chromosomal translocation events and these include mutations in lymphoid gene regulators, cell cycle regulators and lymphoid signalling pathways *TAL1, TLXA, TLX3, LYL1, PAX5, AK1*, JAK2, CDK2NA, CDKN2B and NOTCH1 (Inaba et al., 2013). Treatment of ALL involves induction chemotherapeutics or the use of TKIs for t(9;22) positive disease and allogeneic stem cell transplant upon relapse.

AML is a vastly heterogeneous leukaemic subtype which is categorised by two classification systems; the world health organisation (WHO) and French American British (FAB) systems. AML is ultimately a generic term for a group of myeloid diseases resultant from rapid accumulation of immature myeloid cells through acquisition of self-renewal and hyper-proliferative properties. These abnormal immature myeloid cells then inhibit normal blood cell production. AML related mortality is predominately due to bone marrow failure and organ infiltration. AML to be discussed in extensive detail in *1.3.*

1.3 AML

1.3.1 AML incidence, survival rates and standard treatment

AML is the most common adult leukaemia with the lowest survival rate of all leukaemias (Howlader et al., 2012). The five year survival rates for patients >45 years, >65 years and <65 years are 41 %, 30 % and 4 % respectively (Redaelli et al., 2004). The incidence of AML is predicted to increase with an aging global population. Paediatric AML accounts for 20 % of childhood leukaemias and is the leading cause of paediatric leukaemia related mortality, 50 % of paediatric leukaemia related deaths are due to relapsed AML disease (Pui et al., 2011, Moore et al., 2013). AML may arise as de novo or secondary disease. Secondary AML arises as a result of treatment with cytotoxic agents (therapy related AML) or disease progression. 10-15 % of AMLs are therapy related and have poor prognosis (Kumar, 2011). Secondary AML may occur due to progression of CML, myeloproliferative/myelodyplastic disorders (MPN and MDS), polycynthemia and paroxysmal nocturnal haemoglobinuria. A number of factors will determine patient prognosis and the treatment regime implemented. Age is a factor associated with poor prognosis and older patients are less likely to receive chemotherapeutics due to high cytotoxicity and overall poorer quality of life. For such patients palliative care is available. The standard treatment for AML patients, with no adverse karyotypic features and low risk of relapse is induction therapy, the "3 +7 induction regime". This involves 3 days of intravenous daunorubicin (45-60 mg/m^2/d) along with 7 days of a continuous infusion of standard-dose cytarabine (SDAraC) (100-200 mg/m^2) (Burnett et al., 2011).

1.3.2 AML classification

AML is classified into subtypes by two distinct classification schemes FAB and WHO (Bennett et al., 1976, Vardiman et al., 2009). The older FAB system classifies AML into 8 subtypes M0-M7 based on cytogenetics, morphology and the extent of white blood cell differentiation (Bennett et al., 1976) (**Table 1.3.2 A**). The newer WHO classification system aims to provide a globally applicable classification system based on cytogenetics, morphology, immunological markers and molecular

genetics and divides AML into four disease subgroups (Vardiman et al., 2009) (**Table 1.3.2 B**). The greatest difference between the two systems is FAB requires 30 % blasts in blood or bone marrow while WHO diagnosis AML at 20 %.

FAB subtype	**Description**	**Comments**
M0	Undifferentiated acute myeloblastic leukaemia	Myeloperoxidase negative,myeloid markers positive
M1	Acute myeloblastic leukaemia with minimal maturation	Some evidence of granulocytic differentiation
M2	Acute myeloblastic leukaemia with maturation	Maturation at or beyond the promyelocytic stage of differentiation; can be divided into those with t(8;21) AML1-ETO fusion and those without
M3	Acute promyelocytic leukaemia	APL;most cases have t(15;17) PML-RARα or another translocation involving RARα
M4	Acute myelomonocytic leukaemia	
$M4_{eos}$	Acute myelomonocytic leukaemia with eosinophilia	Characterised by inversion of chromosome 16 involving CBFβ , which normally forms a heterodimer with AML1
M5	Acute monocytic leukaemia	
M6	Acute erythroid leukaemia	
M7	Acute Megakaryoblastic leukaemia	GATA1 mutations in those associated with Down's syndrome

Table 1.3.2 A FAB classification of AML. AML is divided into 8 categorises M0-M7.

Subgroup of Acute Myeloid Leukaemia	Genetic and molecular details of disease
1. Acute myeloid leukaemia (AML) and related precursor neoplasms	AML with recurrent genetic abnormalities AML with t(8;21)(q22;q22), RUNX1-RUNX1T1 AML with inv(16)(p13.1q22) or t(16;16)(p13.1;p22); CBFB-MYH11 Acute promyelocytic leukaemia with t(15;17)(q22;q12);PML-RARA AML with t(9;11)(p22;q23)MLLT3-MLL AML with t(6:9)(p23;q34); DEK-NUP214 AML with inv(3)(q21q26.2) or t(3.3)(q21;q26.2); RPN1-EVl1 AML (megakaryoblastic) with t(1:22)(p13;q13); RBM15-MKL1 AML with mutated NPM1 AML with mutated CEBPA
2. AML with myelodysplasia-related changes. Therapy-related myeloid Neoplasms. Acute myeloid leukaemia, NOS	AML with minimal differentiation AML without maturation AML with maturation Acute myelomonocytic leukaemia Acute monoblastic and monocytic leukaemia Acute erythroid leukaemia Acute megakaryoblastic leukaemia Acute basophilic leukaemia Acute panmyelosis with myelofibrosis
3. Myeloid sarcoma	Myeloid proliferations related to Down syndrome Transient abnormal myelopoiesis Myeloid leukaemia associated with Down syndrome Blastic plasmacytoid dendritic cell neoplasm
4. Acute leukaemias of ambiguous lineage	Acute undifferentiated leukaemia Mixed phenotype acute leukaemia with t(9;22)(q34;q11.2); BCR-ABL1 Mixed phenotype acute leukaemia with t(v;11q23); MLL rearranged Mixed phenotype acute leukaemia, B/myeloid, NOS Mixed phenotype acute leukaemia, T/myeloid, NOS Natural killer (NK) cell lymphoblastic leukaemia/lymphoma

Table 1.3.2 B The 4th edition of WHO classification of AML. AML is classified into four categories.

1.3.3 Chromosomal translocations and aberrations in AML

AML is a vastly heterogeneous disease in terms of both underlying genetic abnormalities and associated disease phenotypes. Cytogenetics is the most important determinant when predicting AML remission rates, relapse rates and overall survival. 50-60 % of newly diagnosed AML patients have chromosomal abnormalities. In 2011 over 749 different chromosome aberrations had been detected in AML (Mitelman et al., 2011). The most common chromosomal translocations result in the generation of a fusion gene/protein which acquires aberrant activity altering expression of target genes which govern myeloid differentiation (summarised in **Table 1.3.3**). A brief discussion of the 5 most frequent translocations is outlined below.

Translocations	Oncofusion Proteins	Frequency in AML	FAB subtype
t(8;21)	AML1-ETO	10%	M2
t(15;17)	PML-RARα	10%	M3
inv(16)	CBFβ-MYH11	5%	$M4_{eos}$
der(11q23)	MLL-fusions	4%	M4/M5
t(9;22)	BCR-ABL1	2%	M1/M2
t(6;9)	DEK-CAN	<1%	M2/M4
t(1;22)	OTT-MAL	<1%	M7
t(8;16)	MOZ-CBP	<1%	M4/M5
t(7;11)	NUP98-HOXA9	<1%	M2/M4
t(12;22)	MN1-TEL	<1%	M4/M7
inv(3)	RPN1-EVI1	<1%	M1/M2/M4/M6/M7
t(16;21)	FUS-ERG	<1%	M1/M2/M4/M5/M7

Table 1.3.3 The 12 most common chromosomal translocations in AML, the resultant oncofusion protein products, their frequency of occurrence in AML and FAB subtype adapted from (Martens and Stunnenberg, 2010).

t(8;21) AML1-ETO

t(8;21) is the most common chromosomal translocation event detected in AML, resulting in the production of the oncoprotein AML1-ETO (Muller et al., 2008). AML1 also known as RUNX1 is a transcription factor encoded on chromosome 21 which regulates expression of myeloid and lymphoid gene targets. AML1 knockout mice are embryonical lethal and display no evidence of definitive haematopoiesis in the foetal liver (Okuda et al., 1996). ETO encoded on chromosome 8,

acts as a transcriptional silencer through binding co-repressors. AML1-ETO has been identified to induce AML in murine models in the presence of additional cooperating mutations reviewed by (Hatlen et al., 2012). AML1-ETO leukaemias display a limited degree of maturation and are classified as FAB subtype M2 (Yamasaki et al., 1995).

t(15;17) PML-RARα

A translocation involving chromosome 15 and 17 results in the generation of promyelocytic leukaemia (PML) - retinoic acid receptor α (RARα) gene fusion. This oncogenic fusion protein is present in 95 % of acute promyelocytic leukaemias (APLs) (Grimwade et al., 2000). APL is a distinct subtype of AML FAB subtype M3 (Vardiman et al., 2009). RARα is a ligand inducible transcription factor which binds DNA response elements upon heterodimerisation with retinoid X receptors (RXRs). PML-RARα acts as an oncogenic transcriptional repressor through oligomeric complexing with RXR disrupting myeloid differentiation, apoptosis and self-renewal (Perez et al., 1993, Zeisig et al., 2007). APL has the best survival rates of all leukaemia subtypes, as 90 % of patients achieve complete remission following treatment with all-trans retinoic acid (ATRA) and arsenic trioxide (Degos and Wang, 2001, Lengfelder et al., 2003).

inv(16) CBFβ-MYH11

Inversion 16 or translocation events involving 16q22 and 16p13 are associated with AML subtype $M4_{eos}$. Patients possess monocytic and granulocytic differentiation but have abnormal eosinophils at various stages of differentiation arrest within the bone marrow (Larson et al., 1986). Aberration of chromosome 16 involves the introns of core binding factor β (CBFβ) and smooth muscle myosin heavy chain 11 gene (MYH11) producing the CBFβ-MYH11 chimeric protein, disrupting the transcription factor activity of CBFβ (Liu et al., 1993, Liu et al., 1995). CBFβ is essential for haematopoiesis, as evidenced in knock out murine models that result in mid-gestational fatalities due to a failure of haematopoiesis within the foetal liver, similar to AML1 knockout animals (Niki et al., 1997). CBFβ regulates transcription of a variety of genes involved in haematopoiesis including *macrophage colony stimulating factor receptor (M-CSFR), IL-3* and *myeloperoxidase* (Nuchprayoon et al., 1994, Cameron et al., 1994, Rhoades et al., 1996). CBFβ binds and stabilises AML1 and also increases its affinity for DNA in a wildtype cellular environment (Huang et al., 2001). However CBFβ-MYH11 stabilises AML1 to a greater extent and adapts AML1 into a constitutive transcriptional repressor resulting in leukaemogenesis.

der(11q23) MLL fusions

Perturbations of MLL through aberrations to chromosome 11 results in oncogenic fusion of MLL with over 50 identified gene partners in approximately 10 % of ALs (Huret et al., 2001, Krivtsov and Armstrong, 2007). MLL is a large multidomain protein which possesses the ability to bind DNA through AT hooks and acts as both a transcriptional repressor and activator. MLL proteins contain plant homology domains, DNA methyltransferase homology domain and CREB binding site. MLL also forms large nuclear multiprotein complexes with various interacting protein partners including Menin and members of the HDAC family of proteins (Martens and Stunnenberg, 2010). MLL is expressed in HSCs and MPPs (Kawagoe et al., 1999). Patients which harbour MLL translocations often have leukaemias which display monocytic features and have a poor prognosis (Byrd et al., 2002). Despite extensive analysis of MLL fusion gene products in primary patients no direct targets have been identified (Martens and Stunnenberg, 2010). In ALL it is thought MLL fusion proteins elicit defects in chromatin modelling however it is not yet known if this also bears true in AML.

t(9;21) BCR-ABL

A reciprocal translocation between chromosome 9 and 22, produces the Philadelphia chromosome, the hallmark of CML results in aberrant tyrosine kinase activity. The Philadelphia chromosome was the first genetic aberration to be determined causative of the pathophysiology of a malignancy. CML is classified into three phases based on clinical and laboratory defined characteristics. In the absence of treatment CML will progress from chronic phase into accelerated phase resulting terminally in blast crisis. Chronic phase which is asymptomatic, the duration of which is variable and largely dependent on drug response and the leukaemogenic chromosomal driver. Progression into the accelerated phase is determined based on several characteristics e.g. 10-19 % circulating myeloblasts and elevated platelet counts. Accelerated phase indicates the disease is progressing. The final stage in the evolution of CML is blast crisis which behaves similar to AML with rapid progression and short survival blast crisis phase is determined by >20 % myeloblasts circulating in blood or in the bone marrow.

1.3.4 Gene mutations in AML

Maturation and differentiation of myeloid cells is coupled to a decreased in self-renewal and proliferation. These processes are tightly regulated by a small number of transcription factors which mediate appropriate target gene expression. Myeloid differentiation is regulated by a relatively small number of transcription factors e.g.; PU.1, CCAAAT/enhancer binding proteins (C/EBPα,

C/EBPβ, C/EBPε), growth-factor independent 1 (GFI1), interferon-regulatory factor 8 (IRF8), AML1, stem cell leukaemic factor (SCL), JUNB, IKAROS and myelocytomatosis (MYC). Mutation of these myeloid governing transcription factors results in severe myeloid defects in murine models and have been identified in AML patients.

AML is proposed to occur through a two hit mechanism involving class I and class II mutations in a myeloid precursor cell (Gilliland and Griffin, 2002). Class I mutations result in an increase in proliferation through alteration to receptor tyrosine kinase activity and cell signalling cascades, and class I mutations typically affect classic oncogenes (Kelly and Gilliland, 2003). Class II mutations result in a differentiation block mediated by dysregulation of transcription factors (Kelly and Gilliland, 2003). Leukaemogenesis results when class I and class II mutations co-operate. This hypothesis is supported as a model of AML disease in murine models. Single mutations are insufficient for transformation while co-operation of class I and class II mutations results in AML, for example C/EBPα and Fms like tyrosine (FLT3)-ITD (McCormack et al., 2005, Reckzeh et al., 2012b). However class I and class II mutational hits are not always readily identifiable in AML patients. Therefore it is proposed the two hit model may be an oversimplification of leukaemogenesis, as with any vastly heterogeneous disease it is not possible to entirely categorise biological entities (Dombret, 2011, Murati et al., 2012, Conway O'Brien et al., 2014). Through the advent of AML genome sequencing, lesions were identified in genes which are not associated with haematopoiesis e.g. *isocitrate dehydrogenase 1/2 (IDH1/2)* and *DNA methyltransferase 3a (DNMT3a)* (Mardis et al., 2009, Ley et al., 2010, Sanders and Valk, 2013). Thus modifications to the two hit model have been proposed to include a third class of mutations, class III, and these include mutations to epigenetic gene regulators (Dombret, 2011, Conway O'Brien et al., 2014)(**Table 1.3.4 A**).

	Class I	Class II	Class III
Pathways	**Signal Transduction**	**Differentiation**	**Epigenetic regulation**
Genes	FLT3	AML1	TET2
	KIT	CBFβ	1DH1
	NRAS, KRAS	CEBPα	1DH2
	JAK2	NPM1	ASXL1
	PTPN11	PU.1	EZH2
		MLL	DNMT3A
		RARα	
		EVI 1	

Table 1.3.4 A Classification of gene mutations identified in AML adapted from (Dombret, 2011, Conway O'Brien et al., 2014).

A further modified and complex model of genetic mutation classification in leukaemogenesis has been proposed, termed "the slot machine model" extending the model to 5 classes of mutations (**Table 1.3.5**) (Murati et al., 2012). Class IV mutations affect tumour suppressor genes resulting in loss of their protective function. Class V mutations are those which affect the spliceosome during pre-messenger RNA (mRNA) processing, and these are mutually exclusive (Yoshida et al., 2011, Murati et al., 2012). Disruption of the spliceomsone results in intron retention, exon skipping, use of incorrect splice sites, resulting in the accumulation of many incorrectly spliced transcripts affecting mRNAs (Yoshida et al., 2011, Makishima et al., 2012). Murati et al propose that ultimately the hits required must affect proliferation and differentiation but that the number of oncogenic hits required to achieve these two phenomena may be greater than previously thought. In the slot machine model they propose the late steps are constrained by the initial steps and it is important to determine the number of "reels" (hits) and "symbols" (genes) and all possible combinations (Murati et al., 2012). Alternatively, a more contemporary model classifies the "hits" as pathways as opposed to specific genetic entities. The pathway model proposes that it is a combination of different "pathway hits", be they genetic or epigenetic targeting the apoptotic, self-renewal, differentiation, cellular metabolism and cell signalling pathways that will govern the initiation of disease (Hatlen et al., 2012).

	Class IV	Class V
Pathways	**Tumour suppressor Genes**	**RNA maturation**
Genes	CDK2NA	SF3B1
	CDKN2B	SRSF2
	TP53	U2AF1
	WT1	ZRSR2
		PRPF40B
		SF1
		SF3A1
		U2AF65

Table 1.3.4 B Further classification of leukaemogenic genes according to (Murati et al., 2012).

1.4 C/EBPα

C/EBPα is expressed in several tissues including adipose, lung epithelium, keratinocytes, hepatocytes and haematopoietic cells including the HSC, CMP and GMP (Zhang et al., 2004). High levels of C/EBPα expression characterises terminal differentiation of the cell type in which it is expressed. C/EBPα is a member of the C/EBP family of basic region leucine zipper transcription factor family. There are 6 family members identified by Greek symbols signifying chronological order of discovery (C/EBP α, β, ζ, ε, γ, ζ) (Cao et al., 1991). The C/EBP N-Terminal regions are highly divergent sharing only ~20 % sequence homology (reviewed by (Ramji and Foka, 2002)). However some N-Terminal short sequence motifs are retained, that are involved in interactions with basal transcriptional machinery (TBP/TFIIB), transcriptional co-activators (CBP/p300), and chromatin remodelling complexes (SWI/SNF) (Nerlov and Ziff, 1995, Erickson et al., 2001, Pedersen et al., 2001). C/EBP C-Terminal regions share regions of highly conserved sequence identity ~90 % (reviewed by (Ramji and Foka, 2002)). The C-Terminal region contains the basic DNA binding region and the leucine rich zipper region which facilitates protein dimerisation (Landschulz et al., 1988). C/EBP dimerisation is a requisite for DNA binding mediated by the basic region, and once C/EBP proteins bind DNA they activate transcription via their N-Terminal transactivation domain 1 (TAD1) (Landschulz et al., 1988, Vinson et al., 1989). C/EBP proteins recognise the consensus DNA binding sequence 5' TKNNGYAAK 3' (Y=C/T, K=T/G) within the

regulatory regions of their target genes. The high degree of C-Terminal homology permits intrafamilial C/EBP dimerisation. C/EBPα has been jokingly termed "Mcbindall" through its ability to bind multiple DNA sequences and vast number of protein partners (McKnight, 2001).

1.4.1 Structure of C/EBPα

C/EBPα exists as two isoforms, a full length p42 isoform and N-Terminally truncated p30 isoform, both generated from shared mRNA. C/EBPαp30 lacks the first 117 amino acids and TAD1 which mediates protein-protein interactions (Cleaves et al., 2004). C/EBPα is an intronless gene encoded on human chromosome 19q13, whose mRNA contains 3 translational AUG start sites. To date the crystal structure is only available for the C-Terminus bound to DNA, as the highly flexible N-Terminus hinders X-ray crystallography (**Fig 1.4.1**) (Miller et al., 2003). The rigid structure of the C-Terminus facilitates structural analysis.

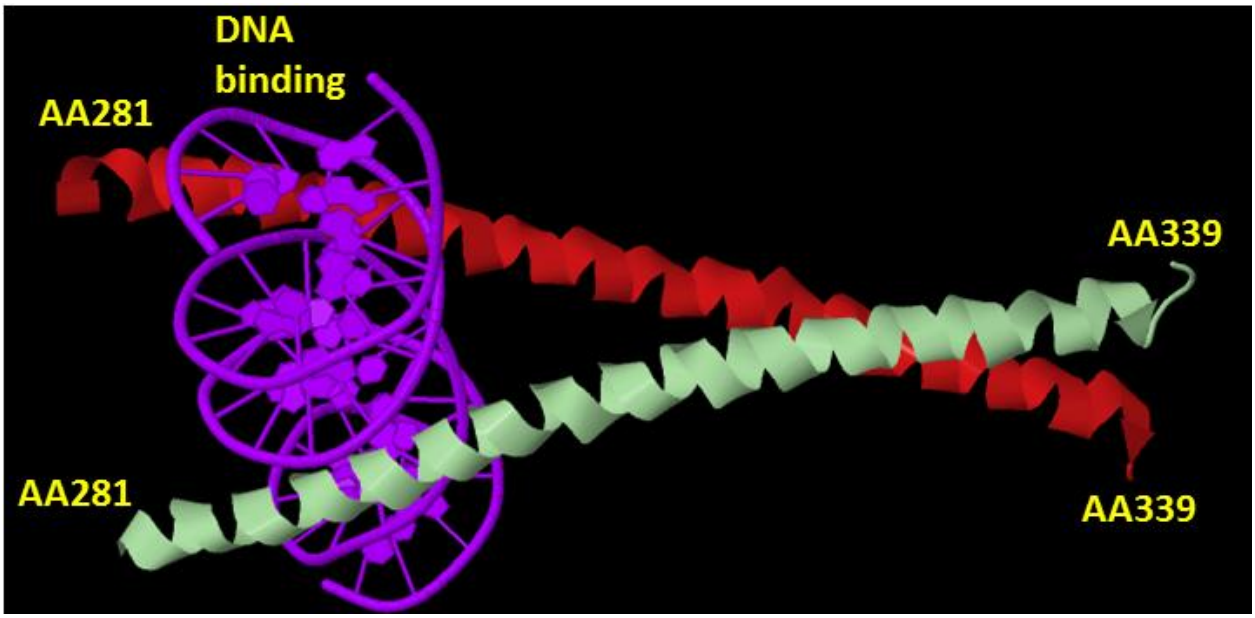

Fig 1.4.1 C/EBPα-DNA complex adapted from www.rcsb.org protein data base published by (Miller et al., 2003) viewed using Jmol viewer. NBD ID: PD0395, PBD ID:1NWQ. Individual C/EBPα monomers highlighted in red and green and DNA double helix highlighted in purple.

Full length C/EBPαp42 is translated from AUG_1 and AUG_2 (**Fig 1.4.2**). However C/EBPα also contains an additional weak upstream AUG site, and translation from this site is out of frame and results in premature protein truncation, causing the ribosome to scan over AUG_1 and AUG_2 and initiate translation from the alternative internal AUG_3 start site generating C/EBPαp30. Ribosomal scanning is controlled by the activity of eukaryotic translation initiation factor 2 (eIF-2α). High eIF-2α activity promotes translation for the weak upstream AUG and C/EBPαp30 translation (Calkhoven et al., 2000b). Alternatively it has also been proposed that generation of C/EBPαp30

occurs through partial proteolysis of C/EBPαp42 as occurs for nuclear factor kappa (NFκB) p105 generating p50 (Lin and Ghosh, 1996). C/EBPαp30 is described to exert a dominant negative effect on C/EBPαp42. C/EBPαp30 isoform negatively affects C/EBPαp42 through heterodimer formation. C/EBPαp30:C/EBPαp42 heterodimers have impaired DNA binding ability and transactivation capacity in comparison to C/EBPαp42 homodimers (Cleaves et al., 2004). C/EBPαp30 only binds DNA with 14 % of the affinity as C/EBPαp42 hence negatively affecting C/EBPα dimers (Pabst et al., 2001b). Additionally C/EBPαp30 mediates sumoylation of C/EBPαp42 through enhanced ubiquitin conjugating enzyme 9 (Ubc9) expression resulting in a decrease in C/EBPαp42 transactivation capacity (Geletu et al., 2007). Reference to C/EBPα within this text refers to both isoforms as a gene or protein entity as often in the literature there is no specification of isoforms. Where information is provided C/EBPα is referred to as either C/EBPαp42 or C/EBPαp30 delineating the isoforms.

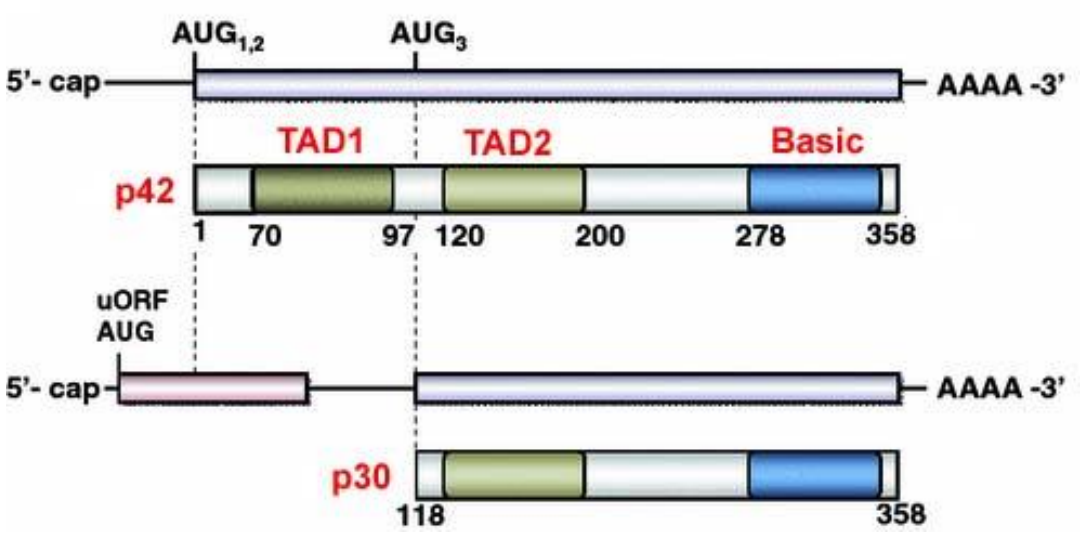

Fig 1.4.2 Functionally distinct isoforms of C/EBPα generated from alternative translational start sites, adapted from (Reckzeh and Cammenga, 2010). C/EBPα is translated from alternative translational start sites. AUG_1 and AUG_2 results in translation of full length C/EBPαp42 isoform while translation from internal start site AUG_3 results in generation of C/EBPαp30 isoform due to initial faulty translation from upstream AUG .

1.5 C/EBPα is a master regulator of haematopoiesis

1.5.1 C/EBPα in the HSC

C/EBPα is a crucial regulator of haematopoiesis, controlling the proliferative capacity of the adult and foetal HSC and mediating myeloid differentiation through governing the transition from CMP

to GMP (Zhang et al., 2004, Mancini et al., 2012, Ye et al., 2013, Hasemann et al., 2014). Foetal liver HSCs cycle rapidly in order to produce a stockpile to maintain adult life (Morrison et al., 1995). Four weeks post partum HSCs stop cycling and acquire a quiescent metabolic signature (Bowie et al., 2006). C/EBPα was identified to mediate this proliferative change in HSC behaviour, with increased C/EBPα expression associated with a decrease in HSC proliferation (Zhang et al., 2004, Ye et al., 2013). Additionally loss of C/EBPα in the adult HSC resulted in a transcriptome signature similar to the foetal liver HSCs through downregulation of *N-MYC* (Ye et al., 2013). Loss of C/EBPα in adult HSC results in an increase in LT-HSC population defined as $Lin^-/Sca1^+/Ckit^+$ (LSK)/$CD150^+/CD48^-$ ($SLAM^+$) and an increase in cells in G1-G2-S/M phase (Ye et al., 2013). Overexpression of C/EBPα in the foetal liver HSC induced cell quiescence determining an inverse relationship between C/EBPα expression and HSC proliferation (Ye et al., 2013). Contrastingly, Hasemann et al report that excision of C/EBPα in the adult HSC does not increase HSC cell numbers and rather it mediates an exit from the quiescent state with a concomitant increase in cell death due to HSC exhaustion (Hasemann et al., 2014). It was observed that C/EBPα expression represses lymphoid and erythroid gene expression while upregulating myeloid gene targets, supporting the idea of HSC lineage priming based on HSC gene expression (Hasemann et al., 2014). While both studies agree on C/EBPα exerting control over adult HSC quiescence, Ye et al did not observe any change to apoptotic gene expression in C/EBPα knockout versus wildtype (WT) LSK $SLAM^+$ murine cell population while Hasemann et al reported an increase in cell death and an increase in apoptotic and DNA damage repair pathways in C/EBPα knockout versus WT LSK $SLAM^+$ murine cell population. The difference between the studies is proposed to be due to methodological differences namely the time difference between poly (I-C) (pIpC) injections used to excise C/EBPα in floxed mice and experimentation (Hasemann et al., 2014). PIpC induces interferon response which influences the HSC parameters investigated. However Ye et al analysed apoptotic gene expression 7 and 21 days post pIpC injection which is approximate to Hasemann et al which performed analysis 14-17 days post injection (Hasemann et al., 2014). Taken together C/EBPα is crucial for regulating HSC biology through regulating self-renewal, quiescence and lineage priming (Zhang et al., 2004, Bereshchenko et al., 2009, Ye et al., 2013, Hasemann et al., 2014).

1.5.2 C/EBPα promotes myeloid differentiation

Expression of C/EBPα increases with myeloid commitment, as cells differentiate from CMPs to GMPs, at which stage C/EBPα expression is no longer required for terminal GMP differentiation (Zhang et al., 2004) (**Fig 1.5.1 and 1.5.2**). C/EBPα promotes the expression of myeloid terminal

differentiation effector genes *G-CSFR, M-CSFR, GM-CSFR, myeloperoxidase* and *C/EBPε*. C/EBPα is not expressed in the lymphoid or MEP cell lineages (Akashi et al., 2000, Miyamoto et al., 2002)(**Fig 1.5.1**).

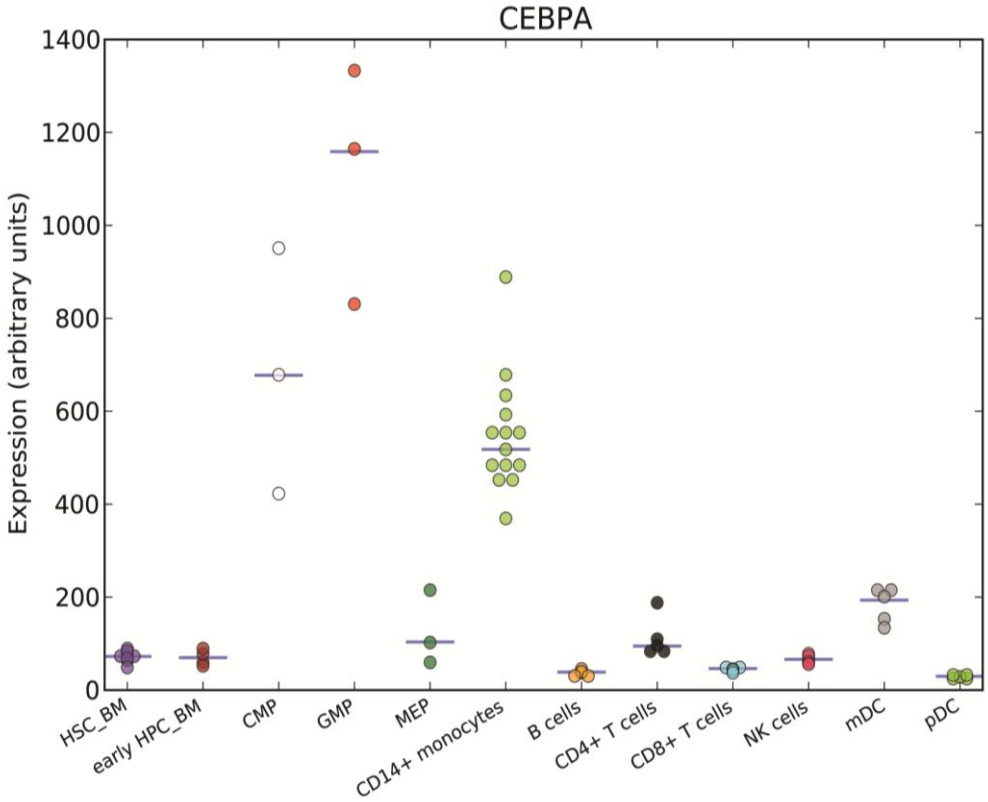

Fig 1.5.1 *C/EBPα* mRNA expression throughout human haematopoiesis analysis from HemaExplorer, each dot corresponds to the expression of *C/EBPα* in a microarray, while horizontal lines represent the median expression for each class of cell (Bagger et al., 2013). *C/EBPα* expressed highly in CMP, GMP and CD14+ monocytes, cells of the myeloid lineage.

Non conditional knockout C/EBPα neonates die due to hypoglycaemia and have no granulocytes within the foetal liver (Wang et al., 1995, Zhang et al., 1997). The obligate haematopoietic requirement for C/EBPα expression was revealed as conditional knockout of C/EBPα in adult mice blocked CMP transition with a decrease in myelomonocytes, eosinophils, granulocytes and monocytes, with no changes observed to erythroid or lymphoid lineages (Zhang et al., 2004). Further refinement identified a pre-granulocyte-monocyte (preGM) $CD41^{-}/CD150^{-}/CD105^{-}$ population which is unable to differentiate to GMPs in the absence of C/EBPα (Mancini et al., 2012). In C/EBPα knockout preGMs, elevated levels of *Globin transcription factor1/2* (*Gata1,Gata2), Fli1* and *friends of GATA1* (*Fog-1)* erythroid lineage mediating genes were identified along with an increase in megakaryocytic and erythroid progenitor cells, indicating loss

of C/EBPα may result in lineage reprogramming (Mancini et al., 2012). Differing levels of C/EBPα expression were proposed to differentially steer terminal GMP differentiation (Paz-Priel and Friedman, 2011). Lower levels of C/EBPα expression in the GMP promote monopoiesis through formation of a heterodimer with activator protein 1 (AP-1), while higher expression levels promote homodimerisation and granulopoiesis (Wang et al., 2006a, Paz-Priel and Friedman, 2011). Committed lymphoid precursor cells may be reprogrammed to myeloid lineage cells via overexpression of C/EBPα (**Fig 1.5.2**). C/EBPα elicits reprogramming through its ability to both extinguish other lineage determining pathways and to elicit its myeloid inducing effects. Overexpression of C/EBPα in pre-T-cells can reprogramme cells to become macrophages (Laiosa et al., 2006b) (**Fig 1.5.2**). Forced expression of C/EBPα in $CD19^{+}$ murine B-cells was able to reprogramme cell fate resulting in a macrophage phenotype (Xie et al., 2004) (**Fig 1.5.2**). C/EBPα mediates transdifferentiation through upregulation of miR-34a and miR-223 which decrease B-cell lineage gene expression (Rodriguez-Ubreva et al., 2014). C/EBPα downregulated B-cell commitment factor PAX5 in collaboration with PU.1 (Xie et al., 2004).

There is an element of redundancy amongst C/EBPα and its family member C/EBPβ in governing haematopoiesis. Replacement of C/EBPα gene locus with C/EBPβ did not affect terminal myeloid differentiation, and cytokine-stimulated or infection-meditated upregulation of C/EBPβ rescued the C/EBPα deficient granulocytic differentiation block (Jones et al., 2002, Hirai et al., 2006).

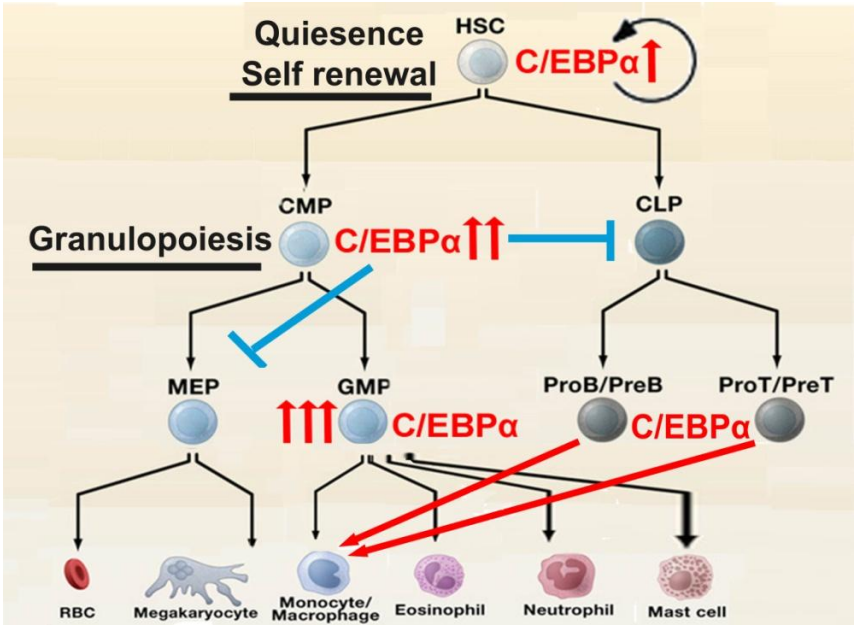

Fig 1.5.2 Cell fate governed by C/EBPα expression during haematopoiesis. Low levels of expression in the HSC promote quiescence and self-renewal capacity. C/EBPα expression levels increase from HSC to CMP and to the GMP. C/EBPα promotes granulopoiesis while

simultaneously inhibiting lymphoid and 2 is described as a myeloid tumour suppressor and its ability to promote myeloid differentiation is coupled to its ability to promote exit from the cell cycle, both functions governed independently by C/EBPα (Porse et al., 2001, Pabst et al., 2001b). C/EBPαp42 inhibits cell cycle progression from G1 to S phase and has been identified to do so independently of its DNA binding transcriptional activation activities, instead involving its association with multiple cell cycle proteins. C/EBPα was identified to inhibit cellular proliferation through repression of E2F dependent transcription and through repression of transcription from *C-MYC* promoter via an E2F binding site (Slomiany et al., 2000, Johansen et al., 2001). E2F controls the expression of genes required for S phase of the cell cycle and DNA replication. C/EBPα represses E2F dependent transcription via its N-Terminal TAD1 and via protein-protein interactions mediated by basic region amino acids I294 and R297 (Porse et al., 2001). C/EBPαp30 which lacks this N-Terminal TAD1 region is unable to mediate terminal myeloid differentiation and to induce cell cycle exit (Keeshan et al., 2003, D'Alo et al., 2003). C/EBPα-BRM2 (C/EBPα mutant BRM2 I294A/ R297A) is also unable to mediate myeloid differentiation in cell based assays and in vivo knockin murine studies identified an absence of neutrophils and expansion of early myeloid progenitor population (Porse et al., 2001, Keeshan et al., 2003, D'Alo et al., 2003, Porse et al., 2005). Long term BRM2 mice developed myeloproliferative disorders which progressed to AML and had a transplantable disease (Porse et al., 2005). C/EBPα mediated repression of E2F is crucial for terminal granulopoiesis; loss of E2F mediated cell cycle control is proposed to promote malignant myeloid transformation.

C/EBPα was also identified to complex with cell cycle regulators cyclin dependent kinase 2 and 4 (CDK2 and CDK4) via their homologous T loop region (Wang et al., 2001). The central C/EBPα proline rich region 177-191 was identified to mediate CDK2 and CKD4 interaction (Wang et al., 2001). C/EBPα and CDK2 interaction inhibited cyclin activation and E2F release, while C/EBPα and CDK4 interaction mediated proteasomal degradation of CDK4 by disrupting its association with protective chaperone proteins (Wang et al., 2001, Wang et al., 2002). Deletion of amino acids 177-191 abrogated C/EBPα ability to inhibit the cell cycle at G1 phase in vitro cell line experiments (Wang et al., 2001). Functional assays however revealed C/EBPα mediated repression of CDK2/CDK4 was not required for granulopoiesis and knockin C/EBPα Δ177-191 mutant mice displayed no haematopoietic disturbances (Keeshan et al., 2003, Porse et al., 2006). It is currently thought C/EBPα mediated repression of CDK2/CKD4 is dispensable for terminal granulocytic differentiation (Johnson, 2005). Additionally C/EBPα expression was identified to increase *p21* expression, a cyclin dependent kinase inhibitor, through an increase in *p21* transcriptional and post

transcriptional stabilisation (Timchenko et al., 1996, Timchenko et al., 1997). The role of p21 in C/EBPα mediated cell cycle exit has also been reported to be dispensable, as it can still do so in p21-deficient murine embryos (Johnson, 2005). The function of such interactions has varying degrees of responsibility and consequence in leukaemic transformation.

1.6 C/EBPα dysregulation in AML

Loss of C/EBPα function may occur directly through genetic mutations, promoter hypermethylation, post-translational modifications or indirectly through perturbations to upstream signalling cascades often mediated by chromosomal translocations in AML. Regardless of the cause of C/EBPα dysregulation patients are reported to display a characteristic haematopoietic cell marker expression profile CD7, HLA-DR, CD34, CD15, CD33, CD34 and CD65 (Fasan et al., 2014).

1.6.1 C/EBPα mutations in AML

C/EBPα is the most frequently mutated transcription factor in AML. C/EBPα mutations are frequently reported to be present in 10-15 % of karyotypically normal AMLs, however a recent report has identified mutated C/EBPα in 31.8 % of elderly karyotypically normal AML patients, suggesting perhaps current figures of 10-15 % maybe an underrepresentation (Pabst et al., 2001b, Pabst and Mueller, 2007, Fasan et al., 2014, Su et al., 2014). These C/EBPα mutant (mutC/EBPα) AMLs are typically classified (77 % of mutC/EBPα AMLs) as M1 and M2 by the FAB classification scheme (Renneville et al., 2008b, Fasan et al., 2014). C/EBPα mutations can occur throughout the single exon gene however they are predominately identified clustered either in the N-Terminus resulting in generation of the truncated C/EBPαp30 isoform, or are found in the C-Terminus between the basic region and the leucine zipper (Pabst et al., 2001b, Leroy et al., 2005). Under normal physiological cell conditions the ratio of C/EBPαp42 to C/EBPαp30 is greater than 1, when this ratio falls below 1 this is considered the leukaemic C/EBPαp42/p30 ratio and is observed in leukaemic cell lines and AML patients (Calkhoven et al., 2000a, Leroy et al., 2005, Keeshan et al., 2006, Koschmieder et al., 2007). N-Terminal mutations result in a disturbance of the wildtype C/EBPαp42:C/EBPp30 ratio, through decreasing C/EBPαp42 levels and increasing C/EBPαp30 levels (Pabst et al., 2001b). The haematopoietic importance of C/EBPαp42:C/EBPp30 ratio has been highlighted by a study identifying pharmacological induced differentiation of leukaemic cells and primary patient AML blasts (Koschmieder et al., 2007). 2-Cyano-3,12-dioxooleana-1,9-dien-28-oic acid (CDDO) treatment increases C/EBPαp42 or decreases C/EBPαp30 via dephosphorylation of eIF2α and phosphorylation of eIF4E (Koschmieder et al., 2007). The resultant change to C/EBPαp42:C/EBPp30 ratio mediates differentiation of leukaemic cell lines via

upregulation of C/EBPα functionality through the reduction of C/EBPαp30 repressive effects (Koschmieder et al., 2007). The C/EBPαp42:C/EBPp30 ratio has also been proposed as a mechanism by which a cell can control its proliferation and state of differentiation in response to extracellular states e.g. nutrient/growth factor/cytokine conditions (reviewed by (Nerlov, 2004)). Thus in a situation of optimum growth, increased activity of eIF2α and eIF4E would permit increased translation of C/EBPαp30 from C/EBPαp42 shared mRNA, which lacks the inhibitory cell cycle control of C/EBPαp42 resulting in increased proliferation and delay to terminal differentiation (D'Alo et al., 2003). However an argument exists against the importance of leukaemic C/EBPαp42:C/EBPp30 ratio presented in a murine model whereby mice with one WT-C/EBPαp42 allele and one C/EBPαp30 allele (L allele) do not develop AML or display any haematopoietic disturbances, despite a 2.5 fold decrease in C/EBPαp42:C/EBPαp30 ratio (Kirstetter et al., 2008). As discussed below L/L mice all developed fully penetrant AML indicating the leukaemogenic potential of C/EBPαp30 or/and the tumour suppressive function of C/EBPαp42. Further studies are required to fully decipher the leukaemogenic significance of alterations to this C/EBPαp42:C/EBPαp30 ratio.

Several in vitro and in vivo studies have been aimed at deciphering the biological effect of N-Terminal and C-Terminal mutations on WT-C/EBPαp42 function in an attempt to elucidate the biological mechanism of mutC/EBPα leukaemogenesis. In vitro studies reveal expression of C/EBPαp30 was insufficient to promote neutrophil differentiation of murine 32Dcl3 cells and granulocytic differentiation of primary murine bone marrow cells unlike C/EBPαp42 (Keeshan et al., 2003, Cleaves et al., 2004, Kato et al., 2011). However C/EBPαp30 retained the ability to stall the cell cycle at G1-S phase (Cleaves et al., 2004). Investigation by Schwieger et al reported C/EBPαp30 delayed but did not block myeloid differentiation in murine $CD34^{+}$/$lineage^{-}$ bone marrow cells but blocked both myeloid and erythroid differentiation in human $CD34^{+}$/$lineage^{-}$ cord blood cells, highlighting differences between murine and human haematopoiesis and other published studies (Schwieger et al., 2004). Murine knockin studies investigating C/EBPαp30 (termed L allele) oncogenicity in the absence of C/EBPαp42 showed that C/EBPαp30 induced fully penetrant transplantable AML (Kirstetter et al., 2008). C/EBPαp30 is sufficient for haematopoietic commitment to the myeloid lineage, it enables transition from the CMP to the GMP stage, however it does not retain the ability to control proliferation and myeloid progenitors have greatly increased self-renewal capacities (Kirstetter et al., 2008). Further investigation of a C-Terminal mutation (K allele K313dup mutation) combined with L allele (C/EBPαp30 expression only) revealed co-operation and possible explanation for the high prevalence of one N-terminal mutation and one C-

terminal mutation in 90 % of biallelic C/EBPα mutAMLs (Bereshchenko et al., 2009). Fetal liver transplanted chimera mice harbouring K/L genotype developed AML with a shorter latency than K/K and L/L mice (Bereshchenko et al., 2009). K/L and L/L shared the similar phenotypic features of AML disease with a distinct myeloid dysregulated signature similar to subtype M2, however only 25 % of K/K mice developed an AML like disease (Bereshchenko et al., 2009). K/K murine induced leukaemia was identified to involve accumulation of erythroid progenitors and display a phenotype similar to C/EBPα null mice (Bereshchenko et al., 2009). The different K/K leukaemic phenotype was reported to be due to the absence of the leukaemia initiating cell (LIC). Both K/L and L/L LICs were identified to be committed myeloid progenitor cells however in K/K mice there was a distinct lack of this cell type (Kirstetter et al., 2008, Bereshchenko et al., 2009). K/K murine leukaemic transformation occurred in erythroid progenitor population with slower kinetics due to absence of GMP population explaining the longer latency observed in K/K disease. K/L and K/K and to a lesser extent L/L HSCs evaded homeostatic control with an increase in cell number (Bereshchenko et al., 2009). LSK subpopulations were identified to have decreased expression of quiescence associated genes and an increase in measurable proliferation (Bereshchenko et al., 2009). Expansion of the HSC population was reported to accelerate leukaemogenesis by providing a pool of premalignant transformable cells. Gene set enrichment analysis identified that myeloid lineage gene expression was decreased in HSCs of K/K, K/L and to lesser extent in L/L mice. K/K HSCs had elevated erythroid gene expression thus it suggests presence of L allele is required for priming to commitment to the myeloid lineage. While the K allele is responsible for expansion of the HSC population (Bereshchenko et al., 2009). Kato et al confirmed the co-operative effect observed by Bereshchenko et al between N and C-Terminal C/EBPα mutations. Their study involved C/EBPα mutant T60fx159 termed the N^M allele, generating the C/EBPαp30 isoform, similar to Bereshchenko and Kirstetter "L allele" and the C-Terminal mutation K304-323dup C^M allele spanned K313dup "K allele" used by Bereshchenko (Kirstetter et al., 2008, Bereshchenko et al., 2009, Kato et al., 2011). Using bone marrow transplantation model (BMT) C^M transduced mice all developed AML with a latency 4-12 months. N^M mice did not develop AML but 37 % developed B-ALL. C^M/N^M transduced mice developed AML with a shorter latency than C^M. Kato et al explained their results in terms of the "the two hit mechanism of leukaemogenesis". They identified C^M as the differentiation inhibiting hit (class II) and N^M to confer a proliferative advantage to the cells (class I) (Kato et al., 2011). Validation of this hypothesis was performed by combining C^M with a FLT3 mutation, a confirmed class I AML mutation, resulting in AML with a very short latency (Kato et al., 2011). An additional study combining biallelic C/EBPα and FLT3-ITD mutations in a knockin murine model which facilitates expression of mutants from their

endogenous promoters at appropriate stages of development verified the co-operation observed by Kato et al (Reckzeh et al., 2012a). C/EBPα and FLT3-ITD mutations reduced the latency of induced AML (Reckzeh et al., 2012a). Differences in the Bereschchenko and Kato et al studies in terms of N and C-Terminal mutation leukaemogenecity were attributed to differences in murine models (knockin versus BMT) and different C/EBPα mutations. However both studies identify distinct roles for the N and C-Terminal C/EBPα mutations and their oncogenic co-operation during leukaemogenesis.

To date there have been three different patterns of C/EBPα mutations observed in AML patients 1) a single mutation on one allele (monoallelic), 2) mutations on both alleles (biallelic) usually a N-Terminal mutation on one allele and a C-Terminal mutation on the second allele or 3) a homozygous mutation due to loss of heterozygosity or uniparental disomy (Fasan et al., 2014). C/EBPα mutations are largely somatically acquired however there have been several reports of germline inheritance of C/EBPα mutations with a resulting familial predisposition to AML (Smith et al., 2004, Sellick et al., 2005, Pabst et al., 2008, Renneville et al., 2008a, Nanri et al., 2010, Gutman and Hoffner, 2012, Debeljak et al., 2013). Upon inheritance of a C/EBPα mutation a second second somatically acquired C/EBPα mutation is required for transformation (Pabst et al., 2008). There is evidence of anticipation upon inheritance of a highly penetrant C/EBPα mutation with age of onset decreasing with successive generations (Pabst et al., 2008). A study by Pabst et al identified 11.1 % of C/EBPα mutations were inherited in germline DNA accounting for 1.1 % of all AMLs. To date reports of inheritance of C/EBPα mutations identified have been predominately N-Terminally localised. Clinically C/EBPα mutAMLs are associated with favourable patient outcomes in response to a chemotherapy regime with a high dose ARA-C component; however the molecular biology surrounding this favourable response remains largely undetermined (Renneville et al., 2008b). The favourable response was later reported to be specific to patients who possessed biallelic versus monoallelic mutations (Wouters et al., 2009, Fasan et al., 2014). This differential treatment response is probably unsurprising as monoallelic and biallelic patients display different gene signature expression patterns (Wouters et al., 2009). Additionally patients who harboured a monoallelic N-Terminal single mutations have a poorer overall survival than monoallelic C-Terminal mutations, indicating the localisation of the mutation may also provide prognostic information (Fasan et al., 2014). C/EBPα mutations remain constant pre and post relapse and are thus thought to be crucial in the initiation of leukaemogenesis. It is now a strongly held view that C/EBPα mutation analyses be included in standard diagnostic cytogenetic tests upon presentation.

1.6.2 AML chromosomal translocations which disrupt C/EBPα expression

While C/EBPα mutations are predominately associated with cytogenetically normal AML patients, dysregulation of C/EBPα also occurs in AML patients with oncogenic fusion proteins created by chromosomal translocations summarised in Fig **1.6.2** (most common AML translocations outlined in Table **1.3.3**). Translocation (8;21) which gives rise to AML1-ETO oncofusion protein downregulates *C/EBPα* expression and its DNA binding activity (Pabst et al., 2001a). AML1-ETO binds the C/EBPα promoter and inhibits its auto regulation repressing *C/EBPα* at the transcriptional level (Pabst et al., 2001a). Knockdown of AML1-ETO restores *C/EBPα* expression in leukaemic cells resulting in myeloid differentiation (Heidenreich et al., 2003). t(3;21) and inv(16) increase the expression levels of Calreticulin, an mRNA binding protein which strongly binds the GC rich *C/EBPα* mRNA (Helbling et al., 2004, Helbling et al., 2005). Calreticulin binding inhibits C/EBPα translation and decreases protein expression (Helbling et al., 2004, Helbling et al., 2005). BCR-ABL the hallmark translocation of CML increases levels of hnRNP-E2 protein in a mitogen-activated protein kinase (MAPK) signalling dependent manner (Perrotti et al., 2002). hnRNP-E2 binds the 5' untranslated region (UTR) of *C/EBPα* mRNA and also represses translation (Chang et al., 2007). Imatinib treatment was identified to restore C/EBPα protein expression and relieving the myeloid differentiation block (Chang et al., 2007). Translocation t(14;19) identified in B-Cell precursor (BCP)-ALL patients results in overexpression of *C/EBPα* through the fusion of the immunoglobulin heavy chain (IGH) transcript on chromosome 14 to *C/EBPα* (Chapiro et al., 2006). Chromosomal translocations involving IGH result in deregulated expression of partner fusion genes due to the proximity of the transcription enhancers within IGH (Willis and Dyer, 2000). The breakpoint on chromosome 19 occurs in the 3'UTR of *C/EBPα* permitting full apparent normal isoform expression (Chapiro et al., 2006). The IGH-C/EBPα fusion results in aberrant ectopic *C/EBPα* expression in response to B-Cell signalling cascades perpetuated by IGH fusion, skewing the path of normal B-Cell differentiation. Indeed other C/EBP family members (C/EBPδ and C/EBPγ t(14;19) C/EBPβ t(14;20) C/EBPε t(14;14)) have also been identified to be up regulated in translocation events involving IGH in ~1 % of all BCP-ALLs (Akasaka et al., 2007). Under normal physiological conditions B-Cell differentiation is thought to be concomitant with decreasing C/EBP expression (Laiosa et al., 2006a). The mechanism by which all C/EBP family members (except C/EBPζ) confer oncogenic pathogenicity in BCP-ALL is as of yet unknown, but is proposed to be perpetuated via the C-Terminal highly conserved leucine zipper and DNA binding regions (Akasaka et al., 2007). Interestingly Akasaka et al is reported as the first evidence of multiple members of the same family being involved in translocations with the same gene locus within the same disease phenotype.

While examples of chromosomal translocations cited up- or down-regulated C/EBPα expression, expression of C/EBPα was identified as a pre-requisite for leukaemic initiation for some chromosomal translocations. In AML, chromosomal translocations involving MLL and 50 other interacting protein partners have been described (Krivtsov and Armstrong, 2007). Leukaemic transformation with MLL-ENL required the expression of C/EBPα for transformation; however C/EBPα expression was not required for disease maintenance (Ohlsson et al., 2014). Hoxa9/Meis1 also requires C/EBPα expression for transformation, while E2A-HLF does not, indicating that C/EBPα is only required for leukaemia initiation in specific genetic backgrounds (Ohlsson et al., 2014). It has been proposed that C/EBPα binds DNA maintaining it in an open configuration for resulting gene-fusion binding (Roe and Vakoc, 2014).

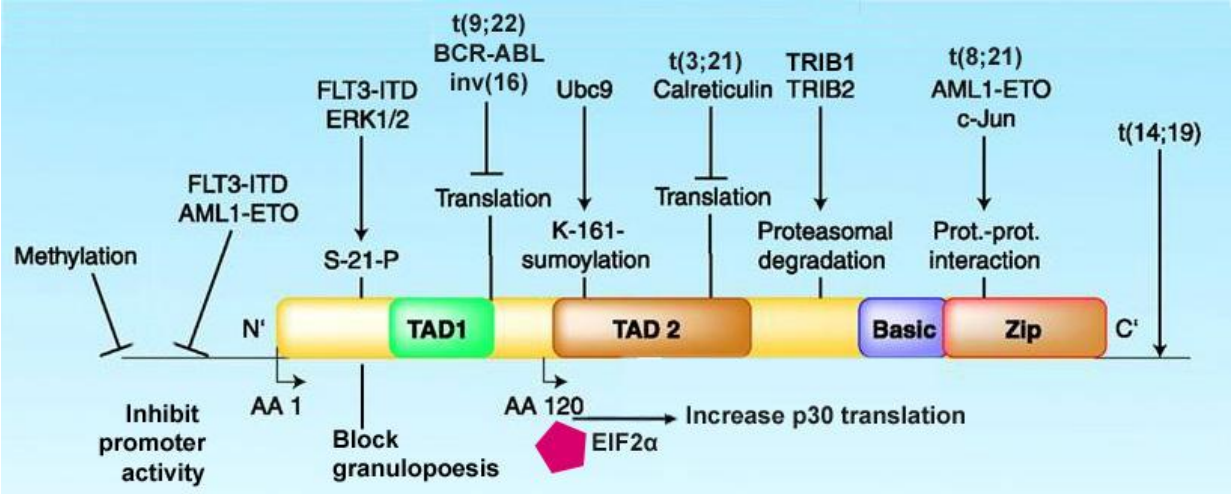

Fig 1.6.2 Schematic of chromosomal and post-translation modifications identified to repress C/EBPα adapted from (Pabst and Mueller, 2009).

1.6.3 Post-translational modifications disrupting C/EBPα in AML

Sumoylation

Sumoylation involves the reversible covalent conjugation of Small Ubiquitin like MOdifier proteins (SUMO) to target proteins thereby modifying their functionality and cell fate. Sumoylation is an evolutionary conserved process, involving a three step mechanism similar to ubiquitination (to be discussed). In general, sumoylation of transcription factors leads to repression of their transactivation activity, through conferring new protein-protein interactions which alter promoter binding (Khanna-Gupta, 2008). Both C/EBPαp42 and C/EBPαp30 isoforms have been identified to be sumoylated by SUMO-1 at K159 within the conserved negative subdomain "the synergy control motif" (Subramanian et al., 2003). Sumoylation was identified to negatively affect C/EBPαp42

functionality during neutrophil maturation (Hankey et al., 2011). Additionally C/EBPαp30 was identified to mediate sumoylation of C/EBPαp42 via upregulation of ubiquitin conjugation enzyme *Ubc9* (Geletu et al., 2007). Knockdown of *Ubc9* in C/EBPαp30 transduced human $CD34^+$ cells was able to restore a C/EBPαp30 induced differentiation block (Geletu et al., 2007). Therefore it has been proposed that C/EBPαp30 mediated sumoylation of C/EBPαp42 is another mechanism by which C/EBPαp30 exerts a dominant negative effect on C/EBPαp42 in AML as the ratio of C/EBPαp42/C/EBPαp30 is often perturbed (Geletu et al., 2007).

Phosphorylation of C/EBPα

Phosphorylation describes the covalent transfer of a phosphate group from ATP to specific amino acids on a target protein subsequently affecting its functionality. Phosphorylation is the most common post-translation modification. C/EBPα to date has several identified phosphorylation sites (summarised in **Table 1.6.3**); however there is not a consensus behavioural response in terms of phosphorylated or dephosphorylated C/EBPα and the ability to differentiate cells in various tissues. This underlines the molecular complexity of these phosphorylation events and the multiple upstream kinases which mediate the phosphorylation events.

Serine 21 (Ser21) was identified to be an extracellular kinase 1/2 (ERK1/2) phosphorylation site on C/EBPα, recognised via a proximal C-Terminal MAP Kinase docking site FXFP (Ross et al., 2004). ERK1/2 mediated phosphorylation of C/EBPα was identified to alter the conformation of the C/EBPα dimer whilst not affecting dimer stability (Ross et al., 2004). Ser21 phosphorylation resulted in the N-Terminal TAD moving apart from the C-Terminal domain (Ross et al., 2004). It was speculated that phosphorylation at Ser21 does not affect the bZIP DNA binding functions rather the phosphorylation event affects N-Terminal interactions with protein partners (Ross et al., 2004). High levels of phosphorylated Ser21 (P-Ser21) are present in the bone marrow and further investigation revealed P-Ser21 inhibited granulopoiesis in K562 cells and inhibited granulocytic differentiation of bipotental U937 cells (Ross et al., 2004). U937 leukaemic cells possess the ability to become either monocytes or granulocytes, phorbol 12-myristate 13-acetate (TPA) stimulation promotes the former, while retinoic acid (RA) stimulation promotes the latter. Expression of C/EBPα phosphorylation mimetic construct, S21D, permits monocytic differentiation while inhibiting granulocytic differentiation (Ross et al., 2004). FLT3 is a receptor tyrosine kinase mutated in ~30 % of AMLs, and classified as a class I mutation (Gilliland and Griffin, 2002). The most common mutation results from an internal tandem duplication (ITD) within the juxatamembrane domain resulting in constitutive signalling and aberrant activation of downstream

kinases including ERK1/2 (Nakao et al., 1996). Analysis of human FLT3-ITD mutant AML cell lines revealed hyperphosphorylation of Ser21 (Radomska et al., 2006). Treatment with both a FLT3 inhibitor MLN518 and a mitogen/extracellular signal-regulated kinase (MEK) inhibitor PD98059 relieved the differentiation block in mutant FLT3 (mutFLT3) AML cell lines and activated differentiation through detectible decreases to P-Ser21 (Radomska et al., 2006). Indeed overexpression of an unphosphorylated Ser21 mimetic (S21A) in mutFLT3 cell line was sufficient to induce differentiation while S21D expression had no effect (Radomska et al., 2006). The induction of differentiation observed upon inhibitor treatment and S21A expression was accompanied by a rapid decrease in *C-MYC* mRNA expression, reiterating the necessity for inhibition of the cell cycle upon initiation of differentiation (Radomska et al., 2006). Further investigation of S21D and S21A effects on cell cycle regulation revealed both phosphorylated and unphosphorylated mimetics displayed reduced inhibition of the cell cycle, reduced E2F repression and differential E2F protein binding to WT-C/EBPα (Ferrari-Amorotti et al., 2010). WT-C/EBPα was identified to associate with E2F2 and E2F3 while S21D and S21A displayed reduced binding to E2F2 and S21A displayed increased binding to E2F3 (Ferrari-Amorotti et al., 2010). Frangalisso et al investigated differentiation mediating properties of S21D and S21A and reported S21D ectopic expression in K562 cells marginally inhibited granulocytic differentiation and in fact S21A displayed a great inhibitory effect contradicting the previous studies by Ross et al, Radomska et al, and Twu et al all of which showed that S21D expression inhibited differentiation and that S21A and WT-C/EBPα expression mediated granulopoiesis in K562. Interestingly P-Ser21 was also identified to inhibit key processes in erythropoiesis (Twu et al., 2010). Unphosphorylated Ser21-C/EBPα upregulates *IGnTC* expression, which is essential for antigen i maturation during erythropoiesis (Twu et al., 2010). Phenotypic transition from antigen i to antigen I is a key process during erythroid development. P-Ser21 has reduced affinity for the *IGnTC* promoter, does not drive *IGnTC* expression and antigen i maturation (Twu et al., 2010). Thus phosphorylation of Ser21 appears to inhibit differentiation of both erythroid and myeloid cells.

The first and only study to date identifying P-Ser21 specific C/EBPα protein partners using a mass spectrometry large scale approach, reports DEK as a specific binding partner for unphosphorylated C/EBPα at Ser21 (Koleva et al., 2012). The assembly of this DEK/C/EBPα complex occurs on the *G-CSFR* promoter, driving its transcription and myeloid differentiation. Thus DEK acts as a phosphospecific C/EBPα co-activator (Koleva et al., 2012). S21D was reported to retain the ability to bind the *G-CSFR* promoter in K562 cells but it was unable to drive its expression (Koleva et al., 2012). Knockdown of DEK in cells expressing WT and S21A-C/EBPα resulted in a 2 fold decrease

in *G-CSFR* mRNA levels and a block in granulocytic differentiation (Koleva et al., 2012). These data corroborates the reported roles of S21D in inhibiting differentiation (Ross et al., 2004, Twu et al., 2010) and the effect of S21A in overcoming a differentiation block (Radomska et al., 2006). While unphosphorylated C/EBPα was identified to act as co-activator in the context of DEK mediated transcriptional activation, P-Ser21 was reported to relieve C/EBPα mediated repression of interleukin-10 (IL-10) production (Kang et al., 2013). IL-10 is an anti-inflammatory cytokine whose production is upregulated in myeloid cells by IL-32β expression (Kang et al., 2013). IL-32β induces Protein Kinase C delta (PKCδ) mediated phosphorylation of C/EBPα at Ser21 and this phosphorylation event relieves C/EBPα inhibitory effect on *IL-10* promoter (Kang et al., 2013). IL-32β binds both C/EBPα and PKCδ while IL-32β binding of C/EBPα is P-Ser21 independent. IL-32β binding site was localised to the DNA binding domain of C/EBPα. It has yet to be elucidated if P-Ser21 recruits other potential co-activators or if C/EBPα promoter binding alone results in repression.

The majority of reports on phosphorylated C/EBPα in haematopoietic cells document a differentiation block of cells committed to the granulocytic lineage however phosphorylation of C/EBPα has also been identified in two reports to skew lineage commitment of cells. p38MAPK was identified as a kinase capable of phosphorylating Ser21 (Geest et al., 2009). Pharmacological inhibition of p38MAPK in human cord blood derived $CD34^+$ ($hCD34^+$) cells resulted in an increase in granulocytes with a concomitant decrease in eosinophil numbers (in granulocyte and eosinophil permissive culture conditions) (Geest et al., 2009). Inhibition of p38 was shown to decrease levels of P-Ser21 in neutrophil progenitors (Geest et al., 2009). Mice transplanted with $hCD34^+$ cells transduced with CA-MKK3 (constitutively active- Mitogen-activated protein kinase 3, upstream p38 activator) had decreased numbers of neutrophils accompanied with an increase in eosinophil development, indicating that P-Ser21 regulates haematopoietic lineage fate (Geest et al., 2009). Co-expression of CA-MKK3 and S21A abrogated activated p38 inhibition of neutrophil differentiation, permitting neutrophil development in colony forming assays. Thus in this context P-Ser21 skews granulocytic differentiation toward eosinophil lineage ultimately still exerting a negative effect on mature granulocyte cell numbers. When the Ser21 phosphorylation site was first identified by Ross et al., pharmacological inhibition of p38MAPK did not decrease ectopically expressed C/EBPα P-Ser21 levels in 3T3-L1 cells, whereas inhibition of ERK1/2 activity alone elicited a decrease in P-Ser21 levels (Ross et al., 2004). Additionally Radomska et al., also observed no increase in endogenous P-Ser21 upon p38 activation (Radomska et al., 2006). Thus to date there appears to be no consensus in the literature regarding activation and subsequent functionality of P-Ser21 with

regard to inhibition of granulopoiesis. There also appears to be a lack of studies investigating the differential effects of P-Ser21 within the HSC and as a regulator of quiescence.

Protein Kinase B (PKB) is a downstream effector of PI3K pathway identified to mediate lineage commitment decisions during myelopoiesis through modulation of glycogen synthase kinase-3 (GSK3) mediated phosphorylation of C/EBPα (Buitenhuis et al., 2008). GSK3 was identified as a kinase responsible for phosphorylation of C/EBPα at threonine 222/226 (Thr222/226) (Ross et al., 1999). P-Thr222/226 also results in a conformational change to the C/EBPα protein as was observed by ERK1/2 mediated P-Ser21, suggesting phosphorylation of C/EBPα may be a mechanism by which it can alter its interactions with protein partners (Ross et al., 1999, Ross et al., 2004). P-Thr222/226 has been suggested to be essential for controlling the autoregulatory function of C/EBPα (Zhang and Ma, 2010). Loss of this phosphorylation site through alanine substitution (T222A/T226A) abrogated the ability of C/EBPα to activate its own promoter, while loss of other phosphorylation sites S21A, S248A, S193A behaved similarly to wildtype C/EBPα (Zhang and Ma, 2010). Expression of a constitutively active isoform of PKB (CA-PKB) inhibited neutrophil differentiation and enhanced eosinophil development in both ex vivo differentiation assays and in murine models while alternatively, the expression of dominant negative isoform of PKB (myr-PKB) enhanced neutrophil expansion and blocked eosinophil development (Buitenhuis et al., 2008). CA-PKB expression was identified to increase P-Thr222/2226 C/EBPα and GSK3 has already been described as a direct substrate for PKB. Thus in this study it was proposed that PKB activation results in GSK3 activation, an increase P-Thr222/226 C/EBPα, resulting in an increase in eosinophil production at the cost of neutrophils (Buitenhuis et al., 2008). Additionally P-Thr222/226 also exerts a role in adipocytic differentiation but has no discernible effect on hepatocytes biology (Ross et al., 1999, Liu et al., 2006). Insulin was identified to decrease phosphorylation of C/EBPα affecting adipocyte biology (Hemati et al., 1997, Ross et al., 1999). Insulin mediates C/EBPα dephosphorylation through both inhibition of GSK3 which phosphorylates C/EBPα at Thr222/226 and through activation of the protein phosphatases 1 and 2A (PP1/ PP2A) which remove phosphate groups from C/EBPα (Ross et al., 1999). Inhibition of GSK3 results in dephosphorylation of C/EBPα at Thr222/226 inhibiting preadipocytic differentiation suggesting in this cell context that unphosphorylated C/EBPα has an inhibitory effect on terminal cell differentiation (Ross et al., 1999). Further studies investigating the functional effects of GSK3 mediated P-Thr222/226 revealed phosphorylation of these sites had no effect on hepatocyte biology and in fact reported C/EBPα was a poor substrate for GSK3 (Liu et al., 2006). However Liu et al did suggest P-Thr222/226 played a role in adipocytic biology as unphosphorylatible Thr222/Thr226

mutants (T222A/T226A) increased transactivation of C/EBPα targets compared to WT-C/EBPα in adipocytes. However no difference to C/EBPα transactivation functions of C/EBPα target promoters regardless of the phosphorylation status of Thr222/226 was observed in another study (Ross et al., 1999). In vivo knockin murine studies investigating the loss of GSK3 consensus phosphorylation site Thr222A/226A/Ser230A (TTS-C/EBPα mutant) identified no apparent physiological abnormalities or specifically no changes to amount or morphology of cells in lung, liver and granulopoiesis (Pedersen et al., 2007). Detailed analysis of TTS livers revealed increased expression of genes expressed upon transition from the fasting to fed metabolic states. Authors propose that Thr222/226 phosphorylation of C/EBPα may serve as a hepatic-specific sensor regulating hepatic gene expression dependent on the metabolic state (Pedersen et al., 2007).

Ser248 is a phosphorylation site identified in C/EBPα which also perturbs myeloid differentiation (Behre et al., 2002, Singh et al., 2008, Hasemann et al., 2012). Enhanced Ras signalling was identified to increase the transactivation capacity of C/EBPα as measured by its ability to drive *G-CSFR* expression, however this was not as a result of altered DNA binding (Behre et al., 2002). Ser248 was identified as a site of Ras signalling-mediated phosphorylation and upon mutation Ser248A lost the ability to induce differentiation of 32Dcl3 and K562 cells (Behre et al., 2002, Singh et al., 2008, Hasemann et al., 2012). In vivo murine knock-in studies showed Ser248A-C/EBPα was dispensable for early haematopoiesis as there was no disruption to the haematopoietic compartment of 8 week old mice (Hasemann et al., 2012). However Ser248A-C/EBPα aged mice developed a low penetrant haematopoietic disorder characterised by increased megakaryocytic and erythroid progenitor cells at the expense of granulocytic-monocytic lineage, accompanied with LSK expansion (Hasemann et al., 2012). Thus both Ser21- and Ser248-C/EBPα are phosphorylated by different mechanism with antagonistic effects on the differentiation function of C/EBPα with Ser21 phosphorylation being anti-differentiation and Ser248 being pro-differentiation (Ross et al., 2004, Radomska et al., 2006, Behre et al., 2002, Singh et al., 2008, Hasemann et al., 2012).

Ectopically expressed Protein Kinase C delta- catalytic fragment (PKCδ-CF) was observed to mediate phosphorylation of C/EBPα at Ser21, Ser 266 and Ser277, the two latter sites identified as novel C/EBPα phosphorylation sites (Wu et al., 2013). PKCδ is cleaved upon induction of apoptosis generating an active PKCδ–CF protein. However initial studies by this group contradict their later findings that reported the absence of both direct PKCδ/C/EBPα binding and any phosphate transfer mediated by PKCδ to C/EBPα (Zhao et al., 2009). Induction of apoptosis, generation of PKCδ-CF, was identified to increase ubiquitination of C/EBPα in leukaemic cells (Zhao et al., 2009). Pharmacological inhibition of PKCδ using rotterlin abrogated the enhanced

C/EBPα ubiquitination observed upon induction of apoptosis (Zhao et al., 2009). PKCδ activation alters the localisation of C/EBPα, by promoting its cytoplasmic sequestration, resulting in enhanced ubiquitination of C/EBPα upon induction of apoptosis. It remains to be clarified whether the phosphorylation events themselves serve to trigger ubiquitination, or if the cytoplasmic localisation of C/EBPα is responsible for the subsequent ubiquitination upon PKCδ activation. Several C/EBPα phosphorylation events have been linked to ubiquitin-dependent proteasomal degradation of C/EBPα. Cellular stresses activate c-Jun N-Terminal kinase 1 (JNK1) which binds the DNA binding region of C/EBPα mediating phosphorylation of C/EBPα at unknown residues within this region (AA 278-352) (Trivedi et al., 2006). Activation of JNK1 and the subsequent C/EBPα phosphorylation stabilizes C/EBPα protein by inhibiting ubiquitination (Trivedi et al., 2006). Alternatively inactive JNK1 is permissive of C/EBPα ubiquitination (Trivedi et al., 2006). Another example of phosphorylation affecting C/EBPα protein stability revealed hyper-phosphorylation of C/EBPα occurs in the livers of aging mice and also induce liver tumourigenesis (Wang et al., 2006b, Wang et al., 2010). Ser193 was identified to be phosphorylated by CDC2 and CDK4 (Wang et al., 2010). Under normal physiological conditions this phosphorylation event results in C/EBPα mediated inhibition of liver proliferation however during carcinogenesis, P-Ser193 is targeted by gankyrin mediated ubiquitin-dependent proteasome degradation. Gankyrin is a proteasomal subunit and only binds C/EBPα when phosphorylated at Ser193 (Wang et al., 2010). Therefore it appears different phosphorylation events mediated by different kinases in different cell types serve to either enhance or inhibit ubiquitination of C/EBPα increasing or decreasing protein stability (summarised in **Table 1.6.3**).

Kinase	Site	Effecter	Reference
ERK1/2	Ser21	-Phosphorylation inhibits granulocytic differentiation	(Ross et al., 2004)
FLT3-ITD via ERK1/2		-Phosphorylation inhibits myeloid differentiation	(Radomska et al., 2006)
ERK1/2		-Phosphorylation does not inhibit differentiation -Differential binding to E2F family members	(Ferrari-Amorotti et al., 2010)

p38MAPK	Ser21	-Inhibits granulocytic differentiation increases eosinophil development	(Geest et al., 2009)
Cdc2	Ser21	-Ubiquitin-dependent C/EBPα degradation in hepatocytes	(Wang et al., 2010)
PKCδ Via IL-32β	Ser21	-Suppress C/EBPα inhibition of IL-10 production	(Kang et al., 2013)
PKCδ	Ser21 Ser266 Ser277	-Cytoplasmic sequestering of C/EBPα and enhanced ubiquitination upon induction of apoptosis	(Zhao et al., 2009) (Wu et al., 2013)
Not investigated	Ser21	-Phosphorylation inhibits granulopoesies and antigen i/I transition and erythroid development	(Twu et al., 2010)
Not investigated	Ser243	-Phosphorylation has no affect on granulopoiesis or erythroid development	(Twu et al., 2010)
Ras signalling	Ser248	-Phosphorylation required for normal haematopoiesis -Loss of phosphorylation results in haematopoietic malignant disease	(Behre et al., 2002) (Singh et al., 2008) (Hasemann et al., 2012)
GSK3 GSK3 via PKB	Thr222/226	-Phosphorylation inhibits adipocytic differentiation -Dephosphorylation increases G6Pc hepatic gene expression, no physiological abnormalites -Skews toward eosinophil differentiation	(Ross et al., 1999) (Pedersen et al., 2007) (Buitenhuis et al., 2008)
Unidentified	Ser230	-Not a GSK3 target kinase	(Ross et al., 1999)
JNK1	DBD unidentified site	-Phosphorylation stabilises C/EBPα protein decreasing ubiquitination	(Trivedi et al., 2006)
CDC2/CDK4	Ser193	-Promotes liver aging and tumourigenesis	(Wang et al., 2010)
ERK1/2 GSK3	Ser21 Thr222/226	-Phosphorylation promotes inhibitory effect mediated by C/EBPα on IL-12/p40 expression in response to Triptolide	(Zhang and Ma, 2010)

treatment in macrophages

Table 1.6.3 Phosphorylation events and their effects on C/EBPα function.

Ubiquitination

Ubiquitination describes the signalled conjugation of an ubiquitin moiety to a target protein subsequent to three steps of an enzyme controlled pathway. The enzymes involved are E1 ubiquitin-activating enzymes, E2 ubiquitin-conjugation enzymes and E3 ubiquitin ligases which conjugate ubiquitin to the target protein. Conjugation of ubiquitin results in alterations to the function of a protein, predominately resulting in proteasomal mediated degradation of its target protein however ubiquitination is now increasingly being attributed with non-degradative functions. Ubiquitination of C/EBPα discussed herein refers to ubiquitin-dependent proteasomal degradation. C/EBPα was first identified to be ubiquitinated resulting in its proteasomal degradation in keratinocytes (Shim and Smart, 2003). Lithium chloride treatment (LiCl) resulted in an increase in C/EBPα protein levels with no change to *C/EBPα* mRNA levels indicating a post transcriptional effect on C/EBPα (Shim and Smart, 2003). LiCl inhibits the chymotryptic activities of the proteasome thus inhibiting the degradation of ubiquitinated proteins. LiCl also inhibits GSK3, however the LiCl induced increase in C/EBPα protein levels was independent of any inhibitory effect on GSK3 and subsequent phosphorylation of C/EBPα (Shim and Smart, 2003). Analysis of TTS-C/EBPα protein expression in murine hepatocytes identified no difference in comparison to WT-C/EBPα mice suggesting loss of this phosphorylation site does not affect protein stability supporting the reports from Shim et al of increased stability of C/EBPα to be GSK3 independent (Pedersen et al., 2007).

As introduced above C/EBPα phosphorylation events have been inextricably linked to protein ubiquitination, P-Ser193, P-Ser266 and P-Ser277 in response to CDC2, CDK4 and PKCδ mediated phosphorylation respectively have been associated with enhanced C/EBPα ubiquitination in leukaemic cells and in liver tumour cells. F-box/WD repeat-containing protein 7 (FBXW7), an E3 ligase was identified to mediate ubiquitination of C/EBPα only upon P-Thr222/226 (Bengoechea-Alonso and Ericsson, 2010). P-Thr222/226 acts as a phosphodegron motif for FBXW7 recognition of C/EBPα, thus FBXW7 only binds P-Thr222/226 and mediates ubiquitination inhibiting adipogenesis (Bengoechea-Alonso and Ericsson, 2010). Thus it appears phosphorylation triggered ubiquitination and subsequent elimination of C/EBPα protein is a common event in dysregulated differentiation of various cell types and in cancer cells.

Other E3 ligases have been identified to associate with C/EBPα mediating enhanced ubiquitination and proteasomal degradation in different cellular contexts (summarised in **Table 1.6.4**). In some instances an increase in ubiquitination has not been directly investigated, however proteasomal degradation has been identified to be dependent on E3 ligase binding which is predominately indicative of ubiquitin mediated proteasomal degradation however requiring further experimental investigation. E6 associated protein (E6AP) is an E3 ligase with a C terminal homologous to the E6-AP Carboxyl Terminus (HECT) domain. E6AP is one of only two E3 ligase identified to date which directly binds to C/EBPα in both myeloid cells and adipocytes (Pal et al., 2013a, Pal et al., 2013b). E6AP binding results in ubiquitin-dependent proteasomal degradation of C/EBPα, resulting in inhibition of both myeloid and adipocytic differentiation, two processes governed by C/EBPα expression (Pal et al., 2013a, Pal et al., 2013b). Knockdown of E6AP or expression of dominant negative catalytically inactive form E6AP-C843A induced myeloid differentiation of K562, U937 and 32Dcl3 cells through increased C/EBPα protein expression (Pal et al., 2013b). While to date E6AP has not been linked to carcinogenesis these studies underline the therapeutic potential of inhibition of C/EBPα ubiquitination in AML.

Proteasomal degradation of C/EBPα has also been associated with the E3 ligase constitutively photomorphogenic 1 (COP1), however COP1 mediated ubiquitination or proteasomal degradation of C/EBPα is dependent on expression of a family of adaptor proteins "Tribbles" (Keeshan et al., 2006, Keeshan et al., 2010, Yokoyama et al., 2010, Yoshida et al., 2013). These adaptor proteins of which there are three family members, Tribbles 1 (TRIB1), Tribbles 2 (TRIB2) and Tribbles 3 (TRIB3), contain a highly conserved C-Terminal COP1 binding motif. TRIB1 and TRIB2 through their ability to bind both COP1 and C/EBPα mediate subsequent C/EBPα proteasomal degradation (Keeshan et al., 2006, Dedhia et al., 2010). TRIB1 and TRIB2 were identified to induce AML in murine models and this leukaemogenecity is dependent on their ability to bind COP1 (Keeshan et al., 2010, Yokoyama et al., 2010, Yoshida et al., 2013). Loss of COP1 binding, or COP1 activity through mutation of its active site, abrogated TRIB1 and TRIB2 ability to mediate ubiquitination and proteasomal degradation of C/EBPα (Yokoyama et al., 2010, Keeshan et al., 2010, Yoshida et al., 2013). TRIB1 and TRIB2 exert a differentiation block on myeloid cells inhibiting terminal differentiation through loss of C/EBPα protein expression (Keeshan et al., 2006, Yokoyama et al., 2010). TRIB3 does not induce AML nor does it induce proteasomal degradation of C/EBPα. Proteasomal degradation of C/EBPα in lung cancer cells has also been identified through TRIB2 adaptor binding however in this context TRIB2 was identified to bind TRIM21, another E3 ligase (Grandinetti et al., 2011). This report did not demonstrate bonafide ubiquitination of C/EBPα in this

context, however based on data identifying proteasomal inhibition rescued C/EBPα protein levels and E3 ligase requirement, it is highly likely TRIB2 mediates ubiquitin-dependent proteasomal degradation of C/EBPα in lung cancer cells via TRIM21 binding (Grandinetti et al., 2011). Thus direct association of C/EBPα with E3 ligases is not always a necessity for its mediated ubiquitination. Adaptor protein binding to C/EBPα also results in ubiquitination through the adaptor protein binding with an E3 ligase resulting in the formation of a multiprotein complex co-localising C/EBPα with an E3 ligase.

Ligase	Cell type	Effect	Reference
FBXW7	Adipocytes	-Recognise phosphodegron. P-Thr222/226 mediates ubiquitination and inhibits adipogenesis	(Bengoechea-Alonso and Ericsson, 2010)
E6AP	Adipocytes Leukaemic cells	-Directly binds C/EBPα mediating ubiquitin-dependent proteasomal degradation, inhibiting terminal differentiation of cells.	(Pal et al., 2013a) (Pal et al., 2013b)
TRIM21 Via TRIB2	Lung cancer cells	-Proteasomal degradation of C/EBPα.	(Grandinetti et al., 2011)
COP1 Via TRIB1	Leukaemic cells	-Ubiquitin-dependent proteasomal degradation of C/EBPα resulting in AML in murine models.	(Yokoyama et al., 2010) (Yoshida et al., 2013)
COP1 via TRIB2	Leukaemic cells	-Proteasomal degradation of C/EBPα resulting in AML in murine models.	(Keeshan et al., 2010)

Table 1.6.4 Ligases identified to date which mediate ubiquitination and/or proteasomal degradation of C/EBPα.

1.7 Tribbles as regulators of haematopoiesis and potent leukaemogenes

As mentioned previously there are three members of the tribbles family of proteins. TRIB1 and TRIB2 both induce proteolytic degradation of C/EBPα and induce AML in murine models and also have been identified to co-operate with Hoxa9 and Hoxa9/Meis1 leukaeamogenes (Keeshan et al., 2006, Jin et al., 2007, Keeshan et al., 2008, Yokoyama et al., 2010). Data mining using leukaemic genome atlas (LGA) has identified elevated *TRIB3* expression in AML harbouring t(15;17) and t(8;21) and in AML subtypes M2 and M3 but as of yet no leukaemogenecity has been attributed to TRIB3 (Dedhia et al., 2010, Liang et al., 2013). Thus this discussion will focus on TRIB1 and TRIB2 not TRIB3 as to date no reports suggest it elicits degradation of C/EBPα or AML in the murine models studied.

1.7.1 Tribbles functional classification and protein structure

TRIB proteins are classified as pseudokinase; while initial discoveries of TRIB1 and TRIB2 described them as phosphoproteins, to date no in vitro kinase assay has identified TRIB-mediated phosphate transfer (Boylan et al., 2003, Hegedus et al., 2007). Lack of detectable kinase activity is either attributable to the kinase having unique untested substrates or that it is a true pseudokinase (Wilkin et al., 1997, Großhans and Wieschaus, 2000, Manning et al., 2002). A pseudokinase is defined as a protein which has a kinase-like domain, but lacks conserved motifs that are necessary for catalytic activity. Pseudokinases are now classified as a family of proteins which are predicted to comprise 10 % of the human kinome, these proteins are present on multiple branches of the human kinase tree, suggesting that they evolved independently of active kinases with distinct cellular roles (Manning et al., 2002). TRIB proteins are structurally comprised of three regions: an N-Terminal region, a C-Terminal region and a central pseudokinase domain (**Fig 1.7.1**). The N-Terminal region is a short 60–80 amino-acid region which is proline- and serine-rich (PEST). Proteins containing PEST regions are indicative of proteins with short half-lives. TRIB1 and TRIB3 are proposed to possess N-Terminal nuclear localisation sequence motifs [K/R]2×2[D/E]X[D/E] as determined by PSORT a protein domain prediction software (Hegedus et al., 2007). In silico analysis of TRIB1 and TRIB2 using PredictNLSonline revealed TRIB2 does not possess a NLS however it does contain a nuclear exportation sequence (NES) within the kinase domain (Unpublished work, Ciaran Forde, Dr. Karen Keeshan). TRIB1 also contains a NES. However experimental validation of these predicted NLS and NES domains is required. The central pseudokinase domain of the tribbles family resembles that of a canonical kinase as they retain some hallmark characteristics of a functional kinase while lacking other critical motifs and residues (Hanks and Hunter, 1995). To date there is no published 3D structure for TRIB proteins. Tribbles

has the predicted three-dimensional structure of a kinase (SWISS-MODEL homology modelling) and retains a critical lysine for ATP binding however it lacks motifs required for ATP catalysis and ATP orientation (Hegedus et al., 2007). The C-Terminal region contains two motifs: a COP1 RING E3 ubiquitin ligase binding motif [D/E]QXVP[D/E] and a MEK1-binding motif IL(L/D)HPWF. Both the COP1 and MEK1 binding motifs are highly conserved in mammalian tribbles homologues (Qi et al., 2006, Yokoyama et al., 2010, Dedhia et al., 2010). The presence of these two distinct protein-binding sites hints at functionally diverse roles of tribbles despite their lack of apparent kinase activity. Control of cell signalling pathways provides a cell with ability to respond to its extracellular environment and to control, proliferation, differentiation, cell survival and apoptosis. TRIB1 was reported to bind MKK4 and TRIB3 was reported to bind MKK7 while both TRIB1 and TRIB3 were identified to bind MEK1 (Kiss-Toth et al., 2004). MAPK binding was suggested to stabilise TRIB proteins and subsequent modulation of MAPK signalling cascades (Kiss-Toth et al., 2004). Further studies identified all TRIB proteins 1, 2 and 3 were able to bind MEK1 and only TRIB1 interacted with MKK4 (Yokoyama et al., 2010). TRIB proteins have been reported to act as adaptor/scaffold proteins, either facilitating the assembly of multiprotein complexes which result in a phosphorylation change, or in the degradation of their target proteins, or alternatively as signalling modulators. A conundrum to date has existed in the definition of tribbles functionality; they have been both proposed to act as degradation-mediation proteins and signal mediators. Additionally TRIB proteins have also been classified as decoy kinases; they do not exert kinase-like activity but have been shown to impede the function of other kinases through obstructive binding. It appears TRIB functionality is largely dependent on the cell context studied and the specific interacting protein partner (Lohan and Keeshan, 2013).

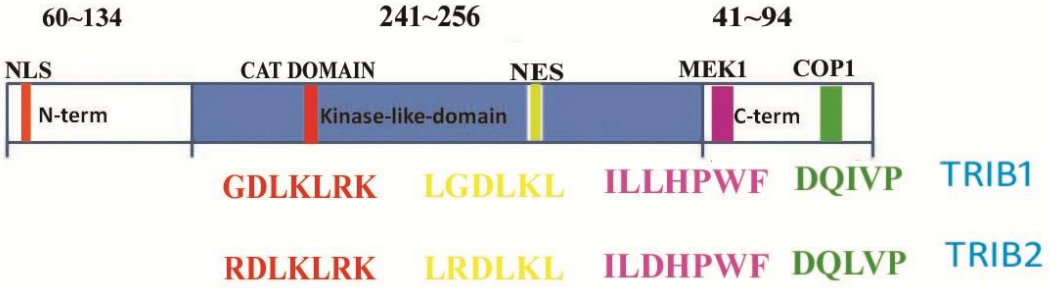

Fig 1.7.1 Schematic of TRIB1/2 highlighting the amino acid sequence of; TRIB1 unique NLS sequence highlighted in orange, the catalytic domain highlighted in red, NES highlighted in yellow, MEK1 binding domain highlighted in purple, COP1 binding domain highlighted in green. Amino acid length of N-terminus, kinase-like domain and C-Terminus is indicated above and the amino acid identify of the domains identified of TRIB1 and TRIB2 indicated below.

1.7.2 Tribbles in haematopoiesis and their association with leukaemic disease

Trib1

To date elevated *TRIB1* expression in leukaemic disease has only been reported in patients harbouring double minute (dmin) acentric chromatin bodies (Röthlisberger et al., 2007, Storlazzi et al., 2006). Dmin are frequent in AML, observed in ~1 % of cases and nearly always involve amplification of chromosome band 8q24 (Röthlisberger et al., 2007). Analyses of the amplicon produced showed that it contained the *MYC* locus however increased *MYC* transcription was not always identified in AML patients who harbour dmins indicating it was not the target gene of the amplification (Storlazzi et al., 2006, Röthlisberger et al., 2007). *TRIB1* is also encompassed in this amplicon and was identified to be elevated in a subset of AMLs and MDS patients presenting with dmins (Storlazzi et al., 2006, Röthlisberger et al., 2007).

TRIB1 was first discovered as a co-operating leukaemogene in BMT models investigating retroviral insertion sites of oncogenic fusion gene *Hoxa9-Meis1* (Jin et al., 2007). *Hoxa9-Meis1* insertion increased *Trib1* expression levels and combining *Hoxa9-Meis1* and *Trib1* in BMT models showed a reduced latency of *Hoxa9-Meis1*-induced AML (Jin et al., 2007). Additionally Trib1 expression was identified to mediate an increase in levels of P-ERK1/2 in bone marrow and leukaemic cells, providing an example of TRIB functionality as signalling modulators (Jin et al., 2007). TRIB1 expression was also identified to protect against apoptosis upon IL-3 withdrawal (Jin et al., 2007). Further BMT models revealed Trib1 expression alone was sufficient to induce murine AML and Trib1 was indeed a potent leukaemogene (Yokoyama et al., 2010). Trib1 leukaemogenecity was intrinsically linked to its ability to bind MEK1, as MEK1 binding mutants lost the ability to induce AML (Yokoyama et al., 2010). Additionally Trib1-mediated increase in P-ERK1/2 previously observed was also identified to be dependent on MEK1 binding (Jin et al., 2007, Yokoyama et al., 2010). Trib1 was identified to bind C/EBPα and mediate proteasomal degradation of C/EBPαp42 (Yokoyama et al., 2010). However investigation by Dedhia et al did not observe any increase in P-ERK1/2 in response to Trib1 expression in 32Dcl3 cell (Dedhia et al., 2010). Trib1 did mediate degradation of C/EBPα and inhibited C/EBPα driven differentiation in response to G-CSF (Dedhia et al., 2010). This study undermines the MAPK involvement in Trib1 induced AML however it further supports the crucial role of C/EBPα mediated degradation.

In an attempt to identify the C/EBPα binding site on TRIB1 a series of deletion constructs were made and their ability to bind C/EBPα was assessed, deletion of the N-Terminal region and part of the kinase-like domain of TRIB1 abrogated its ability to interact with C/EBPα (Yokoyama et al.,

2010). However this N-Terminal deletion construct investigated was 180 amino acids shorter than WT-TRIB1 and may not retain the crucial tertiary structure of a protein required for the sterically complex interaction between two proteins during binding and additionally may alter cellular localisation. MEK1 binding was also observed to be a requisite for TRIB1 mediated degradation of C/EBPαp42, however the increase in P-ERK1/2 levels mediated by MEK1/TRIB1 did not result in an increase in P-Ser21 C/EBPα levels (Yokoyama et al., 2010). Loss of COP1 binding site on TRIB1 inhibited TRIB1-mediated degradation of C/EBPα indicating COP1 E3 ligase involvement in C/EBPα degradation (Yokoyama et al., 2010). Analysis of Down syndrome AML patients identified the existence of a TRIB1-R107L mutation which was proposed to be an early event in leukaemogenesis as it was retained in bone marrow cells during remission and was not identified in non-haematopoietic cell DNA (Yokoyama et al., 2012). Molecular characterisation of this mutant revealed it decreased the latency of TRIB1 induced AML in BMT models and enhanced TRIB1-mediated increase in P-ERK1/2 and enhanced C/EBPα degradation (Yokoyama et al., 2012).

TRIB1 plays a crucial role in regulation of myeloid cell differentiation during normal haematopoiesis (Satoh et al., 2013). *Trib1* knockout (*Trib1*$^{-/-}$) mice had decreased levels of M2-tissue resident macrophages, an absence of eosinophils and increased granulocytes and neutrophils within their spleenic tissue (Satoh et al., 2013). Reversal of differentiation effects observed in colony forming assays was achieved by ectopic WT-*Trib1* expression in *Trib1*$^{-/-}$ bone marrow cells which resulted in a decrease in C/EBPα expression (Satoh et al., 2013). Ectopic expression of TRIB1ΔCOP1 did not rescue the haematopoietic deficient phenotypes or decrease C/EBPα expression (Satoh et al., 2013). Knockdown of *C/EBPα* expression in *Trib1*$^{-/-}$ cells abrogated *Trib1*$^{-/-}$ effects validating that the haematopoietic defects resulting from loss of *Trib1* expression are attributable to increased C/EBPα levels (Satoh et al., 2013). Interestingly the authors noted a decrease in IL-10 production in adipose tissue of *Trib1*$^{-/-}$ mice, and as mentioned previously C/EBPα represses IL-10 production via promoter binding and this inhibitory effect was relieved by P-Ser21 (Kang et al., 2013, Satoh et al., 2013). Investigations by Liu et al showed that knockdown of *Trib1* expression in macrophage cells altered their morphology and their migratory behaviour (Liu et al., 2013). Liang et al investigated *TRIB1* expression using LGA platform in different AML FAB subtypes and showed a significant increase in *TRIB1* expression levels in FAB subtypes M4 and M5 and also in patients with karyotypic abnormalities involving chromosome 16 (Liang et al., 2013). Liang et al also investigated *TRIB1* expression in normal physiological conditions and identified *TRIB1* expression was significantly increase in granulocyte/monocyte and B-Cell

lineages supporting the observed effects of *Trib1* knockout animal models discussed above (Liang et al., 2013).

Trib2

TRIB2 was initially discovered as a transcript down-regulated upon inhibition of NOTCH1 signalling in a T-ALL cell line, and it was further validated as a direct transcription target of NOTCH1 upon identification of NOTCH1 binding to the *TRIB2* promoter (Wouters et al., 2007). NOTCH1 is found mutated in 50% of T-ALLs resulting in aberrant signalling and activation of downstream signalling cascades (Weng et al., 2004). *TRIB2* was also identified as a PITX1 gene target. PITX1 is recurrently activated in T-ALL via chromosome 5 deletion (Nagel et al., 2011). TRIB2 was reported to be essential for T-ALL cell survival; leukaemic transformation resulting in upregulation of TAL1 protects TRIB2 from Ebox proteins which are proposed to have a repressive effect on TRIB2 (Sanda et al., 2012). Additionally elevated *TRIB2* expression is correlated with NOTCH1 activation, resulting from either gain of function NOTCH1 mutations or loss of function FBXW7 mutations, in a cohort of T-ALL paediatric patients (Hannon et al., 2012). Analysis of *TRIB2* mRNA expression in AML FAB subtypes revealed *TRIB2* expression is generally low albeit increased expression was observed in FAB subtypes M0 and M3 (Liang et al., 2013). Analyses of *TRIB2* mRNA expression across 16 acute and chronic leukaemic subtypes from the MILE study identified a statistically significant increase in *TRIB2* expression in T-ALLs specifically in patients with normal karyotypes and t(1;19) (Hannon et al., 2012). Further expression analysis identified genes associated with high *TRIB2* expression in ALL were involved in T-cell and NOTCH1 signalling (Hannon et al., 2012). Analysis of *TRIB2* mRNA expression during normal haematopoiesis (**Fig 1.7.3**) revealed *TRIB2* expression is highest in T-cells, specifically $CD4^+$ T-cells supporting the associations observed between *TRIB2*, T-cell leukaemogenes and T-cell leukaemias and suggesting TRIB2 is involved in T-cell biology (Hannon et al., 2012, Liang et al., 2013). B-Cells and MEPS were also identified to express high levels of *TRIB2* mRNA (Hannon et al., 2012) (**Fig 1.7.3**). Studies on knockout Trib2 mice showed that loss of *Trib2* expression resulted in diminished levels of red blood cells indicating TRIB2 may also be crucial for normal erythropoiesis (ASH conference 2013 poster (Li et al., 2013). Indeed Fog1 and Gata1, megakaryocyte and erythroid governing transcription factors, have been identified to bind the *Trib2* promoter (Mancini et al., 2012). Knockout of Fog1 in preMegEs (bi-potential cells capable of forming megakaryocyte or erythroid lineages but not myeloid) resulted in a myeloid cell fate through upregulation of myeloid cell regulators (Mancini et al., 2012). Knockout of Fog1 decreased

Trib2 expression implicating a crucial role for TRIB2 in megakaryocyte and erythroid cell lineage commitment (Mancini et al., 2012).

TRIB2 was the first member of the TRIB family to be classified as a leukaemogene. Its overexpression drives fully penetrant transplantable AML in BMT models (Keeshan et al., 2006). In these murine models Trib2 overexpression induces a myeloid leukaemic disease exclusively, phenotypically presenting as $CD11b^{intermediate}$/ $Gr\text{-}1^{low}$ which is a profile characteristic of immature myeloid cells and indicative of murine myeloid leukaemias (Keeshan et al., 2006). *TRIB2* mRNA expression was shown to steadily increases as cells commit to the myeloid lineage; an increase in expression is detectible from HSC to CMP to GMP to granulocytes (Hannon et al., 2012) (**Fig 1.7.3**). While as mentioned above *TRIB2* expression has been reported to associate with human T-ALL disease and also implicated in MEP differentiation, analysis of *TRIB2* expression in 285 human AML patients (VALK dataset) revealed elevated *TRIB2* expression clustered with a cohort of patients who displayed a mixed myeloid/lymphoid phenotype (cluster 4) (Valk et al., 2004, Keeshan et al., 2006, Wouters et al., 2007) These patients identified in cluster 4 had elevated levels of T-cell signature genes including CD7 while also expressing $CD34^{+}$ an immature cell marker (Wouters et al., 2007). Gene expression profiling of patients in cluster 4 identified a dysregulated C/EBPα gene expression signature, despite a subgroup of patients possessing no C/EBPα mutations. Patients harbouring C/EBPα mutations displayed high levels of C/EBPα expression while WT-C/EBPα patients had very low or no C/EBPα expression (Wouters et al., 2007). Elevated *TRIB2* levels were identified in patients with no C/EBPα mutations (Keeshan et al., 2006).

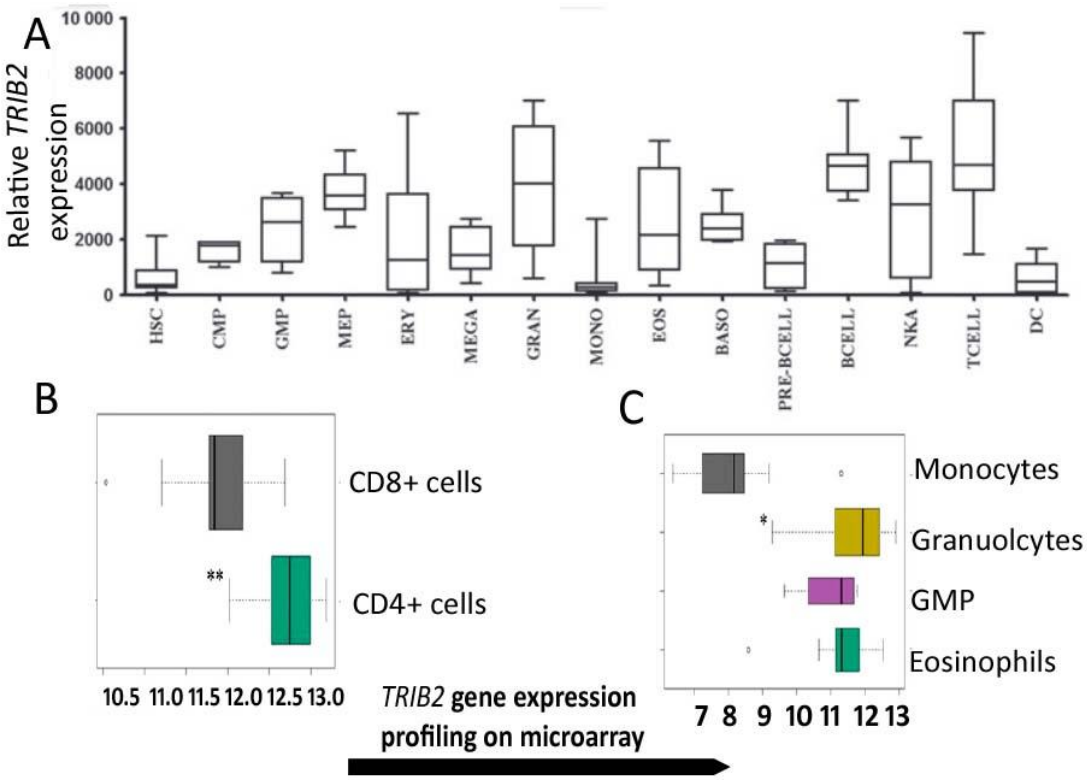

Fig 1.7.3 Profiling *TRIB2* mRNA expression during normal human haematopoiesis from dataset published by (Novershtern et al., 2011). **A)** *TRIB2* expression across multiple haematopoietic lineages adapted from (Hannon et al., 2012) the intersecting line in boxplot represents mean expression while maximum and minimum whiskers represent range in expression. **B)** *TRIB2* expression analysed by LGA in $CD8^+$ and $CD4^+$ T-cells adapted from (Liang et al., 2013). **C**) *TRIB2* expression analysed by LGA in monocytes, granulocytes, GMP and eosinophils adapted from (Liang et al., 2013).

The dysregulated C/EBPα signature and low expression levels of WT-C/EBPα patients may be explained by the TRIB2-mediated proteasomal degradation of C/EBPα, (Keeshan et al., 2006). Additionally the T-lymphoid phenotype of these leukaemic cells may also be attributed to elevated TRIB2 expression due to its association with T-cell gene expression. *TRIB1* levels were decreased with elevated *TRIB2* in this cohort of patients indicating distinct modalities for TRIB1 and TRIB2 induced AML (Keeshan et al., 2006). TRIB2 also co-operates with Hoxa9 and *Nup98-Hoxd13-Meis1* fusion gene reducing the latency of AML in BMT models (Argiropoulos et al., 2008, Keeshan et al., 2008). *Hox* genes are common retroviral integration sites in murine myeloid and are crucial mediators of haematopoiesis reviewed by (Alharbi et al., 2012). Trib2 was identified as an insertion site in the *Hoxa9* gene locus, mediating increased *Hoxa9* expression. Indeed *Hoxa9* was identified to co-operate with Trib2 to rapidly accelerate the onset of Trib2 induced AML in BMT

models by ~100 days (Keeshan et al., 2008). *Meis 1* was identified to directly increase *Trib2* expression via occupancy on the *Trib2* promoter facilitating *Trib2* and *Nup98-Hoxd13-Meis1* co-operation during leukaemogenesis (Argiropoulos et al., 2008).

Structural analysis of the Trib2 protein revealed its leukaemogenecity is dependent on an intact kinase-like domain and its C-Terminal COP1 binding site (Keeshan et al., 2010). Deletion of TRIB2 N-Terminal domain does not abrogate the ability of Trib2 to mediate proteasomal degradation of C/EBPα or to inhibit myeloid cell differentiation. Mutation of the Trib2 kinase-like domain to resemble a canonical kinase (TRIB2-KDM) inhibited the proteolytic effect of Trib2 on C/EBPα and also abrogated its ability to induce AML in BMT models (Karen Keeshan unpublished data and (Keeshan et al., 2010). Mutation of a lysine which is a hallmark of a serine/threonine (ser/thr) kinases within the kinase-like domain of Trib2 to resemble a tyrosine kinase (K177R), was performed to assess if Trib2 possessed any ser/thr kinase activity. Trib2-K177R also abrogated the ability of TRIB2 to degrade C/EBPα and to induce AML (Karen Keeshan unpublished data and (Keeshan et al., 2010). Therefore, while no kinase activity has yet been attributed to TRIB2 perhaps modulation of these amino acids within the kinase-like domain may have major ramifications on its protein structure hence altering its protein-protein interactions. TRIB2 modulation of signalling has been implicated in the immune response through mediation of Toll like receptor (TLR) signalling. TRIB2 was shown to negatively regulate TLR5-mediated activation of NFκB (Wei et al., 2012). This inhibition was attributed to TRIB2 binding directly to NFκB2 decreasing the activity of NFκB2 (p100) (Wei et al., 2012). Indeed, TRIB2 knockdown results in a decrease in TLR mediated phosphorylation of JNK and p38, but not ERK1/2 and knockdown of TRIB2 in macrophages resulted in increased levels of p65 and inhibitor of NFκBα and β (iKKα) and (iKKβ) phosphorylation (Wei et al., 2012). TRIB2 is also induced by TLR5 and this feedback loop contributes to TRIB2-mediated control of the immune response (Wei et al., 2012).

A prominent role for TRIB2 is now emerging as a modulator of cell cycle and proliferation, providing leukaemic cells with increased proliferative advantage (Rishi et al., 2014). Indeed knockdown of TRIB2 expression in leukaemic cells results in a decrease in cell proliferation, an increase in cells paused in G1 with a concomitant increase in apoptosis and cell death indicating a requirement for TRIB2 expression (Rishi et al., 2014). Additionally in Drosophila dTrbl mediates proteasomal degradation of dString/CD25C pausing the cell cycle at the G2/M transition during morphogenesis and gastrulation (Mata et al., 2000). Mammalian conservation of this relationship is currently under investigation in our group. *TRIB2* expression was identified to be directly regulated by E2F1, the master cell cycle regulator (Rishi et al., 2014). E2F1 along with transcriptional

activator family members E2F2, E2F3 were identified to bind the *TRIB2* promoter increasing *TRIB2* expression (Rishi et al., 2014). C/EBPαp42 as mentioned previously elicits a pause in the cell cycle through repression of E2F1 and *C-MYC* transcription. C/EBPαp30 lacks the N-Terminal domain required for this interaction (Johansen et al., 2001, D'Alo et al., 2003). Under normal haematopoietic conditions C/EBPαp42 was identified bound to the TRIB2 promoter via a C/EBP binding site, repressing *TRIB2* expression in GMPs (Rishi et al., 2014). Upon TRIB2-mediated disruption of the C/EBPα42/p30 ratio elevated levels of C/EBPαp30 resulted in an increase in C/EBPαp30 binding to the *TRIB2* promoter, which was identified to co-operate with E2F1 and enhance *TRIB2* expression (Keeshan et al., 2006, Rishi et al., 2014). Indeed pharmacological inhibition of the cell cycle in leukaemic cells resulted in a decrease in E2F1 levels and an associating decrease in TRIB2 levels (Rishi et al., 2014). Pharmacological inhibition of the cell cycle in normal WT and Trib2 knockout bone marrow cells revealed very little cytotoxicity, providing evidence to suggest that targeting this pathway may be a viable option to inhibit the acquired proliferative advantage of leukaemic cells (Rishi et al., 2014).

To date several microRNAs have been identified to modulate *TRIB2* expression. miR-99 decreases *TRIB2* expression and inhibits cervical carcinoma cell proliferation (Xin et al., 2013). miR-511 and miR-1297 also downregulate *TRIB2* expression with an increase in C/EBPα protein expression observed (Zhang et al., 2012a). Overexpression of miR-511 and miR-1297 inhibits adenocarcinoma cell proliferation and increases apoptosis (Zhang et al., 2012b). Thus far two miRNAs have been identified to modulate *TRIB2* expression in haematopoietic cells miR-155 and miR-100 (Zheng et al., 2012, Palma et al., 2014). MiRNAs are multifunctional short stretches of noncoding RNA; miR-155 is upregulated in HSCs, GMPs, granulocytes and macrophages and is required for normal haematopoietic cell maturation (Rodriguez et al., 2007). MiR-155 has been reported to be elevated in AML associated with FLT3-ITD and downregulated in AML with inv(16) thus its functional effects remain largely speculative (Jongen-Lavrencic et al., 2008, Faraoni et al., 2012). Overexpression of miR-155 was identified to upregulate *TRIB2* expression and was also identified to promote differentiation of AML with an associating increasing in Caspase-3 dependent apoptosis (Palma et al., 2014). Induction of myeloid differentiation was reported to be independent of *C/EBPα* as no increase in mRNA levels was observed (Palma et al., 2014). It was proposed that induction of differentiation is occurring through an alternate pathway to that mediated by *C/EBPα* expression as there was no change in expression observed and the increase in *TRIB2* levels is contradictory to induction of myeloid maturation (Palma et al., 2014).

To date TRIB2 and to a large extent TRIB1 leukaemogenecity is inextricable linked to inactivation of C/EBPα. Perhaps overexpression of TRIB proteins may be classified as a type I mutation (as loss of TRIB2 expression inhibits cellular proliferation) and subsequent inactivation of C/EBPα resulting in inhibition of differentiation acts as a class II mutation fitting the Gilliland two hit model of leukaemogenesis (Kelly and Gilliland, 2003).

1.8.1 Ubiquitin proteasome system

The ubiquitin proteasome system (UPS) is the main protein proteolysis pathway in eukaryotic cells (Hershko et al., 2000). Ubiquitination involves the hierarchical sequential action of three ubiquitin enzymes; E1, E2 and E3 resulting in degradation performed by the proteasome, a nonspecific protease. Specificity is applied by the action of the three ubiquitin enzymes.

The actions of E1 at the beginning of the cascade are required for activation of the 76 amino acid ubiquitin moiety and its transfer to the E2 enzyme. To date the functions of the E1 enzyme are the most characterised of the whole UPS system (Kleiger and Mayor, 2014). E1 activation of ubiquitin and transfer to E2 is a multistep ATP-dependent process involving; the adenylation of the ubiquitin C-terminus, the formation of a thioester bond between the C-Terminus of ubiquitin and the E1 catalytic cysteine residue in its active site and the subsequent transfer of ubiquitin from E1 to E2's catalytic cysteine residue (Kleiger and Mayor, 2014). The absolute requirement for E1 activity was identified upon chemical inhibition of E1 resulting in almost immediate shutdown of the UPS (Yang et al., 2007). In order for E1 to bind both ubiquitin and deliver it to E2 a high degree of rapid protein flexibility is required (Huang et al., 2007). Additionally E1 enzymes must recognise 40 human E2 ligases. Structural analysis revealed E1 is capable of multiple domain rearrangements and shows no apparent selectivity for E2 binding as the rate of ubiquitin transfer is similar for different E2 proteins (Tokgoz et al., 2012).

The next step of UPS involves E3 ubiquitin ligases. E3 ligases function like adaptor or protein scaffolds mediating co-localisation of the substrate protein and the E2-ubiquitin adduct and the subsequent ubiquitin transfer to the lysine side chain of the amino terminus of the substrate protein. E3 ligases may accelerate the rate of ubiquitin transfer however catalysis of the reaction is dependent on the E2 enzyme (Ohta et al., 1999). Upon formation of the E2-ubiquitin thioester linkage the conformational location of this linkage against particular E2 interphases optimises ubiquitin transfer (Pruneda et al., 2011). E3 ligases may accelerate the transfer by acting to stabilise the E2-ubiqutin-E3 complex. Indeed E3 ligases possessing a really interesting new gene (RING) domain recruit E2-ubiqutin adducts (Plechanovova et al., 2012). In such circumstances, ubiquitin

contacts E3 RING ligase resulting in stabilisation of the interaction. Alternatively phosphorylation of residues neighbouring the RING domain have been identified to further aid ubiquitin binding (Dou et al., 2013). Not all E3 ligases possess RING domain, some possess HECT domains, the molecular mechanism for ubiquitination with such ligases varies greatly from that of RING E3 ligases. HECT E3 ligase require an additional trans-thioesterification step, ubiquitin is first transferred from E2 to E3 before its conjugation to the substrate protein. HECT domains are comprised of two lobes an N-Terminal lobe and a C-Terminal lobe separated by a linker region. The E3 ligase's N-lobe binds E2~ubiquitin adduct and ubiquitin is then transferred from the E2 to the catalytic cysteine of the C-lobe of the E3 ligase. The C-lobe then undergoes a 130 degree rotation about a linker region to juxtapose E2~Ubiquitin and the ubiquitination target site (usually a lysine residue) on the substrate protein to facilitate ubiquitin transfer (reviewed by (Kamadurai et al., 2013)).

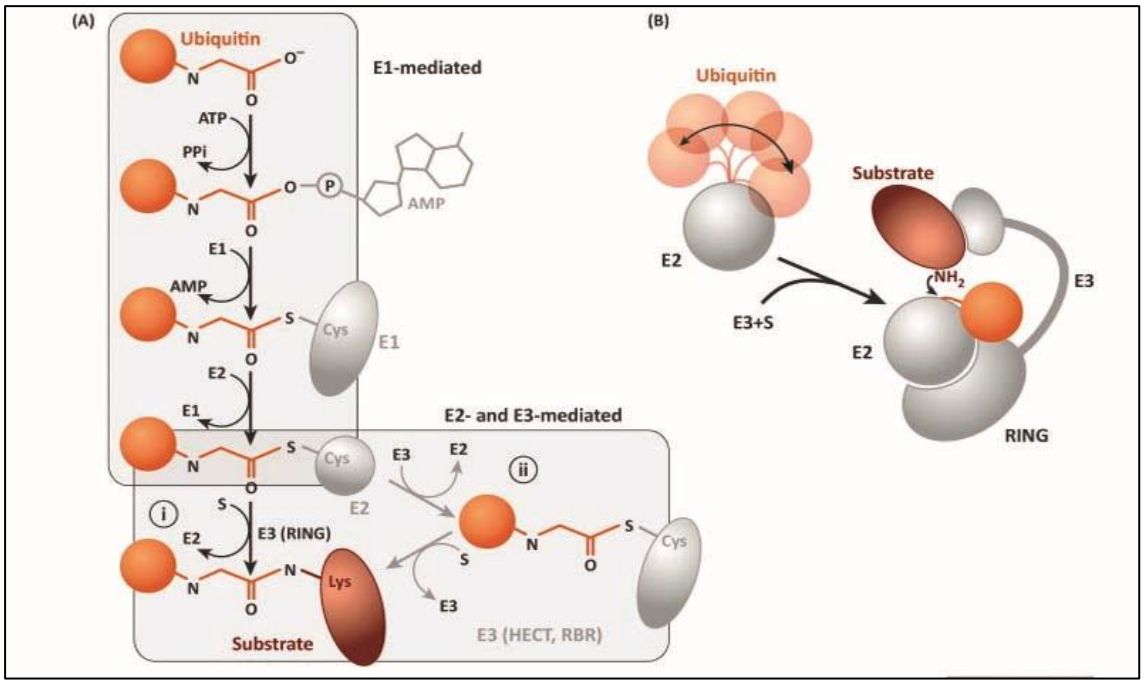

Fig 1.8.1 Mechanism of ubiquitination A) Schematic representation of the chain of E1, E2 and E3 mediated events during ubiquitination. ATP-dependent activation of ubiquitin following adenylation of C-Terminus of ubiquitin producing an E1-ubiqutin adducts. E2 ubiquitin conjugating enzyme receives ubiquitin from E1 and forms a thioester bond with a cysteine residue in its active site. E3 ligase is responsible for conjugation of ubiquitin to target protein. **B)** Model of RING E3

ligase mediated conjugation of ubiquitin to substrate protein adapted from (Kleiger and Mayor, 2014).

E2 enzymes have been identified to function maximally only when in the presence of E3 ligases. This is proposed to occur to prevent the high cellular concentrations of E2-ubiqutin from ubiquitinating non target substrate proteins (Kleiger and Mayor, 2014). In order for a protein to be targeted for proteasomal degradation by its ubiquitin linkers it requires the attachment of at least 4 ubiquitin moieties. Upon transfer of the first ubiquitin to substrate protein the rate of substrate dissociation is sufficiently slow to allow ubiquitin chain formation. Ubiquitination and subsequent proteasomal degradation of regulatory proteins is a rapid process providing abrupt termination to effects propagated, however ubiquitination also serves to degrade misfolded proteins for protein quality control purposes (Pierce et al., 2009, Comyn et al., 2014). In some instances a protein may acquire the correct fold when provided with time, the lack of consensus E3 ligase motifs is proposed to slow polyubiquitination providing time for correct conformational folding. Once the ubiquitinated protein dissociates from the E3 ligase it is exposed to, deubiquitination enzymes (DUBs) that remove and edit ubiquitin polychains. Some DUBs associate with the proteasome (the final resting place of degradation ubiquitin linked proteins), and are proposed to enable efficient proteolysis by removing the ubiquitin motifs facilitating their proteasomal processing (Kleiger and Mayor, 2014). Several types of ubiquitination chains may be produced through the identity of the lysine in ubiquitin which forms the linkage e.g. K6, K11, K27, K29, K33, K48 and K63. K48 polyubiquitination targets the substrate protein for degradation while alternative ubiquitination chains are increasingly being identified with distinct molecular roles (discussed in greater detail in Chapter 4).

1.8.2 The 26S proteasome

The 26S proteasome a highly dynamic holocomplex, of 2.5mDA size, comprised of two multisubunit components, the 20S subunit and its regulatory subunit the 19S (**Fig 1.8.2**). Only recently has the structure of the 26S proteasome been described in detail using electron microscopy based approaches reviewed by (Förster et al., 2013). The 20S subunit is arranged in a hollow cylindrical structure with the proteolytic active subunits facing in (Peters et al., 1993). Within this, protein proteolysis occurs. The ends of the 20S barrel are gated by the 19S regulatory subunits. Ubiquitinated proteins dock on the 19S subunit through binding proteasome receptors Rpn13, Rpn10 (Zhou et al., 2013). The Rpn11 subunit then cleaves the ubiquitin polychain from the substrate protein enabling recycling of the ubiquitin proteins and reducing the size of the substrate protein, which now enters the 20S core (**Fig 1.8.2**).

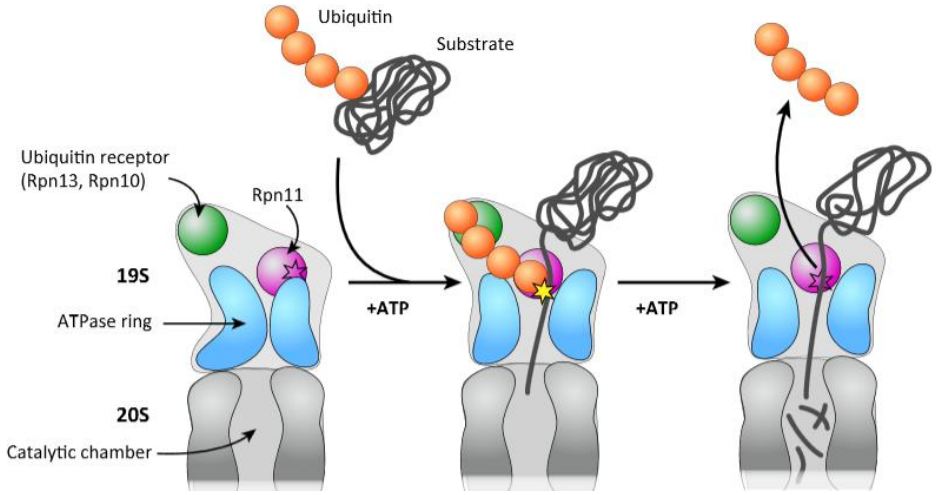

Fig 1.8.2 Schematic of ubiquitinated protein proteolysis at the 26S proteasome. The grey chambers represent the 20S core, the blue chambers represent the 19S regulatory subunit. Rpn10/13 are represented in green and Rpn11 is pink. Upon ubiquitinated-protein binding to Rpn10/13, alterations to the 19S conformation permit entry of unfolded and deubiquitinated protein after the actions of Rpn11. The protein is then passed into 20S core in an ATP dependent manner adapted from (Kleiger and Mayor, 2014).

1.8.3 Proteasome inhibitors as chemotherapeutic agents

Loss of apoptosis (cellular suicide), is one of the major causes of tumourigenesis. The UPS is a crucial modulator of cell cycle, proliferation and apoptosis. Indeed disruption of the UPS is increasingly being associated with neoplastic disease. Aberrant activation of NOTCH1 signalling observed in T-ALL is often due to loss of function mutations in FBXW7 an E3 ligase. The first food and drug administration (FDA) approved inhibitor of the UPS, Bortezomib, which targets the proteasome is used in the treatment of refractory multiple myeloma and currently in phase II and phase III trials as a potential treatment for B-cell lymphoma and follicular non-Hodgkin's lymphoma (Richardson et al., 2006, Kane et al., 2007). Carfilzomib a mechanistically and structurally distinct proteasome inhibitor has been reported to induce cell cycle arrest, apoptosis and displays sensitivity against Bortezomib resistant disease (Kuhn et al., 2007, Rentsch et al., 2013). The promising results of these proteasome inhibitors has fuelled the search for other antagonists of the UPS (reviewed by (Zhang and Sidhu, 2014)). An allosteric E2 inhibitor has been identified which is able to inhibit ubiquitination of cell cycle regulators leading to inhibition of proliferation human cancer cells (Ceccarelli et al., 2011). Ubistatins have been described which bind to the K48 ubiquitin polychain disrupting the conformation of ubiquitin polychains and affecting proteasome receptor binding of K48 ubiquitinated proteins (Verma et al., 2004). Ubistatins have a strong

negative charge and are not cell permeable however they represent another promising emerging therapeutic agent (Nalepa et al., 2006).

Aims of this project

TRIB2 possesses potent murine leukaemogenic potential and has also been shown to be elevated in cohorts of AML patients. Trib2 was previously identified to mediate murine AML via its proteolytic effect on C/EBPα, a crucial regulator of haematopoiesis frequently identified mutated in patient AML. The aims of this project were to determine the mode by which TRIB2-mediated the degradation of C/EBPα and to investigate the proteolytic requirement for direct TRIB2-C/EBPα interaction through elucidation of the direct regions of C/EBPα interaction on TRIB2. TRIB2 is classified as a pseudokinase as it lacks kinase function despite possessing some hallmark of kinase characteristics. The aims of this work were to investigate TRIB2 functionally required regions and their effect on C/EBPα. TRIB2 is classified as an adaptor protein facilitating the formation of multiprotein complexes which mediate proteasomal degradation and modulation of cell signalling cascades. Phosphorylation of C/EBPα exerts differing differentiation inhibiting effects on C/EBPα function, governed by the action of upstream kinases. This work investigates TRIB2 effects on C/EBPα phosphorylation and attempts to further define the role of TRIB2 as an adaptor protein. Improvement of AML survival rates has stalled during the last decade owing to limited knowledge of the vastly heterogeneous nature of the disease and a subsequent lack of targeted therapies. Through increased knowledge of TRIB2-mediated disease this study aims to identify a potential therapy to target TRIB2-mediated AML. This research was conducted using peptide array technology, in vivo binding, ubiquitination and drug cytotoxicity assays. The therapeutic effect of TRIB2 overexpression on the leukaemic cell and on AML patient cell biology was explored by measuring the in vitro response to proteasome inhibition.

Chapter 2: Materials and Methods

2.1 Materials

2.1.1 General Chemicals and Reagents

All salts and reagents including protease and phosphatase inhibitors were purchased from Sigma-Aldrich unless otherwise stated. Protein G-Sepharose Fast Flow 4 Beads and Nitrocellulose membrane were procured from GE Life Sciences, United Kingdom (UK). Prestained molecular weight protein markers and chemiluminescent Clarity ^{TM} Western ECL substrate detection kit for Chemidoc^{TM} XRS$_{+}$ system were purchased from Biorad Laboratories, UK. Bradford protein quantification solution, Immunoblot stripping buffer, CL-XPosure Film, Ponceau S Solution, chemiluminescent detection kits ECL Pico and Femto were purchased from Thermo Scientific, UK. Restriction enzymes were purchased from New England Biolabs, UK. Purified C/EBPα protein was purchased from Genway, United States of America (USA). Bortezomib was purchased from LC Labs, USA. Peptide arrays and specific alanine scanning substitution arrays (SASSA) were generated by Dr. Patrick Kiely, University of Limerick.

2.1.2 Molecular Biology Reagents

2.1.2.1 Immunoblotting antibodies

Antibody	**Clone**	**Species**	**Incubation**	**Blocking Soln.**	**Dilution**	**Company**
TRIB2 sc-100878	B-06	Mouse	Overnight	5% milk	1:250	Santa Cruz
C/EBPα sc-61	14AA	Rabbit	1 hr at RT (O/E) Overnight (E/N)	5% milk	1:2000 (O/E)* 1:114 (E/N)**	Santa Cruz
C/EBPαX sc-61X	14AA	Rabbit	Overnight CO-Immuno precipitation	-	5µg per Immuno-precipitation	Santa Cruz
Myc-tag	9E10	Mouse	Overnight	5% milk	1:250	Homemade
P-Ser21 C/EBPα 2841	No clone number	Rabbit	Overnight	5% BSA	1:500 (E/N) 1:1000(O/E)	Cell Signaling

P-Thr222/ 226 C/EBPα 2844	No clone number	Rabbit	Overnigh	5 % BSA	1:500 (E/N) 1:1000 (O/E)	Cell Signaling
Actin A5441	AC-15	Mouse	Overnight/ 1 hr RT	5% Milk	1:2500	Sigma
HA H9658	HA-7	Mouse	Overnight	5% Milk	1:1000	Sigma
K48-Ubiquitin 05-1307	APU-2	Rabbit	Overnight	5% Milk	1:1000	Millipore
K63-Ubiquitin 05-1308	APU-3	Rabbit	Overnight	5% Milk	1:1000	Millipore
P-ERK1/2 4695s	D13.1.4 E	Rabbit	Overnight	5% BSA	1:2000	Cell Signaling
ERK1/2 4370s	137F5	Rabbit	Overnight	5% BSA	1:2000	Cell Signaling

*O/E-overexpression, ** E/N-Endogenous, RT-room temperature

2.1.2.2 FACS antibodies

Antibody	**Clone**	**Fluorophore**	**Incubation**	**Dilution**	**Company**
Annexin V 556422 550475	No clone number	PE APC	15 mins RT	1:100	BD
Cd14 557700	M5E2	PE	30 mins 4°C	1:100	BD
Cd15 560827	H198	PECY7	30 mins 4°C	1:100	BD
Cd11b	M1/70	PE	30 mins	1:100	BD

557397 553312 553310		APC FITC	4°C		
Cd34 345803	8G12	PE CY	30 mins 4°C	1:100	BD

2.1.2.3 Cell lines

Human embryonic kidney (HEK) 293t cells (ATCC) were maintained in Dulbecco Modified Eagle Medium (DMEM) (Invitrogen) supplemented with 10 % Fetal Bovine Serum (FBS) (Invitrogen), 12 μM L-glutamine, 100 U/mL penicillin and 100 μg/mL streptomycin (Invitrogen). U937 cells (a kind gift Dr. Martin Carroll) were maintained in rpmI 1640 medium supplemented with 10 % FBS, 12 μM L-glutamine, 100 U/mL penicillin and 100 μg/mL streptomycin. NIH-3T3 fibroblast cells were maintained in DMEM supplemented with 10 % Cosmic (Invitrogen), 12 μM L–glutamine, 100 U/mL penicillin and 100 μg/mL streptomycin. Cells were maintained in culture for no longer than three months and were routinely tested for mycoplasma infection using MycoAlert Mycoplasma detection kit purchased from Lonza (Dublin, Ireland).

2.1.2.4 Plasmid Sources

Expression constructs murine (m) TRIB2-pcDNA3.1, mTRIB2-VPM-pcDNA3.1, mTRIB2-KDM-pcDNA3.1, rat (r) C/EBPα-pcDNA3.1–Myc-His (PHMA), MigR1-eGFP, mTRIB2-MigR1-eGFP and mTRIB2-VPM-MigR1-eGFP were described previously (Keeshan et al., 2006, Keeshan et al., 2010). See PHMA and MIGR1 backbone vector maps below (**Fig 2.1.2.4 A, B and C**). Retroviral packaging plasmids pCPg and envelope encoding VSVg were used in order to produce retrovirus using respective retroviral expression vectors (**Fig 2.1.2.4 D and E)**. Ubiquitin (Ub) - haemagluttin (HA), Ubiquitin mutant K48R-HA and Ubiquitin mutant K63R-HA were kind gifts from Dr. R. J. Carmody, University of Glasgow. mC/EBPα-S21D-pcDNA3, mC/EBPα-S21A-pcDNA3, mC/EBPα-S21D-ER-IRES-MSCV-eGFP and mC/EBPα-S21A-ER-IRES-MSCV-eGFP were kind gifts from Dr. D. Tenen, Harvard Medical School and described previously (Ross et al., 2004). mTRIB2 mutants R77A, S227A/S229A/S231A/K233A and K322A with a N-Terminus fused FLAG tag were created in PHMA expression vector by GenScript, USA. rC/EBPα mutant K313R noSTOP-myc in PHMA expression vector was generated by GenScript, USA. C/EBPα mutants R333A, R393A and R343A-HA-PHMA were previously generated in the laboratory by C. Forde using SDM primers (eurofins MWG operon) outlined below. Complete list of plasmids used see table below (**Table 2.1.2.4 A**).

Primer	Sequence
R333A forward	5’GTG GAA CAG CTG AGC GCT GAA CTG GAC ACG CT 3’
R333A reverse	5’AGC GTG TCC AGT TCA GCG CTC AGC TGT TCC AC 3’
R339A forward	5’AAC TGG ACA CGC TGG CGG GTA 5’TCT TCC GCC 3’
R339A reverse	5’GGC GGA AGA TAC CCG CCA GCG TGT CCA GTT 3’
R343A forward	5’TGC GGG GTA TCT TCG CCC AGC TGC CTG AG 3’
R343A reverse	5’CTC AGG CAG CTG GGC GAA GAT ACC CCG CA 3’

Table 2.1.2.4 A Primer pairs used for construction of various C/EBPα mutants

Vector maps

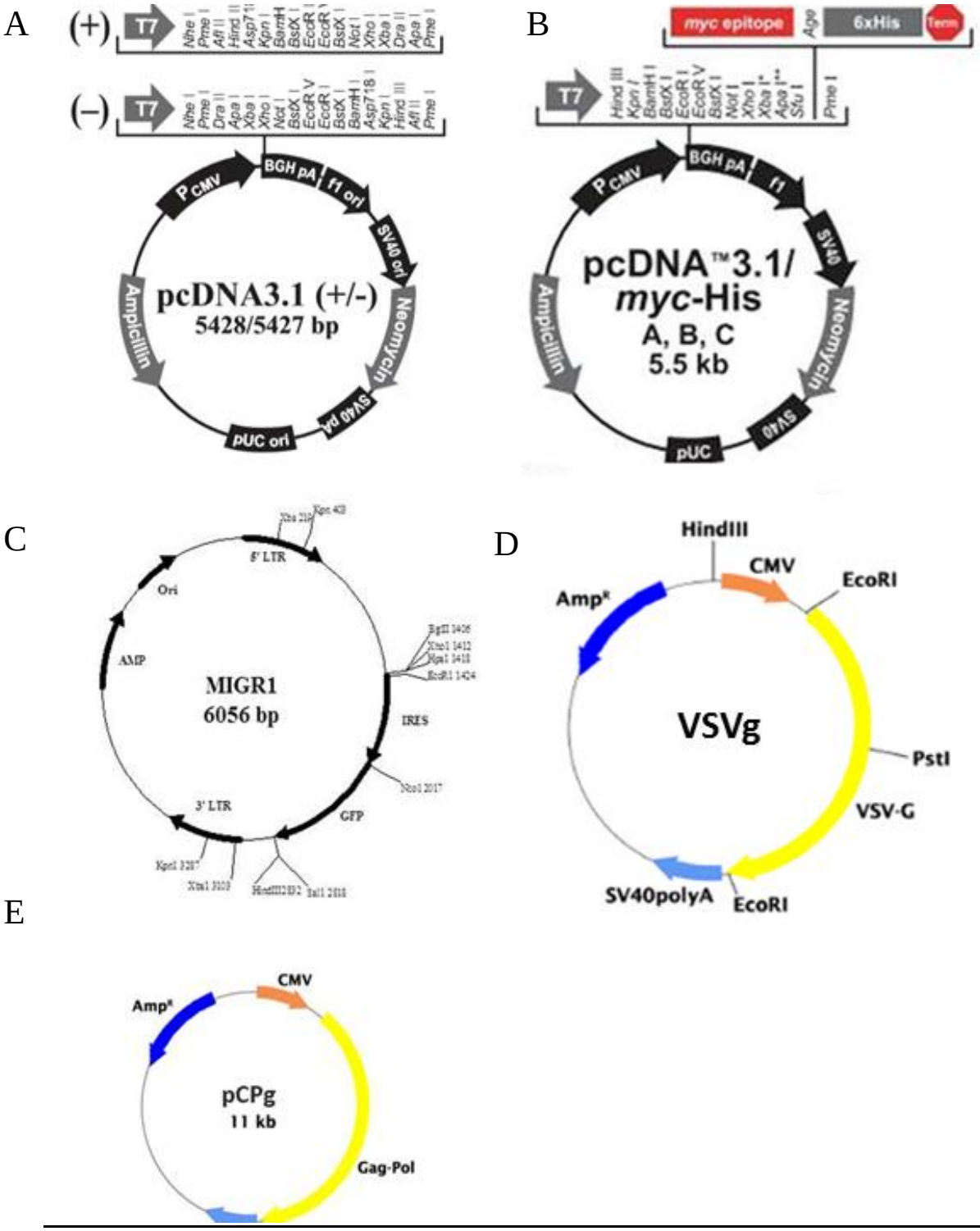

Fig 2.1.2.4 Backbone vector maps used. A) pcDNA3.1 **B)** pcDNA 3.1 myc-His A (PHMA) vector map. **C**) MigR1 retroviral expression vector. **D**) VSVg retroviral packaging vector. **E**) pCPg retroviral envelope producing vector.

Gene	Vector	Tag
C/EBPα	PHMA	HA/Myc
C/EBPα-R339a	PHMA	HA
C/EBPα-R333a	PHMA	HA
C/EBPα-R343a	PHMA	HA
C/EBPα-K313R	PHMA	Myc
C/EBPα-S21D	pcDNA3.1	-
C/EBPα-S21A	pcDNA3.1	-
C/EBPα-L12V	PHMA	HA
Ubiquitin-WT	PHMA	HA
Ubiquitin-K48R	Unknown	HA
Ubiquitin-K63R	Unknown	HA
WT-TRIB2	PHMA	Myc
TRIB2-KDM	PHMA	Myc
TRIB2-VPM	PHMA	Myc
TRIB2-R77A	PHMA	Flag
TRIB2-S227A/S229A/S231A/K233A	PHMA	Flag
TRIB2-K322A	PHMA	Flag
Expression vector control	PHMA	-
pCPg	Retrovirus production	
VSVg	Retrovirus production	
WT-TRIB2	MigR1	GFP
TRIB2-VPM	MigR1	GFP
C/EBPα-S21D	IRES	ER
C/EBPα-S21A	IRES	ER
Retrovirus control	MigR1	GFP

Table 2.1.2.4 B List of plasmids used

2.2 Methods

2.2.1 Molecular Biology

2.2.1.1 Competent cell preparation and transformation

DH5α were streaked for single colonies and grown on an LB plate overnight at 37 °C. A single colony was picked and grown in 5 mL of LB medium overnight at 37 °C. 3 mL of overnight grown DH5α cells were inoculated into 100-200 mL of LB solution and grown for 2-3 hours (hrs). Once cell density reached OD_{595} 0.6-1.0, cells were harvested by centrifugation of cells at 3000xg for 15 mins at 4 °C. The supernatant was discarded and the pellet resuspended in pre-cooled 0.1 M Magesnium sulphate ($MgS0_4$) at one third the volume of the bacterial culture volume. Cells were then harvested as above and the pellet resuspended in 0.1 M Calcium chloride ($CaCl_{2)}$ containing 15 % (v/v) of glycerol with 1/25 of bacterial culture volume. Aliquots were stored in pre-cooled eppendorfs, frozen on dry ice and then stored at -80 °C.

2.2.1.2 Transformation of DH5α competent cells for plasmid production

DH5α cells thawed on ice for 10 mins. DH5α were inoculated with 1 µL of plasmid DNA (10-50 ng) and placed in water bath at 37 ℃ for 1 min. 100 µL of LB broth was added, the inoculate was smeared on sterile LB + Ampicillin (AMP)(100 µg/mL) plates and incubated at 37 ℃ overnight. Single colonies were selected and grown in 3 mL of sterile starter culture (LB broth + 37 ℃ AMP) for 8 hrs in shaker at 37 ℃. Starter culture was added to 150 mL of LB broth + AMP and incubated overnight in shaker at 37 ℃. Plasmid preparation was performed using PureYield ™ Plasmid Midiprep kit. DNA was quantified using Nanodrop 2000 (Thermo).

2.2.1.3 Restriction enzyme digests and verification of plasmid preparation.

Plasmid preparations were checked by restriction enzyme digests. All C/EBPα constructs (1 µg) were digested with 0.5 µL Xho1 and 0.5 µL EcoR1 high fidelity in 10 µL NEB buffer 4, supplemented with 2 µL bovine serum albumin (BSA) in a final volume of 20 µL for 1 hr at 37 ℃. WT-TRIB2, TRIB2-KDM and TRIB2-VPM constructs were digested similarity instead using Xho1 and BamH1 NEB buffer 3. TRIB2 mutants R77A, S227A/S229A/S231A/K233A and K322A were digested with Xho1 and EcoR1. Digests were run on an agarose 1 % gel alongside DNA ladder and visualised using the Chemidoc. Plasmid preparation were screened for 1.5 kb (C/EBPα constructs) and 1.2 kb (TRIB2 constructs) insert drop outs and 5.4 kb PHMA vector back bone as restriction enzymes chosen each had only one recognition site.

2.2.2 Cell Biology

2.2.2.1 X-tremeGENE transfection of HEK293t cells

Transient overexpression of respective plasmid vectors was performed using X-tremeGENE HP DNA Transfection reagent (Roche) following manufactures guidelines in HEK293t cells. Cells were seeded on day 1 at a density of 4X10^6 cells per 10 cm dish, or 0.3X10^6 cells per well in 6 well plate. Twenty four hrs post seeding, when cells were at optimum confluency (70-90 %), cells were transfected as required using a DNA to X-tremeGENE ratio of 3:1. The total amount of DNA transfected was 6 μg or 2 μg for 10 cm and 6-well plate respectively. Cells were lysed 24 hrs post transfection as outlined in ***2.2.4***.

2.2.2.2 Retroviral production using calcium phosphate method and virus titration.

Retrovirus was produced in HEK293t cells and titered by transduction of NIH-3T3 cells. On day 1 5X10^6 HEK293t cells were seeded in 10 cm plate in a final volume of 10 mL. Day 2 cells were replenished with 3 mL fresh DMEM medium. For the transfection, 1 volume transfection buffer was added to 1 volume DNA cocktail drop by drop. The buffer/cocktail mixture was incubated with cells overnight. Each 10 cm plate used 500 μL of buffer and 500 μL of cocktail. The transfection buffer contained 0.05 M HEPES, 0.18 M sodium chloride (NaCl), 2 mM sodium phosphate (Na_2HPO^4) made up to a final volume 500 μL using ddH_2O. The DNA cocktail contained 31 μg total DNA (15 μg of transfer plasmid, 10 μg pCPg and 6 μg VSVg), 0.25 M $CaCL_2$, 10X NTE (0.01 M ethylenediaminetetraaceteic acid (EDTA) pH8.0, 0.1 M Tris hydrochloric acid (HCl) pH7.4, 0.15 M NaCl and ddH_2O) made up to a final volume 500 μL using ddH_2O. HEK293t cells were transfected no longer than 16 hrs at which time the medium was aspirated from the cells and 4.5 mL of fresh warm medium was added. Viral harvests were collected 24 hrs, 48 hrs and 72 hrs post medium replenishment. Viral harvests were centrifuged at 1500rpm for 5 mins at 4 °C, the supernatant was snap frozen on dry ice and stored at -80 °C. NIH-3T3 cells were transduced in order to titer the virus. 2X10^5 NIH-3T3 cells were seeded in 3 cm dish in 3 mL of medium. Twenty four hrs later medium was aspirated and the cells were incubated with 100 μl of viral supernatant to be titered and 2 μg/mL polybrene in 1 mL of medium. 2 mL of medium were added 24 hrs later. Twenty four hrs later cells were trypsinised and percentage transduction as measured by green fluorescent protein (GFP) expression was determined by comparing GFP expression to non-transduced control by fluorescent activated cell sorting (FACS) analysis.

2.2.2.3 Retroviral transduction of U937 cells

U937 cells were seeded at a density of 2X10^5 cells per mL 12 hrs prior to transduction. 1-5X10^6 cells were resuspended in 3-5 mL fresh medium supplemented with 20 % FBS, 1-3 mL of virus

(dependent on titre and cell number required), 2 ug/mL polybrene in 6 well plate. Cells were centrifuged for 90 mins at 1500rpm at room temperature. Six hrs post transduction, transduced cells were replenished with fresh medium to reach a final volume of 10 mL. Percentage transduction was determined by GFP expression measured by flow cytometry at desired time points.

2.2.2.4 Preparation of cellular protein extracts, protein quantification and SDS–polyacrylamide gel electrophoresis and western blotting

Cellular protein extracts were prepared using lysis buffer optimized for extraction of respective proteins. For TRIB2 protein expression, cells were lysed in Tris Lysis buffer (50 mM Tris pH7.4, 150 mM NaCl, 1 mM EDTA, 0.5 % NP-40, 5 % glycerol, supplemented with tyrosine phosphatase inhibitors;1 mM sodium orthovanadate (Na_3VO_4) and 1 mM Sodium Flouride (NaF) and protease inhibitors;1 mM phenylmethylsulfonyl fluoride (PMSF), 1 μM Pepstatin A, 2 ug/mL Aprotonin and 2 ug/mL Leupeptin) for 30 mins on ice, vortexing every 5 mins, then centrifuged at 14,000rpm for 10 mins at 4 °C. Lysates were stored at -80 °C. Direct lysis was performed in order to assess C/EBPα protein expression. 15X10^5 cells were suspended in 25 μL of 2x Laemmli buffer (120 mM Tris-CL pH 6.8, 20 % Gylcerol, 4 % sodium dodecyl sulphate (SDS), 0.02 % bromophenol blue), vortexed, boiled at 95 °C for 5 mins and then stored at -80 °C. Protein quantification was performed using Bradford solution graphing the absorbance of BSA protein concentration standards versus the absorbance of protein lysates to be determined. Absorbance was measured at wavelength 595 nm using a spectrophotometer. Protein concentration was determined using SoftMax Pro software ®. Typically, 50-100 μg of protein was resolved by 8-12 % SDS–polyacrylamide gel electrophoresis (PAGE). Proteins were transferred to nitrocellulose membrane. Post transfer membrane was washed with Ponceau S solution in order to visualise efficiency of protein transfer. Membranes were blocked for 1 hr at room temperature in 5 % milk/BSA in Tris-buffered saline-T (TBST) (20 mM Tris, 150 mM NaCl and 0.05 % Tween 20, pH 7.6). Primary antibodies were diluted and incubated with membrane at concentrations outlined previously **Table 2.1.2**. Horse radish peroxidise (HRP)-conjugated secondary antibodies were incubated with membranes at dilution of 1:2000 for 1 hr at room temperature. Membranes were washed 3 X 15 mins in TBST. Protein detection was visualised by two methods 1) using CL-XPosure Film on KODAK X-MAX developer post incubation with SuperSignal West Pico/Femto Chemiluminescent Substrate. 2) Using ChemiDoc TM XRS Biorad ® post incubation with Clarity TM Western ECL substrate.

2.2.2.5 In vivo overexpression HA ubiquitination assay

For in vivo overexpression HA ubiquitination assays, 4X10^6 HEK293t cells were seeded in a 10 cm plate. Twenty four hrs later cells were transiently transfected with 2.5 μg of Ubiquitin vectors,

0.5 µg of C/EBPα vectors and 3 µg of TRIB2 vectors for 24 hrs. Five hrs prior to cell lysis, cells were treated with 10 µM Z-Leu-Leu-Leu-al (MG-132). Cells were incubated with 100 mM N-Ethylmaleimide (NEM) for 30 seconds (sec) and then washed in ice cold phosphate-buffered saline (PBS), boiled at 95 °C for 5 mins in 1 % SDS, sonicated for 20 sec and centrifuged at 14,000rpm for 10 mins at 4 °C. Total inputs were collected by harvesting 10 µL of lysate and combining it with 10 µL of 2X Laemlli buffer. Inputs were boiled at 95 °C for 5 mins and stored at -20 °C. Remaining lysates were diluted in 900 µL radio-immuno precipitation assay (RIPA) lysis buffer (50 mM Tris, pH 8.0, containing 0.5 % NP-40, 0.25 % sodium deoxycholate, 150 mM NaCl, 1 mM EDTA, supplement with 20 mM NEM, protease and phosphatase inhibitors). Lysates were precleared with 25 µL Protein G Sepharose 4 fast flow beads rotating for 30 mins at 4 °C. Precleared lysates were centrifuged at 1500rpm for 5 mins at 4 °C, supernatant was incubated with 5 µg of C/EBPα antibody and 25 µL of fresh Protein G beads rotating overnight. The following day lysates were washed three times in RIPA lysis buffer. Post final wash all RIPA buffer was eluted from the beads using a 1 mL insulin syringe with a 26G needle attached, 30 µL of 2X Laemmli buffer was added and beads were then boiled at 95 °C in for 5 mins. Lysates and beads were centrifuged at 1500rpm for 5 mins at 4 °C. Supernatant was eluted using 1 mL insulin syringe with a 26G needle and equal volumes were separated on an 8 % SDS-PAGE, whilst total inputs were separated on a 12 % SDS-PAGE and immunoblotted as indicated.

2.2.2.6 Co-immunoprecipitation of overexpression proteins in HEK293t cells.

For co-Immunoprecipitation (co-IP) 4X10^6 HEK293t cells were transiently transfected with 4 µg of C/EBPα vectors and 4 µg of TRIB2 vectors as described for 24 hrs. Five hrs prior to cell lysis, cells were treated with 10 µM MG-132 cells were lysed in Tris lysis buffer. Immunoprecipitation reaction was performed as described for in vivo ubiquitination assay. Lysates were separated on 12 % SDS-PAGE.

2.2.2.7 Peptide array and specific alanine scanning substitution arrays (SASSA).

Essentially, scanning libraries of overlapping 18-mer peptides (shifted to the right by 3 amino acids) covering the entire TRIB2 murine protein (NCBI reference NM_144551.5) were produced by automatic SPOT synthesis and attached on continuous cellulose membrane supports on Whatman 50 cellulose using 9-fluorenylmethyloxycarbonyl (Fmoc) chemistry with the AutoSpot-Rosbot ASS 222 (Intavis Bioanalytical Instruments), schematic representation of peptide array synthesis see blow (**Fig 2.2.2.7 A and B**). Arrays were produced in collaboration with Dr. Patrick Kiely, University of Limerick. The specific alanine scanning substitution arrays (SASSA) were generated for selected peptides on TRIB2 using the same synthesis procedure, see schematic

representation below (**Fig 2.2.2.7 C**). Peptide arrays were activated in 100 % ethanol for 5 mins then washed with TBS-T 0.1 % (v/v). Arrays were blocked for 1 hr with 5 % (w/v) Marvel milk/TBS-T 0.1 % (v/v). TRIB2 arrays were then incubated in purified protein buffer (20 mM Tris-HCL pH7.5, 0.1 M NaCl, 5 mM β-Mercaptoethanol) or 2 µg/mL of purified CEBPα protein (Genway 10-002-38004). Arrays were washed with TBS-T 0.1 % (v/v) and incubated with 1/114 anti-C/EBPα, washed, then incubated in 1/2000 anti-rabbit HRP conjugated secondary or with specific Alexa Fluor 800-coupled anti-rabbit secondary antibodies (LI-COR Biosciences) (for SSASs). Bound protein was detected and visualised using ECL or the Odyssey® Infrared Imaging System (LI-COR Biosciences). True positive results were determined by comparison of the binding pattern with the controls (protein buffer) to the results from the protein incubations.

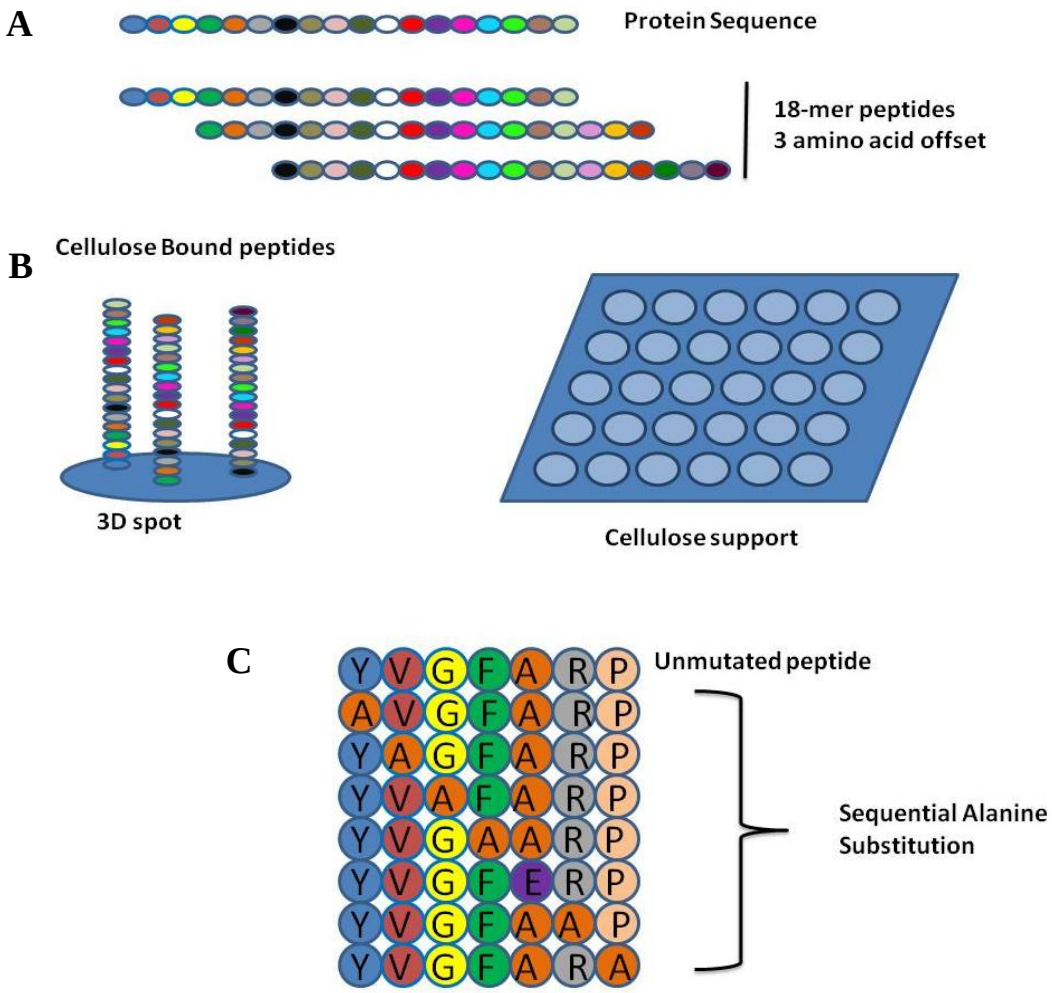

Fig 2.2.2.7 Schematic Representation of SPOT synthesis technology. A) Production of amino acid library spanning TRIB2 protein shifted by 3 amino acids **B)** Graphical representation of amino acid peptides spotted on cellulose support. **C)** Depiction of production of alanine scanning substitution arrays.

2.2.2.8 FACS analysis and cell sorting.

Cell pellets were resuspended in chilled PBS supplemented with 10 % FBS and incubated with antibodies on ice for 30 mins. Samples were washed with PBS and 10 % FBS before fluorescence intensity was analysed by flow cytometry (FACS CantoTM II BD). Data analysis was performed using Flow Jo Version 10 software (Treestar). For apoptosis assays cell suspensions were prepared in Hanks buffered Saline Solution (HBSS) (Life technologies) and stained with Annexin V-PE (BD Biosciences 556422) or Annexin V-APC (BD Biosciences 550475) and 4',6-diamidino-2-phenylindole (Dapi) (Sigma) for 15 mins at room temperature in the dark. Cells were washed with HBSS and analysed on FACS within 60 mins of cell staining. Annexin V is a member of the Annexin family of proteins which bind intracellular phosphatidylserine (PS). Upon induction of apoptosis cell membrane asymmetry is lost and PS translocates external to the cell membrane. Thus Annexin V staining can be exploited to detect apoptotic cells. Dapi is a fluorescent stain that strongly intercalates at AT rich regions of DNA. Dapi passes less efficiently through the membranes of live cells therefore strong Dapi staining serves as a marker of dead cells. Cell sorting was performed as requested by Ms. Jennifer Cassels using FACS Aria I (BD Biosciences, UK).

2.2.2.9 Cryopreserved AML patient sample thawing and culturing

AML peripheral blood samples were collected in accordance with the Declaration of Helsinki; all patients provided written consent. Samples were kindly provided by Dr. Mary Cahill, University College Cork and Dr. Ruud Delwel, Erasmus University. Mononuclear cells were isolated using Histopaque (Sigma) according to manufacturer's instructions. Cryopreserved AML patient samples were defrosted by rapidly warming cyrovials in 37 °C water bath. Cells were added drop by drop over 20 mins to pre-warmed thawing medium (IMDM supplemented with 20 % ES Fetal Calf Serum (Biosera), 5000 U/mL Heparin, 200 mM L-Glutamine and 100 u/mL DNAse (Stem Cell Technologies)) using Pasteur pipette. AML patient samples were then centrifuged for 15 mins at 1000rpm. The supernatant was discarded and cells were washed in thawing media and centrifuged for 10 mins at 1000rpm. The supernatant was removed and AML patient samples were cultured overnight at a density of ~ 1X10^6 cells/mL in StemSpan medium (Stem Cell Technologies) supplemented with 10 % Myelocult (Stem Cell Technologies), hIL-3, hIL-6, hSCF and hFLT3 cytokines at final concentrations of 10 ng/mL (Peprotech).

2.2.2.10 Pharmacological inhibition of the ubiquitin-proteasome degradation pathway in U937 cells and AML patient samples

Bortezomib a proteasome inhibitor was stored in 1M aliquots solubilised in dimethyl sulfoxide (DMSO) at -20 °C. U937 cells were seeded at density of 0.2X10^6/mL 24 hrs prior to treatment. AML patient sample seeding densities were dependent on cell number, where possible AML patient

cells were kept at density of 1X10^6/mL. U937 cells were plated at a density of 0.2X10^6 cells/mL in final volume of 200 µl in 96 well plate. Cells were treated with 10 nM Bortezomib diluted in PBS for indicated time points.

2.2.2.12 Cycloheximide treatment

For overexpression cycloheximide (CHX) treatment 2X10^5 HEK293t cells were seeded in 6 well plate. Twenty four hrs later cells were transfected as necessary. Twenty four hrs post transfection cells were treated with 100 ng/mL CHX for indicated time points. Cells were lysed, protein extracted and quantified followed by SDS-PAGE and western blotting as previously described.

2.2.2.13 Bioinformatical Analysis

SARPRED a real value prediction of surface accessibility software, generates a prediction of solvent-accessible surface area amino acids (ASA) (http://imtech.res.in/raghava/sarpred/). The ASA score is generated by performing PSI- Basic Local Alignment Search Tool (BLAST) which compares distant relationships between proteins and then predicts the secondary structure of a protein from its amino acid sequence (Garg et al., 2005). UbPred online software, predictor of protein ubiquitination sites http://www.ubpred.org/help.htmL (USCD). UbPred predicts potential ubiquitination sites in a protein through analysis of the amino acids identity of a protein. It was trained on 266 known ubiquitination sites and is reported to have a class based of accuracy 72% (Radivojac et al., 2010). NCBI BLAST (http://blast.ncbi.nlm.nih.gov/BlastAlign.cgi) finds regions of similarity between two sequences (Altschul et al., 1997). Chou Fasman secondary structure prediction software (http://www.biogem.org/tool/chou-fasman/) was used to determine the predicted secondary structure of TRIB2. This is an empirical technique whereby the frequencies of amino acids in secondary structures of know protein structures is applied to the amino acids of unknown secondary structure to get a probable secondary structure prediction (Chou and Fasman, 1974). Protein-protein interaction prediction engine was used to predict sites of protein interactions PIPE (Pitre et al., 2006). Neural Network Prediction of Beta-turns (NetTurnP) (http://www.cbs.dtu.dk/services/NetTurnP/) uses information on evolutionary and predicted protein sequences to determine the presence of β-turns based on protein amino acid sequence (Peterson et al., 2010).

2.2.2.14 Statistical Analysis

Statistical analysis was performed using Microsoft Excel and Prism Graphpad software

Chapter 3: Results

Investigating the TRIB2 and C/EBPα direct protein-protein interaction

3.1 Introduction

The interaction between the TRIB family of proteins and C/EBP family of proteins is evolutionary highly conserved in a cell type specific manner. In Drosophila the tribbles ortholog dTrbl was identified to bind dSlbo the homolog of mammalian C/EBP proteins resulting in its ubiquitination and subsequent degradation (Rørth et al., 2000, Masoner et al., 2013). There are three mammalian isoforms of dTrbl (TRIB1, TRIB2 and TRIB3). The TRIB family of proteins are structurally comprised of three regions or domains. TRIB proteins contain a large central kinase-like domain flanked by two smaller N-Terminal and C-Terminal regions. Sequence analysis of the TRIB protein family in different species revealed the N-Terminal region is highly divergent amongst family members but the kinase-like domain retained regions of high sequence similarity as did pockets of the C-Terminus (Hegedus et al., 2007).

The N-Terminal is rich in Serines and Prolines indicative of a Proline (Pro-P), Glutamic acid (Glu-E), Serine (Ser-S) and Threonine (Thr-T) (PEST) region. Canine Trbl was identified to be a laible protein with a half life of approximately 1 hr (Wilkin et al., 1997). The half life of TRIB2 in human cells was reported to be 2 hrs increasing upon deletion of its first 5 amino acids (MNIHR) (Wang et al., 2013a). Within the C-Terminal all TRIB proteins retain MEK1 (IL(L/D)HPWF) and the E3 ligase COP1 (DQXVPL) binding sites (Kiss-Toth et al., 2004, Qi et al., 2006, Yokoyama et al., 2010).

Canonical kinases have 12 distinct subdomains each comprised of 10-30 amino acids, and within these subdomains certain sequences are functionally highly conserved (Hanks and Hunter, 1995). Analysis of the TRIB2 kinase-like domain revealed it contained some characteristics of an active kinase but not all (Hegedus et al., 2007). The kinase domain of a protein is folded in 2 lobed 3D structures (Hanks and Hunter, 1995). Subdomains I-IV are located in the amino terminal lobe and subdomains VIA-XI are located in the carboxy terminal lobe. Subdomain V is located in the hinge region between the two lobes which acts to catalyse enzymatic reactions. The amino terminal lobe is largely structured in β-sheets and is responsible for anchoring the phosphate donor, ATP (Hanks and Hunter, 1995). The carboxy terminal lobe is largely α-helical and responsible for anchoring the phosphate acceptor. Conservation of subdomains I, II and VIB is considered to be the most important for kinase functionality (Hegedus et al., 2007). Within subdomain I is a highly conserved GXGXXG sequence which is necessary for ATP orientation, and is lacking in TRIB2. Subdomain II contains a highly invariant lysine (K) within the sequence VAIK which binds ATP, and all TRIB proteins retain this critical lysine. Subdomain VIB contains the catalytic loop LR**D**LKLRNF, the third residue of this sequence is a crucial aspartic acid (D) which is retained by all TRIB proteins.

The majority of canonical kinases retain an asparagine (N) residue, 5 residues downstream of the crucial asparagine whilst in TRIB2 it is replaced with a lysine (LR**D**LKLR**K**F). Within subdomain VII there is a conserved tripetpide sequence APE which is responsible for the stability for the C-Terminal lobe through formation of a salt bridge between the gluatamic acid (E) of the tripeptide and an arginine (R) residue in subdomain IX. TRIB2 retains the second and third amino acids in this sequence but has a serine in the first position (SPE) (Hegedus et al., 2007). The DVWSXG heptapeptide in subdomain IX is also a signature of functional kinases retained by TRIB2. TRIB2 lacks a DFG triplet motif in subdomain VII, which is the most striking difference between functional kinases and the TRIB family of proteins (Hegedus et al., 2007). The aspartic acid in the DFG motif chelates $Mg+^{2}$ ions, necessary for catalysis of the phosphate transfer and is also essential for orientating ATP through binding of α and β phosphates in the ATP binding cleft. There are of course examples of functionally active kinases which lack some of these functionally conserved motifs (reviewed by (Boudeau et al., 2006)).

TRIB proteins are currently defined as pseudokinases as they lack phosphate transfer activity despite having the predicted 3D structure of a kinase (Wilkin et al., 1997, Boudeau et al., 2006, Hegedus et al., 2007). When first identified in canine thyroid cf5W/Trbl was described as a phosphoprotein as it is phosphorylated upon stimulation however it was unable to autophosphorylate or phosphorylate substrates (Wilkin et al., 1997). Further in vitro kinases assays investigating the kinase-like domain of SKIP3/TRIB3 homolog of TRIB2 also stated that TRIB3 was unable to autophosphorylate or phosphorylate substrates (Boylan et al., 2003). TRIB2 retains the ability to bind ATP through this critical lysine K90 in subdomain II and TRIB2 is able to turnover ATP but not sufficiently to result in kinase function (Unpublished result, personal communication Dr. P Eyers, University of Liverpool). Despite the apparent lack of kinase activity of TRIB2 its kinase-like domain still remains crucial for its biological functions (Keeshan et al., 2010, Masoner et al., 2013).

TRIB1 and TRIB2, unlike TRIB3, both possess the ability to perturb normal haematopoiesis resulting in malignant leukaemic disease (Keeshan et al., 2006, Dedhia et al., 2010, Yokoyama et al., 2010, Yoshida et al., 2013). TRIB1 and TRIB2 were identified to bind C/EBPα and induce its proteasomal degradation, whilst TRIB3 which retained a low binding affinity for C/EBPα was unable to induce degradation and AML (Dedhia et al., 2010). Overexpression of TRIB2 results in degradation of the C/EBPαp42 isoform with a concomitant increase in the levels of the N-Terminally truncated C/EBPαp30 isoform, disrupting the normal C/EBPαp42:C/EBPαp30 ratio (Keeshan et al., 2006). TRIB2 expression resulting in altered C/EBPαp42:C/EBPαp30 ratio disrupts

haematopoiesis (Keeshan et al., 2006). BMT models identified TRIB2 mice had reduced numbers of BM granulocytes and increased BM and splenic monocytes with mice finally succumbing to an AML like disease (Keeshan et al., 2006). Reversal of low C/EBPαp42:C/EBPαp30 ratio has been identified to induce differentiation of leukaemic cell lines and patient derived primary AML blasts (Koschmieder et al., 2007). Pharmacological treatment with CDDO increases C/EBPαp42:C/EBPαp30 ratio resulting in overcoming of differentiation block, highlighting the importance of C/EBPαp42:C/EBPαp30 ratio in controlling haematopoietic cell differentiation (Koschmieder et al., 2007). TRIB2 degradation of C/EBPαp42 can be inhibited by treatment with the proteasomal inhibitor MG-132. C/EBPαp42 co-immunoprecipitates with TRIB2 only in the presence of MG-132 whilst C/EBPαp30 co-immunoprecipitates in the absence and in the presence of MG-132, indicating that the direct interaction of C/EBPαp42 and TRIB2 results in its subsequent proteasomal degradation (Keeshan et al., 2006).

In order to assess the functional regions required for TRIB2 leukaemogenecity, the domains of TRIB2 were investigated. All TRIB proteins retain a COP1 binding site in their C-Terminus (Qi et al., 2006). COP1 is a RING-Finger E3 ubiquitin ligase responsible for conjugation of ubiquitin proteins to lysine residues on target substrates. It was determined loss of the COP1 binding to TRIB2 through deletion of the COP1 binding site (1-324 TRIB2-dCOP1) or mutation of COP1 binding site (DQVPL to AQLAA TRIB2-VPM) abrogated its ability to degrade C/EBPαp42 and ultimately to induce AML in murine models (Keeshan et al., 2010). TRIB2-dCOP1 still retained the ability to bind C/EBPα indicating that abrogation of C/EBPα-TRIB2 interaction was not responsible for the loss of TRIB2 function. COP1 binding was necessary for TRIB2-mediated degradation of C/EBPαp42 and the resultant leukaemic disease (Keeshan et al., 2010).

Further structural analysis into the essential functional domains of TRIB2 required for this proteolytic relationship revealed that the N-Terminus was not essential, whilst an intact central kinase-like domain was necessary for TRIB2 leukaemogenecity (Keeshan et al., 2010). Deletion of the N-Terminal dNTRIB2 (63-343) did not abrogate WT-TRIB2 function however extension of the deletion into the N-Terminus of the kinase-like-domain (121-343 ΔNS) did abrogate TRIB2 ability to degrade C/EBPα (Keeshan et al., 2010). As mentioned, within the kinase-like domain TRIB2 does not retain the canonical kinase motif HRDLKPEN characteristic of a catalytic loop (**Table 3.1.1**). Mutation of TRIB2 to resemble a canonical kinase (LRDLK**LRK** to LRDLK**PEN** TRIB2-KDM) resulted in a loss in its ability to degrade C/EBPα and induce leukaemia (Unpublished data, Karen Keeshan and (Keeshan et al., 2010). TRIB2 does retain the lysine at position 5 LRDL**K**LRK which defines active Ser/Thr kinases. Mutation of TRIB2 to resemble a tyrosine kinase

LRDL**R**LRK (TRIB2-K177R) also abrogated TRIB2s ability to degrade C/EBPα and induce leukaemia (Unpublished data, Karen Keeshan and (Keeshan et al., 2010). The homologous mutation to K177R was investigated in Drosophila dTrbl K266R, and this mutant retained dTrb*l* functionality and the ability to degrade the C/EBPα homolog dSlbo (Großhans and Wieschaus, 2000). However mutation of the essential aspartic acid retained by dTrbl (position 3) in Drosophila **D**LK to **N**LK reduced dTrbl ability to interact with dSlbo and mediate its degradation (Masoner et al., 2013). These data proved the TRIB protein sequence LRDLKRK is crucial for protein functionality. Mutation of these crucial amino acids may not affect kinase-like activity of TRIB but perhaps the amino acid changes are structurally crucial for protein folding. Investigation of other crucial kinase motifs VAIK in subdomain II and SLE in subdomain VII in Drosophila determined that neither mutation of the crucial ATP binding lysine in VAIK nor mutation of crucial Glu in SLE abrogate dTrbl function (Masoner et al., 2013).

H	R	D	L	K	P	E	N	Canonical kinase motif subdomain VIB
L	R	D	L	K	L	R	K	Mammalian TRIB2
L	R	D	L	K	P	E	N	Mammalian TRIB2 KDM mutant
L	R	D	L	R	L	R	K	Mammalian TRIB2 K177R mutant
L	R	D	L	K	L	R	K	Drosophila Trbl
L	R	D	L	R	L	R	K	Drosophila Trbl K266R mutant
L	R	N	L	K	L	R	K	Drosophila Trbl NLK mutant
1	2	3	4	5	6	7	8	Position

Table 3.1.1 TRIB protein kinase subdomain VIB mutants

TRIB proteins were demonstrated to bind MEK1, MKK4 and MKK7 and share a conserved MEK1 binding site in the C-Terminus (Kiss-Toth et al., 2004, Yokoyama et al., 2010). TRIB1 binding to MEK1 is reported to be essential for mediating degradation of C/EBPα and induction of murine AML in BMTs. TRIB1 and C/EBPα binding was localised to the N-Terminus of TRIB1. TRIB1ΔN1 (1-90) mutant retained the ability to bind C/EBPα whilst an extension of the deletion further into the kinase-like domain of TRIB1 to 160 amino acids (TRIB1ΔN2) resulted in loss of C/EBPα binding, loss in TRIB1 ability to degrade C/EBPα and a loss in TRIB1 induced AML. TRIB1 binds C/EBPα resulting in its degradation but this proteolytic association requires MEK1 binding (Yokoyama et al., 2010). Thus, although both TRIB1 and TRIB2 bind C/EBPα resulting in its degradation and AML, there are mechanistic differences and similarities. Deletion of TRIB1 N-Terminus and N-Terminal region of kinase-like domain (TRIB1ΔN2) resulting in a loss in C/EBPα

binding and degradation, and similarly deletion of N-Terminus and N-Terminal region of kinase-like domain TRIB2 (TRIB2ΔNS) also abrogated TRIB2s ability to degrade C/EBPα. Despite low percentages of sequence similarities between the N-Termini of TRIB1 and TRIB2 loss of both N-termini results in loss of C/EBPα binding, thus suggesting possible conservation of protein binding site on homologous proteins despite low sequence similarities between the proteins.

Much literature exists attempting to identify protein binding sites and any conservation of protein binding sites amongst protein families (Nooren and Thornton, 2003, Korkin et al., 2005, Tyagi et al., 2009). Protein binding sites are generally sought through physiochemical investigation of protein size, binding surface areas, residue composition, polarity and hydrophobicity but there still remains no consensus for protein binding site identification, due in part to the transient nature of many interactions and lack of published 3D structures (Nooren and Thornton, 2003, Korkin et al., 2005). There are several factors governing protein-protein interactions such as protein concentrations (Nooren and Thornton, 2003), cellular localisation and ultimately the proteins must be geometrically compatible (Lawrence and Colman, 1993). It is postulated that only a very small number of amino acids are involved in protein binding, in small proteins even just one amino acid (Bogan and Thorn, 1998) and there is also reports of selection bias regarding the identity of amino acids at protein interaction sites (Murakami, 1995, James and Tawfik, 2003, Ofran and Rost, 2007).

Aim

The COP1:TRIB2:C/EBPα multiprotein degradation complex is a key event in TRIB2 induced leukaemogenesis. Loss of COP1:TRIB2 binding through mutation or deletion abrogates the ability of TRIB2 to degrade C/EBPα and induce AML (Keeshan et al., 2010). TRIB2 directly binds C/EBPα. Previous work in the laboratory identified the TRIB2 binding site on C/EBPα as R339, through use of peptide array analyses, SASSA, SDM and confirmation by GST-IP. In order to understand this malignant interaction, detailing of the sites of C/EBPα interaction on TRIB2 was necessary. In our study through use of peptide array analyses, SASSA, SDM and verification by co-IP I determine mutation of TRIB2-S227/S229/S231/K233 results in a loss in C/EBPα binding, while mutation of TRIB2 residues R77 and K322 does not abrogate C/EBPα binding. I also confirm using mammalian co-IP R339 as the TRIB2 binding site on C/EBPα.

Result 3.2.1 Peptide array analysis identified TRIB2 interacting sites on C/EBPα-array 1

It has previously been reported by our group that TRIB2 and C/EBPα interact as ascertained by co-IP assay in HEK293t cells (Keeshan et al., 2006). However the identity of the TRIB2 protein domains and amino acids involved in C/EBPα binding had yet to be determined. TRIB1 the homolog of TRIB2 was identified to bind C/EBPα and the crucial TRIB1 region was mapped to an N-Terminal pseudokinase spanning region (Yokoyama et al., 2010, Dedhia et al., 2010). TRIB3 was identified to associate very weakly with C/EBPα (Dedhia et al., 2010). In order to assess the TRIB2 amino acids responsible for mediating the interaction with C/EBPα, peptide arrays were produced which spanned the entire TRIB2 protein. The arrays were produced by Dr. Patrick Kiely as described in Materials and Methods ***2.2.2.7***. Two identical peptide arrays were produced, one was incubated with the stabilisation C/EBPα protein buffer (referred to from this point as control buffer) in order to control for any nonspecific binding and the second was incubated with 2 μg/mL C/EBPα purified protein in its stabilisation buffer (Genway, USA). Arrays were then incubated with anti C/EBPα antibody and anti rabbit HRP conjugated secondary antibody and visualised using ECL. True positive results were determined by comparison of the binding pattern of the control array to that of array incubated with the C/EBPα protein. Dark spots were indicative of C/EBPα protein binding to the respective 18mer peptides. Five binding spots unique to the C/EBPα incubated array were identified as is indicated by red numbering (**Fig 3.2.1 A).** Characterisation of these TRIB2 18mer peptides revealed that C/EBPα interaction sites spanned throughout the TRIB2 protein from amino acids 25-318 indicating a strong pattern of C/EBPα binding **(Fig 3.2.1 B).**

A

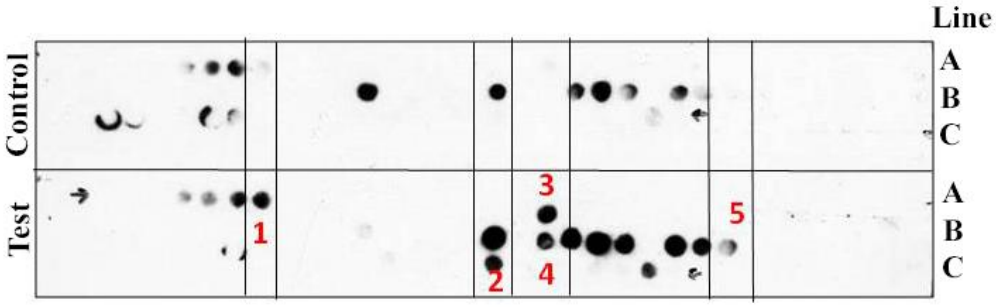

B

SPOT	Position	Residues	Sequence
1	A7	25-42	E-E-L-S-S-I-R-S-A-E-P-S-Q-S-F-S-P-N
2	C16	301-318	E-I-L-D-H-P-W-F-S-T-D-F-S-V-S-N-S-G
3	A18	69-86	P-L-E-G-D-H-V-F-R-A-V-H-L-H-S-G-E-E
4	B18	189-206	T-R-V-K-L-E-S-L-E-D-A-Y-I-L-R-G-D-D
5	B25	217-234	A-Y-V-S-P-E-I-L-N-T-S-G-S-Y-S-G-K-A

Fig 3.2.1 Analysis of C/EBPα binding sites on TRIB2 peptide array A) Peptide array analysis of identical TRIB2 arrays incubated with Control buffer and Test (2 μg/mL of purified C/EBPα protein). Arrays were then incubated with anti C/EBPα primary antibody and secondary anti rabbit HRP. Binding was visualised using ECL. Dark spots are indicative of binding sites. Numbers 1-5 indicate the binding sites unique to protein incubation versus control buffer. **B)** Table lists the 17 amino acid residues in each of the binding spots.

Result 3.2.2 Peptide array analysis identified TRIB2 interacting sites on C/EBPα-array 2

Results from C/EBPα protein incubation with TRIB2 peptide array 1 identified the potential involvement of multiple TRIB2 amino acids in C/EBPα protein binding (**Fig 3.2.1**). In order to verify these results before generation of specific alanine scanning substitution arrays a third TRIB2 peptide arrays (array 2) was produced. The array was first incubated with the control buffer and then purified C/EBPα protein (**Fig 3.2.2)**. In order to confirm the previous results these arrays were visualised using a different secondary approach on an Odyssey® Infrared Imaging System (LI-COR Biosciences) following incubation with specific Alexa Fluor 800-coupled anti rabbit secondary antibody (LI-COR Biosciences). The binding pattern between control buffer incubation and protein incubation was compared. Ten unique binding spots were identified in the array incubated with purified C/EBPα protein in stabilisation buffer versus incubation with control buffer alone (**Fig 3.2.2 A**). The background signal detected using Odyssey® Infrared Imaging System was greater than that observed using ECL detection as has been previously reported for use of fluorescent antibodies (Frank, 2002). Binding sites throughout the TRIB2 protein were identified replicating the results from array 1 (**Fig 3.2.1).** An observable cluster of C/EBPα binding sites was observed for amino acids ranging from 199-249 spots C7, C8, C16, C17 and C18 highlighting a distinct C/EBPα potential binding region (**Fig 3.2.2 B**).

A

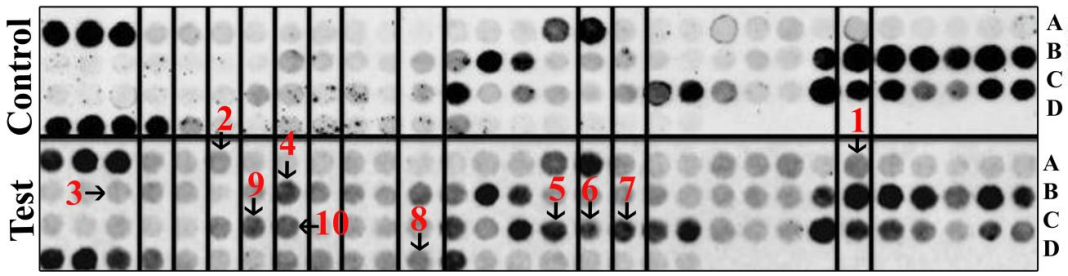

B

Spot	Position	Residue	Sequence
1	A25	72-90	D-H-V-F-R-A-V-H-L-H-S-G-E-E-L-V-C-K
2	A6	16-33	R-S-R-N-K-T-Q-F-E-E-L-S-S-I-R-S-A
3	B3	97-114	Y-Q-E-S-L-A-P-C-F-C-L-S-A-H-S-N-I-N
4	B8	112-129	N-I-N-Q-I-T-E-I-L-L-G-E-T-K-A-Y-V-F
5	C16	226-243	T-S-G-S-Y-S-G-K-A-A-D-V-W-S-L-G-V-M
6	C17	229-246	S-Y-S-G-K-A-A-D-V-W-S-L-G-V-M-L-Y-T
7	C18	232-249	G-K-A-A-D-V-W-S-L-G-V-M-L-Y-T-M-L-V
8	D12	304-321	D-H-P-W-F-S-T-D-F-S-V-S-N-S-G-F-G-A
9	C7	199-216	A-Y-I-L-R-G-D-D-D-S-L-S-D-K-H-G-C-P
10	C8	202-219	L-R-G-D-D-D-S-L-S-D-K-H-G-C-P-A-Y-V

Fig 3.2.2 Identification of C/EBPα interacting sites on TRIB2. Peptide array analysis of TRIB2 array first incubated with control buffer then C/EBPα protein. The peptide array was visualised on Odyssey® Infrared Imaging System (LI-COR Biosciences) following incubation with Alexa Fluor 800-coupled anti rabbit secondary antibodies. **A)** Ten unique binding spots were identified on test incubation versus control buffer incubation. **B)** Table lists the amino acid identity of the 10 binding spots unique to the test array.

Result 3.2.3 Identification of six TRIB2 regions as potential C/EBPα binding sites from array 1 and array 2

Generation of two independent sets of TRIB2 peptide arrays yielded a list of 5 and 10 potential C/EBPα binding sites (**Fig 3.2.1 and Fig 3.2.2**). Comparison of the amino acid sequences identified in both peptide arrays yielded a list of 6 stretches of amino acid sequence, i.e. potential binding sites. The amino acid sequences identified were largely clustered within TRIB2 pseudokinase domain, (4 of the 6 common binding sites, DHVFRAVHLHSGEE, AYILRGDDD, AYV and SGSYSGKA). One binding site was located in the N-Terminus EELSSIRSA and one binding site was identified at the bridge of the kinase-like domain and the C-Terminus DHPWFSTDFSVSNSG (**Fig 3.2.3 A**). As previously mentioned TRIB1 has the ability to interact with C/EBPα and an N-Terminal region was determined to be crucial for C/EBPα binding (Dedhia et al., 2010, Yokoyama et al., 2010). Therefore TRIB2 was blasted against TRIB1 to identify any conservation of amino acids within the N-Terminus of the protein, thus identifying any potential common C/EBPα binding sites. The EELSSIRSA sequence is located in N-Terminus of the TRIB2 protein, was a region identified not conserved with TRIB1. Investigation of this sequence does not support the previously outlined hypothesis of conservation of protein binding localisation sites amongst family members TRIB1 and TRIB2, however an equally compelling argument exists for non conservation of protein binding sites (Nooren and Thornton, 2003). TRIB1 and TRIB2 do not retain 100% sequence similarity therefore there are unquestionable differences in protein tertiary structure and protein interactions. As this sequence was strongly identified in both peptide arrays, further investigation as a C/EBPα binding site was warranted (**Fig 3.2.3 C**). The DHVFRAVHLHSGEE TRIB2 sequence from amino acids 74-86 in subdomain I of the kinase-like domain, retains 50% homology with TRIB1 (**Fig 3.2.3 C**). TRIB2-R77 is homologous to TRIB1-R107 which, which when mutated to R107L increased C/EBPα degradation with a resulting decrease in TRIB1 AML latency (Yokoyama et al., 2012). Thus, as the degradation of C/EBPα by TRIB1 was reported to be binding dependent and mutation of this arginine results in increased degradation perhaps R77 may act as C/EBPα binding site in TRIB2. The sequence AYILRGDDD is a stretch of TRIB2 sequence which is homologous to a region of TRIB1 sequence which when deleted loses the ability to bind C/EBPα. (Yokoyama et al., 2010) (**Fig 3.2.3 C**). Examination of this sequence will determine conservation of protein binding sites between homologous proteins. The sequence AYV is located within subdomain VII of the kinase-like domain of TRIB2 and located beside a region SPE which is highly conserved throughout evolution across tribbles family members and species. PE sequence is one of the vestiges of an active kinase which TRIB2 retains (Hegedus et al., 2007). Multiple sequences within the kinase-like domain of TRIB2 were identified as potential sites strongly

suggesting kinase-like domain involvement; this warranted further investigation of this site. The sequence SGSYSGKA resembles the consensus GSK3 phosphorylation site motif S/TXXXS/T. The N-Terminal S/T is the target and the second S/T serves as a phosphorylation priming site. Phosphorylation priming is reported to increase the efficiency of substrate transfer thought not always necessary (Doble and Woodgett, 2003). Potential phosphorylation at this site within the kinase-like domain of TRIB2 may be important for structure of TRIB2 and its resulting protein-protein interactions. The DHPWFSTDFSVSNSG sequence is located at the junction between the kinase-like domain and the C-Terminus of TRIB2. It contains part of the MEK1 binding site ILDHPWF on TRIB2 (Yokoyama et al., 2010). Analysis of promiscuous protein binding has identified the existence of "multiple protein binding interfaces", whereby the same "hotspot" is capable of binding multiple different protein partners involved in different cell pathways (Tyagi et al., 2009). Therefore pre-existing knowledge of a known protein binding site on a protein may suggest the presence of one such multiprotein binding hotspot. Thus this MEK1 binding site on TRIB2 warranted further investigation as it may potentially also be involved in C/EBPα binding. Each of these 6 TRIB2 sequences were further analysed for their involvement in C/EBPα binding by SASSA.

A

B

SPOT	Sequence	Significance
1	EELSSIRSA	N-term of TRIB2 region unconserved with TRIB1
2	DHVFRAVHLHSGEE	TRIB2-R77A is homologous with TRIB1-R017 which when mutated R107L increases degradation of C/EBPα
3	AYILRGDDD	The only sequence in TRIB2 which aligns with TRIB1 90-160AA which is reported to contain C/EBPα binding site
4	AYV	Kinase domain region
5	SGSYSGKA	Putative GSK3 phosphorylation site
6	DHPWFSTDFSVSNSG	Contains MEK1 binding site ILDHPWF

C

```
TRIB2 68  EPLEGDHVFRAVH  80
            E +HV RA+
TRIB1 98  PLAEREHVSRALC  101

TRIB2 214 GCPAYVSPE  222
            GCPAYVSPE
TRIB1 244 GCPAYVSPE  252

TRIB2 301 EILDHPWFS 309
            +IL HPWF
TRIB1 322 QILLHPWFE 321

TRIB2 193 LESLEDAYILRGDDDSL 209
            LESLED +I++G+DD+L
TRIB1 223 LESLEDTHIIKGEDDAL 239

TRIB2 226 TSGSYSGKAAD 236
            T+G+YSGKAAD
TRIB1 256 TTGTYSGKAAD 266
```

Fig 3.2.3 Identification and annotation of six potential C/EBPα binding sites on TRIB2. A) A schematic of TRIB2 protein domains with the localisation of the potential binding sites. **B**) A brief annotation of the binding sites identified on TRIB2. **C)** BLAST of TRIB2 versus TRIB1 identifying homologous sequences with regard to identified potential binding sites.

Result 3.2.4 SASSA identifying TRIB2 peptides D, G, H and J are important for C/EBPα binding

In order to determine specific amino acids involved in C/EBPα and TRIB2 binding, SASSA was generated as described in Materials and Methods ***2.2.2.7*** and designed based on combined results from peptide arrays 1 and 2 and annotation of sequences identified (**Fig 3.2.1, 3.2.2 and 3.2.3).** Each identified sequence was mutated twice on the array in order to validate its importance in the interaction. Array A represents the results from the first incubation of the SASSA with purified C/EBPα protein (**Fig 3.2.4A).** The array was stripped, re-activated and re-blocked as detailed in Materials and Methods ***2.2.2.7***. The efficacy of stripping was tested by incubation with Alexa Fluor 800-coupled anti rabbit secondary and visualised on Odyssey® Infrared Imaging System. The array was then reincubated with purified C/EBPα protein and data represented as Array B (**Fig 3.2.4 B)**. Analysis of Spot 1 in Peptides A-J represents the unmutated peptide sequence, a dark spot is indicative of the importance of that particular peptide sequence in C/EBPα binding. Array B directly matched the binding pattern trends observed in Array A for Spot 1 in Peptides A, B. C .D. F. G. I and J. **Figures 3.2.4 C** and **3.2.4 D** plot the intensities of the unmutated peptide sequence (i.e. the 18 amino acid peptide stretch anlaysed Spot 1) as total percentages. From these graphs the importance of the TRIB2 peptides in C/EBPα binding can be directly compared. High signal intensity for Spot 1 Peptides D, H and J confirmed the importance of these amino acid sequences in C/EBPα binding. Peptide D strongly binds C/EBPα indicating amino acids 73-90 are important for TRIB2 binding. Peptide H, residues 221- 238, displayed low signal intensity in Array A, however in Array B the observed signal intensity was much stronger confirming the importance of these residues. Peptide J had the highest intensity of C/EBPα binding on the alanine array. Low signal intensity for Spot 1-19 in Peptides A, B, C, E, F and I indicated these sequence are not important in C/EBPα binding. Low binding signal intensity for A, B and C suggest that the N-Terminus of TRIB2 does not bind C/EBPα. Peptides E and F, residues 193-230 and Peptide I, residues 301-318 do not appear important for C/EBPα binding as is evident by the low intensity. Comparison of Array A to Array B confirmed the circumference of Spots E1, E4 and E7 were clarified to be artefacts. Peptide G, which overlaps with the sequence of Peptide H determined to be important for C/EBPα binding, displayed low signal intensity for the unmutated sequence Spot 1 but the signal intensity increased from Spot 3-Spot 17 suggesting Peptide G may be important for C/EBPα binding. Of note, lower overall signal intensity was observed in Array B owing probably to the stripping procedure.

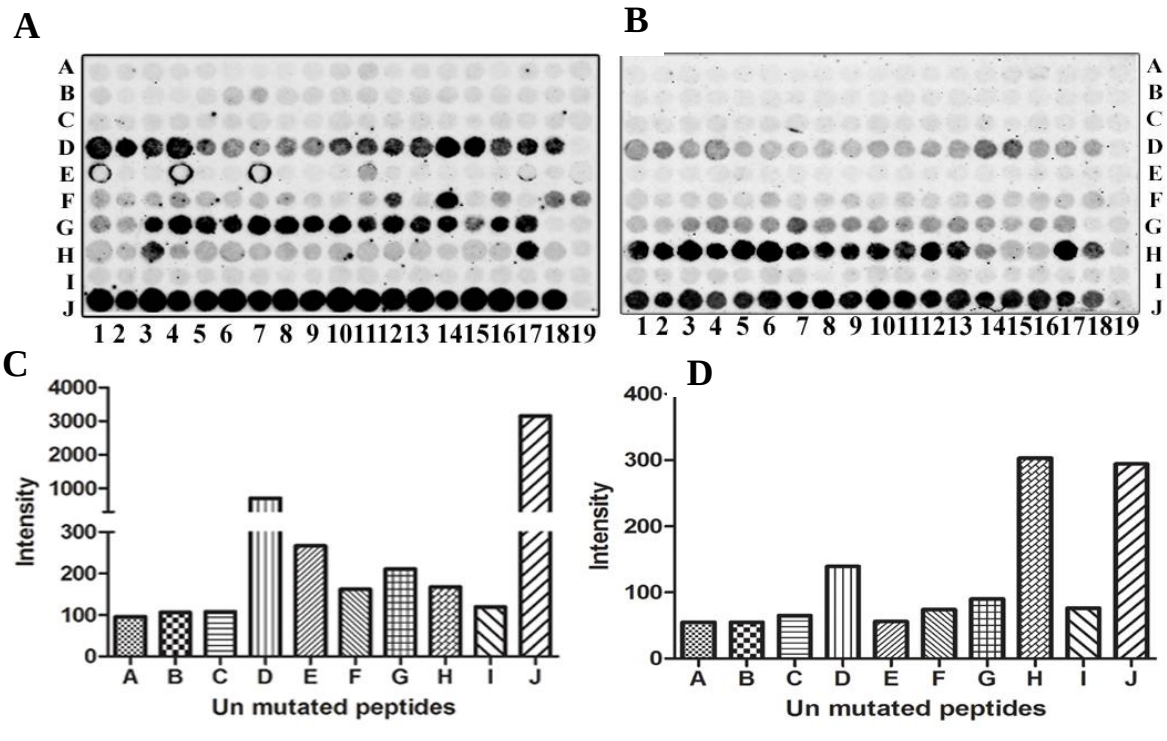

E

Peptide	Residues	Sequence
A	21-38	T Q D F E E L S S I R S A E P S Q S 21 22 23 24 25 26 27 28 29 30 31 32 33 34 35 36 37 38
B	25-42	E E L S S I R S A E P S Q S F S P N 25 26 27 28 29 30 31 32 33 34 35 36 37 38 39 40 41 42
C	69-86	P L E G D H V F R A V H L H S G E E 69 70 71 72 73 74 75 76 77 78 79 80 81 82 83 84 85 86
D	73-90	D H V F R A V H L H S G E E L V C K 73 74 75 76 77 78 79 80 81 82 83 84 85 86 87 88 89 90
E	193-210	L E S E K E D A Y I L R G D D D S L S 193 194 195 196 197 198 199 200 201 202 203 204 205 206 207 208 209 210
F	213-230	H G C P A Y V S P E I L N T S G S Y 213 214 215 216 217 218 219 220 221 222 223 224 225 226 227 228 229 230
G	217-234	A Y V S P E I L N T S G S Y S G K A 217 218 219 220 221 222 223 224 225 226 227 228 229 230 231 232 233 234
H	221-238	P E I L N T S G S Y S G K A A D V W 221 222 223 224 225 226 227 228 229 230 231 232 233 234 235 236 237 238
I	301-318	E I L D H P W F S T D F S V S N S G 301 302 303 304 305 306 307 308 309 310 311 312 313 314 315 316 317 318
J	305-322	H P W F S T D F S V S N S G F G A K 305 306 307 308 309 310 311 312 313 314 315 316 317 318 319 320 321 322

Fig 3.2.4 SASSA identifying C/EBPα binding sites on TRIB2. SASSA was generated as described in Materials and Methods and designed based on results from both peptide arrays. Spot 1 on each lane represents the wild type un-mutated 18 amino acid peptide. Each subsequent amino is sequentially mutated to an alanine. **A)** SASSA were incubated with 2 µg/mL purified C/EBPα protein, anti C/EBPα primary antibody and Alexa Fluor 800-coupled anti rabbit secondary antibody and visualised on Odyssey® Infrared Imaging System. **B)** Array was stripped and probed as in **(A)**. **C)** and **D)** The binding intensity of C/EBPα protein to each un mutated Peptide Spot 1 (A-J), quantified by densitometry was plotted as the percentage binding intensity of both arrays A and B. **E)** The amino acid identity of the array.

Result 3.2.5 SASSA identifying amino acids in TRIB2 peptides D, G, H and J important for C/EBPα binding

High binding signal intensities indicated Peptides D, G, H and J are potential C/EBPα binding sites on TRIB2 (**Fig 3.2.4**). Within Peptide D mutation of amino acids F76A, R77A, A78E, V79A, H80A, L81A, H82A and K90A resulted in a greater than 50 % reduction in intensity relative to the un-mutated wildtype peptide sequence Spot 1 (**Fig 3.2.5 A).** Previous analyses identified the amino acids phenylalanine, alanine, valine and leucine to be under-represented at protein binding sites (Ofran and Rost, 2007, Tyagi et al., 2009), whilst arginines have been identified to be over abundant at protein binding sites (Villar and Kauvar, 1994, Ofran and Rost, 2007, Tyagi et al., 2009). Arginines have been implicated in being energetically important for protein binding. Mutation of K90 reduced binding signal intensity of C/EBPα to TRIB2. K90 is a critical lysine for ATP-binding located in subdomain II of the pseudokinase domain and one of the vestiges of an active kinase which TRIB proteins retain (Hegedus et al., 2007). Mutation of K90M ablates the ability of TRIB2 to turnover ATP as measured by autophosphorylation assays (Personal communication, unpublished data, Fiona Bailey and Dr. P. Eyers). It is hypothesised that TRIB proteins retain the ability to bind ATP like a kinase but do not posses sufficient kinase activity to engage in phosphate transfer. Thus K90 was not investigated as a C/EBPα binding site as it had a defined role in TRIB2 ATP-binding and subsequent mutation may perturb the highly conserved functional structure of the TRIB2 kinase-like domain. Thus as arginines have been identified to be strongly involved in protein binding and TRIB2-R77 is homologous to TRIB1-R107 with an already identified link to C/EBPα, TRIB2-R77 from Peptide D was chosen as an amino acid to be investigated for its role in binding C/EBPα. Peptide G Spot 1 (unmutated peptide sequence) displayed low binding intensity with an increase in binding from amino acid Y218A to G232A. This trend was observed in both arrays suggesting Peptide G is important for C/EBPα binding. Mutation of K233A and A234E resulted in a greater than 50 % reduction in binding signal intensity (**Fig 3.2.5 B**). Peptide G (residues 217-234) spanned some of the same amino acids as Peptide H (221-238). Amino acids K233A and A234E were also contained within Peptide H again showing a greater than 50 % reduction in binding intensity. Also within Peptide H mutation of A235E and W238A resulted in a 50 % drop in binding signal intensity (**Fig 3.2.5 C**). Alanines at protein binding sites are selected against as mentioned previously. Initial annotation of this sequence of TRIB2 from its identification on both peptide arrays 1 and 2 (**Fig 3.2.1 and 3.2.2**) identified a putative GSK3 phosphorylation site. SGSYSGKA resembles the consensus GSK3 phosphorylation site motif S/TXXXS/T. Analyses of amino acid identity at protein binding sites revealed an over abundance of serines and glycines at protein binding sites (Ofran and Rost, 2007, Tyagi et al.,

2009). Glycines are common at protein binding sites as they provide flexibility to the region (James and Tawfik, 2003). Serines and glycines are common amino acids in β turns which are prominent 2° structures at protein binding sites (Murakami, 1995, Ofran and Rost, 2007, Murakami and College, 2014). TRIB2 secondary structure analysis confirmed the presence of 2 predicted β turns within the sequence GSYSG (residues 228-232) using Chou and Fasman Secondary structure prediction server (**Appendix 8.1.1)** (Chou and Fasman, 1974). Additional in silico analysis using β turns specific software NetTURN B, identified β turns structures encompassing S227-S231 (Peterson et al., 2010) **(Appendix 8.1.2**). Protein-protein interaction prediction engine (PIPE) analysis predicted amino acids 227-258 in TRIB2 as C/EBPα interaction site (**Appendix 8.2**). PIPE predicts protein interaction sites based on primary protein sequence and comparison of sequences to known interaction sites (Pitre et al., 2006). Combining bioinformatic analyses performed, knowledge of amino acid identity at protein-protein binding sites, peptide array and SASSA results S227/S229/S231/K233 was investigated as a potential C/EBPα binding site. Peptide J displayed the strongest binding signal for C/EBPα on the array. Binding intensity remained high for all alanine substitution within Peptide J, except for substitution of K322A (**Fig 3.2.5 D**). Mutation of K322A resulted in a near complete ablation of binding signal. Thus with such a profound effect of binding this lysine warranted further investigation as a potential C/EBPα binding site on TRIB2.

A

Peptide D (Fig 3.2.5A)

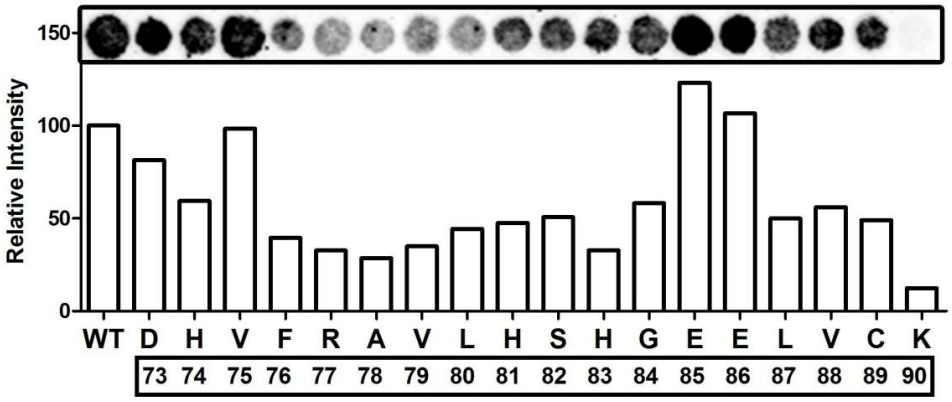

B

Peptide G (Fig 3.2.5 B) ımino Acid Subsituted

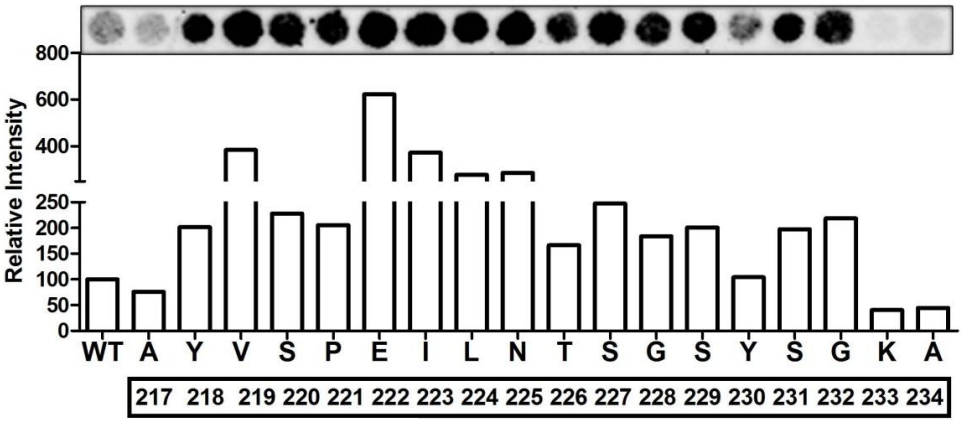

C

Peptide H (Fig 3.2.5 C) nino Acid Subsituted

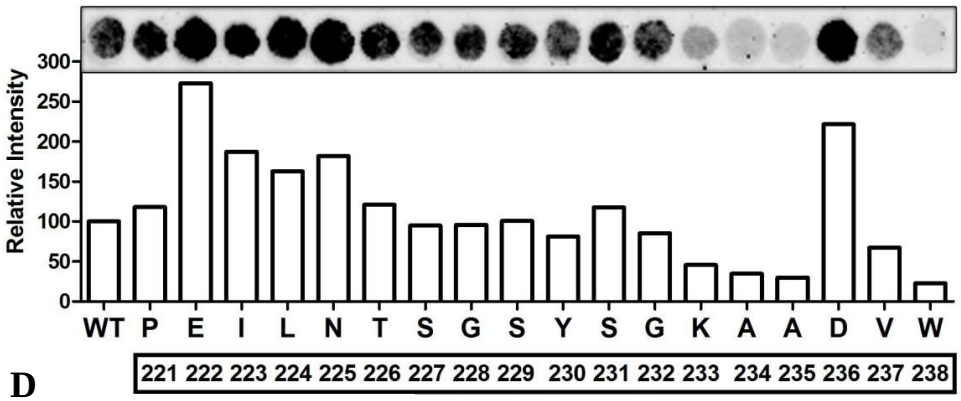

D

Peptide J (Fig 3.2.5 D) nino Acid Subsituted

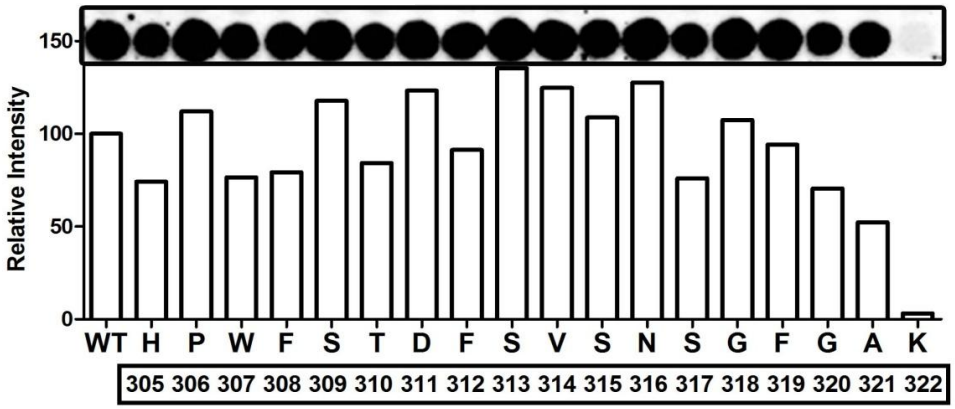

Amino Acid Subsituted

Fig 3.2.5 SASSA of Peptide D, G, H and J. SASSAs were probed with purified C/EBPα protein. The binding of C/EBPα protein to each alanine substituted peptide was quantified by densitometry and presented as relative intensity of the control unmutated WT sequence, with an underlay identifying the amino acid which was substituted with an alanine.

Result 3.2.6 TRIB2 binding mutant expression in HEK293t cells

Based on the results from the SASSA and interpretation of these data three binding mutants were selected for further study, R77A, S227A/S229A/S231A/K233A and K322A (**Fig 3.2.5**). In the absence of 3D structures for interacting proteins the most conclusive method to identify the important residues in an interaction is to experimentally mutate them to alanine and determine any effect these mutations have on the protein interaction (Ofran and Rost, 2007). R77A is located in subdomain I, S227A/S229A/S231A/K233A is located in subdomain VIII and K322A is located in the C-terminus. Mutants were produced by GenScript (USA) in PHMA expression vector backbone (**Fig 3.2.6 A**). In order to determine expression levels and validate antibody recognition of TRIB2 mutants, HEK293t cells were transiently transfected with 4 μg of WT-TRIB2, R77A, S227A/S229A/S231/K233A, K322A and an untransfected lane served as a control to confirm specificity of antibody binding. Both WT-TRIB2 and K322A expression were similar, running at approximately 38 kDa as a tight doublet. S227A/S229A/S231/K233A ran lower than both K322A and WT-TRIB2 as a singlet at 37 kDa. This could be due to mutation of a putative GSK3 phosphorylation site, as it has been known for phosphorylation events to be detected on SDS–PAGE as a doublet and to slightly increase the molecular weight that the protein runs at. R77A expression was the weakest expressing mutant and ran as a single band like S227A/S229A/S231/K233A but higher at approximately the same level of the bottom singlet of WT-TRIB2 and K322A. Actin showed that while there was equal protein loading, TRIB2 mutants were not expressed equivalent to WT-TRIB2 (**Fig 3.2.6 B**). Densitometry of mutant expression relative to Actin levels determined that S227A/S229A/S231/K233A expression was greater than 2 fold R77A expression, whilst K322 and WT-TRIB2 expression was nearly 3 fold stronger than R77A and approximate to each other (**Fig 3.2.6 C**).

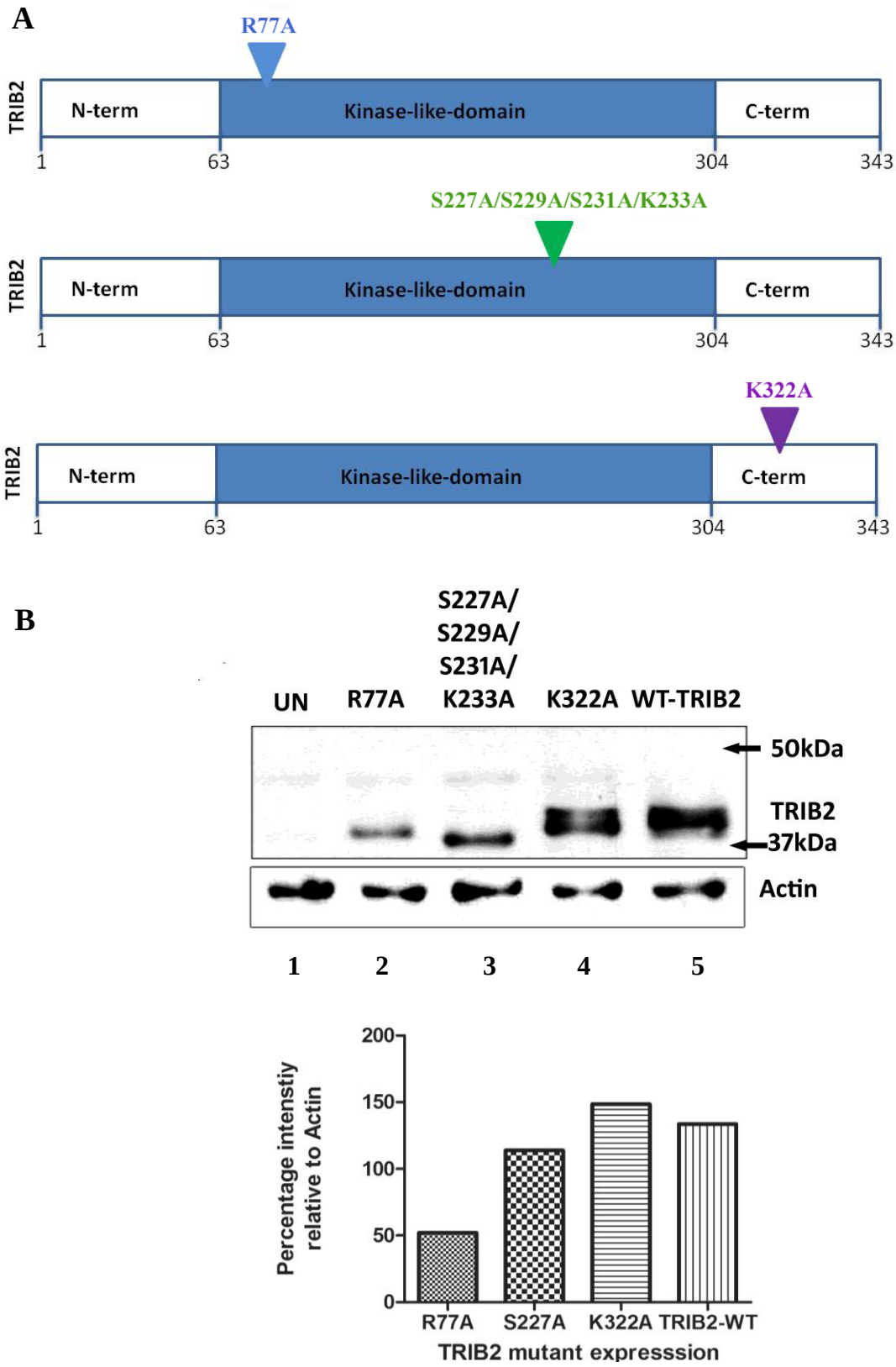

Fig 3.2.6 TRIB2 binding mutant expression in HEK293t cells A) A Schematic diagram of TRIB2 mutants R77A, S227A/S229A/S231A/K233A and K322A. **B)** HEK293t cells were t **C** cted to express WT-TRIB2 and mutants R77A, S227A/S229A/S231A/K233A and K322A. Lysates were collected 24 hrs post transfection and were separated by 12 % SDS-PAGE and

immunoblotted with anti TRIB2 and Actin serving as a loading control. **C**) Densitometry on expression levels of the proteins relative to their respective Actin levels.

Result 3.2.7 TRIB2-S227A/S229A/S231/K233A loses the ability to interact with C/EBPα in vitro.

Having identified potential C/EBPα binding sites on TRIB2 following SASSA (**Fig 3.2.5**) an overexpression co-IP was performed in order assess their importance as C/EBPα binding sites. HEK293t cells were transiently transfected to overexpress 4 μg TRIB2-R77A, TRIB2-S227A/S229A/S231/K233A, TRIB2-K322A, WT-TRIB2 and 4 μg C/EBPα. C/EBPα was immunoprecipitated overnight and the immunoprecipitates were immunoblotted with anti TRIB2 and anti C/EBPα (**Fig 3.2.7 A** top panel). WT-TRIB2 as previously described (**Fig 3.2.1,** (Keeshan et al., 2006) strongly associates with C/EBPα (**Fig 3.2.7 A** lane 3, top panel). Surprisingly mutation of K322A retains TRIB2s ability to interact with C/EBPα (**Fig 3.2.7 A** lane 6); R77A also faintly retained the ability to bind C/EBPα (**Fig 3.2.7 A** lane 4). S227A/S229A/S231A/K233A loses the ability to interact with C/EBPα (**Fig 3.2.7 A** lane 5). Immunoblotting of input lysates with TRIB2 and C/EBPα confirmed the expression of constructs **(Fig 3.2.7 A** bottom panel**)**. Densitometry analysis of TRIB2 immunoprecipitate relative to input expression, determined approximate equal C/EBPα binding to WT-TRIB2 and K322A (**Fig 3.2.7 B)**. R77A immunoprecipitated more strongly with C/EBPα than WT-TRIB2 and K322A, suggesting this mutant may in fact have increased affinity for C/EBPα, which is interesting as the equivalent mutation R107L in TRIB1 is a gain of function mutation associated with increased C/EBPα degradation (Yokoyama et al., 2012). These results show that mutation of TRIB2-S227A/S229A/S231/K233A affects its ability to interact with C/EBPα (**Fig 3.2.7 A and B)**.

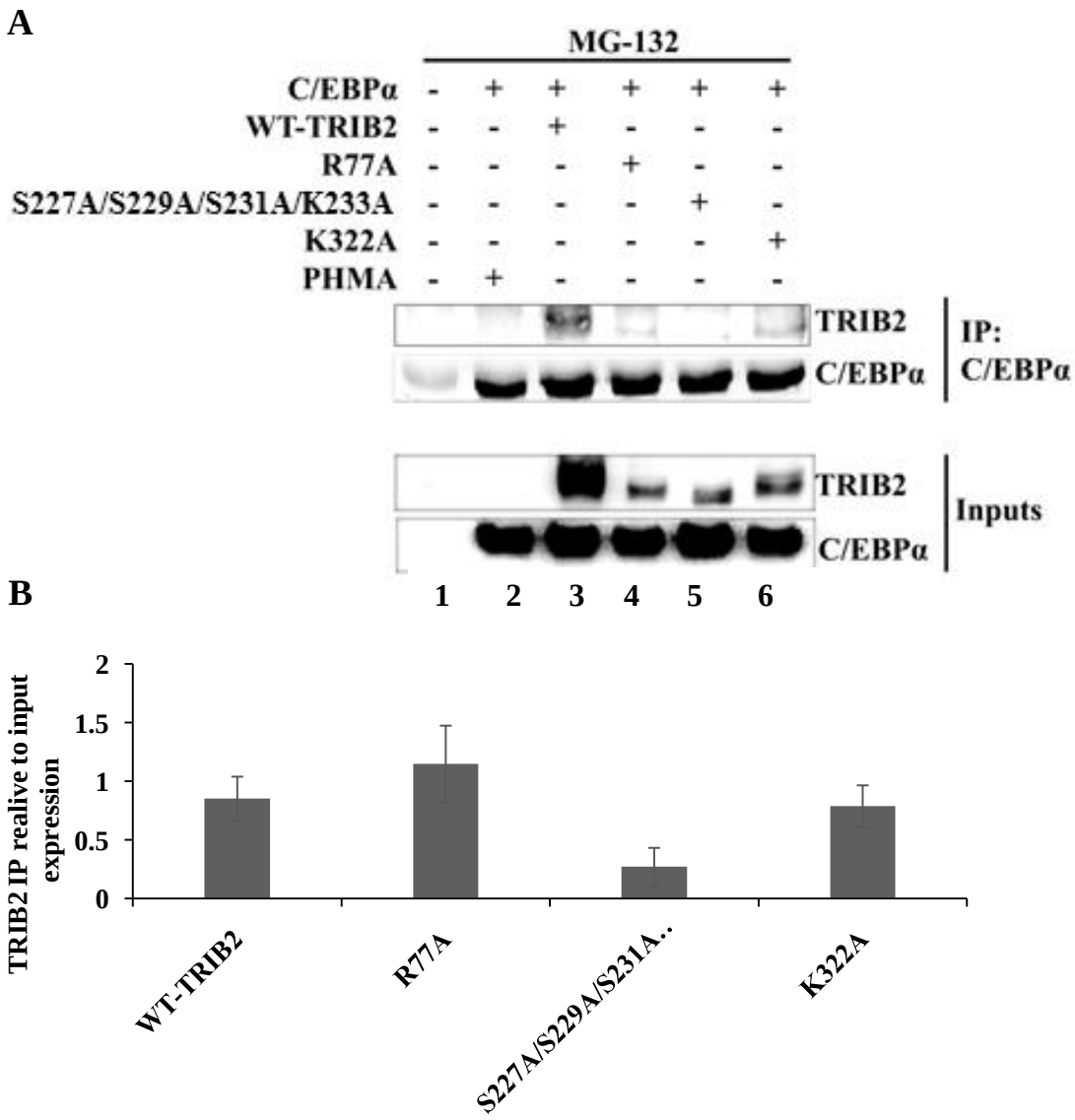

Fig 3.2.7 TRIB2-S227A/S229A/S231A/K233A loses ability to interact with C/EBPα in vivo. **A**) HEK293t cells were transiently transfected with C/EBPα alone and in combination with WT-TRIB2, R77A, S227A/S229A/S231A/K233A and K322A for 24 hrs. Five hours prior to lysate harvest cells were treated with 10 μM MG-132. C/EBPα was immunoprecipitated overnight; lysates were separated by 12 % SDS-PAGE and immunoblotted with anti TRIB2 and anti C/EBPα (top panel). Immunoblot analysis of inputs confirmed expression of all constructs (bottom panel). Data presented is representative of three independent transfection experiments. **B**) Densitometric analysis quantified TRIB2 immunoprecipitation relative to TRIB2 input expression from three independent experiments. The mean of input expression relative to immunoprecipitation of the three experiments was plotted +/- SEM.

Results 3.2.8 C/EBPα R339A loses its ability to interact with TRIB2.

Previous work in the laboratory identified R339 as the TRIB2 binding site on C/EBPα using peptide array analysis, SASSA and subsequent verification by GST-IP using site direct mutant C/EBPα-R339A (**Appendix 8.4**). A schematic diagram indicates the location of R339 within the C-Terminus which is common to both C/EBPαp30 and C/EBPαp42 isoforms of C/EBPα (both isoforms of capable of binding TRIB2 (Keeshan et al., 2006))(**Fig 3.2.8 A**). Therefore, a co-IP assay was performed in mammalian cells to verify the requirement of this amino acid for the interaction between TRIB2 and C/EBPα in mammalian whole cell lysates. HEK293t cells were transfected with 4 μg WT-TRIB2-MYC and 4 μg WT-C/EBPα or C/EBPα-R339A. MYC-TRIB2 was immunoprecipitated and immunoprecipitates were immunoblotted with anti C/EBPα. C/EBPα-R339A does not immunoprecipitate with MYC-TRIB2 (**Fig 3.2.8 B** top panel lane 3), whilst WT-C/EBPα does immunoprecipitate with TRIB2. Immunoblot analysis of input lysates confirmed expression of all constructs (**Fig 3.2.8 B** bottom panel). These results verify previous identification of C/EBPα-R339A as the TRIB2 binding sites and also display evidence of WT-TRIB2 and C/EBPα binding through reciprocal IP.

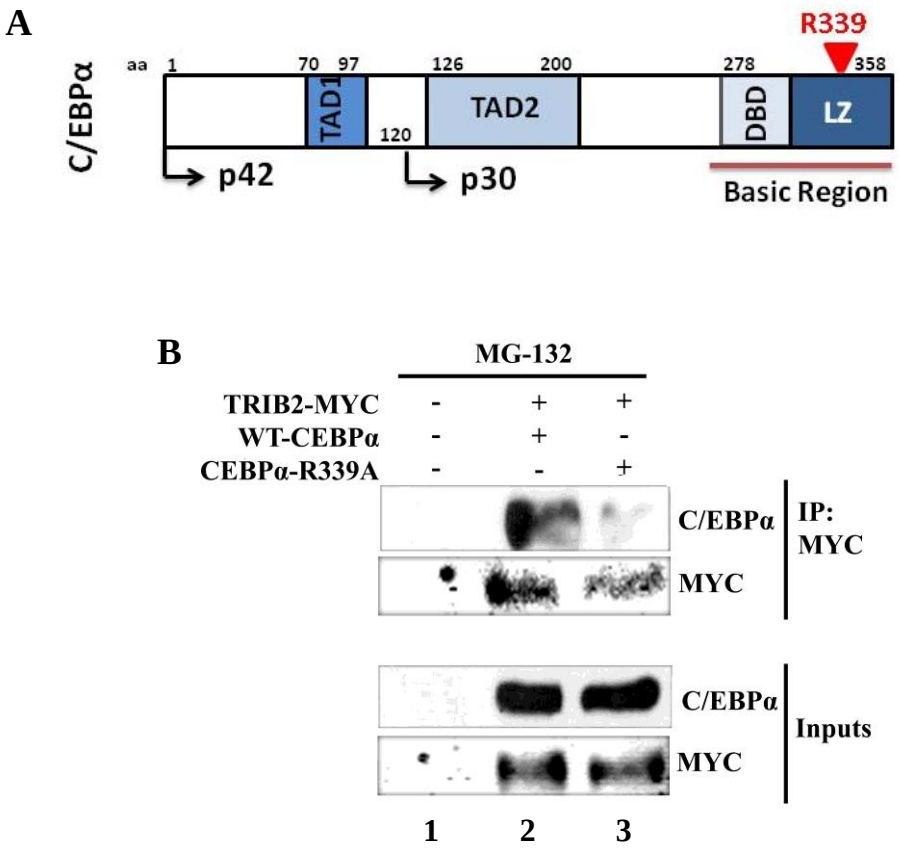

Fig 3.2.8 C/EBPα-R339A loses the ability to interact with TRIB2 in vivo. A) Schematic of C/EBPα highlighting location of R339 and C/EBPαp30, C/EBPαp42 translational start sites. **B)** HEK293t cells were transfected with WT-C/EBPα-WT, C/EBPα-R339A and WT-TRIB2- MYC for 24 hrs. Five hours prior to lysate harvest cells were treated with 10 μM MG-132. MYC was immunoprecipitated overnight, lysates were separated by 12 % SDS-PAGE and immunoblotted with anti MYC and anti C/EBPα.

3.3 Discussion

TRIB2 binds C/EBPα and mediates proteasomal degradation of the C/EBPαp42 isoform increasing levels of the N-Terminally truncated C/EBPαp30 isoform (Keeshan et al., 2006). Disturbance of the C/EBPαp42/p30 ratio results in disruption of myeloid differentiation and AML disease (Keeshan et al., 2006). TRIB2-induced AML is dependent on its proteolytic effect on C/EBPα (Keeshan et al., 2010). Structurally TRIB2 relies on 2 distinct domains for C/EBPα degradation 1) a COP1 binding site in its C-Terminus and 2) an intact kinase-like domain (Keeshan et al., 2010). The N-Terminus was identified not to be essential for TRIB2s functionality (Keeshan et al., 2010). Previous work in our laboratory identified the TRIB2 binding site on C/EBPα at R339. Herein I identify and confirm the amino acid features of the TRIB2:C/EBPα protein-protein interaction to consist of S227A/S229A/S231A/K233A in TRIB2 kinase-like subdomain VIII and R339 in the bZIP domain of C/EBPα.

Examinations of protein-protein interaction amongst family members identified that there is generally a conservation of protein binding localisation amongst protein homologs and the existence of multiprotein binding hotspots (Korkin et al., 2005, Tyagi et al., 2009). Evolution strives to conserve existing biological functions e.g. conservation of the dTrbl and dSlbo interaction identified in Drosophila, but it also strives to generate novel biological functions. dTrbl mediated degradation of dSlbo abrogates the ability of border cells within the ovarian epithelium to migrate during oogenesis resulting in generation of eggs which are unable to be fertilized (Montell et al., 1992). Further investigations revealed conservation of the interaction between mammalian TRIB proteins and C/EBP protein families in different cellular contexts. It was reported that TRIB2 binds and degrades the LAP isoform of C/EBPβ disrupting adipogenesis (Naiki et al., 2007). The N-Terminus of TRIB3 was reported to bind C/EBP homologs protein (CHOP) in response to Endoplasmic reticulum (ER) stresses caused by accumulation of unfolded or misfolded proteins in the ER (Ohoka et al., 2005). Preservation of the biological function of TRIB1 and TRIB2 in mediating leukaemic disease through binding and degradation of C/EBPα places constraints on amino acid sequence identity thus perhaps towards conservation of the C/EBPα binding site. TRIB1 and TRIB2 are the most similar family members in terms of amino acid sequence (71.3 %). Both the N-Terminal regions of the kinase-like domains of TRIB1 and TRIB2 were identified to be essential for maintaining WT-TRIB leukaemic function (Yokoyama et al., 2010, Dedhia et al., 2010).

In order to localise C/EBPα binding site(s) on TRIB2 we generated peptide arrays spanning the entire TRIB2 protein. Comparison of C/EBPα binding regions identified on two independent sets of peptide arrays identified sequences which mostly clustered to the pseudokinase region of TRIB2 protein, a region known to be critical for TRIB2 function (Keeshan et al., 2010, Masoner et al., 2013). Identification of protein binding on a peptide array is suggestive of the binding site being a linear sequence and not a conformational sequence formed by the folding of the protein (Beutling and Frank, 2010). Thus C/EBPα binding to the TRIB2 peptide array indicates that its binding site is a linear sequence and not formed during TRIB2 protein folding. In order to functionally annotate the 6 identified amino acid sequences common to both arrays, TRIB2 sequence was aligned to the TRIB1 sequence to determine if there was any conservation of residues in the regions of TRIB1 identified to be functionally important for C/EBPα binding**.** Subsequently we generated a TRIB2 SASSA which allowed identification of individual amino acid involvement in C/EBPα binding within the stretches of 6 amino acids identified from the peptide arrays. Peptides D, G, H and J were identified to be involved in C/EBPα binding. Sequential mutation of the amino acids within Peptide D to alanine identified a loss in C/EBPα binding upon mutation of amino acids F76-K90 to alanine. Comparisons of the reported prevalence of amino acids common in protein binding sites with TRIB2 functional data narrowed the selection for mutagenesis as a potential C/EBPα binding site. R77 was chosen as a candidate to be investigated from Peptide D. It possessed several qualities promoting its choice 1) arginines are heavily present at protein binding sites, 2) it is homologous to TRIB1-R107 which when mutated increases degradation of C/EBPα and 3) it is located in the N-Terminus of the kinase-like domain supporting the hypothesis of conservation of binding sites within families of proteins (Villar and Kauvar, 1994, Korkin et al., 2005, Ofran and Rost, 2007, Tyagi et al., 2009, Yokoyama et al., 2010). Peptide G and H both spanned the same stretch of amino acids including a putative region of β-turn secondary structure and GSK3 phosphorylation site SGSYSGK. S227/S229/S231/K233 was chosen as a site warranting further investigation from Peptides G and H due to prevalence of serine in protein binding site (Ofran and Rost, 2007), presence of predicted β-turn secondary structures and near complete ablation in binding upon mutation of K233. Mutation of K322 on Peptide J resulted in a complete loss of C/EBPα binding, this was very striking as Peptide J had the strongest binding intensity of all peptides investigated on the array. Thus K322 was chosen as a candidate binding site. Verification of the TRIB2- R77, S227/S229/S231/K233 and K322 role in C/EBPα binding was assessed by co-IP. Surprisingly K322A retained the ability to strongly bind C/EBPα similarly to WT-TRIB2, concluding this lysine had no role in C/EBPα binding, perhaps suggesting that in the folded protein this site may not be accessible. Indeed, initial peptide array analysis identifying C/EBPα binding sites on the TRIB2

array did not include this amino acid suggesting why K322A is not required for C/EBPα binding. Despite lower expression levels of R77A this mutant still retained the ability to bind C/EBPα, and in fact densitometry normalising protein input expression to protein pulldown identified that R77A actually had stronger affinity for C/EBPα. TRIB1-R107L increased C/EBPα degradation a phenomenon suggestive of binding dependency from published data (Yokoyama et al., 2012), therefore TRIB2-R77A possessing increased affinity for C/EBPα may suggest mutation of this amino acid increases TRIB protein affinity for C/EBPα. Mutation of S277A/S229A/S231A/K233A abrogated TRIB2:C/EBPα binding. This sequence is located in subdomain VIII of TRIB2 kinase-like domain. It is not contained in either of the TRIB1 or TRIB2 N-Terminal/N-Terminus kinase-like domain deletion mutants identified to lose their effect on C/EBPα; however both of these mutations involve deletion of a very large portion of the protein (Keeshan et al., 2010, Yokoyama et al., 2010). Their subsequent loss of effect on C/EBPα may be secondary to protein misfolding due to the large deletions and not due to actual loss of the C/EBPα binding site.

With no crystal structure currently available for TRIB2 it is not possible to identify where these amino acids lie within the folded conformation of the protein or if these amino acids are exposed for direct interactions. Analysis using SARPRED: Real Value prediction of surface accessibility software generates a prediction of solvent-accessible surface area amino acids (ASA) and also the extent to which an amino acid is buried in and involved in protein folding (Durham et al., 2009). The ASA score is generated by performing PSI-BLAST which compares distant relationships between proteins and then predicts the secondary structure of a protein from its amino acid sequence (Garg et al., 2005). Provisional analysis of TRIB2 to identify the probability of the identified residues being on the surface of the protein generated ASA scores of S227=39, S229=23, S231=35 and K233=55 (**Appendix 8.3**). K233 generated the highest ASA score of 55. The high scores of S227=39, S231-35 and K233-55 indicate strong evidence for their presence on the exposed surface necessary for protein interactions. Also as previously mentioned serine and glycine residues are frequently identified in β-turn secondary structures (Ofran and Rost, 2007, Murakami, 1995). β-turns are proposed to be favourable secondary structure of protein binding sites. β-turns structures were predicted within SGSYSGK sequence (**Appendix 8.1 and 8.1.2**). PIPE analysis identified TRIB2 amino acids 227-258 to be involved in the TRIB2 and C/EBPα interaction (**Appendix 8.2**). Together, the in silico and in vitro experimental data strongly support the importance of S227/S229/S231/K233 in the interaction between TRIB2 and C/EBPα.

Gene expression analysis of 285 AML patients identified a cohort of patients which had dysregulated C/EBPα signature (Keeshan et al., 2006). However within this cohort not all patients had mutated C/EBPα, and it was identified that patients with WT-C/EBPα had high *TRIB2* expression explaining the dysregulated C/EBPα signature in these AML patients (Keeshan et al., 2006). With increasing demand for personalised target therapies, small molecule inhibitors of protein binding may provide a novel specific approach and offers huge therapeutic potential. Current antibody based therapies while highly specific to their molecular interaction are difficult and costly to manufacture and have problems permeablising the cell wall. Small molecule protein-protein inhibitors overcome these problems but are currently an under-used option due to the lack of well defined binding pockets (reviewed by (Arkin and Wells, 2004)). Targeted inhibition of the TRIB2-C/EBPα interaction may provide a therapeutic opportunity for such elevated TRIB2 AMLs with a dysregulated C/EBPα signature. In summary, in this study I identify and confirm the TRIB2 and C/EBPα reciprocal binding sites as R339 on C/EBPα and S227/S229/S231/K233 on TRIB2 which may be an opportunity to develop such targeting therapies.

Chapter 4: Results

TRIB2-mediates K48 ubiquitin-dependent degradation of C/EBPαp42

4.1 Introduction

C/EBPα is a crucial regulator of haematopoiesis controlling the self-renewal capacity of HSCs and mediating GMP differentiation of myeloid cells (Zhang et al., 1998, Zhang et al., 2004, Ye et al., 2013, Hasemann et al., 2014). C/EBPα is often referred to as a gatekeeper gene in AML, as loss of functional C/EBPα results in uncontrolled proliferation of immature myeloid precursor cells (reviewed by (Reckzeh and Cammenga, 2010)). C/EBPα may be disrupted by several modalities: suppression of transcription, post-transcriptional modification, post-translational modification and DNA mutations affecting protein functionality (summarised in **Fig 4.1.1** adapted from (Reckzeh and Cammenga, 2010)). C/EBPα is reported to be mutated in approximately 5-14 % of cytogenetically normal AMLs (Taskesen et al., 2011). Mutations predominately occur either in the N-terminus, resulting in an out-of-frame shift generating the C/EBPαp30 truncated protein. Mutations also occur in the C-Terminus affecting C/EBPα ability to bind DNA and to dimerise. C/EBPα mutations are predominately associated with AML FAB subtypes M1 and M2 (Fasan et al., 2014). To date post-translational modifications identified to functionally disrupt C/EBPα include phosphorylation (to be discussed in Chapter 5), sumoylation and ubiquitination. The focus of this chapter is post-translational modification of C/EBPαp42 through TRIB2-mediated ubiquitination.

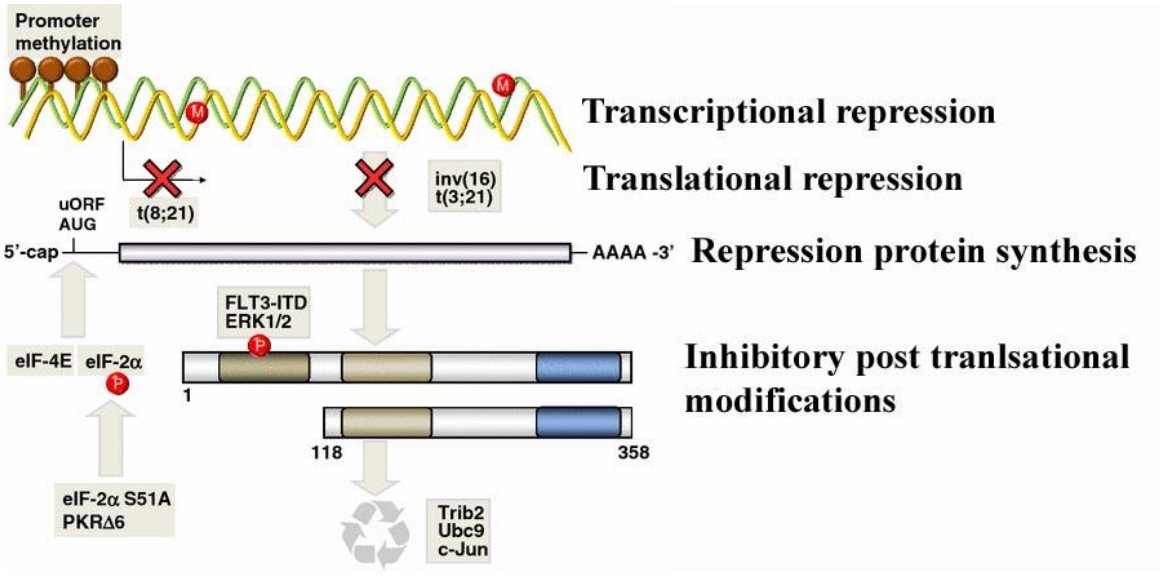

Fig 4.1.1 Schematic diagram of C/EBPα deregulation in AML adapted from (Reckzeh and Cammenga, 2010).

Ubiquitination is a highly regulated ATP dependent process, involving the covalent attachment of 76 amino acid ubiquitin polypeptide(s) to a substrate protein. Ubiquitination triggers a plethora of effects within the cell but predominately signals the target protein for proteasomal degradation.

Ubiquitin is conjugated through the formation of a thioester bond between C-Terminal of ubiquitin (G76) and ε amino side chain of a lysine on the target protein (Hershko et al., 1983). Lysine is the predominate amino acid identified to serve as the ubiquitin conjugation site on a protein. However the amino acids cysteine, threonine, serine and the free ε amino side chain at the N-Terminal of a protein have also been identified to bind ubiquitin in rare cases (Cadwell and Coscoy, 2005, Scaglione et al., 2013). Single ubiquitin polypeptides may be conjugated (mono or multi-monoubiquitination) or polymers of ubiquitin may be conjugated termed polyubiquitination (Schematic **Fig 4.1.2**). There are several species of ubiquitination which are determined by the identity of the lysine in ubiquitin which forms the polychain linkage with the adjacent ubiquitin (K6, K11, K27, K29, K33, K48 and K63). K48 ubiquitination signals proteasomal degradation and four K48 linked ubiquitin polypeptides are the minimum length polychain recognised by the proteasome (Chau et al., 1989, Pickart, 1997, Thrower et al., 2000). K63 ubiquitination triggers endocytosis, protein trafficking and DNA repair responses but not proteasomal degradation (Schematic **Fig 4.1.2**) (reviewed by (Chen and Sun, 2009)). K48 and K63 to date are the most widely studied ubiquitin polychains.

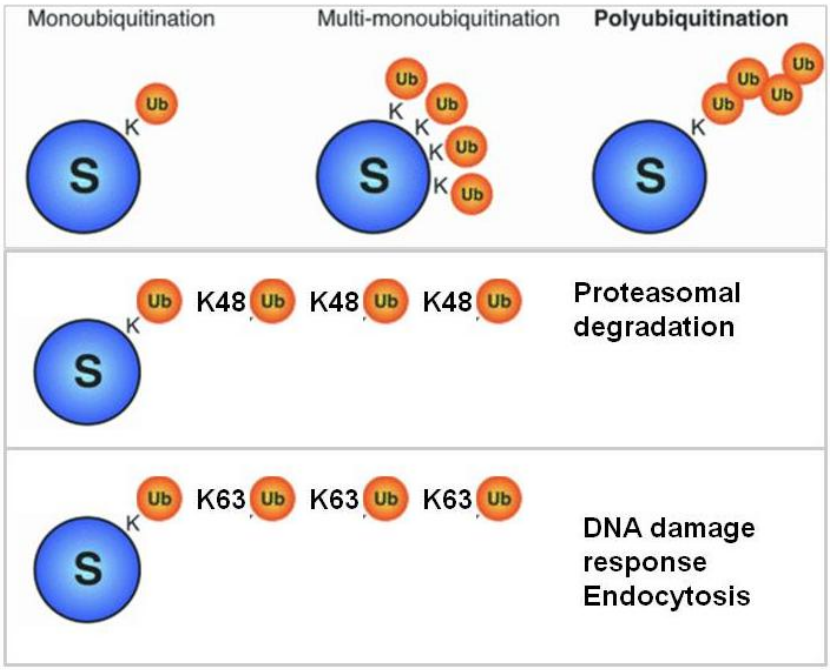

Fig 4.1.2 Schematic of mono- and poly-ubiquitination.

Conjugation of ubiquitin to a substrate protein involves the hierarchical action of three enzymes, E1, E2 and E3 ubiquitin ligases. A cell is estimated to contain only 2 E1, 37 E2 and >600 E3 ligases, which can tightly control the UPS through stringent substrate identification (Deshaies and

Joazeiro, 2009). The 26S proteasome is the primary site of controlled protein proteolysis within the cell. The proteasome is comprised of 2 multisubunit components, the 20S and the 19S regulatory subunit. Upon proteasome binding the polyubiquitinated protein is degraded rapidly thus promptly and irreversibly terminating any signal transduction propagated by the protein. C/EBPα has been identified to be targeted by the UPS as a result of direct binding to a number of E3 ligases and also through associations with adaptor proteins which facilitate subsequent ubiquitination in a variety of mammalian tissues.

Mammalian C/EBPα was first identified to be ubiquitinated in keratinocytes upon Lithium induced proteasomal inhibition (Shim and Smart, 2003). To date the E3 ligases E6AP and FBXW7 have been identified to directly bind C/EBPα mediating its ubiquitination (Bengoechea-Alonso and Ericsson, 2010, Pal et al., 2013a, Pal et al., 2013b). The E3 ligases COP1 and TRIM21 have also been identified to degrade C/EBPα however in an adaptor protein dependent manner (Yokoyama et al., 2010, Keeshan et al., 2010, Grandinetti et al., 2011, Yoshida et al., 2013). Additionally the phosphorylation status of C/EBPα has been linked to its ubiquitination in response to various proteins. PKCδ and JNK1 have been reported to mediate ubiquitination of C/EBPα upon phosphorylation and dephosphorylation in response to apoptosis induction and stress signal responses in AML cells (Trivedi et al., 2006, Zhao et al., 2009, Wu et al., 2013).

E6AP was identified as an E3 ligase upregulated in Tamoxifen treated Henrietta Lacks (HeLa) cells with a resultant decrease in C/EBPα protein levels (Cheng et al., 2007). E6AP was identified to directly bind C/EBPα mediating its ubiquitination in myeloid cells and in adipocytes resulting in a block in cell differentiation (Pal et al., 2013a, Pal et al., 2013b). Mutation of E6AP catalytic site C834A abrogated C/EBPα ubiquitination (Pal et al., 2013a, Pal et al., 2013b). Knockdown of E6AP or overexpression of E6AP-C834A induced myeloid differentiation of U937 cells, K562 and 32Dcl3 cells through increasing C/EBPα protein expression (Pal et al., 2013b). While similarly knockdown of E6AP or E6AP-C834A overexpression promotes adipocyte differentiation through increasing C/EBPα protein levels (Pal et al., 2013a).

FBXW7 is a tumour suppressor controlling the expression of C-MYC, NOTCH1, Cyclin E and C-jun (Koepp et al., 2001, Wei et al., 2005, Malyukova et al., 2007, Welcker and Clurman, 2008). Inactivating FBXW7 mutations are frequently associated with activated NOTCH1 T-ALL disease (Kraszewska et al., 2012). Interestingly elevated levels of *TRIB2* have been identified in a cohort of paediatric T-ALL patients which harbour NOTCH1 or FBXW7 mutations (Hannon et al., 2012). Differential phosphorylation has been reported to both protect and promote UPS degradation of

C/EBPα (Trivedi et al., 2006, Bengoechea-Alonso and Ericsson, 2010, Wu et al., 2013). FBXW7 has been identified to mediate ubiquitination through recognition of a phosphodegron motif. FBXW7 only binds and mediates ubiquitination of C/EBPα upon phosphorylation of residues Thr222/Thr226 resulting in the inhibition of adipocyte differentiation (Bengoechea-Alonso and Ericsson, 2010).

Induction of apoptosis through PKCδ cleavage and Caspase-3 activation results in UPS degradation of C/EBPα in AML cells (Zhao et al., 2009). PKCδ was identified to mediate phosphorylation of C/EBPα, disrupting C/EBPα nuclear localisation resulting in proteasomal degradation (Wu et al., 2013). Alternatively activated JNK1 in response to stress signals was identified to bind C/EBPα resulting in phosphorylation through an unidentified site, mediating a decrease in levels of C/EBPα ubiquitination and increasing protein stability, whilst inactive JNK1 which does not phosphorylate C/EBPα resulted in an increase in the levels of ubiquitinated protein (Trivedi et al., 2006).

TRIB proteins are often reported to function as scaffold or adaptor proteins as they facilitate the formation of multiprotein binding complexes. dTrbl mediates binding dependent ubiquitination of dSlbo in border cells of Drosophila (Rørth et al., 2000, Masoner et al., 2013). Evolutionary conservation of this relationship is evident by both TRIB1- and TRIB2- mediating proteasomal degradation of C/EBPαp42 but this proteolysis is dependent on TRIB E3 ligase binding (Yokoyama et al., 2010, Keeshan et al., 2010, Grandinetti et al., 2011). Overexpression of TRIB1 and TRIB2 in BMTs results in AML disease with TRIB leukaemogenecity dependent on the E3 ligase COP1. Loss of the COP1 binding site on TRIB1 and TRIB2 through deletion, mutation or expression of dominant negative isoforms of COP1 relieves TRIB1 and TRIB2 proteolytic effect on C/EBPα (Keeshan et al., 2010, Yokoyama et al., 2010, Yoshida et al., 2013). Overexpression of COP1 in the presence of TRIB1 expression was identified to mediate ubiquitination of C/EBPα inhibiting myeloid differentiation and reported to reduce the latency of TRIB1 mediated AML in BMTs (Yoshida et al., 2013). Knockdown of TRIB1 abrogated the effects of overexpressed COP1 in AML cells (Yoshida et al., 2013). Similarly TRIM21 was identified as an E3 ligase inducing degradation of C/EBPα in a TRIB2 dependent manner in NSCLS (Grandinetti et al., 2011). Overexpression of TRIM21 did not mediate degradation of ectopically expressed C/EBPα but co-expression of TRIB2 and TRIM21 mediated degradation of C/EBPα (Grandinetti et al., 2011). Thus TRIB proteins facilitate ubiquitination and proteasomal degradation of C/EBPα through binding an E3 ligase and through direct binding to C/EBPα. To date there are no published reports on the effects of TRIB2 on the ubiquitination status of C/EBPα.

C/EBP family members are highly homologous within their C-Terminal leucine zipper. The leucine zipper allows for formation of homo and heterodimers between C/EBP proteins and other proteins which contain leucine zippers such as C-fos and C-Jun (Williams et al., 1991, Hsu et al., 1994). Dimer formation was reported to stabilize C/EBPζ and C/EBPγ as it prevented ubiquitin-dependent degradation (Hattori et al., 2003). An intact leucine zipper region, mediating dimerisation, was identified to be essential for ubiquitination of C/EBPδ, however this ubiquitination was reported to not correlate with increased degradation (Zhou and Dewille, 2007). Thus there is not a consensus pattern of behaviour regarding C/EBP ubiquitination upon dimerisation. In frame C-Terminal C/EBPα AML patient mutations affecting the ability of C/EBPα to dimerise are frequently identified. Investigation of the functional role of monomeric C/EBPα revealed it inhibits C/EBPα ability to induce monopoiesis when ectopically expressed in lineage negative murine cells (Wang et al., 2006a). Thus monomeric C/EBPα does not function similarly to dimeric C/EBPα. C/EBPα dimer formation was also identified to vary with its nuclear localisation and in response to environmental stresses (Schaufele et al., 2003). There have been no reports to date investigating the ubiquitination and subsequent proteasomal degradation of monomeric C/EBPα or investigation of TRIB2 effect on monomeric C/EBPα.

Aim

TRIB2 has been reported to mediate proteasomal degradation of C/EBPα in an E3 ligase dependent manner. However there have been no investigations detailing the molecular biology of this proteolytic relationship. In this study I present the first reports of C/EBPα K48 ubiquitin-dependent degradation and of TRIB2-mediated K48 ubiquitination of C/EBPα identified by performing in vivo overexpression ubiquitination assays. I identified that TRIB2 and C/EBPα direct binding is essential for TRIB2-mediated ubiquitination having previously identified the amino acid features involved in the interaction as TRIB2-S227A/S229A/S231/K233A and C/EBPα-R339. In vivo ubiquitination assays identified TRIB2-S227A/S229A/S231/K233A was unable to mediate ubiquitination of WT-C/EBPα and C/EBPα-R339A was unable to be ubiquitinated by WT-TRIB2. I also verified that COP1 is the bona fida E3 ligase used by TRIB2 for ubiquitination of C/EBPα as TRIB2-VPM cannot mediate ubiquitination of C/EBPα. I propose that K313 is the potential site of ubiquitin conjugation on C/EBPα as K313R was unable to be ubiquitinate by TRIB2. I also determined TRIB2 preferentially ubiquitinates dimeric C/EBPα over monomeric C/EBPα despite the ability of TRIB2 to bind both monomeric and dimeric C/EBPα.

Result 4.2.1 Overexpression of TRIB2-mediates increased ubiquitination of overexpressed C/EBPα

Previous data determined TRIB2-mediated the proteasomal degradation of C/EBPαp42 and this proteolytic relationship is dependent on COP1 E3 ligase binding to TRIB2, suggesting TRIB2 may mediate ubiquitin-dependent degradation of C/EBPα (Keeshan et al., 2006, Keeshan et al., 2010). However, it is incorrect to assume the proteasomal degradation process is ubiquitin-dependent. Recently a growing list of proteins have been identified which undergo proteasomal degradation in an ubiquitin-independent manner, e.g. ornithine decarboxylase, p21, and C/EBPδ (Hoyt et al., 2003, Chen et al., 2004, Zhou and Dewille, 2007). In order to determine if TRIB2 was in fact mediating ubiquitination of C/EBPα an in vivo ubiquitination assay was performed in HEK293t cells transiently transfected to overexpress C/EBPα-MYC, TRIB2-FLAG and Ubiquitin (Ub)-HA. Upon treatment with the proteasome inhibitor MG-132 the levels of ubiquitinated C/EBPα increased as determined by immunoblotting for HA and evident by the polyubiquitinated smear in lane 3 versus the untreated ubiquitination levels in lane 2 (**Fig 4.2.1** top panel). Ubiquitination levels in lane 3 determine the basal ubiquitination status of C/EBPα in the cell, suggesting ubiquitination may serve to control protein turnover of C/EBPα in a wildtype environment. Overexpression of TRIB2 in the presence of MG-132 (**Fig 4.2.1** lane 5) increased the ubiquitination of C/EBPα versus C/EBPα in the absence of TRIB2 (**Fig 4.2.1** lane 3). Immunoblotting for TRIB2 and C/EBPα confirm input protein expression and equal Actin levels confirmed equal protein loading (**Fig 4.2.1** bottom panel). Overexpression of TRIB2 does not mediate degradation of overexpressed C/EBPα as detected in protein inputs in HEK293t cells in the in vivo ubiquitination assay, highlighting a limitation of this assay. In all cell systems/murine models with endogenous C/EBPα expression TRIB2-mediates proteasomal degradation (Keeshan et al., 2006, Keeshan et al., 2010, Rishi et al., 2014). This is proposed to be due to highly expressive nature of the HEK293t cells, transfection of highly expressive constructs and perhaps due to a protein overload of the proteasome. The in vivo ubiquitination assay is optimised and published for identifying ubiquitination (Carmody et al., 2007). Thus it may now be stated that TRIB2-mediates increased ubiquitination of C/EBPα.

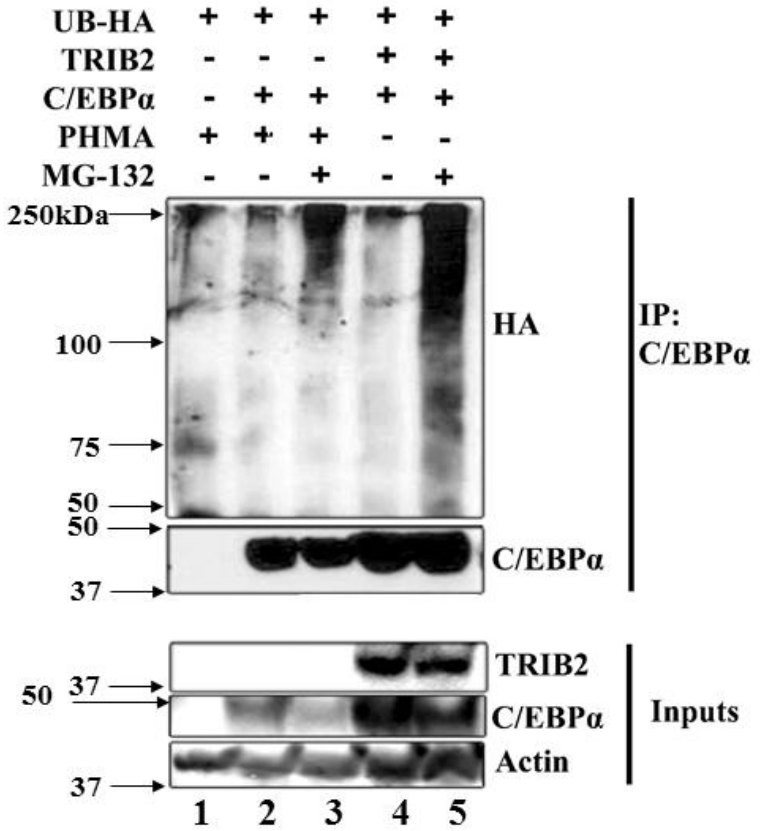

Fig 4.2.1 TRIB2-mediates increased ubiquitination of C/EBPα HEK293t cells were transfected to overexpress Ub-HA, TRIB2, C/EBPα and PHMA served as an empty vector control. Indicated samples were treated with 10 μM MG-132 5 hrs prior to harvesting lysates. C/EBPα was immunoprecipitated and an in vivo ubiquitination assay was performed. Lysates were separated by SDS-PAGE and immunoblotted for anti HA. Immunoblotting for anti TRIB2 and anti C/EBPα detects input levels and Actin serves as a loading control (bottom panel). Representative molecular weight markers in kDa are presented for ubiquitination blots and TRIB2, C/EBPα and Actin immunoblots presented herein. Data presented is representative of three independent transfection experiments. The mean fold increase in C/EBPα ubiquitination in the presence of TRIB2 is 3.4 +/- 0.43 SEM.

Result 4.2.2 TRIB2-mediates K48 specific ubiquitination of C/EBPα as determined by ubiquitin polychain specific antibodies

In order to determine the type of ubiquitination mediated by TRIB2, immunoprecipitates were immunoblotted using antibodies specific to K48 and K63 polychains of ubiquitination. K48 ubiquitination polychains target the substrate protein for proteasomal degradation (Pickart, 1997), while K63 ubiquitination induces endocytosis, regulates protein localisation and protein-protein interactions (Arnason and Ellison, 1994, Mukhopadhyay and Riezman, 2007). An in vivo ubiquitination assay was performed in HEK293t cells transiently transfected to overexpress C/EBPα, TRIB2 and Ub-HA. C/EBPα was immunoprecipitated and lysates were immunoblotted with an antibody specific to K48 ubiquitin polychain (**Fig 4.2.2 A**). Additionally the membrane from **Fig 4.2.1** was stripped and incubated with an antibody specific to K63 ubiquitin polychain (**Fig 4.2.2 A** and **B**). Overexpression of TRIB2 mediated an increase in K48 ubiquitination of C/EBPα (**Fig 4.2.2 A** lane 4 and 5 top panel). K48 ubiquitination signal was stronger than detection of ubiquitination through immunoblotting for HA from the overexpression WT-Ub-HA construct as K48 antibody detects both endogenous K48 ubiquitination and K48 ubiquitination expressed from the WT-Ub-HA expression construct. Immunoblotting for K63 antibody determined that TRIB2 was not mediating an increase in K63 ubiquitination (**Fig 4.2.2 B**). TRIB2 thus mediates K48 specific ubiquitin-dependent degradation of C/EBPα.

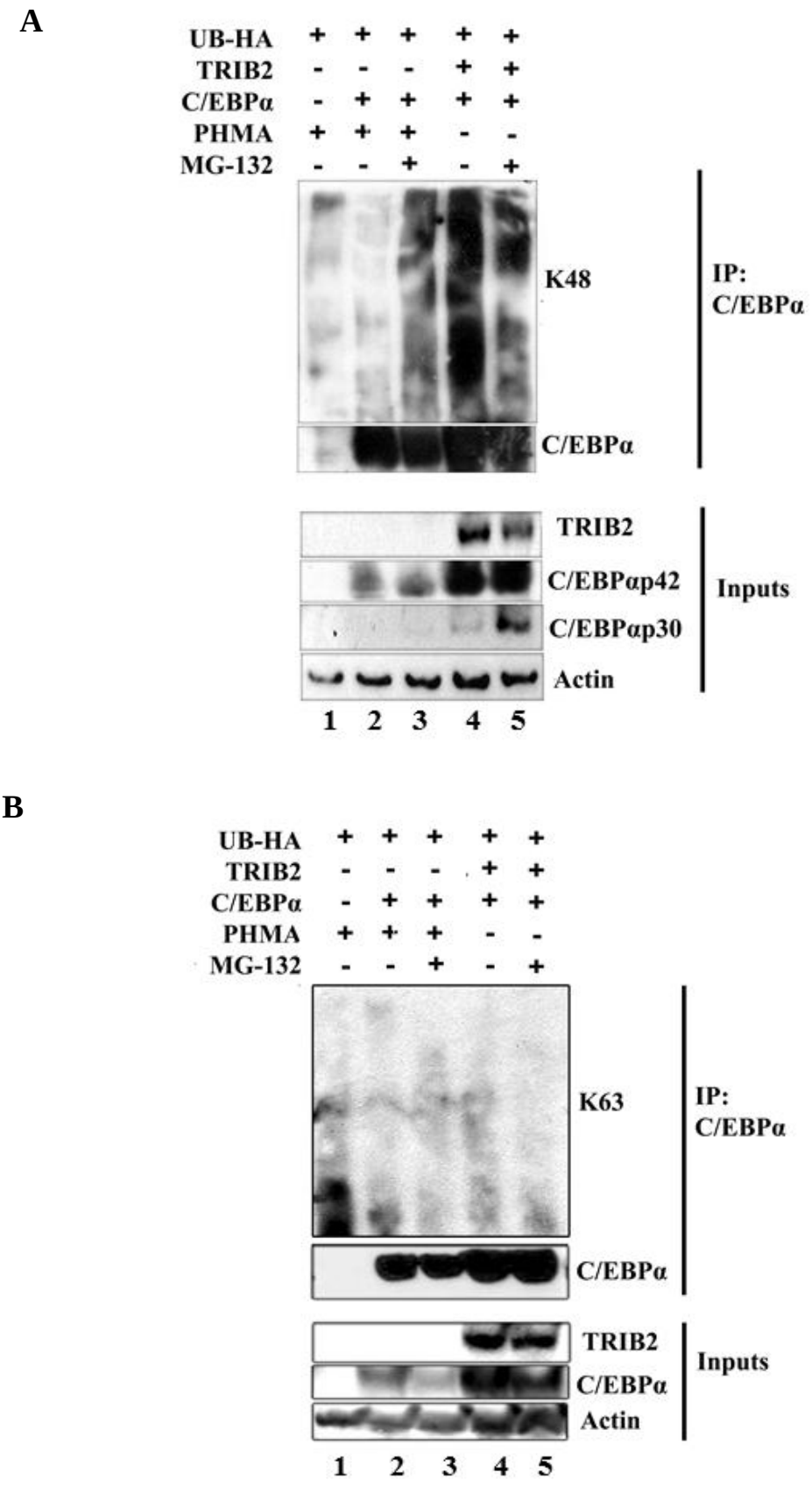

Fig 4.2.2 TRIB2 mediates increased K48 ubiquitination of C/EBPα. HEK293t cells were transfected to overexpress Ub-HA, TRIB2, C/EBPα and PHMA empty vector control. Indicated

samples were treated with 10 μM MG-132 5 hrs prior to harvesting lysates. C/EBPα was immunoprecipitated and an in vivo ubiquitination assay was performed. Lysates were separated by SDS-PAGE and immunoblotted for **A)** anti K48 and **B)** anti K63 species of ubiquitination. Immunoblotting input lysates confirms expression of TRIB2 and C/EBPα and Actin confirmed equal protein loading. Data presented is representative of three independent transfection experiments.

Result 4.2.3 TRIB2-mediates K48 specific ubiquitination of C/EBPα as determined by ubiquitin polychain mutants

In order to confirm the TRIB2 mediated K48- and not K63- specific ubiquitination of C/EBPα by another method an in vivo ubiquitination assay was performed including ubiquitin mutants which do not express the K48 ubiquitin polychain (K48R) and the K63 ubiquitin polychain (K63R). Immunoprecipitation of C/EBPα in cells transfected to expression UB/K63R alone produced a very strong background signal subsequent to immunoblotting for anti HA (**Fig 4.2.3** lane 3). Immunoprecipitation of C/EBPα in cells transfected to express WT-Ub-HA and UB/K48R did not produce any background signal upon immunoblotting for anti HA. Thus when characterising the effect of UB/K63R on C/EBPα ubiquitination changes relative to the background signal in lane 3 were assessed. Overexpression of UB/K48R was unable to mediate ubiquitination of C/EBPα in the presence of TRIB2 (**Fig 4.2.3** lane 8). Both WT-Ub and UB/K63R mediated increased ubiquitination of C/EBPα in the presence of TRIB2 versus C/EBPα alone (**Fig 4.2.3** lane 4 and lane 6, lane 7 and lane 9) as both ubiquitin constructs express the K48 polychain. Overexpression of TRIB2-mediated an increase in C/EBPα ubiquitination in the presence of WT-Ub (lane 7) and UB/K63R (lane 9) but not in the presence of UB/K48R (lane 8) (**Fig 4.2.3** top panel). Immunoblotting for anti TRIB2 and anti C/EBPα confirmed equal input expression and immunoblotting for Actin confirmed equal protein loading (**Fig 4.2.3** bottom panel). Thus this validates TRIB2-mediates K48 and not K63 specific ubiquitination of C/EBPα resulting in its proteasomal-dependent degradation.

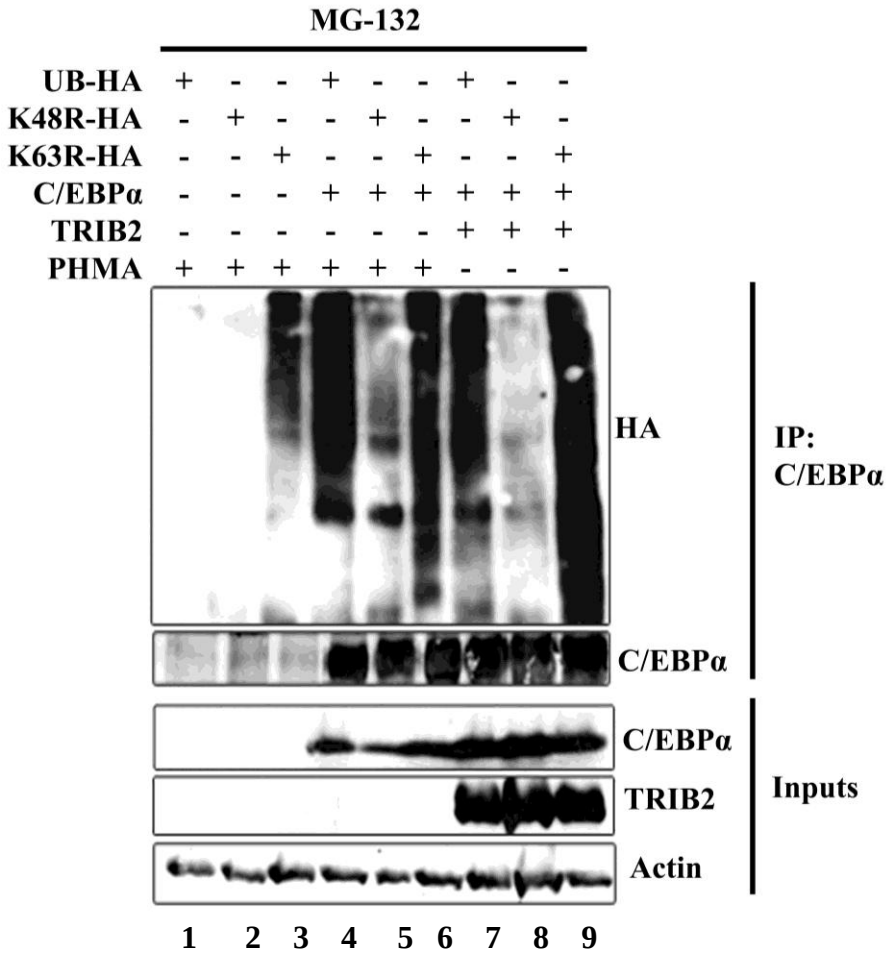

Fig 4.2.3 TRIB2-mediates increased K48 ubiquitination of C/EBPα. HEK293t cells were transfected to overexpress Ub-HA, UB/K48R-HA, UB/K63R-HA, TRIB2, C/EBPα and PHMA empty vector control. Cells were treated with 10 μM MG-132 5 hrs prior to harvesting lysates. C/EBPα was immunoprecipitated and an in vivo ubiquitination assay was performed. Lysates were separated by SDS-PAGE and immunoblotted for anti HA. Immunoblotting input lysates confirms expression of TRIB2 and C/EBPα and Actin confirms equal protein loading. Data presented is representative of one independent transfection experiments.

Result 4.2.4 TRIB2 is unable to mediate ubiquitination of C/EBPα-R339A

R339 was identified as the TRIB2 binding site on C/EBPα (unpublished data, Ciaran Forde, Dr. Karen Keeshan, **Appendix 8.4**, **Fig 3.2.8 B**). Thus analysis of the ubiquitination profile of C/EBPα-R339 in the presence of TRIB2 would determine if TRIB2 binding was essential for its ubiquitin-dependent degradation of C/EBPα. An in vivo ubiquitination assay was performed overexpressing WT-Ub-HA, WT-C/EBPα, C/EBPα-R339A and C/EBPα-R343A in the presence of TRIB2 in HEK293t cells treated with MG-132. C/EBPα-R343A was identified as a potential TRIB2 binding site by SASSA however GST-IP verification revealed it retained the ability to bind GST-TRIB2 (unpublished data, Ciaran Forde **Appendix 8.4**). WT-C/EBPα was ubiquitinated in the presence of TRIB2 as was R343A mutant which retained the ability to interact with TRIB2 (**Fig 4.2.4** lane 1 and lane 3 top panel), however R339A was not ubiquitinated in the presence of TRIB2 (**Fig 4.2.4** lane 2 top panel) indicating that TRIB2 and C/EBPα binding is essential for TRIB2-mediated ubiquitination and proteasomal degradation of C/EBPα. Immunoblotting for TRIB2 and C/EBPα confirmed equal input expression and immunoblotting for Actin confirmed equal protein loading (**Fig 4.2.4** bottom panel).

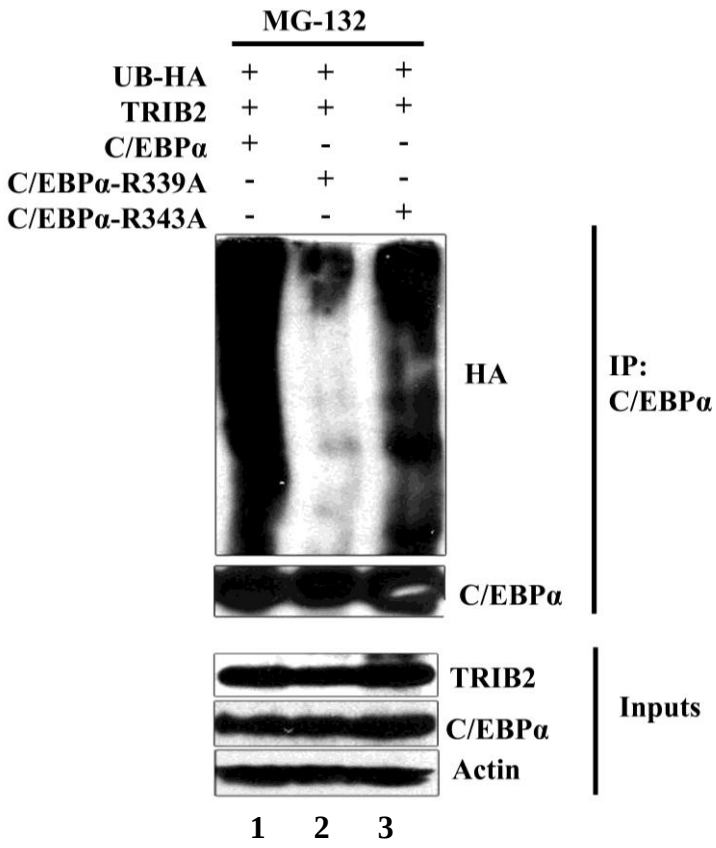

Fig 4.2.4 TRIB2:C/EBPα binding is essential for mediating ubiquitination. HEK293t cells were transfected to overexpress WT-C/EBPα, C/EBPα-R339A and C/EBPα-R343A in the presence of overexpressed TRIB2 and Ub-HA. Cells were treated with 10 μM MG-132 5 hrs prior to harvesting lysates. C/EBPα was immunoprecipitated and an in vivo ubiquitination assay was performed. Lysates were separated by SDS-PAGE and immunoblotted for anti HA. Immunoblotting input lysates confirms expression of TRIB2 and C/EBPα and Actin confirmed equal protein loading. Data presented is representative of two independent transfection experiments.

Result 4.2.5 TRIB2-S277A/S229A/S231A/K233A is unable to mediate ubiquitination of C/EBPα

Direct TRIB2 and C/EBPα binding was determined as a requisite for TRIB2-mediated ubiquitination of C/EBPα (**Fig 4.2.4**), thus in order to validate the identification of S227A/S229A/S231A/K233A (**Fig 3.2.7**) as a region responsible for C/EBPα interaction with TRIB2 an in vivo ubiquitination assay was performed. HEK293t cells were transfected to express WT-Ub-HA, WT-C/EBPα, WT-TRIB2, TRIB2-R77A, TRIB2-S227A/S229A/S231A/K233A and TRIB2-K322A and treated with MG-132 for 5 hrs. TRIB2-R77A and TRIB2-K322A retained the ability to directly bind C/EBPα (**Fig 3.2.7).** Immunoblotting for HA determined TRIB2-S227A/S229A/S231A/K233A is unable to mediate ubiquitination of C/EBPα, unlike TRIB2-R77A and TRIB2-K322A mutants which both retained the ability to mediate ubiquitination of C/EBPα, similar to WT-TRIB2 (**Fig 4.2.5** top panel). Immunoblotting protein inputs for C/EBPα expression determined overexpression of TRIB2-R77A and TRIB2-K322 mediated an increase in C/EBPαp30; however TRIB2-S227A/S229A/S231A/K233A did not increase C/EBPαp30 levels similar to WT-TRIB2 (**Fig 4.2.5** bottom panel). Thus TRIB2 and C/EBPα direct binding is essential for TRIB2-mediated ubiquitination and proteasomal degradation of C/EBPαp42 and C/EBPαp30 generation.

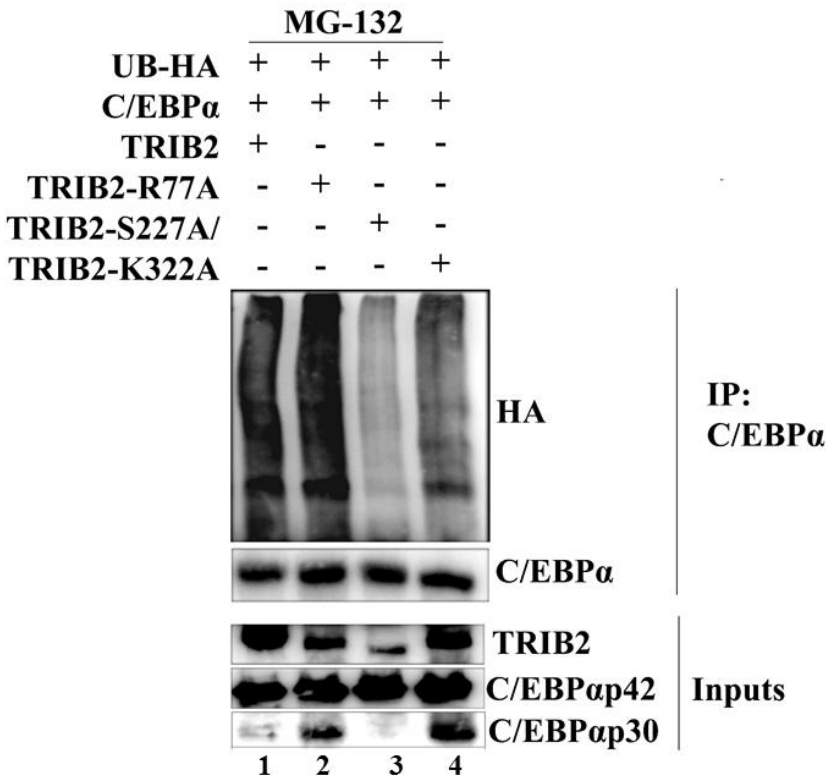

Fig 4.2.5 TRIB2 binding to C/EBPα is essential for mediated ubiquitination. HEK293t cells were transfected to overexpress WT-TRIB2, TRIB2-R77A, TRIB2-S227A/S229A/S231A/K233A, TRIB2-K322A, C/EBPα and Ub-HA. Cells were treated with 10 μM MG-132 5 hrs prior to harvesting lysates. C/EBPα was immunoprecipitated and an in vivo ubiquitination assay was performed. Lysates were separated by SDS-PAGE and immunoblotted for HA. Immunoblotting protein input lysates confirms expression of TRIB2 and C/EBPα. Data presented is representative of three independent transfection experiments.

Result 4.2.6 Prediction of potential ubiquitination sites on C/EBPα

Much debate surrounds the prediction of ubiquitination sites in substrate proteins. There has been consensus in the lack of a discernible ubiquitination site motif (Danielsen et al., 2011) however reports on the identity of the flanking amino acid sequences surrounding the ubiquitination site vary (Radivojac et al., 2010, Kim et al., 2011, Zhou et al., 2013, Udeshi et al., 2013). Ubpred online software was used to identify the probability of each lysine in C/EBPα acting as a ubiquitination site. Ubpred assigns probability scores based on the amino acid identity surrounding lysines, as it was trained on known ubiquitination sites (Radivojac et al., 2010). Ubpred analysis of C/EBPα identified six residues as potential ubiquitination sites K90, K92, K159, K169, K250 and K313 (**Fig 4.2.6 A**). Annotation of the predicted lysines identified a recurrent C/EBPα mutation K313dup which has been reported in 10 % of C/EBPα mutated AMLs and was identified to have a shorter protein half life than wildtype C/EBPα as determined by cycloheximide (CHX) assay (Carnicer et al., 2008). K313dup mutation results in an extra lysine adjacent to K313, which I predict to be a potential ubiquitination site (**Fig 4.2.6 A**). K313 is located in the C-Terminal region of C/EBPα between the DNA binding domain and the zipper region (**Fig 4.2.6 B**). Murine BMT and knock-in models report the ability of K313dup to induce AML (Bereshchenko et al., 2009, Kato et al., 2011). Investigations in the laboratory identified K90 and K92 were not essential lysines for C/EBPα ubiquitination (Personal communication, Dr. Karen Keeshan). K159 was previously identified as the site of C/EBPα sumoylation (Geletu et al., 2007). K313 was chosen as potential C/EBPα ubiquitination site to be investigated based on the leukaemogenecity of this mutation in AML.

A

Residue	Score	Ubiquitinated
90	0.76	Yes -Medium
92	0.64	Yes - Low
159	0.85	Yes -High
169	0.90	Yes -High
250	0.71	Yes -Medium
273	0.26	No
275	0.51	No
276	0.26	No
280	0.30	No
298	0.31	No
302	0.24	No
304	0.23	No
313	0.77	Yes -Medium
326	0.56	No
352	0.54	No

Confidence ranges

Low confidence $0.62 \leq s \leq 0.69$

Med confidence $0.69 \leq s \leq 0.84$

High confidence $0.84 \leq s \leq 1.00$

B

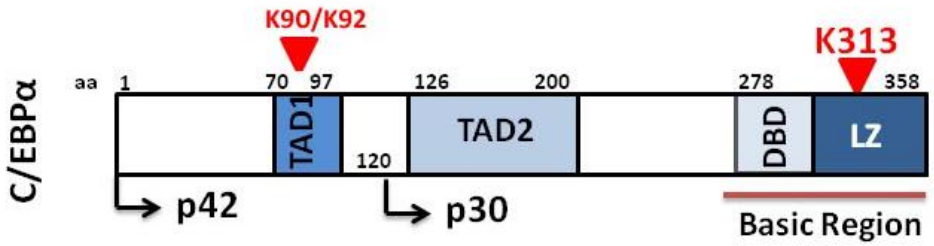

Fig 4.2.6 Identification of C/EBPα ubiquitination site. A) Ubpred analysis of rat C/EBPα Ensembl ID ENSRNOG00000010918; displaying the probability of each lysine acting as an ubiquitin conjugation site. **B)** Schematic diagram displaying the localisation of K90/K92 and K313dup in terms of C/EBPα domains adapted from (Mueller and Pabst, 2006).

Result 4.2.7 Identification of K313 as a site of C/EBPα ubiquitination

C/EBPα-K313R mutant was produced by GenScript in order to investigate the role of this lysine in TRIB2-mediated ubiquitination of C/EBPα. Substitution of a lysine for an arginine residue is often performed as arginine is a positive amino acid and retains the electrostatic interactions performed by lysine, required for protein stability. However arginine lacks the required ε amino side chain for ubiquitin conjugation thus creation of K313R would assess the role of this lysine in the ubiquitination of C/EBPα without disrupting C/EBPα protein structure. An in vivo ubiquitination assay was performed in HEK293t cells overexpressing WT-Ub-HA, TRIB2, WT-C/EBPα, and C/EBPα-K313R and treated with MG-132 for 5 hrs. Immunoblotting for anti HA determined that mutation of K313R reduced basal ubiquitination levels of C/EBPα compared to WT-C/EBPα after equal immunoprecipitation of C/EBPα (**Fig 4.2.7** top panel lane 3). Overexpression of TRIB2 was unable to mediate increased C/EBPα-K313R ubiquitination unlike WT-C/EBPα (**Fig 4.2.7** top panel lane 4 and lane 5). Overexpression of TRIB2-mediated an increase in WT-C/EBPαp30 levels as expected (**Fig 4.2.7** bottom panel lane 4). However TRIB2 was unable to mediate an increase in C/EBPα-K313Rp30 levels (**Fig 4.2.7** bottom panel lane 5). Immunoblotting input protein lysates confirmed C/EBPαp42 and TRIB2 expression (**Fig 4.2.7** bottom panel). This suggests that K313 serves as the site of ubiquitin conjugation on C/EBPα in the presence and absence of TRIB2 and mutation of K313 abrogates TRIB2-mediated ubiquitin-dependent proteasomal degradation of C/EBPα.

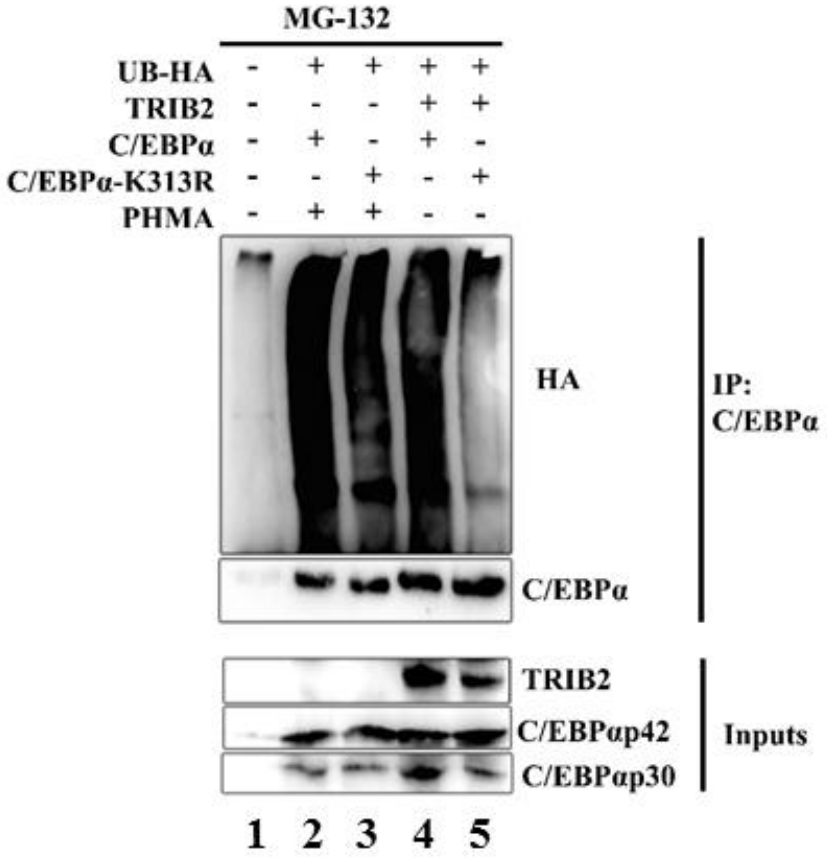

Fig 4.2.7 C/EBPα-K313 is a site of ubiquitin conjugation. HEK293t cells were transfected to overexpress Ub-HA, WT-TRIB2, WT-C/EBPα and C/EBPα-K313R. Cells were treated with 10 μM MG-132 5 hrs prior to harvesting lysates. C/EBPα was immunoprecipitated and an in vivo ubiquitination assay was performed. Lysates were separated by SDS-PAGE and immunoblotted for anti HA after equal immunoprecipitation of C/EBPα. Immunoblotting protein inputs for anti TRIB2 and anti C/EBPα detects TRIB2, WT-C/EBPα42, WT-C/EBPαp30, K313R-C/EBPαp42 and K313R-C/EBPαp30 levels (bottom panel). Data presented is representative of three independent transfection experiments.

Result 4.2.8 Mutation of the COP1 binding site and the kinase-like domain of TRIB2 abrogate its ability to mediate C/EBPα ubiquitination

An intact COP1 binding site and kinase-like domain were reported to be essential for TRIB2 oncogenicity (Keeshan et al., 2010). Mutation or deletion of the COP1 binding site abrogated TRIB2 ability to degrade C/EBPαp42 (Keeshan et al., 2010). In order to ascertain that COP1 was responsible for the conjugation of ubiquitin to C/EBPα through direct TRIB2 and C/EBPα binding an in vivo ubiquitination assay was performed overexpressing the TRIB2 mutant TRIB2-VPM which is unable to bind COP1 through mutation of the COP1 binding site DQVPL to AQLAA (Keeshan et al., 2010). Additionally an intact kinase domain was reported to be essential for TRIB2-mediated oncogenicity (Keeshan et al., 2010). Immunoblotting for anti HA determined that COP1 binding is essential for TRIB2-mediated ubiquitination of C/EBPαp42 as TRIB2-VPM was unable to mediate ubiquitination of C/EBPαp42 (**Fig 4.2.8 A** top panel lane 2). TRIB2-VPM was also unable to increase CEBPαp30 levels similarly to WT-TRIB2 (**Fig 4.2.8 A** bottom panel lane 2). In order to assess the effect of mutating the TRIB2 kinase-like domain on C/EBPαp42 ubiquitination an in vivo ubiquitination assay was performed using TRIB2-KDM. Immunoblotting for anti HA determined that mutation of TRIB2 to resemble a canonical kinase (TRIB2-KDM) abrogated its ability to mediate ubiquitination of C/EBPαp42 (**Fig 4.2.8 B** top panel). TRIB2-KDM was also unable to mediate an increase in C/EBPαp30 compared to WT-TRIB2 (**Fig 4.2.8 B** bottom panel). Immunoblotting input protein lysates confirmed TRIB2 and C/EBPαp42 protein expression while Actin confirmed equivalent protein loading.

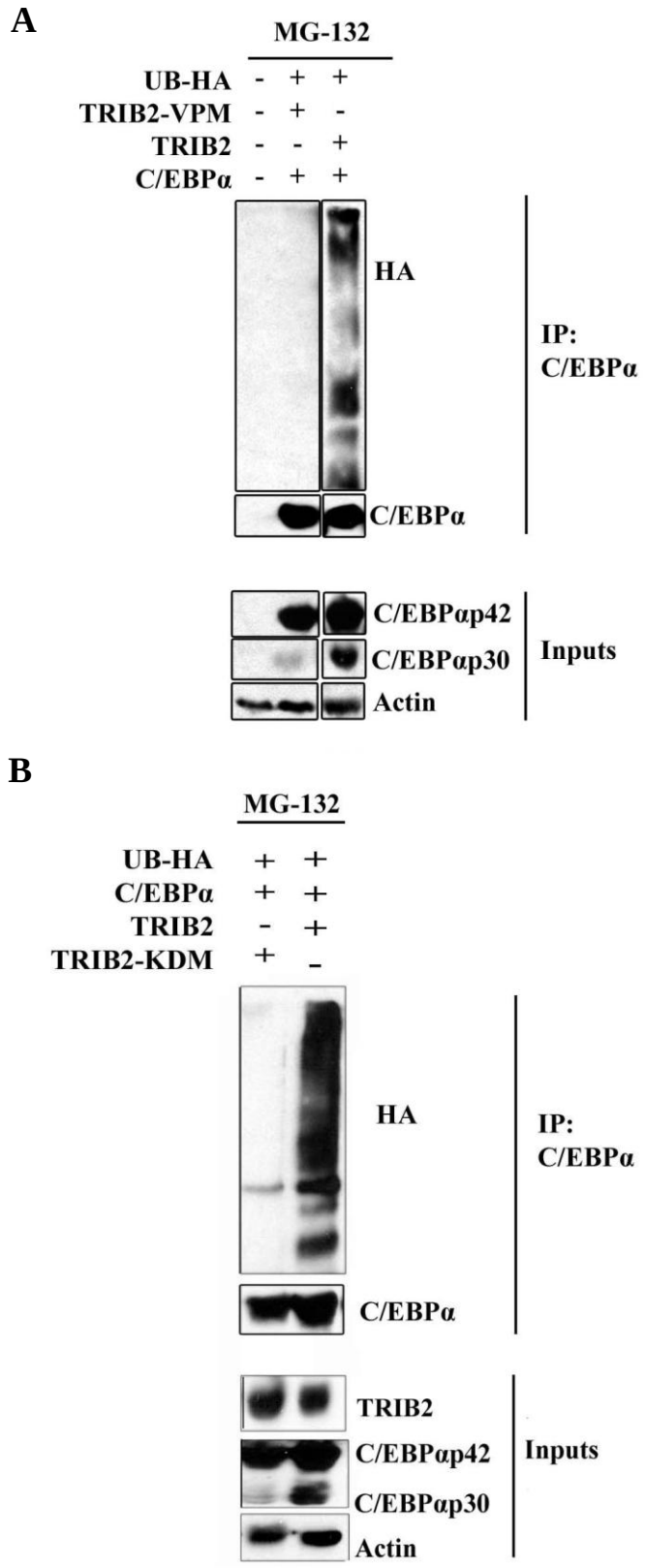

Fig 4.2.8 TRIB2-VPM and TRIB2-KDM are unable to mediate ubiquitination of C/EBPα. A) HEK293t cells were transfected to overexpress Ub-HA, WT-C/EBPαp42, WT-TRIB2, TRIB2-VPM. Note the TRIB2 sample was included in the same experiment however it was loaded several lanes down, the figure was cropped in order to display relevant data only. **B)** HEK293t cells were

transfected to overexpress Ub-HA, WT-C/EBPαp42, WT-TRIB2, and TRIB2-KDM. Cells were treated with 10 μM MG-132 5 hrs prior to harvesting lysates. C/EBPα was immunoprecipitated and an in vivo ubiquitination assay was performed. Lysates were separated by SDS-PAGE and immunoblotted for anti HA after equal immunoprecipitation of C/EBPα. Immunoblotting for anti C/EBPα confirms input protein expression and Actin confirms equal protein loading (bottom panel). Data presented is representative of three independent transfection experiments.

Result 4.2.9 TRIB2 preferentially ubiquitinates dimeric C/EBPα

The C/EBP family of proteins are able to homo and heterodimerise via their highly conserved C-Terminal leucine zipper dimerisation domains. It had previously been reported that formation of dimers increased C/EBP protein family stability (Hattori et al., 2003). Thus we sought to determine if monomeric C/EBPα is more susceptible to TRIB2-mediated ubiquitin-dependent degradation. Mutation of C/EBPα leucines 1 and 2 in the dimerisation domain (leucine 317 and 324) to valines (C/EBPα-L12V) abrogate C/EBPα ability to dimerise (Liu et al., 2003). Previous work in the laboratory determined TRIB2 is able to bind both monomeric and dimeric C/EBPαp42 (Ciaran Forde, unpublished data, **Appendix 8.5**), thus an in vivo ubiquitination assay was performed to identify whether TRIB2 preferentially degrades monomeric or dimeric C/EBPαp42 (**Fig 4.2.9 A**). Immunoblotting for anti HA and anti K48 revealed WT-C/EBPαp42 is ubiquitinated more strongly than C/EBPα-L12V (**Fig 4.2.9 A** lane 2 vs. lane 3 top panel) indicating monomeric C/EBPα protein is more stable that dimeric C/EBPα. Overexpression of TRIB2-mediated an increase in dimeric C/EBPα ubiquitination as is evident by immunoblotting for HA and K48 ubiquitin polychain (**Fig 4.2.9 A** lane 2 vs. lane 4 top panel). TRIB2 overexpression also mediated an increase in C/EBPα-L12V ubiquitination (**Fig 4.2.9 A** lane 3 vs. lane 5) however the increase mediated was not equivalent to that of dimeric C/EBPαp42. Immunoblotting for K63 polychain revealed TRIB2 is not mediating a non degradative ubiquitination signal to C/EBPα-L12V (**Fig 4.2.9 A** top panel). Immunoblotting protein inputs lysates confirmed TRIB2, C/EBPαp42 and C/EBPα-L12V expression while Actin confirmed equal protein loading (**Fig 4.2.9 A** bottom panel).

As the in vivo ubiquitination assay suggested that TRIB2 does not mediate ubiquitination of monomeric C/EBPα-L12V similar to dimeric C/EBPαp42 (**Fig 4.2.9 A**), CHX treatment was performed to determine the protein stability of monomeric versus dimeric C/EBPαp42 in the presence of TRIB2. HEK293t cells were transfected to overexpress TRIB2, C/EBPαp42 and C/EBPα-L12V for 24 hrs. Cells were treated with 100 ng/mL CHX for the indicated timepoints. Immunoblotting for C/EBPαp42 revealed WT-C/EBPαp42 had much reduced protein stability in the presence of TRIB2 than C/EBPα-L12V (**Fig 4.2.9 B).** WT-C/EBPα displayed 18% relative expression at 270 min post CHX vs C/EBPα-L12V displayed 86% relative expression at 270 min post CHX. Carnicer et al report expression of WT-C/EBPαp42 in HEK293t displays a relative decrease of 63 % in protein expression 270 min post CHX treatment (Carnicer et al., 2008). In the presence of TRIB2 immunoblotting for WT-C/EBPαp42 determined relative protein expression is

reduced by 72 % (**Fig 4.2.9 B and C**), indicating as expected that the half life of WT-C/EBPαp42 is reduced in the presence of TRIB2. TRIB2 itself displayed a half life of 180 minutes similar to reported literature (**Fig 4.2.9 B and D)** (Wang et al., 2013b). Thus despite TRIB2 having a shorter protein half life than WT-C/EBPαp42 it still exerts a proteolytic effect on C/EBPαp42 reducing its protein stability (**Fig 4.2.9 B**, **C and D**). Immunoblotting for C/EBPα determined C/EBPα-L12V relative protein expression at 270 min only decreased by 14 % in the presence of TRIB2 (**Fig 4.2.9 B and C)**, indicating that the dimeric C/EBPαp42 is more susceptible to TRIB2-mediated ubiquitin-dependent degradation resulting in a shorter protein half life than its monomeric form.

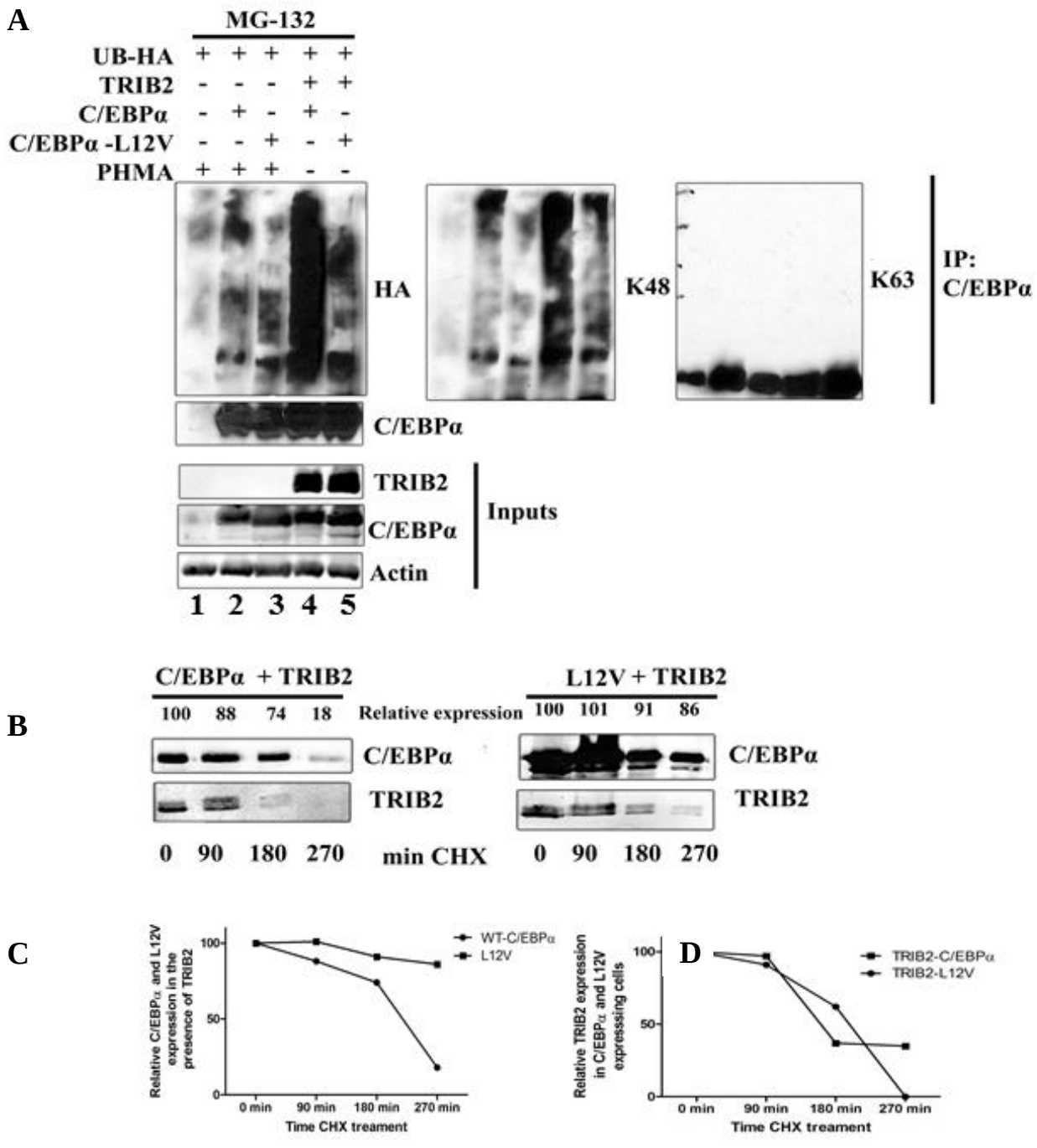

Fig 4.2.9 TRIB2-mediates increased ubiquitination of dimeric C/EBPαp42. A) HEK293t cells were transfected to overexpress Ub-HA, WT-TRIB2, WT-C/EBPαp42, C/EBPα-L12V and PHMA empty vector control. Cells were treated with 10 μM MG-132 5 hrs prior to harvesting lysates. C/EBPα was immunoprecipitated and an in vivo ubiquitination assay was performed. Lysates were separated by SDS-PAGE and immunoblotted for anti HA, anti K48 and anti K63 species of ubiquitin after equal immunoprecipitation of C/EBPα. Immunoblotting for anti TRIB2 and anti C/EBPα confirms input protein expression and Actin confirms equal protein loading (bottom

panel). **B)** HEK293t cells were transfected to overexpress TRIB2, C/EBPαp42 and C/EBPα-L12V. Cells were treated with 100 ng/mL CHX for 0, 90, 180 and 270 mins. Lysates were collected 24 hrs post transfection, separated by SDS-PAGE and immunoblotted for anti C/EBPα and anti TRIB2. Relative expression normalised to expression at 0 mins is displayed. **C**) Graphical representation of WT-C/EBPα and C/EBPα-L12V relative expression over course of CHX treatment. **D**) Graphical representation of TRIB2 relative expression in WT-C/EBPα and C/EBPα-L12V transfected cells over course of CHX treatment. Data presented is representative of one independent transfection experiments.

4.3 Discussion

TRIB2 mediates proteasomal degradation of C/EBPαp42 suggestive of ubiquitin involvement. This proteolytic relationship is a nexus in TRIB2-mediated AML disease. To date there are no published reports on TRIB2 and the subsequent ubiquitination status of C/EBPα. In this study in vivo ubiquitination assays offered the ability to assess the effect of TRIB2 function via mutational analysis on C/EBPα ubiquitination status. It was determined that TRIB2 overexpression mediated an increase in C/EBPαp42 ubiquitination. In order to unequivocally determine that TRIB2 mediates UPS degradation of C/EBPαp42 we immunoblotted for both the K48 and K63 polychain of ubiquitin. Immunoblotting for K48 proteasome degradation polychain of ubiquitin determined TRIB2-mediates an increase in K48 ubiquitination of C/EBPαp42, with no identifiable K63 ubiquitination. K48 ubiquitination was identified as the sole type of ubiquitination mediated by TRIB2 through co-expression of ubiquitin mutant constructs which do not express the K48 polychain of ubiquitin and do not express the K63 polychain of ubiquitin, K48R and K63R respectively. Expression of UB/K48R in the presence of TRIB2 was unable to mediate ubiquitination of C/EBPα, confirming TRIB2 meditates K48 ubiquitination of C/EBPαp42.

Previously the E3 ligases FBXW7 and E6AP have been identified to directly bind C/EBPα mediating its ubiquitination, inhibiting both terminal adipocytic and granulocytic differentiation (Bengoechea-Alonso and Ericsson, 2010, Pal et al., 2013a, Pal et al., 2013b). In this study I determined that direct binding of TRIB2 and C/EBPα was essential for TRIB2-mediated proteolysis despite TRIB2 not possessing E3 functionality. Binding mutants C/EBPα-R339A and TRIB2-S227A/S229A/S31A/K233A abrogated C/EBPαp42 ubiquitination. Previous reports elegantly determined that TRIB2 proteolytic effect was reliant on its ability to bind COP1 (Keeshan et al., 2010). In order to confirm that COP1 is the bona fida E3 ligase responsible for C/EBPαp42 ubiquitination in the presence of TRIB2 we assessed TRIB2-VPM ability to mediate ubiquitination of C/EBPαp42. TRIB2-VPM is unable to ubiquitinate C/EBPαp42. These data support the classification of TRIB2 as a adaptor or scaffold protein forming a multiprotein complex comprising of COP1:TRIB2:C/EBPα (Keeshan et al., 2006, Keeshan et al., 2010). Direct binding of TRIB2 and C/EBPα facilitates ubiquitin conjugation to C/EBPα through the action of the TRIB2 bound COP1. TRIB proteins have been proposed to function as both adaptor molecules and signalling modulators as they lack any discernible kinase activity (reviewed by (Lohan and Keeshan, 2013)). In this context TRIB2 provides a molecular platform, anchoring both C/EBPα and COP1.

Lysines serve as the premier site of ubiquitin conjugation through thioester bond formation. To date there remains much debate regarding the identification of a lysine as an ubiquitination site based on

analysis of its surrounding amino acid environment. Zhou et al report an increase in hydrophobic and small residues, with a decrease in charged amino acids surrounding a ubiquitination site (Zhou et al., 2013). Kim et al report that there is a preference for an overall net negative charge surrounding the ubiquitination site and a disfavouritism toward arginines on the N-Terminal side and lysine and histidine on both sides (Kim et al., 2011). Radivojac et al concurred with Kim et al reporting an increase of polar charged amino acids especially negatively charged aspartic acid and glutamate, however disagreed with Kim et al reporting a depletion of hydrophobic residues isoleucine, leucine, phenylalanine and proline at ubiquitination sites (Radivojac et al., 2010). Using Ubpred online software the probability score of each lysine in C/EBPα to behave as an ubiquitin conjugation site was calculated based on knowledge of identified protein ubiquitination sites and their surrounding amino acids. Six potential ubiquitination sites were identified with medium-high probability scores. K90 and K92 were identified as lysines with medium probability scores of behaving as C/EBPα sites of ubiquitin conjugation. Interestingly these lysines are unique to the C/EBPαp42 isoform and were thought to perhaps provide a mechanism by which TRIB2 mediates degradation of C/EBPαp42 alone. However, investigation in the laboratory revealed K90R/K92R mutants are ubiquitinated similarly to WT-C/EBPα and therefore do not act as sites of ubiquitination (Personal communication, Dr. Karen Keeshan). Annotation of site K159 revealed it acts as a sumoylation site as it has been shown that C/EBPαp30 mediates increased sumoylation of C/EBPαp42 on K159 via Ubc9 (Geletu et al., 2007).

Annotation of K313 revealed it is found mutated in ~ 10 % of mutated C/EBPα patient AMLs resulting in a duplication K313dup (Carnicer et al., 2008). Analysis of K313 surrounding amino acids sequence revealed it was neighboured by hydrophobic amino acids at n+1 n+2 and n+4 with polar glutamine present at n-1 and n-2, there was a disfavouritism for lysine, histidine and arginine with no surrounding charged amino acids (data not shown). In order to assess the role of K313 as an ubiquitin conjugation site in C/EBPα a K313R mutant was created and an in vivo ubiquitination assay was performed. TRIB2 was unable to mediate ubiquitination of C/EBPα-K313R thus identifying K313 as the potential ubiquitination site. C/EBPα-K313R was also ubiquitinated less than WT-C/EBPα in the absence of TRIB2 suggesting K313 may also govern homeostatic control of C/EBPα protein stability. The K313dup mutation results in an additional lysine beside a lysine which we suggest serves as an ubiquitination site, thus K313dup may result in enhanced ubiquitination of C/EBPα, increased degradation, resulting in a block in myeloid differentiation and AML. This hypothesis is supported by data indicating that K313dup protein is less stable than WT-C/EBPα despite displaying higher expression levels (Carnicer et al., 2008). K313dup murine

knockin studies report induction of AML in 25 % of mice, the remaining 75 % developing leukaemia with erythroid involvement (Bereshchenko et al., 2009). K313dup mice displayed increased HSC expansion through an increase in cell proliferation and a decrease in genes associated with stem cell quiescence (Bereshchenko et al., 2009). K313dup mice also lacked GMPs (Bereshchenko et al., 2009). Further studies involving C/EBPα-304_323dup, encompassing K313, reported this mutant blocked granulocytic differentiation and also gained self-renewal capacity (Kato et al., 2011). Analysis of cell marker expression revealed AML patients with K313dup mutation expressed CD7 a T-Cell marker (Carnicer et al., 2008). HSC expansion, decreased HSC quiescence, reduction in GMPs and increased CD7 expression have all been associated with C/EBPα null and K313dup genotypes (Zhang et al., 2004, Wouters et al., 2007, Ye et al., 2013). Investigation of K313dup in knockin murine models deciphering the role of C/EBPα in keratinocyte biology revealed, this lysine duplication increased keratinocyte proliferation, resulting in subsequent defects in cell commitment and differentiation and loss of the barrier function of epithelial cells (Lopez et al., 2009). K313dup mutation has been identified to abrogate C/EBPα ability to bind DNA and also to mediate E2F repression (Lopez et al., 2009). Thus the phenotypes observed in K313dup mice may be due to both the loss of C/EBPα transactivation capacity through its inability to bind DNA, loss of its ability to couple exit of the cell cycle with differentiation through loss of E2F repression and now I propose through reduced protein stability mediated by enhanced C/EBPα ubiquitination. Thus the identification of K313 as the site of ubiquitin conjugation on C/EBPα may provide further understanding into the molecular biology behind the phenotype of this K313dup mutation, in patient and murine AMLs.

TRIB proteins retain a highly conserved kinase-like domain. As mentioned previously an intact kinase domain is essential for TRIB2 leukaemogenecity (Keeshan et al., 2010). Mutation of TRIB2 to resemble a canonical kinase TRIB2-KDM was identified to abrogate TRIB2 differentiation inhibition and self-renewal enhancing effects as determined by differentiation assays and colony reforming assays (Keeshan et al., 2010). TRIB2-KDM lost the ability to mediate degradation of C/EBPα while still retaining the ability to bind COP1 (unpublished data and (Keeshan et al., 2010). In vivo ubiquitination assays performed using TRIB2-KDM confirmed this mutant is unable to mediate ubiquitination of C/EBPα and is also unable to generate increased C/EBPαp30 levels similar to WT-TRIB2. Thus these amino acids within subdomain VIB remain crucial for TRIB2 functionality, their exact role in TRIB2 biology remains to be determined. Perhaps mutation may result in reduced affinity for C/EBPα through conformational changes to the 3D structure of TRIB2.

C/EBP proteins exist as homo or heterodimers mediated via their C-Terminal domain leucine zipper domains. C/EBP dimerisation was reported to stabilize C/EBPY and C/EBPζ proteins, reducing ubiquitination and subsequent proteasomal degradation (Hattori et al., 2003). C/EBPδ was identified to require an intact leucine zipper to facilitate its ubiquitination however this was inversely related to its protein stability, the increase in C/EBPδ ubiquitination upon dimerisation did not result in increased proteasomal degradation (Zhou and Dewille, 2007). C/EBPα functionality is also controlled through dimerisation, alteration in the ratio of C/EBPαp30 isoform results in C/EBPαp42:C/EBPαp30 heterodimers which abrogate WT-C/EBPαp42 function in haematopoiesis (Pabst et al., 2001b, Cleaves et al., 2004). Further investigation into the functional consequence of monomeric C/EBPα revealed C/EBPα-L12V was able to stall cell cycle at G1 similar to WT-C/EBPα however it was unable to promote granulocytic differentiation (Wang et al., 2003, Liu et al., 2003). To our knowledge there have been no reports to date assessing the stability of monomeric C/EBPαp42. Here we report monomeric C/EBPαp42 is ubiquitinated similarly to dimeric C/EBPαp42. Thus it appears in the experimental context studied dimerisation does not greatly increase C/EBPα stability unlike its family members C/EBPY and C/EBPζ. TRIB2 was previously identified to bind both monomeric and dimeric C/EBPαp42 however I observe it preferentially mediates increased ubiquitination of dimeric C/EBPαp42. While there is an increase in C/EBPα-L12V ubiquitination in the presence of TRIB2 it is not equivalent to its effect on dimeric C/EBPαp42. Increased monomeric stability in the presence of TRIB2 was further confirmed by cycloheximide treatment. Cycloheximide treatment inhibits de novo protein synthesis thus allowing assessment of protein stability over time. Despite TRIB2 protein possessing a shorter half life that C/EBPαp42, expression of TRIB2 reduced WT-C/EBPαp42 protein stability compared to previously published reports documenting WT-C/EBPαp42 half life (Carnicer et al., 2008). Comparison of WT-C/EBPαp42 and C/EBPα-L12V protein stability revealed C/EBPα-L12V had increased stability compared to WT-C/EBPαp42 in TRIB2 expressing cells. Together these data strongly suggest TRIB2 preferentially mediates ubiquitination and proteasomal degradation of dimeric C/EBPαp42 despite possessing the ability to bind both monomeric and dimeric forms. This preference for dimeric degradation may be due to differential localisation of monomeric and dimeric C/EBPαp42 as it has been reported that differences in C/EBPα dimer structure exists between regions of euchromatin and heterochromatin in the nucleus (Schaufele et al., 2003). Similarly monomeric and dimeric C/EBPα may each occupy a distinct location within the cell. Alternatively I hypothesize dimeric C/EBPα may be structurally permissive for increased TRIB2-mediated ubiquitination.

The data presented herein reports TRIB2-mediates K48 specific ubiquitination of C/EBPα via interaction with the E3 ligase COP1 and preferentially ubiquitinating dimeric C/EBPα. Elucidation of the molecular features of the TRIB2:C/EBPα interaction reveal direct TRIB2 and C/EBPα binding are required for ubiquitination and K313 within C/EBPα C-Terminus serves as the site of ubiquitin conjugation. These data indicate that inhibition of the proteolytic effect of TRIB2 on C/EBPαp42 would provide a good therapeutic target and suggest that proteasomal inhibition may provide a novel target approach to treat high TRIB2 disease and cases of mutC/EBPα-K313dup AML (investigated in chapter 6).

Chapter 5: Results

TRIB2 preferentially binds phosphorylated Ser21-C/EBPα mediating ubiquitin-dependent proteasomal degradation

5.1 Introduction

"Phosphorylation of a protein can alter its behaviour in almost every conceivable way (Cohen, 2000)." Phosphorylation events may alter the 3D conformation of a protein, its subcellular localisation, protein half life, docking partners, ultimately changing the function of the protein. Phosphorylation may occur at multiple sites on a protein providing multiple pathways with the ability to regulate substrate protein function and often these multisite phosphorylation events have antagonistic effects on protein function (reviewed by (Cohen, 2002). Phosphorylation involves the reversible transfer of a phosphate group (PO_4^{3-}) from ATP to the hydroxyl group of the eukaryotic amino acids serine, threonine, tyrosine, lysine, arginine, aspartic acid/glutamate and cysteine. Phosphorylation mediated regulation of C/EBPα protein function has been widely studied particularly in the context of haematological malignancies due to the crucial role of C/EBPα in regulating myeloid differentiation (Zhang et al., 2004). C/EBPα to date has several identified phosphorylation sites serine Ser21, Ser193, Thr222/226, Ser230, Ser248, Ser266 and Ser277 each with their own function, kinases' and predisposition toward occurrence in different tissues (Ross et al., 1999, Behre et al., 2002, Ross et al., 2004, Wang et al., 2004, Wu et al., 2013). This study will focus primarily on Ser21 and Thr222/226. **Fig 5.1.1** summarises the C/EBPα phosphorylation events.

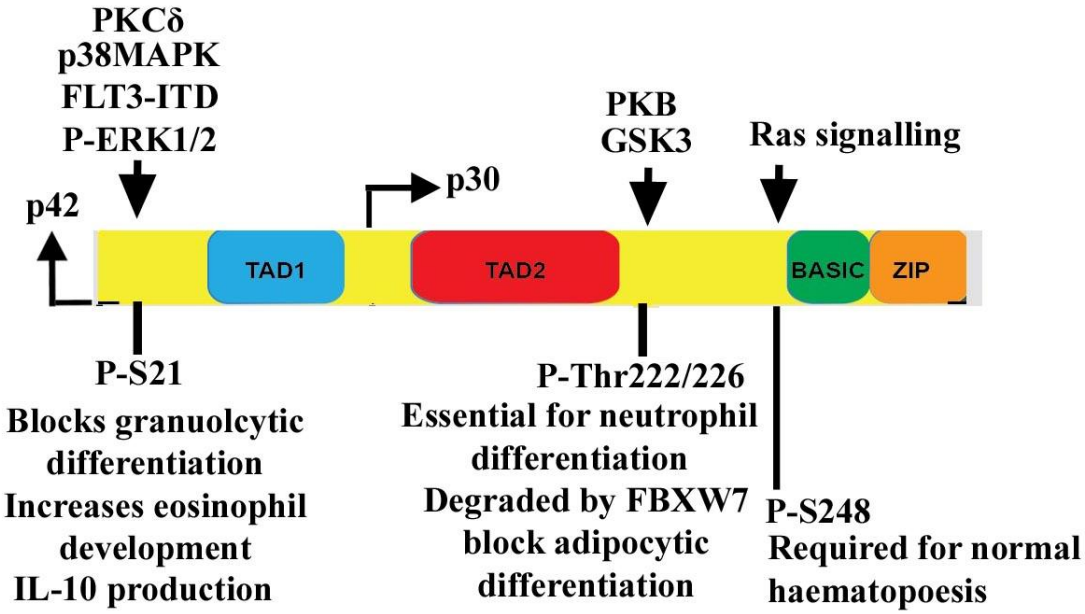

5.1.1 Schematic summarising localisation, kinases and biological consequences of C/EBPα phosphorylation events.

To date phosphorylation of C/EBPα at Ser21 in haematopoietic cells is the most widely studied C/EBPα phosphorylation event, however a dichotomy exists regarding the effect of P-Ser21-C/EBPα on its ability to regulate myeloid differentiation. Phosphorylation of C/EBPα at Ser21 by ERK1/2 was identified to change the dimer conformation of C/EBPα, separating the N-Terminal transactivation domains (Ross et al., 2004). This change in dimer conformation however did not alter the ability of C/EBPα to bind DNA at its target myeloid gene promoter binding sites (Ross et al., 2004, Fragliasso et al., 2012). Ross et al report expression of a phosphomimetic of C/EBPα at Ser21 (S21D) inhibits C/EBPα-mediated differentiation of K562 cell line measured by morphology, NBT reduction and expression of terminal differentiation gene targets *G-CSFR* and *C/EBPε* (Ross et al., 2004). Both WT and S21A-C/EBPα were able to mediate K562 granulocytic differentiation. Overexpression of S21D in U937 myeloid cell line treated with RA also blocked differentiation while WT and S21A-C/EBPα RA treated cells underwent granulocytic differentiation (Ross et al., 2004). In addition, increased P-Ser21-C/EBPα was identified downstream of FLT3 mutations (Radomska et al., 2006). FLT3-ITD results in a constitutively active receptor which blocks differentiation, increases P-ERK1/2 with a resultant increase in P-Ser21-C/EBPα (Radomska et al., 2006). FLT3-ITD and P-ERK1/2 pharmacological inhibition mediated the differentiation of AML cells via decreased P-Ser21 levels, corroborating the differentiation inhibitory role of P-Ser21 reported by Ross et al (Radomska et al., 2006). Additionally, overexpression of S21A in FLT3-ITD mutant AML cells showed that it could relieve the differentiation block as it is unable to be phosphorylated (Radomska et al., 2006). The dichotomy exists where Fragliasso et al reported overexpression of S21D and S21A minimally effects C/EBPα-induced differentiation of K562 cells. In fact they report that S21A exhibits a greater inhibitory effect on induction of granulocytic differentiation than S21D (Fragliasso et al., 2012). Both S21D and S21A displayed indistinguishable *G-CSFR* promoter binding from WT-C/EBPα (Fragliasso et al., 2012).

C/EBPα induced differentiation is not only mediated by its ability to transactivate expression of genes necessary for terminal differentiation but also through its ability to inhibit cell proliferation, as a pause in the cell cycle permits cellular differentiation. C/EBPα stalls the cell cycle via inhibition of E2F, CDK2/4 and also through upregulation of p21 (Timchenko et al., 1996, Slomiany et al., 2000, Wang et al., 2001). Overexpression of S21A, which was identified to rescue the FLT3-ITD differentiation block, coincided with a huge decrease in *C-MYC* mRNA, an E2F transcriptional target suppressed upon inhibition of the cell cycle (Johansen et al., 2001, Radomska et al., 2006). Overexpression of S21D which was unable to rescue differentiation did not decrease *C-MYC* mRNA levels (Radomska et al., 2006). However in this study it was not investigated if the

differential effects on *C-MYC* mRNA were as of a direct result of differential S21D and S21A inhibition of E2F. Fragliasso et al investigated S21D and S21A inhibition of an E2F driven promoter and determined S21D inhibited E2F to a lesser extent than WT-C/EBPα and also displayed reduced binding to both E2F2 and E2F3. However S21A which displayed similar E2F inhibitory effects to WT-C/EBPα displayed increased E2F3 binding (Fragliasso et al., 2012). Thus despite the discrepancies between the studies perhaps the S21D inhibitory effects observed by Ross et al may be explained by the reduction in E2F binding observed by Franliasso et al. Ultimately the three studies hypothesised the existence of phosphorylation specific interacting partners, which are responsible for exerting the differential effects of phosphorylated and unphosphorylated C/EBPα.

Phosphorylation of C/EBPα at Thr222/226 was also identified to exert an effect on haematopoiesis through skewing granulocyte lineage commitment (Buitenhuis et al., 2008). Inhibition of PI3K and of its downstream effector PKB results in a block in neutrophil differentiation with an increase in eosinophil differentiation in human $CD34^+$ BM cells (Buitenhuis et al., 2008). PKB is thought to regulate lineage commitment through inactivation of GSK3 which was previously identified to phosphorylate C/EBPα at Thr222/226 (Ross et al., 1999, Buitenhuis et al., 2008). When C/EBPα is unphosphorylated at Thr222/226 it promotes neutrophil differentiation however inactivation of PKB results in active GSK3 mediating P-Thr222/226-C/EBPα and blocks neutrophil differentiation with a concomitant increase in eosinophils observed. It is postulated that the differences observed in differentiation outcomes are mediated by co-factor associations with phosphorylated and unphosphorylated C/EBPα at Thr222/226 (Buitenhuis et al., 2008). P-Thr222/226 C/EBPα was first identified as a GSK3 phosphorylation site in adipocytes, and pharmacological GSK3 inhibition decreased P-Thr222/226-C/EBPα and inhibited preadipocytic differentiation (Ross et al., 1999). Phosphorylation of C/EBPα at Thr222/226 was identified to change the structural confirmation of C/EBPα similarly to phosphorylation at Ser21 (Ross et al., 1999, Ross et al., 2004). P-Thr222/226-C/EBPα in hepatocytes was reported to not effect C/EBPα functionality, thus suggesting functional effects of P-Thr222/226 are cell type specific (Liu et al., 2006).

A crosstalk between phosphorylation and ubiquitination often results in phosphorylation acting as an ubiquitination trigger (reviewed by (Hunter, 2007)). Phosphorylation of a protein may facilitate ubiquitination by multiple mechanisms; regulation of E3 ligase activity, regulation of substrate/ligase complexes through alteration of subcellular localisation or through the creation of phosphodegron motifs which are recognised by E3 ligases (reviewed by (Hunter, 2007)). Phosphorylation of C/EBPα has been reported to affect both its half life through creation of a

phosphodegron and its nuclear and subcellular localisations (Schaufele et al., 2003, Bengoechea-Alonso and Ericsson, 2010).

PKCδ activation results in ubiquitin-dependent proteasomal degradation of C/EBPα in leukaemic cells, in response to induction of apoptosis as a result of DNA damage (Zhao et al., 2009). PKCδ was identified to mediate phosphorylation of C/EBPα at 3 sites (Ser21, Ser266 and Ser277) however this was not due to direct PKCδ and C/EBPα binding (Zhao et al., 2009, Wu et al., 2013). Activation of PKCδ increased phosphorylation of C/EBPα and cytoplasmically sequestered C/EBPα resulting in its ubiquitination and proteasomal degradation (Zhao et al., 2009, Wu et al., 2013). Phosphorylation of C/EBPα at Thr222/226 also serves to increase C/EBPα ubiquitination. P-Thr222/226 creates a phosphodegron motif recognised by the E3 ligase FBXW7 mediating ubiquitination and proteasomal degradation of C/EBPα in adipocytes (Bengoechea-Alonso and Ericsson, 2010). In contrast phosphorylation of C/EBPα by JNK1 was identified to decrease levels of ubiquitinated C/EBPα and to increase C/EBPα protein half life (Trivedi et al., 2006).

This brief summary on the phosphorylation of C/EBPα at Ser21 and Thr222/226 highlights the complexity of the functional effect of this post-translational modification on C/EBPα function. Phosphorylation of C/EBPα at Ser21 by ERK1/2 is reported to both inhibit and not effect granulocytic differentiation and exert preferences on interacting protein partners (Ross et al., 2004, Radomska et al., 2006, Fragliasso et al., 2012, Koleva et al., 2012). P-Thr222/226 is reported to skew granulocytic differentiation toward increased eosinophils at the cost of neutrophils while P-Thr222/226-C/EBPα is an E3 ligase target mediating C/EBPα ubiquitination in adipocytes (Buitenhuis et al., 2008, Ross et al., 1999, Bengoechea-Alonso and Ericsson, 2010). Thus it appears the phosphorylation site of C/EBPα and the cell context all have different effects on C/EBPα protein function.

Aim

The aim of this study was to determine the effect of TRIB2 expression on C/EBPα phosphorylation and to investigate any crosstalk between TRIB2-mediated ubiquitination and C/EBPα phosphorylation. I show that TRIB2-mediated a decrease in C/EBPα phosphorylation at Ser21 and Thr222/226. TRIB2 mediates increased ubiquitination of the C/EBPα S21D phosphomimetic construct. Additionally TRIB2 was identified to preferentially bind S21D compared to the unphosphorylatible C/EBPα construct S21A. Thus I propose phosphorylation of C/EBPα at Ser21 results in increased TRIB2 binding and ubiquitin-dependent proteasomal degradation. Retroviral overexpression of TRIB2 in U937 leukaemic cells was performed to assess the effect on

endogenous C/EBPα phosphorylation. Overexpression in vivo ubiquitination and co-IP assays were performed to determine TRIB2 effect on C/EBPα phosphomimetic ubiquitination and preference for protein binding.

Result 5.2.1 TRIB2 overexpression decreases P-Ser21 and P-Thr222/226 C/EBPα in U937 cells

In order to determine the effect TRIB2 overexpression may have on the phosphorylation profile of C/EBPα and to optimise endogenous phosphorylated C/EBPα protein detection, the U937 cell line was transduced with MigR1-TRIB2-eGFP and MigR1-eGFP empty vector control. U937 cells are a promyelomonocytic cell line which express both TRIB2 and C/EBPα that can be readily detected at the protein level (Rishi et al., 2014). Viral transduction of U937 with TRIB2 recapitulates the cellular environment of high TRIB2 AML cell, enabling investigation of the effects of overexpressed TRIB2 on endogenous C/EBPα (Keeshan et al., 2006). Validation of TRIB2 overexpression from these retroviral vectors has been previously published (Keeshan et al., 2006). In order to robustly assess growth factor induced phosphorylations in the presence and absence of TRIB2, U937 cells transduced and sorted for GFP positive population (48 hrs post transduction) were serum starved overnight in 1 % FBS followed by stimulation for 30 min with 20 % FBS. Direct lysates were collected and separated by SDS page to assess C/EBPα status. Stimulation following serum starvation was performed as it increases the levels of phosphorylated C/EBPα (Ross et al., 2004), thus if TRIB2-mediated an effect on phosphorylation levels it would be more evident. To date several C/EBPα phosphorylation sites have been identified however at the time of experimentation there were only antibodies commercially available recognising P-Ser21 and P-Thr222/226. Lysates were immunoblotted for anti P-Ser21 and anti P-Thr222/226, the membrane was stripped and incubated with anti C/EBPα antibody to detect total C/EBPα protein levels. Serum stimulation increased the levels of phosphorylated C/EBPα at both phosphorylation sites as is evident for the MigR1 transduced cells (**Fig 5.2.1** compare lane 1 and lane 3). Overexpression of TRIB2 decreased the levels of phosphorylated C/EBPα in the presence and absence of stimulation (**Fig 5.2.1** lane 2 and lane 4). TRIB2 overexpression also decreased the levels of C/EBPαp42 as expected (**Fig 5.2.1** lane 2 and lane 4). A non specific band frequently detected with anti C/EBPα antibody at ~75 kDa served as the protein loading control to confirm equal protein loading (**Fig 5.2.1**). Thus the decrease in phosphorylated C/EBPα observed may be due to the decrease in total C/EBPα protein levels. These data show that TRIB2 promotes degradation of both the phosphorylated and total C/EBPα protein levels.

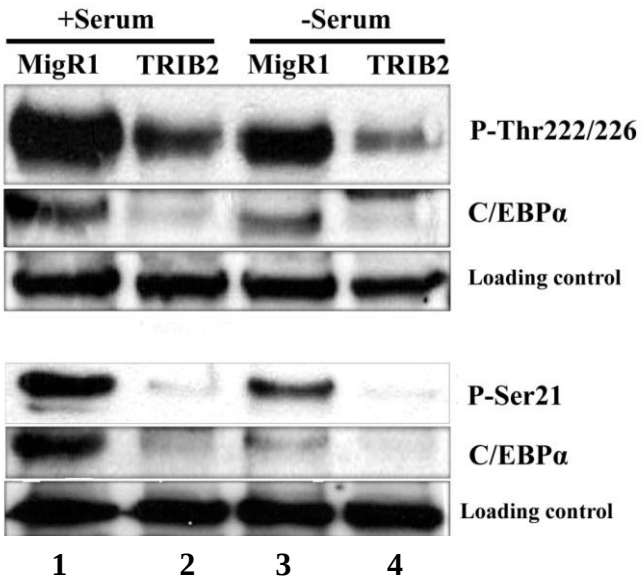

Fig 5.2.1 TRIB2 overexpression decreases P-Ser21 and P-Thr222/226 C/EBPα levels in U937 cells. U937 cells were transduced with MigR1-TRIB2-eGFP and MigR1-eGFP, 48 hrs post transduction the cells were sorted for GFP positive population. Cells were serum starved overnight in 1 % FBS stimulated with 20 % FBS for 30 min. Direct lysates were collected, separated by SDS page and immunoblotted for anti P-Thr222/226 and anti P-Ser21. The membranes were stripped and incubated with anti C/EBPα. A nonspecific band detected by anti C/EBPα confirmed equal protein loading. Data presented is representative of two independent transfection experiments.

Result 5.2.2 Proteasomal inhibition rescues the TRIB2-mediated decrease of P-Ser21 C/EBPα in U937 cells

In order to determine if the decrease in phosphorylated C/EBPα observed was due to a signalling effect mediated by TRIB2 or due to proteasomal degradation, U937 cells transduced with TRIB2 and MigR1 were treated with two different proteasomal inhibitors, MG-132 and Bortezomib/Velclade ™. Due to the documented role of P-Ser21-C/EBPα in blocking granulopoiesis I focused solely on this phosphorylation site for the rest of the study (Ross et al., 2004, Radomska et al., 2006). TPA was used to stimulate an increase in P-Ser21-C/EBPα level as previously reported (Ross et al., 1999). U937 cells were serum staved in 1 % FBS overnight, treated with 10 μM MG-132 for 6 hrs and stimulated with 200 nM TPA for 30 mins. Direct lysates were collected and immunoblotted for P-Ser21. TPA stimulation increased P-Ser21 levels in control MigR1 cells as is evident in lane 3 compared to lane 1 (**Fig 5.2.2 A**). As expected, MG-132 treatment rescued C/EBPα total levels in TRIB2 expressing cells. P-Ser21 levels are equivocal in both MigR1 and TRIB2 transduced U937 cells in the absence and presence of TPA induced stimulation indicating MG-132 treatment rescues TRIB2-mediated proteasomal degradation of P-Ser21 (**Fig 5.2.2 A**). Furthermore, it indicates that TRIB2 does not abrogate the signalling mediated-induction of C/EBPα phosphorylation.

In the absence of proteasomal inhibition TRIB2 decreased the levels of both P-Ser21-C/EBPα and total C/EBPα protein levels as seen in **Fig 5.2.1**. In order to validate proteasomal inhibition rescuing TRIB2-mediated decrease in P-Ser21-C/EBPα, cells were treated with a second proteasomal inhibitor Bortezomib. Upon treatment with Bortezomib in the absence of growth stimulation both P-Ser21-C/EBPα and total C/EBPα levels increased to MigR1 control cells level. Thus proteasomal inhibition abrogated the TRIB2-mediated decrease in P-Ser21-C/EBPα (**Fig 5.2.2 B).** These data indicate that TRIB2-mediated decrease in P-Ser21-C/EBPα is proteasomal degradation dependent and not due to an alteration in cell signalling cascades perpetuated by TRIB2.

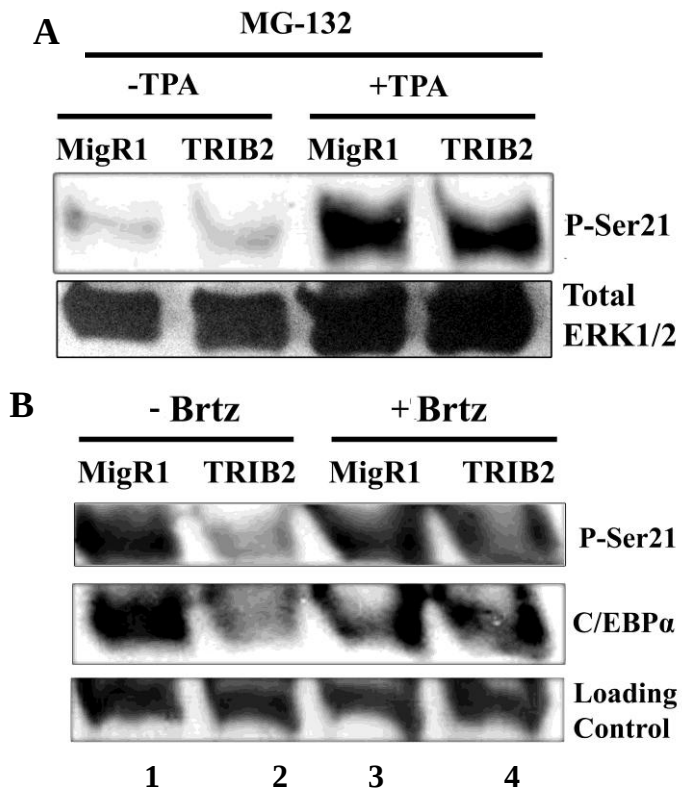

Fig 5.2.2 Proteasomal inhibition rescues TRIB2-mediated decrease in P-Ser21-C/EBPα. U937 cells were transduced with MigR1-TRIB2-eGFP and MigR1-eGFP, 48 hrs post transduction the cells were sorted for GFP positive population. **A**) Cells were treated with 10 μM MG-132 for 6 hrs and stimulated with 200 nM TPA. Direct lysates were collected, separated by SDS page and immunoblotted for anti P-Ser21-C/EBPα. T-ERK1/2 served as loading control. **B**) Cells were treated with 10 nM Bortezomib for 6 hrs. Direct lysates were collected, separated by SDS page, immunoblotted for anti P-Ser21-C/EBPα the membrane were stripped and then incubated with anti-C/EBPα.

Result 5.2.3 Expression of C/EBPα phosphomimetic mutants S21D and S21A

In order to investigate the binding and ubiquitination relationship between TRIB2 and P-Ser21-C/EBPα expression vectors were used that expressed the mutated forms of P-Ser21. pcDNA3.1-C/EBPα-S21D and pcDNA3.1-C/EBPα-S21A were a kind gift from Dr. D. Tenen (Harvard Medical School) and previously published (Ross et al., 2004). Mutation of Ser21 to aspartic acid (S21D) produces a chemically similar substitution to a phosphorylated serine resulting in a constitutive phosphorylation signal, while mutation of Ser21 to alanine (S21A) results in abrogation of phosphorylation as alanine lacks –OH group necessary for phosphate transfer. Expression of S21D and S21A were analysed by transfection of HEK293t cells. Lysates were immunoblotted with anti P-Ser21, the membrane was stripped and immunoblotted with anti C/EBPα to detect total protein levels. As expected, P-Ser21 is strongly detected in cells transfected to express WT-C/EBPα and S21D while there is no detection of P-Ser21-C/EBPα in cells transfected with S21A **(Fig 5.2.3** top panel**)**. Immunoblotting with anti C/EBPα against total C/EBPα confirms equivocal expression of total C/EBPα from S21D, S21A and WT-C/EBPα vectors (**Fig 5.2.3** bottom panel). WT-C/EBPα runs at a slightly higher molecular weight as it is expressed from a different expression vector, PHMA. Thus these constructs may be used to model the interaction of TRIB2 with phosphorylated and unphosphorylated C/EBPα at Ser21.

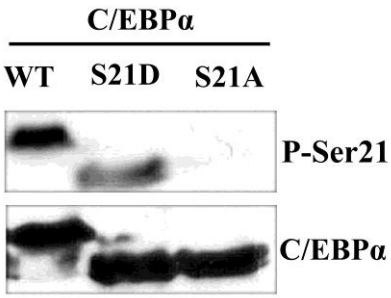

Fig 5.2.3 Expression of WT-C/EBPα, S21D and S21A in HEK293t. HEK293t cells were transfected to overexpress WT-C/EBPα, S21D-C/EBPα and S21A-C/EBPα. Cells were lysed, separated by SDS PAGE immunoblotted for anti P-Ser21-C/EBPα and anti C/EBPα.

Result 5.2.4 TRIB2-VPM preferentially binds S21D-C/EBPα in HEK293t cells

Several C/EBPα interacting proteins have been identified to preferentially interact with either the phosphorylated or unphosphorylated form of C/EBPα (Fragliasso et al., 2012, Koleva et al., 2012). This preference supports differential functions of phosphorylated and unphosphorylated C/EBPα. In order to determine if TRIB2 displays a preference for either phosphorylated or unphosphorylated C/EBPα, a co-IP was performed using C/EBPα mutants S21D and S21A (Ross et al., 2004). TRIB2-VPM-MYC was expressed in HEK293t cells as it is unable to degrade C/EBPα negating the use of MG-132. HEK293t cells were transfected to overexpress TRIB2-VPM-MYC in the presence of WT-C/EBPα, S21D-C/EBPα and S21A-C/EBPα. Untransfected cells served as the control. Twenty four hrs post-transfection cells were lysed and TRIB2 was immunoprecipitated overnight using an anti MYC tag antibody. Immunoblotting for C/EBPα revealed TRIB2 preferentially bound S21D as compared to WT-C/EBPα, whereas reduced binding to S21A-C/EBPα was observed. Equal immunoprecipitation was confirmed by immunoblotting for anti MYC expression as readout of TRIB2-VPM expression (**Fig 5.2.4** top panel). Protein input lysates were immunoblotted for TRIB2 and C/EBPα confirming protein expression while β-Tubulin confirmed equal protein loading (**Fig 5.2.4** bottom panel). Thus TRIB2 preferentially binds C/EBPα when phosphorylated at Ser21, while it could still bind unphosphorylated C/EBPα albeit at reduced levels.

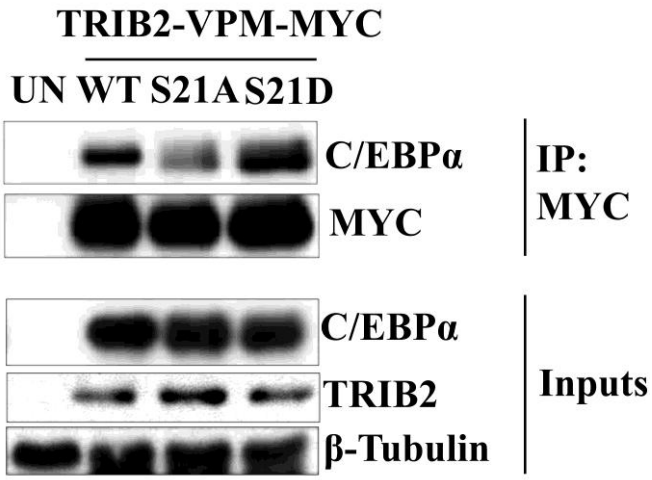

Fig 5.2.4 TRIB2-VPM preferentially binds S21D over S21A. HEK293t cells were transfected to overexpress TRIB2-VPM-MYC, WT-C/EBPα, S21D-C/EBPα, S21A-C/EBPα. MYC was immunoprecipitated overnight; lysates were separated by 12 % SDS-PAGE and immunoblotted with anti C/EBPα and anti MYC (top panel). Protein inputs lysates were immunoblotted with anti C/EBPα, anti TRIB2 and anti β-Tubulin (bottom panel). Data presented is representative of three independent transfection experiments. **Performed with the assistance of Mara Salome.**

Result 5.2.5 TRIB2 preferentially ubiquitinates S21D-C/EBPa

TRIB2 displayed preferential binding to S21D-C/EBPα thus in order to determine if TRIB2 increased binding resulted in increased ubiquitination, an in vivo ubiquitination assay was performed. HEK293t cells were transfected to overexpress Ub-HA, TRIB2, WT-C/EBPα, S21D-C/EBPα and S21A-C/EBPα and treated with 10 μM MG-132 for 5 hrs. Following immunoprecipitation of C/EBPα, lysates were immunoblotted for K48. As expected TRIB2-mediated an increase in K48 ubiquitination of WT-C/EBPα (**Fig 5.2.5** lane 2 compared to lane 5 top panel). TRIB2 also mediated an increase in S21D-C/EBPα ubiquitination (**Fig 5.2.5** lane 3 compared to lane 6, top panel). However TRIB2 did not mediate increased ubiquitination of S21A-C/EBPα (**Fig 5.2.5** lane 4 compared to lane 7). These results show that TRIB2 preferentially ubiquitinates P-Ser21-C/EBPα.

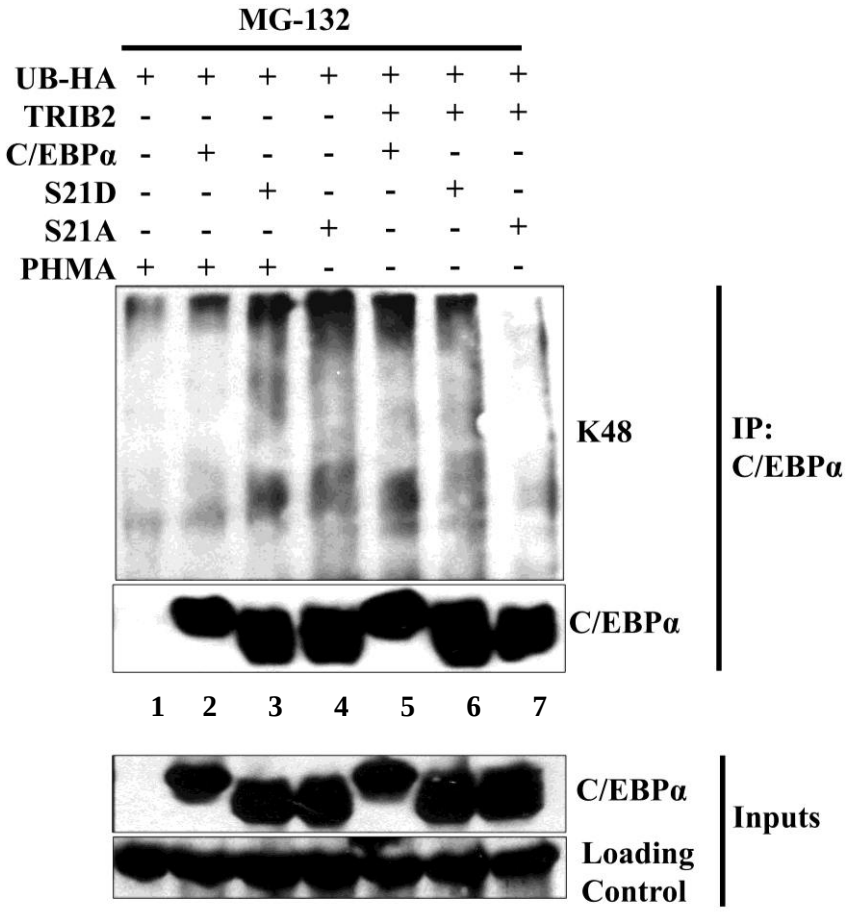

Fig 5.2.5 TRIB2 mediates increased ubiquitination of S21D. HEK293t cells were transfected to overexpress Ub-HA, WT-TRIB2, WT-C/EBPα S21D-C/EBPα, S21A-C/EBPα and PHMA the empty vector control. Cells were treated with 10 μM MG-132 5 hrs prior to lysis. C/EBPα was immunoprecipitated and an in vivo ubiquitination assay was performed. Lysates were separated by SDS-PAGE and immunoblotted for anti K48 ubiquitin. Immunoblotting protein inputs for C/EBPα confirm input protein expression, while a high molecular weight nonspecific detected with C/EBPα antibody serves as a loading control (bottom panel). Data presented is representative of three independent transfection experiments.

5.3 Discussion

In this study I report TRIB2-mediates ubiquitin-dependent proteasomal degradation of P-Ser21-C/EBPα through preferentially binding the phosphorylated protein. This degradation may be relieved through treatment with proteasomal inhibitors Bortezomib and MG-132.

TRIB2 is a pseudokinase and while retaining certain kinase-like features (as discussed in Chapter 3), it does not possess the ability to transfer phosphate groups. In the context of TRIB2-mediated AML, we propose that TRIB2 is functioning as an adaptor protein facilitating the formation of a COP1:TRIB2:C/EBPα multiprotein complex ultimately resulting in C/EBPα ubiquitin-dependent proteasomal degradation. However in other cellular contexts TRIB proteins have been described as signalling modulators and decoy kinases. TRIB1 and TRIB3 up and downregulate MAPK signalling cascades (Kiss-Toth et al., 2004). Knockdown of TRIB2 results in decreased JNK and p38 signalling (Wei et al., 2012). TRIB1 leukaemogenicity and degradation of C/EBPα is reported to be P-ERK1/2 dependent (Yokoyama et al., 2010). Interestingly TRIB1 overexpression increases P-ERK1/2 signalling with no accompanying increase P-Ser21-C/EBPα despite Ser21-C/EBPα reported to be a P-ERK1/2 phosphorylation site (Ross et al., 2004, Yokoyama et al., 2010, Yokoyama et al., 2012). However some innate differences exist between TRIB1 and TRIB2-mediated degradation of C/EBPα, as TRIB2 was reported to have no effect on P-ERK1/2 signalling in the context of both haematological cells and overexpression in HEK239t cells (Dedhia et al., 2010, Wei et al., 2012). I observed a TRIB2-mediated decrease in P-Ser21-C/EBPα in myeloid cells, however this was due to increased ubiquitination and degradation of the P-Ser21-C/EBPα protein. Treatment with both proteasomal inhibitors Bortezomib and MG-132 rescued P-Ser21-C/EBPα levels in the presence of TRIB2.

Phosphorylation events are known to alter protein subcellular localisation (Cohen, 2000). Phosphorylation of C/EBPα by PKCδ at Ser21, Ser266 and Ser277 was identified to result in C/EBPα cytoplasmic translocation and ubiquitin-dependent proteasomal degradation (Zhao et al., 2009, Wu et al., 2013). In the context of TRIB2 overexpression C/EBPα localisation does not change. TRIB2 and C/EBPα co-localise within the nucleus of HeLa cells as determined by immunofluorescence and analysis of nuclear and cytoplasmic protein fractions (Ciaran Forde, unpublished data, **Appendix 8.6**). Thus while TRIB2 does effect C/EBPα ability to bind DNA, this I believe is not as a result of TRIB2-mediating cytoplasmic sequestering of C/EBPα (Keeshan et al., 2006). Rather TRIB2 binds C/EBPα at R339 which lies within its DNA binding domain, disrupting DNA binding. Therefore the results indicate that the increased ubiquitination of S21D-C/EBPα mediated by TRIB2 is as a direct result of increased binding and ubiquitination and not as a result

of C/EBPα mislocalisation within the cell. Additionally leukaemic proteasomes were identified to be abnormally highly expressed compared to normal mononuclear cells (Kumatori et al., 1990). Leukaemic proteasomes are localised within the nucleus unlike cytoplasmic localisation in normal cells (Kumatori et al., 1990). Thus the abundance of nuclear leukaemic proteasomes facilitates TRIB2-mediated proteasomal degradation of C/EBPαp42.

When first identified by Ross et al both phosphorylation events P-Ser21 and P-Thr222/226 were identified to alter the 3D conformation of C/EBPα as determined by FRET, tryptic digestion and SDS-PAGE analysis (Ross et al., 1999, Ross et al., 2004). C/EBPα exists as a dimer and phosphorylation results in an increase in spatial separation between the N-Termini of the individual monomers (Ross et al., 2004). Stimulation with phorbol 12-myristate 13-acetate (PMA) also induced a conformational change in C/EBPα dimers (Schaufele et al., 2003). C/EBPα dimers were identified to cluster at pericentric heterochromatic nuclear regions. Stimulation with PMA resulted in a torsional rotation of the transactivation domains away from each other, similar to the effect reported by Ross et al upon phosphorylation of P-Ser21, probably owing to the PMA mediated phosphorylation of C/EBPα at Ser21 (Schaufele et al., 2003, Ross et al., 2004). In this study I propose that phosphorylation of C/EBPα at Ser21 results in a permissive C/EBPα dimer confirmation change, structurally favouring increased TRIB2 binding at R339. TRIB2 binding results in COP1 mediated conjugation of ubiquitin at K313 resulting in proteasomal degradation. Validation of the dynamics of this protein interaction awaits the deciphering of TRIB2 and C/EBPα crystallised structures.

Murine studies investigating the leukaemogenicity of P-Ser21-C/EBPα revealed it does not possess the ability to induce leukaemic disease (Unpublished data, personal communication Dr. D. Tenen, Harvard Medical School). Reports from Ross et al and Ramdoska et al show the ability of P-Ser21-C/EBPα to block granulopoiesis but suggest it may be co-factor dependent, or that another genetic hit or signalling disturbance is required for the final transformation (Ross et al., 2004, Radomska et al., 2006). Here I reported preferential binding of TRIB2 to P-Ser21-C/EBPα leading to its ubiquitin-dependent proteasomal degradation. Much investigation remains to be done in order to further elucidate the differential functions of P-Ser21 and unphosphorylated Ser21-C/EBPα. Perhaps different phosphorylation patterns of C/EBPα occur throughout haematopoiesis mediating differential regulation of C/EBPα target gene expression. While it has been reported that there is no difference in DNA binding capabilities of P-Ser21 and unphosphorylated Ser21-C/EBPα these analyses were confined to investigation of terminal granulocytic C/EBPε and G-CSFR promoter regions (Ross et al., 2004, Radomska et al., 2006, Fragliasso et al., 2012, Koleva et al., 2012). P-

Thr222/226-C/EBPα has been reported to skew neutrophil differentiation toward eosinophil differentiation and P-Ser21-C/EBPα promotes monocytic differentiation at the expense of terminal granulocytic differentiation (Ross et al., 2004, Buitenhuis et al., 2008). Thus it may be hypothesised that phosphorylated C/EBPα may have different effects in regulating HSC self-renewal, erythroid gene expression and myeloid differentiation through its differential association with co-factors. Experimental investigation of early myelo/erythroid and lymphoid progenitor cells may identify different patterns of C/EBPα phosphorylation governing lineage fate decisions through differential association with interacting protein partners and transcriptional activation of lineage governing genes.

Chapter 6: Results

Leukaemic cells expressing high levels of TRIB2 displayed increased sensitivity to Bortezomib induced cytotoxicity

6.1 Introduction

Bortezomib/Velcade is a first class boronic dipeptide compound ($C_{19}H_{25}BN_4O_4$) which reversibly and selectively inhibits the proteasome. It binds a threonine residue within the 26Sl subunit of the proteasome inhibiting its chymotryptic activity necessary for controlled target protein degradation (Bonvini et al., 2007). Bortezomib received FDA approved for treatment of relapsed and refractory multiple myeloma and mantle cell lymphoma in 2003(Aghajanian et al., 2002, Richardson et al., 2003, Jagannath et al., 2004, Orlowski et al., 2005, Kane et al., 2007). Bortezomib has also been trialed as an acute leukaemia therapeutic, used both as a single agent and in combination with AML induction chemotherapy in order to determine its efficacy in phase I and phase II clinical trials (Cortes et al., 2004, Orlowski et al., 2005, Attar et al., 2005, Attar et al., 2013, Sarlo et al., 2013). Modest anti-leukaemic activity was observed as a single agent treatment (Cortes et al., 2004). However encouraging and complete remission responses were reported when Bortezomib treatment was combined with standard AML induction therapy (Attar et al., 2005, Attar et al., 2013). CD74 has been identified as a poor prognosis marker for AML patients (Attar et al., 2008). CD74 expression on AML blast cells is proposed to serve as a novel biomarker capable of identifying patients associated with complete remission in response to Bortezomib treatment in combination with induction therapy (Attar et al., 2008, Attar et al., 2013). Despite promising results involving incorporation of Bortezomib into AML treatment regimes little is yet known about its mechanism of action at the molecular cell level.

Investigations into the apoptosis inducing effects of Bortezomib suggest it mediates cytotoxicity by a variety of mechanisms. Inhibition of proteasomal mediated degradation ultimately results in an accumulation of K48 ubiquitin linked proteins. This acquired abundance of defective, misfolded and unwanted proteins results in ER stress, triggering autophagy and apoptosis (Obeng et al., 2006). Bortezomib treatment also stabilizes the expression of pro-apoptotic protein p53 while decreasing the expression of anti-apoptotic proteins c-FLIP and XIAP (Pei et al., 2003, Poulaki et al., 2007, Riccioni et al., 2007, Dijk et al., 2011). Bortezomib treatment stabilises cell cycle regulators p21 and p27 inhibiting cell cycle progression and inhibits NFκB activation by stabilising IκB inhibitor levels (Bonvini et al., 2007, Colado et al., 2008). Aberrant NFκB signalling is prevalent in AML, particularly in the leukaemic stem cell and often observed in chemotherapeutic resistance AML (Guzman et al., 2001, Guzman et al., 2002). Apoptotic induction through proteasomal inhibition is ultimately dependent on cell proteasome expression levels. Malignant haematopoietic cell lines and primary leukaemic samples were identified to have very large number of proteasomes compared to normal peripheral blood mononuclear cells and hence display high sensitivity to proteasomal

inhibition induced cell death (Kumatori et al., 1990, Dijk et al., 2011). However, variation in sensitivities of AML cell lines and primary patient responses have been reported (Colado et al., 2008, Matondo et al., 2010, Dijk et al., 2011). This difference in malignant haematopoietic cell response has been attributed to proteasome activity levels, proteasome subunit expression levels, mutation of Bortezomib binding pocket and FAB leukaemic subtypes (Riccioni et al., 2007, Matondo et al., 2010, Dijk et al., 2011, Fang et al., 2012).

The 26S proteasome is composed of the 20S catalytic subunit and the 19S or the 11s regulatory subunits. The 20S subunit possesses three different types of catalytic activity; chymotrypsin-like, trypsin–like and peptidyl-glutamyl peptide hydrolyzing like activity, provided by the subunits β5 (PSMB5), β2 (PSMB7) and β1 (PSMB6) respectively. Increased 20S proteasome content in the leukaemic cell line KG1 compared to U937 (FAB subtype M1 compared to M5) was identified to be responsible for the increased sensitivity of the KG1 cells to Bortezomib induced cell death (Matondo et al., 2010). Ex vivo treatment of AML patient samples also supported the increased sensitivity of samples with increased 20S content (Matondo et al., 2010). Two different types of proteasomes exist; immunoproteasomes and constitutive proteasomes, the difference being the catalytic subunits β5, β2 and β1 are replaced with β5i, β2i and β1i which can be activated by interferon γ. The resultant immunoproteasomes participate in MHC class I antigen presentation resulting in more efficient T-cell activation than constitutive proteasomes. It was identified that the ratio of immune to constitutive proteasomes also affected Bortezomib response in leukaemic cells (Niewerth et al., 2013). A higher ratio of immune to constitutive proteasomes resulted in increased sensitivity to Bortezomib induced cell death in paediatric acute leukaemic cells (Niewerth et al., 2013). Interestingly it was also identified that Bortezomib resistance may be overcome by interferon γ stimulated increase in immunoproteasomes (Niewerth et al., 2014). Studies investigating acquired resistance to Bortezomib treatment have attributed chemoresistance to altered expression or mutation of proteasome subunit genes. Upregulation of PSMB5 or mutation of Bortezomib binding pocket was identified to abrogate Bortezomib mediated cell death (Oerlemans et al., 2008, Franke et al., 2012). Similarly knockdown of PSMA1 was identified to resensitise Bortezomib resistant leukaemic cell line (Fang et al., 2012).

Bortezomib potential as an anti-leukaemic agent is supported by reports of Bortezomib selectively killing the leukaemic cell and having no significant cytotoxic effects on normal mononuclear bone marrow or cord blood derived $CD34^+$ or aldehyde dehydrogenase $(ALDH)^+$ cells (Riccioni et al., 2007, Colado et al., 2008, Fang et al., 2012). Primary AML samples treated with Bortezomib were categorised as high or low responders based on induction of cell death (Riccioni et al., 2007). FAB

subtypes M4 and M5 were classified as high responders while M1 and M2 were classified as low responders. However there is no consensus regarding sensitivity of AML primary samples based on FAB subtype. Bortezomib was shown to mediate increased cytotoxicity to M1 subtype versus M5 subtype based on cell line response (KG1 versus U937) and AML patient sample response (Matondo et al., 2010). The different outcome compared to earlier studies was suggested to be associated with difference in cell culture medium (Riccioni et al., 2007, Matondo et al., 2010).

Aim

Elevated *TRIB2* expression was identified as a feature of a distinct cohort of 285 AML patient samples clustered into 16 groups based on gene expression (Valk et al., 2004, Keeshan et al., 2006). Within this cluster 4, elevated *TRIB2* expression was associated with the cluster defining dysregulated C/EBPα signature which included both wild type and mutated C/EBPα, although high *TRIB2* levels correlated with the *WT-C/EBPα* samples (Valk et al., 2004, Keeshan et al., 2006). Patients presented with leukaemias with a mixed myeloid lymphoid phenotype (Wouters et al., 2007). Elucidation of the molecular mechanism of TRIB2-induced AML in murine models has shown that the proteolytic effect TRIB2 exerts on C/EBPαp42 is a key leukaemogenic driver (Keeshan et al., 2006, Keeshan et al., 2010). I have identified that TRIB2 mediates K48 ubiquitin-dependent proteasomal degradation of C/EBPαp42 (**Fig 4.2.2** and **4.2.3**). Thus as Bortezomib functions as a clinically available proteasome inhibitor with high selectivity for the leukaemic cell and results in accumulation of K48 ubiquitinated proteins. I investigated whether Bortezomib may serve as a potential targeted therapy for elevated TRIB2 leukaemias. The data shows that overexpressing MigR1-TRIB2-eGFP in the U937 cell line led to increased sensitivity to Bortezomib induced cell death. The increased cytotoxicity associated with high TRIB2 expression was shown to be dependent on TRIB2-mediated ubiquitination of C/EBPαp42. The results were supported in AML primary samples categorised for their TRIB2 expression levels.

Result 6.2.1 Determination of optimum Bortezomib concentration to assess cell death in U937 cells.

Previous reports determined that leukaemic cell lines are very sensitive to Bortezomib treatment in the 5-10 nanomolar range (Colado et al., 2008, Dijk et al., 2011). Bortezomib is proposed to induce cytotoxicity through several mechanisms, facilitating the accumulation of K48 ubiquitin linked proteins and also through stabilization of pro-apoptotic and cell cycle inhibitory proteins (Obeng et al., 2006, Riccioni et al., 2007, Colado et al., 2008, Dijk et al., 2011). U937 cells were treated with increasing concentrations of Bortezomib 0-15 nM in order to deduce the optimum Bortezomib concentration for U937 cell death. Cells were counted 24 hrs post treatment and plotted against the log of Bortezomib concentration. Nonlinear regression analysis was performed and the mean IC_{50} of two independent 24 hr treatments calculated an IC_{50} of 8.45+/- 0.45 nM SEM (**Fig 6.2.1 A**). This supports a previously reported Bortezomib IC_{50} of 8.1 nM in U937 cells (Matondo et al., 2010). In order to assess the effect of Bortezomib on apoptosis induction, U937 cells were stained with Annexin V and Dapi following 24 hrs of treatment and analysed by FACs. Dual staining of Dapi and Annexin V permits assessment of apoptotic induction by presenting Annexin V on x-axis vs Dapi on y-axis (**Fig 6.2.1 B** gating strategy employed). Annexin V and Dapi negative cells represent the live population Q4, Annexin V+/Dapi- cells represent cells undergoing early stages of apoptosis Q3, Annexin V+/Dapi+ cells represent late apoptosis stage cells Q2. Q1 quadrant represents the dead cell population however in this assay dead cells are usually not present within this quadrant due to fragmentation of cells. Cells were treated with DMSO as the no drug control (NDC) in order to determine if cell death observed was due to the effect of the Bortezomib solvent. There was no change to the live cell population of untreated and NDC treated cells indicating any decrease in cell viability observed was not due to DMSO induced toxicity but due to specific Bortezomib drug effects (**Fig 6.2.1 C** and **D**). Bortezomib treated samples received DMSO at a concentration less than 0.0001 %. Increasing concentrations of Bortezomib treatment 5-15 nM resulted in decreased percentage of live cells in Q4 from 69.7 % to 41 % with a concomitant increase in cells staining positive for Annexin V and Dapi. There was near a twofold increase in late stage apoptotic cells with increasing Bortezomib treatment. 10 nM Bortezomib treatment resulted in an approximate 50 % decrease in cell viability with 55.7 % of cells remaining Annexin V and Dapi negative. Combining the IC_{50} determined from cell counts of 8.45 +/- 0.45 nM (**Fig 6.2.1 A**) with the results from the apoptosis assay (**Fig 6.2.1 B** and **C**) and published literature on Bortezomib treatment on leukaemic cell lines, 10 nM was chosen as the optimum Bortezomib concentration for the remainder of this study (Dijk et al., 2011, Du et al., 2012, Fang et al., 2012).

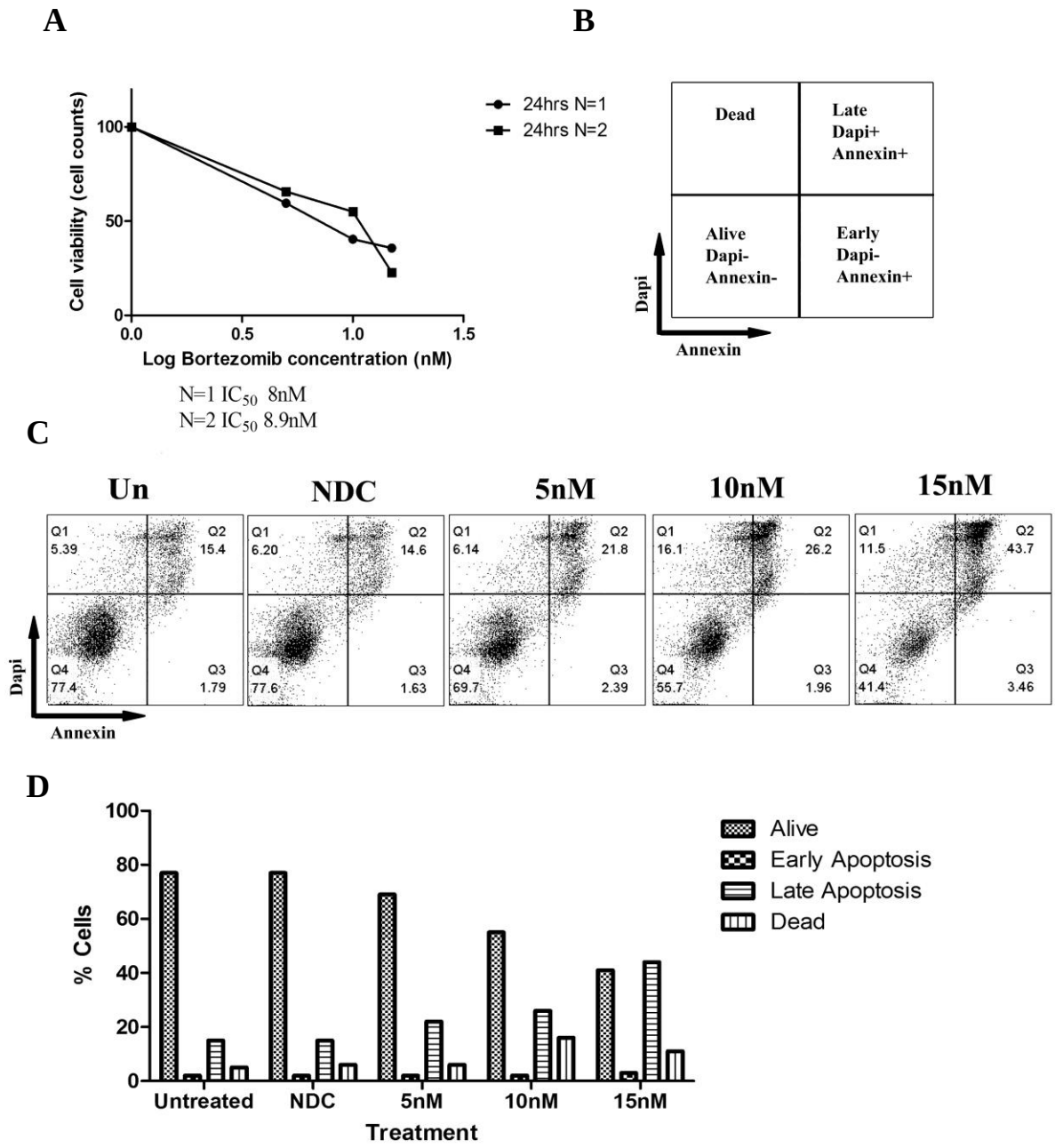

Fig 6.2.1 10 nM optimum Bortezomib concentration to assess cell death in U937 cells. A) 5, 10 and 15 nM Bortezomib treated U937 cell counts were normalised to untreated cell count and plotted against the log of Bortezomib concentration. Nonlinear regression calculated mean IC_{50} 8.45 nM. **B)** Apoptosis assay gating strategy. **C)** Apoptosis assay of U937 cells treated with 0, 5, 10 and 15 nM Bortezomib and NDC DMSO for 24 hrs. Cells were stained with Annexin V and Dapi and analysed by FACs. **D)** Graphical representation of apoptosis assay.

Result 6.2.2 TRIB2 overexpression increases Bortezomib induced cell death in U937 cells

Oncogenic perturbation perpetuated by high TRIB2 expression is dependent on its ability to mediate ubiquitin-dependent proteasomal degradation of C/EBPαp42 (**Fig 4.2.1**) (Keeshan et al., 2006, Keeshan et al., 2010). In order to determine if the high TRIB2 leukaemic cell could be pharmacologically targeted, cells were treated with Bortezomib at the selected concentration of 10 nM. U937 cells were transduced with bicistronic retroviral MigR1-eGFP control and MigR1-TRIB2-eGFP. As mentioned previously overexpression of TRIB2 in U937 cells recapitulates the high TRIB2 AML cell (Keeshan et al., 2006). Cells were transduced for 48 hrs, sorted for the GFP positive population and treated for 24 hrs with 10 nM Bortezomib. GFP expression was measured as a marker of cell viability by FACs analysis. Bortezomib treatment resulted in a decrease in GFP levels in both MigR1 and TRIB2 transduced cells indicative of cell death (**Fig 6.2.2 A**). However the decrease in GFP expression in Bortezomib treated TRIB2 overexpressing cells was much greater than MigR1 Bortezomib treated cells (MigR1 mean 67.3 % +/-1.40 SD vs TRIB2 42.03 % +/-1.37 SD). In order to control for slight variation in GFP expression in the untreated cells (MigR1 91.05 % +/-0.69 SD vs TRIB2 82.1 % +/-2.06 SD) GFP expression post-Bortezomib treatment was normalised to untreated mean GFP expression levels. TRIB2 overexpression results in a statistically significant decrease in cell viability, as determined by GFP expression, compared to MigR1 transduced cells (MigR1 0.757 +/-0.014 SD, TRIB2 0.608 +/-0.003 SD, t-test, p=0.0002) (**Fig 6.2.2 B**).

Assessment of apoptosis revealed Bortezomib treatment resulted in a shift in cell distribution from the Q4 live cell quadrant largely to the Q2 late apoptotic cell quadrant (**Fig 6.2.2 C**). Graphical representation of the mean percentage cells +/- SD from the apoptosis assay depicts the concomitant increase in late apoptosis Q2 corresponding with the decrease in live cells in Q4 (**Fig 6.2.2 D**). In order to validate the decrease in high TRIB2 cell viability observed through measurement of GFP upon Bortezomib treatment the cell viability was assessed through characterisation of live cells as those determined to be Annexin V-/Dapi-, thus assessing cell viability by two additional factors. Bortezomib treatment resulted in a decrease in cells in Q4 for both MigR1 and TRIB2 transduced cells, however the decrease observed for TRIB2 expressing cells was greater (MigR1 56.73 % +/- 1.12 SD, TRIB2 32.9 % +/- 1.20 SD). Bortezomib treated MigR1 cell viability was similar to Bortezomib treated untransduced U937 cell viability (55.7 %) (**Fig 6.2.1 C and D**), indicating empty vector MigR1 control did not differentially effect U937 cell response to Bortezomib treatment. Normalising treated Annexin-/Dapi- cell population to untreated

mean of Annexin-/Dapi- population to control for slight variation in MigR1 (93.25 % +/- 0.77 SD) and TRIB2 (85.2 % +/-2.17 SD) live populations revealed there was a statistically significant decrease in cell viability upon treatment in cells expressing TRIB2 (MigR1 0.608 +/- 0.012 SD, TRIB2 0.396 +/-0.014 SD, t-test p=0.0004) (**Fig 6.2.2 E**). These results show that the leukaemic cell line U937 transduced to express high levels of TRIB2 are more sensitive to Bortezomib induced cell death.

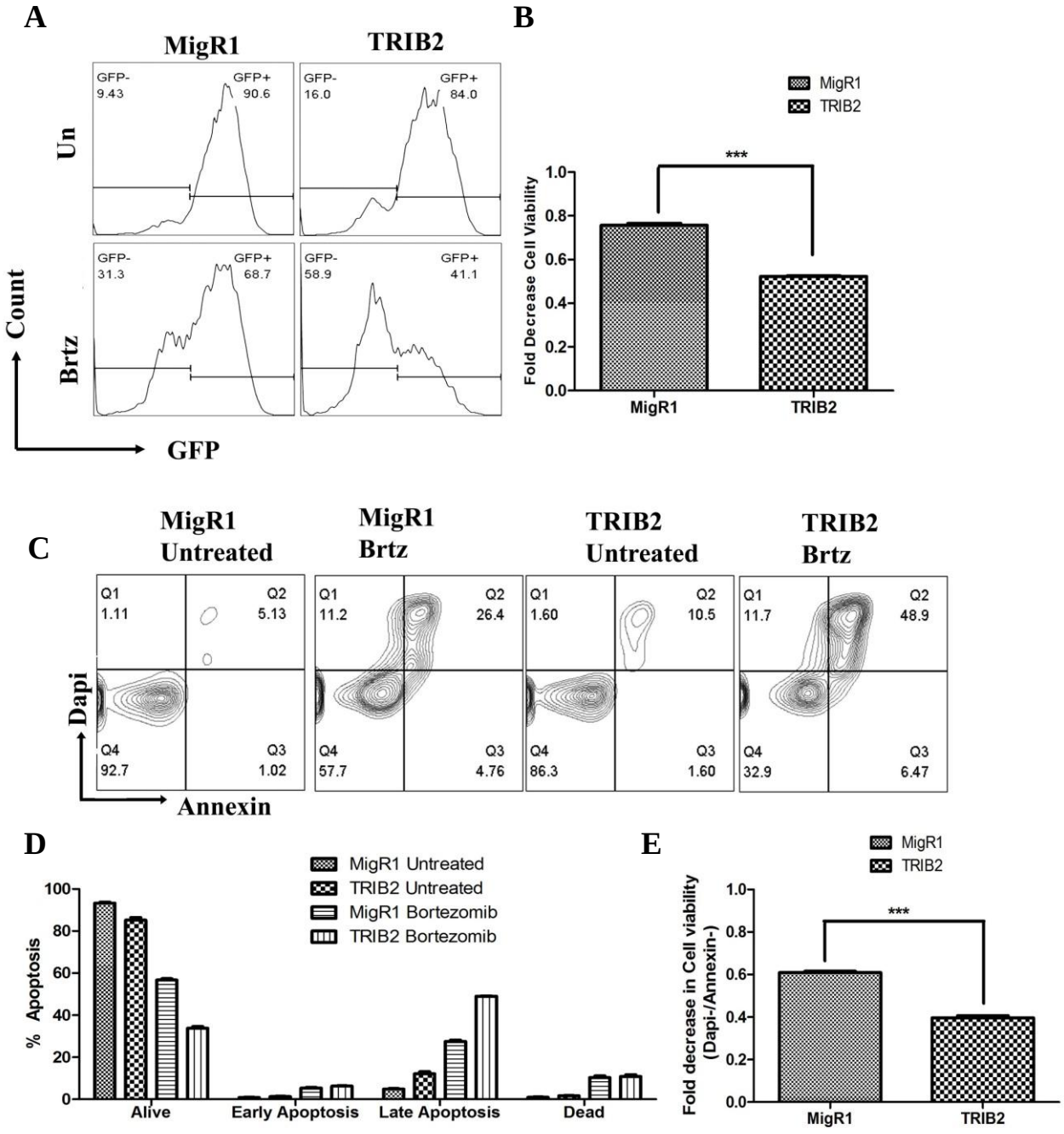

Fig 6.2.2 TRIB2 overexpression increases Bortezomib induced cell death. U937 cells were transduced with bicistronic retroviruses expressing TRIB2-eGFP and MigR1-eGFP empty vector control. 48 hrs post-transduction GFP positive cells were sorted and treated with 10 nM Bortezomib for 24 hrs. **A)** Percentage GFP expression was measured by FACS. **B)** GFP expression was normalised to untreated controls and plotted as the mean +/- SD, t-test p=0.0002. **C)** Apoptosis assay of cells stained with Annexin V and Dapi. **D)** Graphical representation of apoptosis assay plotting the mean +/- SD. **E)** Live cell population as measured by Annexin V-/Dapi- normalised to the untreated live population and plotted as the mean +/- SD, t-test p=0.0004. Data presented is representative of three independent transduction experiments containing 3 sample replicates.

Result 6.2.3 Loss of TRIB2-mediated ubiquitination of C/EBPαp42 abrogates TRIB2 sensitivity to Bortezomib-induced cell death

Overexpression of TRIB2 was identified to decrease U937 cell viability upon Bortezomib treatment (**Fig 6.2.2**) and Bortezomib treatment was reported to mediate cytotoxicity through accumulation of K48 ubiquitin linked proteins (Obeng et al., 2006). In order to determine if the increased sensitivity of TRIB2 overexpressing cells was attributable to the ubiquitination of C/EBPαp42, the drug treatment assay was performed using TRIB2-VPM-GFP construct which is unable to mediate C/EBPα ubiquitination (**Fig 4.2.8**) and subsequent proteasomal degradation of C/EBPαp42 through loss of the E3 ligase COP1 binding site (Keeshan et al., 2010). U937 cells were transduced with MigR1-eGFP, MigR1-TRIB2-eGFP and MigR1-TRIB2-VPM-eGFP for 48 hrs. GFP positive cell population was sorted and treated for 24 hrs with 10 nM Bortezomib. GFP expression was measured as a marker of cell viability by FACs analysis. Bortezomib treatment resulted in a decrease in GFP levels in MigR1, TRIB2 and TRIB2-VPM transduced cells indicative of cell death (**Fig 6.2.3 A**). In order to control for variation in GFP expression in the untreated cells GFP expression post Bortezomib treatment was normalised to the untreated mean GFP expression levels (MigR1 0.605 +/-0.040 SD, TRIB2 0.475 +/-0.016 SD, TRIB2-VPM 0.567 +/-0.002 SD) (**Fig 6.2.3 B**). TRIB2 overexpression resulted in a statistically significant decrease in cell viability as compared to MigR1 and TRIB2-VPM transduced cells (t-test MigR1 vs TRIB2 p=0.0041, TRIB2 Vs TRIB2-VPM p=0.0046). There was no statistically significant difference between MigR1 and TRIB2-VPM transduced cells (MigR1 vs TRIB2-VPM p=0.207) (**Fig 6.2.3 B**). The percentage of live cells determined by Annexin-/Dapi- population was approximately similar amongst transduced untreated cells (MigR1 74.9 5% +/- 3.32 SD, TRIB2 74.9 % +/- 4.42 SD, TRIB2-VPM 67.45 % +/- 10.39 SD) (**Fig 6.2.3 C**). Graphical representation of the mean percentage cells +/- SD in each quadrant from the apoptosis assay depicts the concomitant increase in both early apoptosis Q3 and late apoptosis Q2 corresponding with the decrease in live cells in Q4 (**Fig 6.2.3 D**). Bortezomib treatment resulted in a decrease in cells in Q4 for MigR1, TRIB2 and TRIB2-VPM transduced cells, however the decrease observed for WT-TRIB2 expressing cells was greater (MigR1 44.9 % +/- 1.41 SD, TRIB2 36.5 % +/- 2.80 SD, TRIB2-VPM 41.4 % +/- 0.60 SD) (**Fig 6.2.3 D**). Bortezomib treated Annexin V-/Dapi- cell population was normalised to untreated mean of Annexin V-/Dapi- population to control for slight variation in live populations (MigR1 0.599 +/- 0.02 SD, TRIB2 0.487 +/- 0.037, TRIB2-VPM 0.614 +/- 0.009 SD) (**Fig 6.2.3 E**). A statistically significant decrease in cell viability upon treatment in cells expressing WT-TRIB2 as compared to MigR1 and TRIB2-VPM was evident (t-test TRIB2 vs MigR1 p=0.034, TRIB2 vs TRIB2-VPM p=0.0046 and MigR1 Vs TRIB2-VPM p=0.306) (**Fig 6.2.3 E**). These results show that the loss of

TRIB2 proteolytic effect on C/EBPαp42 abrogates the sensitivity to Bortezomib-induced cell death in TRIB2 expressing U937 cell

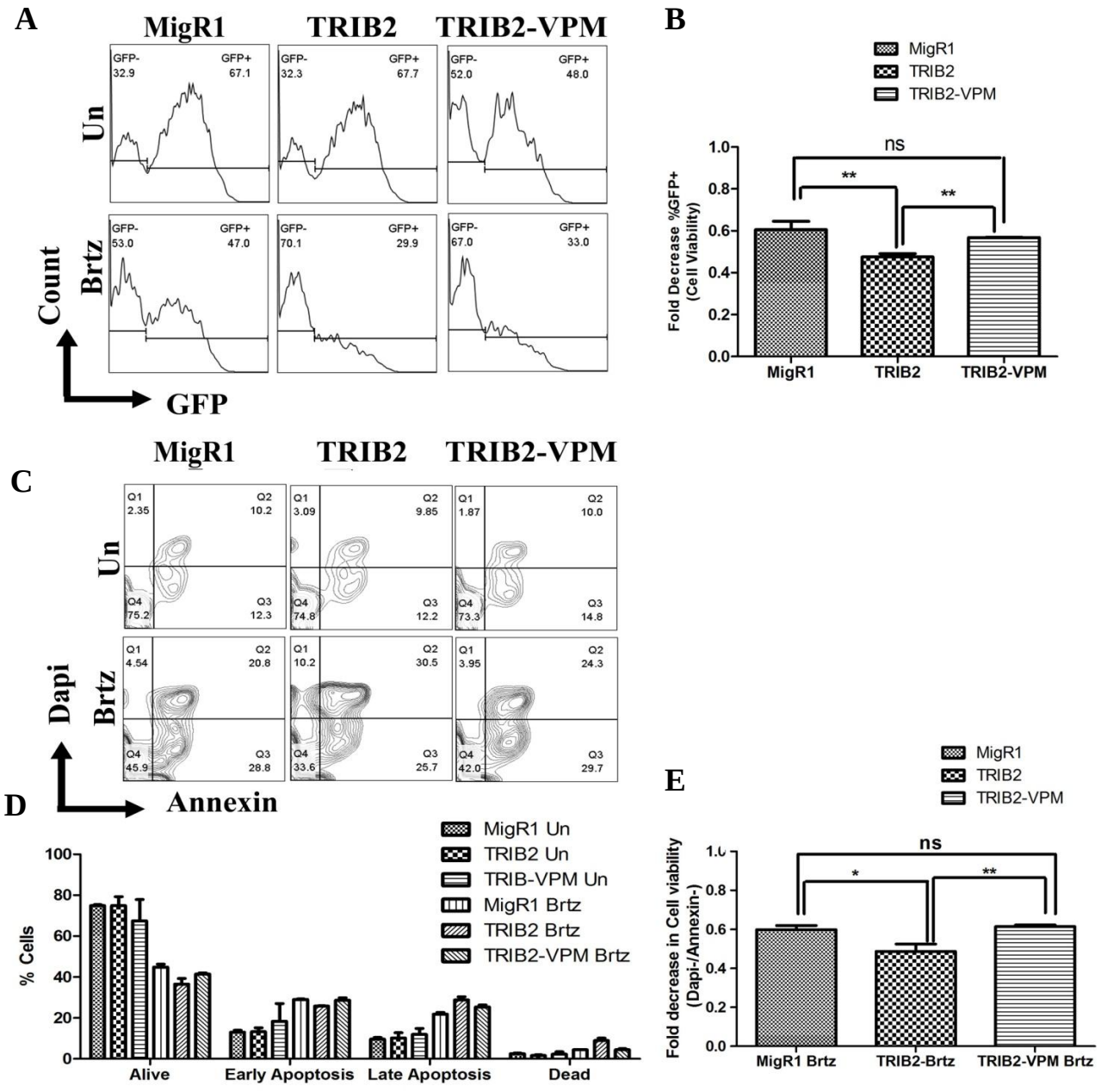

Fig 6.2.3 TRIB2-VPM abrogates TRIB2 increased Bortezomib induced cell death. U937 cells were transduced with TRIB2-VPM-GFP TRIB2-GFP and MigR1-GFP empty vector control. 48 hrs post transduction GFP positive cells were sorted and treated with 10 nM Bortezomib for 24 hrs. **A)** Percentage GFP expression was measured by FACS. **B)** GFP expression was normalised to untreated controls and plotted as the mean +/- SD. Bortezomib treatment resulted in a statistically significant decrease in TRIB2 cell viability vs MigR1 control and TRIB2-VPM. **C)** Apoptosis assay

of cells stained with Annexin V and Dapi. **D)** Graphical representation of Apoptosis assay plotting the mean +/- SD. **E)** Graphical representation of the live cell population as measured by Annexin V-/Dapi- normalised to the mean of the untreated Annexin V-/Dapi- population and plotted as the mean +/- SD. Bortezomib treatment does not result in a statistically significant decrease in TRIB2-VPM cell viability vs MigR1 control. Data presented is representative of two independent transduction experiments containing 3 sample replicates.

Result 6.2.4 High TRIB2 AML patient samples display increased cell death in response to Bortezomib treatment

To investigate if the high TRIB2 cell response to Bortezomib treatment observed in a leukaemic cell lines was evident in primary AML patient samples, peripheral blood derived mononuclear AML patient samples positive and negative for TRIB2 expression were treated with Bortezomib. Patient samples were genotyped on diagnoses as AML1 (JAK (anus kinase) V617F subtype M4), AML2 (karyotypically normal subtype M4) and AML3 (mutNPM1 mutDNMT3A no subtype available)**.** AML samples 1 and 2 were kindly provided by Dr. M. Cahill (University College Cork) while AML sample 3 was kindly provided by Dr. R. Delwel (Erasmus University). AML3 sample was a sample identified in the Valk dataset where gene expression analysis was performed on 285 AML patients and expression analysis identified high levels of TRIB2 expression associating with a cohort of patients with dysregulated C/EBPα signature (Valk et al., 2004, Keeshan et al., 2006). Cryopreserved primary AML patient samples 1 and 2 were characterised previously based on their TRIB2 expression levels (Rishi et al., 2014). There was no detectible TRIB2 protein expression in AML1 while AML2 and AML3 both had robust levels of TRIB2 protein expression (**Fig 6.2.4 A** top panel). AML1 expressed C/EBPαp42 protein while both AML2 and AML3 samples displayed low levels of C/EBPαp42 protein expression, coinciding with high TRIB2 expression status of these patients. Bortezomib treatment of AML3 restored C/EBPαp42 protein expression levels as confirmed by equal Actin expression confirming equal protein loading (**Fig 6.2.4 A**) Western blotting for AML samples 1 and 2 was performed by Dr. L. Rishi (**Fig 6.2.4 A**) (Rishi et al., 2014). AML samples were cultured in 10 nM Bortezomib for 24 hrs and cell death was measured by Dapi staining. Due to cell number limitations single replicates were collected for AML1 and AML2 while two replicates were collected for AML3. AML1 displayed only a 1 % change in cell death as measured by Dapi upon treatment. AML2 displayed a 30 % increase in Dapi staining and AML3 displayed a 49.70 % +/-1.4 SD increase (mean +/-SD) (**Fig 6.2.4 B** and **C**). Untreated AML samples displayed varying degrees of cell death indigenous to each sample (**Fig 6.2.4 B** and **C).** In order to normalise for background cell death the fold increase in cell death upon Bortezomib treatment was plotted. Bortezomib treatment did not result in a change in cell death in AML1, there was a 2.13 fold increase in AML2 cell death and a 8.17 +/-0.028 SD fold increase in cell death in AML3 treated with 10 nM Bortezomib (**Fig 6.2.4 D**). Therefore these data in primary patient samples show that the high TRIB2 cell is more sensitive to Bortezomib mediated cell death and strongly support the cell line data in the previous section.

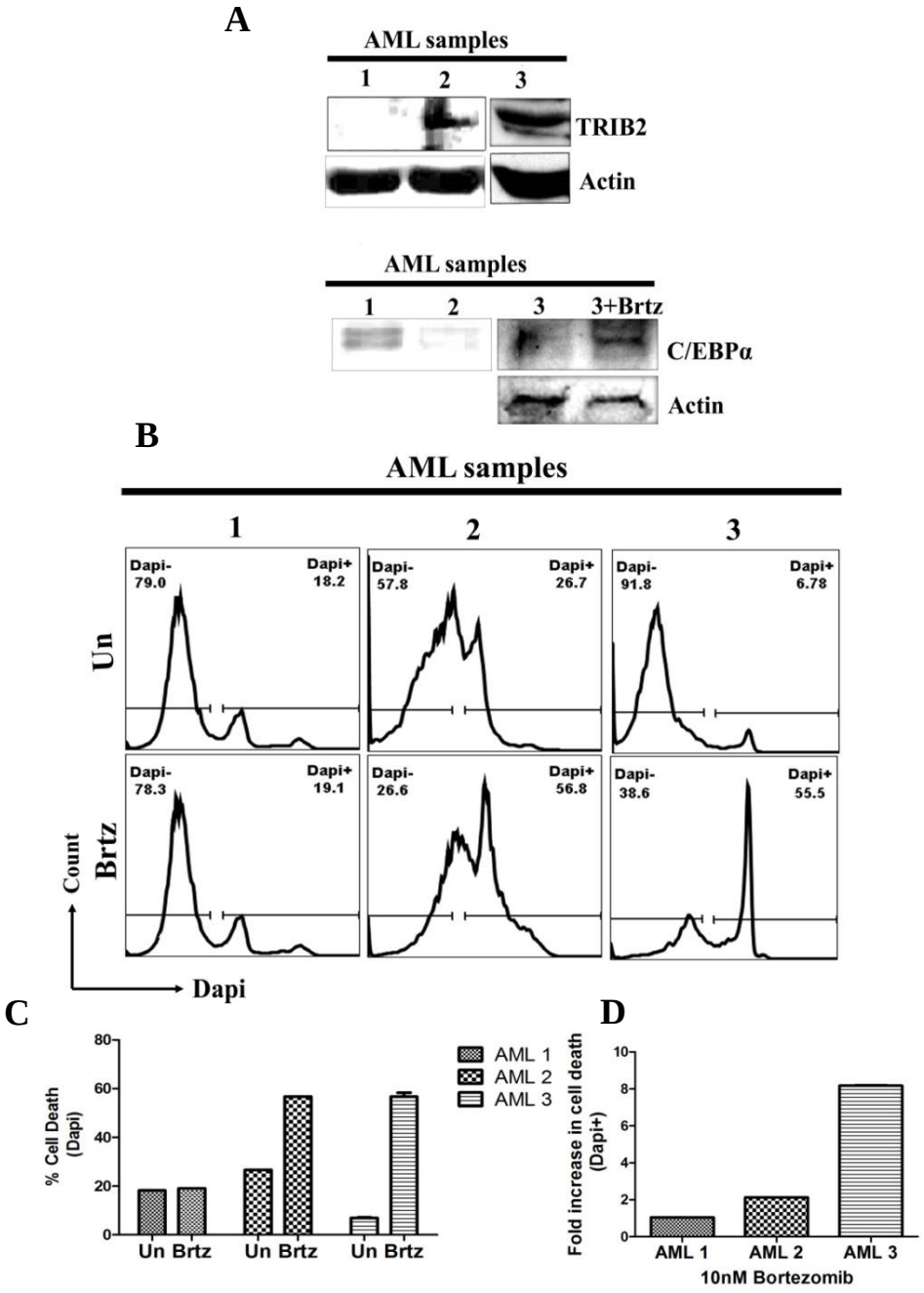

Fig 6.2.4 High TRIB2 AML samples display increased cytotoxicity in response to Bortezomib treatment. A) AML patient sample lysates were immunoblotted with anti TRIB2, anti C/EBPα and with anti Actin which served as a loading control. AML lysates were all prepared by Fíona Lohan; immunoblotting for AML samples 1 and 2 was performed by Dr. L. Rishi. Western blot for TRIB2 is published by (Rishi et al., 2014). **B)** AML samples were treated with 10 nM Bortezomib for 24 hrs, stained with Dapi and cell death was analysed by FACs. **C)** Graphical representation of percentage cell death as measured by Dapi staining. **D)** Fold increase in cell death as determined by Dapi positive cells. Percentage Dapi positive Bortezomib treated samples were normalised to percentage cell death in untreated samples.

Result 6.2.5 Bortezomib treatment increased the percentage of CD14$^+$ and/or CD11b$^+$ cells in high TRIB2 AML samples

Bortezomib treatment has been previously reported to mediate increased cytotoxicity to patients expressing high levels of granulocytic surface markers CD11b/CD14/CD15 than patients expressing lower levels of CD11b/CD14/CD15 (Riccioni et al., 2007). Additionally Bortezomib was identified to target the Aldehyde ALDH^{++} leukaemic stem cell (Riccioni et al., 2007). In order to determine the effect of Bortezomib exerted on the differentiated CD11b$^+$ myeloid cell population in the presence and absence of TRIB2 expression, AML1, AML2 and AML3 were stained for the myeloid cell marker CD11b in the absence and presence of Bortezomib treatment. CD11b is expressed on leukocytes including monocytes, neutrophils, NK cells, macrophages and granulocytes. The change in CD11b expression was assessed in the viable cell population (Dapi negative population). AML3 was also stained for CD14. CD14$^+$ is a marker of macrophages and monocytes. CD11b expression varies between individual leukaemias. AML1, AML2 and AML3 contained 22.2 %, 19.1 % and 63.6 % CD11b$^+$ cells respectively (**Fig 6.2.5 A**). Upon Bortezomib treatment there is a 1 % decrease in AML1 CD11b$^+$ population however there is a 22.3 % increase in CD11b$^+$ AML2 population. Bortezomib treatment of AML3 resulted in a decrease in CD11b$^+$ cells, but an increase in CD14$^+$ cells (**Fig 6.2.5 B**). As this assay was performed over a 24 hr period and AML samples were not maintained in culture media permissive of inducing differentiation, the decrease in CD11b$^-$/CD14$^-$ cells is potentially due to Bortezomib preferentially promoting cell death of this high TRIB2 less mature myeloid cell population resulting in the increase in CD11b$^+$ /CD14$^+$ cells observed. Thus ex vivo treatment of patients AML2 and AML3 resulted in an increase in terminally differentiated cell markers, while there was only a 1% change in CD11b$^+$ in patient AML1 which was not sensitive to Bortezomib induced cytotoxicity.

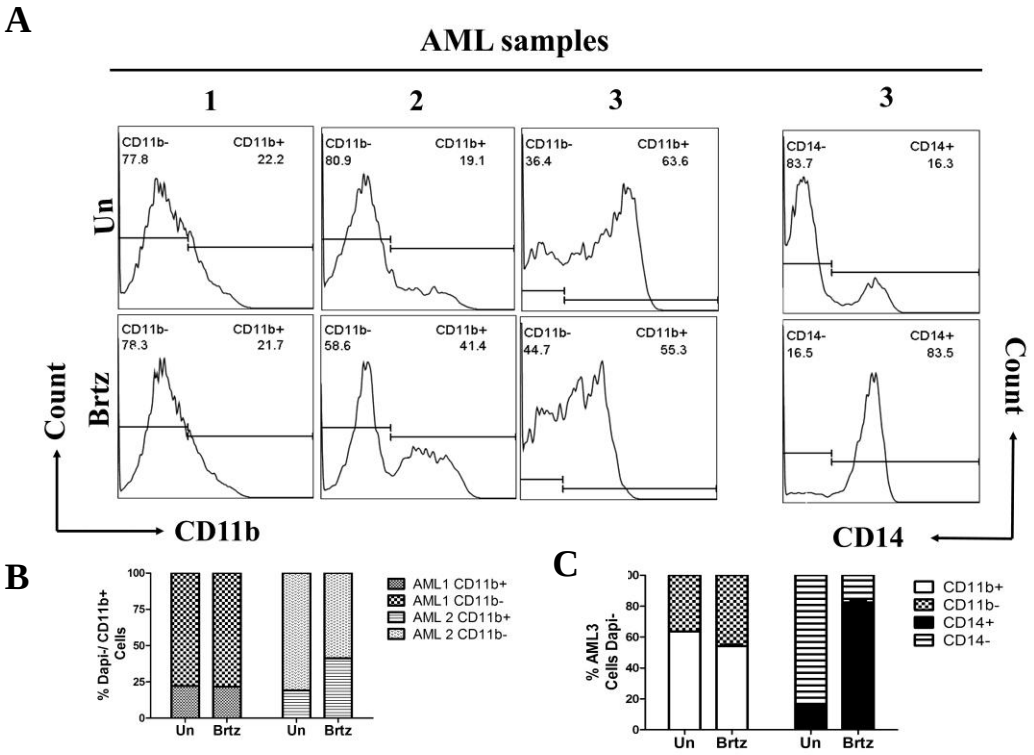

Fig 6.2.5 Bortezomib targets an immature myeloid cell population. A) AML1, AML2 and AML3 were stained with CD11b and CD14 (AML3 only) and analysed by FACs. Cells were gated on the Dapi negative population**. B)** Graphical representation of percentage Dapi negative $CD11b^{+}/CD11b^{-}$ cells in the absence and presence of Bortezomib treatment in AML1 and AML2. **C**) Graphical representation of percentage Dapi negative $CD11b^{+}/CD11b^{-}$ and $CD14^{+}/CD14^{-}$ cells in the absence and presence of Bortezomib treatment in AML3. (Note AML samples 1 and 2 were investigated at the same time while AML3 was investigated at a later date hence the different CD11b FACS gates employed).

6.3 Discussion

AML is a vastly heterogeneous disease with many associated genetic lesions. Bortezomib has been tested for efficacy in the treatment of AML as a single agent, in combination with standard induction therapy and recently with sorafenib tosylate in an ongoing phase III trial (AAML1031) with varying successes (Cortes et al., 2004, Attar et al., 2005, Attar et al., 2008, Sarlo et al., 2013, Attar et al., 2013). Perhaps the differential response of AML patients may reflect the effect of Bortezomib on the underlying genetic abnormalities. One of the main issues with AML treatment is a high relapse rate, due to proposed aberrant signalling cascades, particularly NFκB activation in the quiescent leukaemic stem cell (Guzman et al., 2001, Wang et al., 2011). There are several advantages to the clinical use of Bortezomib as a leukaemic treatment option. Leukaemic cells carry a large number of proteasomes and Bortezomib treatment results in low cytotoxicity to normal mononuclear $CD34^+$ cells, so it selectively targets the leukaemic cell (Kumatori et al., 1990, Riccioni et al., 2007, Colado et al., 2008, Attar et al., 2008, Fang et al., 2012). Bortezomib induced cell death, unlike cytrabine and Ara-C (induction therapy), does not require the cell to be actively cycling in order to induce cell death (online communication, Dr. E. Attar , Massachusetts General Hospital of http://www.dfhcc.harvard.edu/news/news/article/3287/,(Castaigne et al., 2004)). Thus Bortezomib treatment may prove to be an strong option to target the quiescent leukaemic stem cell (Attar et al., 2008). Additionally Bortezomib treatment has been proposed to act as a chemosensitiser. It is not a victim of the action of multi-drug resistant proteins, whose expression do not effect efflux of the drug (Oerlemans et al., 2008, Dijk et al., 2011, Wang et al., 2012). Thus in this manner Bortezomib treatment has been identified to sensitise leukaemic cells to many cytotoxic agents e.g. TRAIL, doxorubicin, idarubicin, valporic acid and cytrabine treatment (Colado et al., 2008, Dijk et al., 2011, Stapnes et al., 2014).

TRIB2 induces transplantable murine AML through multiprotein complex formation with an E3 ubiquitin conjugating ligase COP1, resulting in K48 ubiquitin-dependent proteasomal degradation of C/EBPαp42 as shown in chapter 4 (Keeshan et al., 2006, Keeshan et al., 2010). Additionally, I have shown that loss of the COP1 binding site on TRIB2 (TRIB-VPM) abrogates its ability to mediate ubiquitination of C/EBPαp42, and to induce murine AML (Keeshan et al., 2010). TRIB2-mediated degradation of C/EBPαp42 was inhibited by treatment with both proteasomal inhibitors MG-132 and Bortezomib as shown in chapter 5. To date, studies of *TRIB2* expression in AML patients have identified elevated mRNA expression in a specific subset of AML patients with dysregulated C/EBPαp42 signatures (Valk et al., 2004, Keeshan et al., 2006). A recent study identified elevated *TRIB2* mRNA and protein expression in AML cell lines and AML patient

samples (Rishi et al., 2014). This provided the rational to investigate Bortezomib as a potential targeted therapy for high TRIB2 leukaemic cells.

In this chapter I have determined that TRIB2 overexpression in U937 cells resulted in increased cytotoxicity to Bortezomib treatment versus MigR1 transduced control cells. Additionally I confirmed that the increased cytotoxicity mediated by TRIB2 was dependent on its E3 ligase binding capabilities. TRIB2-VPM transduced cells displayed similar reduction in cell viability to Bortezomib treatment of MigR1 control cells. Thus it may be postulated that loss of TRIB2-mediated ubiquitination, through loss of its COP1 binding site, served to inhibit the increased cytotoxicity observed. As TRIB2 is proposed to function as an adaptor protein with E3 ligase binding capabilities I propose elevated TRIB2 expression increases Bortezomib cytotoxicity due to the increased accumulation of K48 ubiquitinated proteins, specifically C/EBPαp42. As previously reported the accumulation of K48 ubiquitinated proteins is thought to mediate Bortezomib cytotoxicity on a cellular level through triggering ER stress, autophagy and apoptosis (Obeng et al., 2006, Fang et al., 2012). Bortezomib mediated cytotoxicity may be caused by more than an increase in K48 ubiquitinated proteins. Inhibition of proteasomal degradation in the presence of TRIB2 ultimately results in an increase in C/EBPαp42 protein levels. Tamoxifen mediated cell death was attributed to an increase in C/EBPαp42 protein levels through its association with p21 (Cheng et al., 2007). Also ER stress results in expression of pro-apoptotic BIM (Puthalakath et al., 2007). This induction of BIM is mediated by CHOP and C/EBPαp42 transcriptional activation of BIM (Puthalakath et al., 2007). Thus Bortezomib treatment results in accumulation of K48 ubiquitinated proteins maintaining C/EBPαp42 protein levels and potentially also triggering apoptosis through activation of BIM and through its association with p21 (Cheng et al., 2007, Poulaki et al., 2007).

Bortezomib treatment also induces cell death in AML patient samples identified to express TRIB2 protein supporting the U937 cell line data. Bortezomib treatment of an AML1 patient sample negative for TRIB2 expression did not result in an increase in cytotoxicity. AML1 patient possessed JAKV617F mutation, occurrence of which results in aberrant STAT activation (Kundranda et al., 2012). I propose the large cytotoxicity observed by AML2 and AML3 compared to AML1 is due to the high levels of TRIB2 expression in those samples. However one would expect a small degree of cytotoxicity upon Bortezomib treatment in AML1 sample. The presence of JAKV617F mutation may provide resistance to Bortezomib cytotoxicity through aberrant STAT pathway activation (reviewed by (Lee et al., 2013)). Furthermore there is great variation in AML primary sample response to Bortezomib treatment. Analysis of the literature identifies reports of 0-

10 % increase in apoptotic cells in AML samples upon Bortezomib treatments of 20-100 nM (Matondo et al., 2010). Assessment of additional AML samples response to Bortezomib is thus warranted.

The ability of Bortezomib to inhibit NFκB aberrant signalling through stabilisation of inhibitory IκB suggests proteasomal inhibition may preferentially target specific haematopoietic cells, as aberrant NFκB signalling is a hallmark of a leukaemic stem cell (Guzman et al., 2001, Guzman et al., 2002). Bortezomib has been identified to show enhanced specificity for an immature $CD34^{+}$ cell in comparison to doxorubicin (Colado et al., 2008). Indeed I identified Bortezomib induced cytotoxicity resulted in a decrease in $CD11b^{-}$ cells in AML2 patient sample and decreased $CD14^{-}$ cells in AML3 patient sample. However Bortezomib treatment increased $CD11b^{-}$ cells in AML3 patient sample. A 1% change was identified in AML1 which exhibited no cytotoxicity to Bortezomib treatment. Thus perhaps the immature cell population targeted by Bortezomib is dependent on the individual leukaemia and the respective differentiation status of the leukaemias ultimately affecting the cell death response.

As is often common with chemotherapeutics there are dose limiting side effects. In the case of Bortezomib these include peripheral neuropathy and thrombocytopenia (Argyriou et al., 2008). Development of second generation proteasomal inhibitors Carfilzomib and ONX 0912 which are epoxyketones may ameliorate these effects (Demo et al., 2007). Preclinical investigations determined both AML and ALL cells are sensitive to Carfilzomib and ONX and these second generation inhibitors may overcome Bortezomib resistance disease (Niewerth et al., 2013). Recently Carfilzomib has been identified to induce apoptosis in CML cells sensitive and resistant to tyrosine kinase inhibition and the CML cell immunoproteasomal load was identified to associate with Carfilzomib response (Crawford et al., 2014). Combinational treatment of CML cells with Carfilzomib and TKIs synergised, identifying a potential treatment regime for TKI resistant CML disease (Crawford et al., 2014). Here I have documented the first report of a targeted therapy for TRIB2 leukaemic disease. Additional to TRIB2 leukaemias Bortezomib may also selectively target high TRIB2 NSCLCs also identified to mediate degradation of C/EBPαp42 (Grandinetti et al., 2011). In vivo murine model trials will be necessary to support the molecular data presented.

Chapter 7: General Discussion

7.1 Summary and overall conclusions

TRIB2 is a potent oncogene driving fully penetrant transplantable murine AML in BMT models and shown to be elevated in a cohort of patient AMLs (Keeshan et al., 2006). TRIB2 leukaemogenicity is intrinsically linked to its proteolytic relationship with C/EBPα (Keeshan et al., 2006, Keeshan et al., 2010). Indeed TRIB2 is unable to induce murine AML in the absence of C/EBPα degradation and elevated TRIB2 expression in AML patients associate with a dysregulated C/EBPα signature (Keeshan et al., 2006, Keeshan et al., 2010). To date the information regarding TRIB2 effect on C/EBPα was limited to direct binding and proteasomal degradation of C/EBPαp42 full length isoform (Keeshan et al., 2006). This project further elucidated the features of this molecular interaction and provided additional insight into the molecular biology of TRIB2-mediated AML. TRIB2 is currently classified as a pseudokinase as it lacks demonstrable kinase-like activity. In the context of our study TRIB2 is functionally defined as an adaptor or scaffold protein as it facilitates the formation of a multiprotein complex through multiple protein-binding domains. TRIB2 requires C/EBPα binding, its kinase-like domain and C-Terminal E3 ligase COP1 binding in order to elicit its leukaemic effects (Keeshan et al., 2010). TRIB2 increased expression resulting in inhibition of C/EBPα fits the Gilliland two hit model of leukaemogenesis (Kelly and Gilliland, 2003). TRIB2 may be classified as type I mutation "a classic oncogene" resulting in loss of C/EBPα function, classified as a type II mutation halting differentiation.

TRIB2 direct binding mediated K48 ubiquitin-dependent degradation of C/EBPαp42

Molecular analysis performed within this study determined TRIB2 amino acids S227/S229/S231/K233 within subdomain VIII of the kinase-like domain are required for direct TRIB2 and C/EBPα binding. These amino acids were identified as a crucial site for C/EBPα binding initially in peptide arrays and subsequent SASSAs. The role of the specific amino acids was supported by in silico analysis using protein-protein interaction software PIPE which predicted TRIB2 amino acids 227-258 mediated C/EBPα binding. SDM of TRIB2-S227A/S229A/S231A/K233A abrogated TRIB2 ability to bind C/EBPα in mammalian cells as determined by co-IP. Additionally, investigation into this TRIB2 region required for C/EBPα binding revealed it was rich in secondary structure permissive of protein-protein interactions. Identification of TRIB2-S227A/S229A/S231A/K233A supports the use of peptide array technology in the identification of protein interaction sites. To date no 3D structure exists for TRIB2, and predictive structural analysis has been performed in an attempt to get some idea of the structure of

this protein. TRIB2 has been modelled on PIM1 using Swiss Model homology modelling service and predicted to have a structure similar to that of an active kinase (Hegedus et al., 2007). TRIB proteins have been identified as phosphoproteins capable of being phosphorylated however the pseudokinase classification extends from their inability to mediate transfer of phosphates (Boylan et al., 2003, Hegedus et al., 2007, Wang et al., 2013b). Amino acids S227/S229/S231/K233 span a putative GSK3 phosphorylation site S/TXXXS/T. Mutation of S227A/S229A/S231A/K233A may alter the 3D structure of the TRIB2 protein, indeed upon SDS-PAGE analysis immunoblotting with anti TRIB2 antibody identified TRIB2-S227A/S229A/S231A/K233A runs at a slightly lower molecular weight than WT-TRIB2 and it loses the tight top doublet band detected by TRIB2 antibody upon expression of WT-TRIB2. Perhaps mutation of this site results in loss of a phosphorylation site required for TRIB2 interaction with C/EBPα. Regardless of the molecular dynamics resulting from mutation of S227A/S229A/S231A/K233A, this region is essential for C/EBPα binding. Upon documentation of TRIB2 3D structure this may be fully elucidated. Previous investigation of TRIB2 family member TRIB1 and its site of C/EBPα binding was performed by creation of deletion constructs, generated by deletion of up to 180 amino acids which is ~ 1/3 of the protein, localising C/EBPα binding site in N-Terminal/N-Terminus of the kinase-like domain of TRIB1 (Yokoyama et al., 2010). These deletion constructs undoubtedly alter protein 3D structure. It is proposed that SDM of specific amino acids is the most conclusive and easily accessible option available for assessing sites of protein-protein interaction (Ofran and Rost, 2007). Interestingly homologous analysis revealed TRIB1 partially retains elements of SSSK binding sequence identified in TRIB2. TRIB1 contains T2572/T259/S261/K262 which also classifies as a putative GSK3 phosphorylation site and therefore may also exert a role in C/EBPα interaction.

TRIB2 was identified to mediate proteasomal degradation of full length C/EBPαp42 suggestive of an ubiquitin-dependent mechanism. Indeed in vivo ubiquitination assays identified TRIB2 expression in HEK293t cells, which endogenously express COP1, mediated K48 specific ubiquitination of C/EBPαp42. Loss of COP1:TRIB2 binding abrogated the ability of TRIB2 to mediate C/EBPα ubiquitination verifying it as the bona fida E3 ligase involved in ubiquitin conjugation. Analysis involving C/EBPαp42-R339A (previously identified as TRIB2 binding site on C/EBPα) revealed TRIB2 was unable to mediate its ubiquitination supporting the binding dependency for TRIB2-mediated ubiquitination of C/EBPα. This theory was validated as TRIB2-S227A/S229A/S231A/K233A was also unable to mediate ubiquitination of C/EBPαp42 additionally supporting its identification as a crucial site for C/EBPα binding.

Upon investigation of putative C/EBPα binding sites on TRIB2, R77 was identified in the analysis. This arginine is homologous to TRIB1-R107 identified mutated in an AML patient (Yokoyama et al., 2012). Molecular analysis of TRIB1-R107L revealed it had an increased proteolytic effect on C/EBPα compared to WT-TRIB1 (Yokoyama et al., 2012). The functions of TRIB1 and TRIB2 slightly differ in that TRIB1 is identified as a modulator of MAPK signalling and its degradation of C/EBPα is dependent on MEK1 binding (Yokoyama et al., 2010, Dedhia et al., 2010). The authors report TRIB1 increases P-ERK1/2 and TRIB1-R107L further enhanced ERK1/2 phosphorylation, suggesting it may be due to either enhanced modulation of MAPK signalling pathway or alternatively due to a conformational change to TRIB1 protein that may alter its affinity for protein partners. However, examination of the data provided by the authors for the affect of TRIB1 and TRIB1-R107L on P-ERK1/2 reveals initially the increases mediated to P-ERK1/2 are equivocal and only upon IL-3 stimulation do TRIB1-R107L cells retain the enhanced increase in P-ERK1/2 while WT-TRIB1 cells do not (Yokoyama et al., 2012). This supports the notion of TRIB1-R107 acquiring a conformational state which enhances increased MEK1 protein binding, propagating increased P-ERK1/2 and increased C/EBPα binding as increased degradation was observed (Yokoyama et al., 2012). Co-IP analysis of TRIB2-R77 revealed despite lower expression levels and a slightly lower molecular weight as observed during SDS-PAGE, that it had increased C/EBPα binding. Additional to this, ubiquitination assays revealed it also displayed increased ubiquitination of C/EBPαp42 compared to WT-TRIB2. Based on the observation that TRIB1-R107L increased degradation of C/EBPα (a binding dependent effect) and the observation herein of TRIB2-R77A displaying increased binding to C/EBPα and resultant increase in mediated C/EBPα ubiquitination, I propose loss of this homologous arginine facilitates TRIB proteins acquiring a structurally permissive state for increased protein binding. TRIB1-R017L reduced the latency of TRIB1 induced AML and perhaps TRIB2-R77A may also result in a gain of functionality.

Bortezomib treatment as a targeted therapy for TRIB2-mediated ubiquitination of dimeric P-Ser21-C/EBP at K313

C/EBPα is commonly referred to as the "master regulator of haematopoiesis" or as a "gatekeeper of AML", indicative of its nonredudant role in haematopoiesis (Zhang et al., 2004). C/EBPα exists as two isoforms a full length C/EBPαp42 isoform and an N-Terminally truncated C/EBPαp30 isoform (Pabst et al., 2001b). C/EBPα is classified as a tumour suppressor whilst C/EBPαp30 is reported to have oncogenic potential through its ability to exert a dominant negative effect on C/EBPαp42 function through repressive heterodimerisation and through Ubc9 mediated sumoylation of C/EBPαp42 (Pabst et al., 2001b, Cleaves et al., 2004, Geletu et al., 2007). TRIB2 mediates K48

ubiquitin-dependent proteasomal degradation of C/EBPαp42 resulting in a concomitant increase in C/EBPαp30 isoform. A leukaemic feedback loop has been identified whereby C/EBPαp30 can further drive *TRIB2* expression through direct promoter binding in an E2F dependent manner (Rishi et al., 2014). TRIB2 retains the ability to bind both C/EBPαp42 and C/EBPαp30 however its interaction with C/EBPαp30 does not require proteasomal inhibition unlike C/EBPαp42 (Keeshan et al., 2006). This suggests that TRIB2 binding to C/EBPαp30 does not mediate its degradation, also supported by the increase in C/EBPαp30 observed upon TRIB2 expression (Keeshan et al., 2006). TRIB2-mediating proteasomal degradation of C/EBPαp42 but not C/EBPαp30 remains to be fully elucidated. It may be postulated that the increase in C/EBPαp30 observed is due to partial proteolysis of C/EBPαp42. Secondary structures and glycine rich regions (GRR) are known to proteolytically protect protein isoforms, e.g. generation of p50 from p105 is due to partial proteolysis and p50 was identify to be protected due to presence of a GRR which affects proteasomal processing (Lin and Ghosh, 1996). Alternatively TRIB2 may perturb ribosomal scanning and encourage eIF-2α translation from the alternative internal C/EBPαp30 translation start site. TRIB3 has been reported to regulate eIF-2α activity under conditions of cell stress (Ohoka et al., 2005). However in light of my work I propose an additional hypothesis. C/EBPα possesses several phosphorylation sites regulated by different kinases in response to cellular stresses, induction of apoptosis and activation of MAPK cascades. P-Ser21-C/EBPα was identified to inhibit C/EBPα induced differentiation and was identified to exert additional selectivity over protein partner binding (Ross et al., 2004, Radomska et al., 2006, Graham et al., 2009, Koleva et al., 2012). P-Ser21-C/EBPα and unphosphorylated-Ser21-C/EBPα were identified to differentially interact with specific protein partners (Koleva et al., 2012, Fragliasso et al., 2012). TRIB2 decreases the levels of P-Ser21 through preferentially binding the phosphorylated form and mediating increased ubiquitination. P-Ser21 was identified to result in a conformation change to C/EBPα dimer culminating in the TADs migrating away from each other ultimately increasing the space between the individual monomers which are homodimerised (Ross et al., 2004). I propose this phosphorylation event results in a sterically favourable confirmation for increased TRIB2 binding at C/EBPαR339 and increased ubiquitin conjugation. C/EBPαp30 lacks this P-Ser21 site and therefore cannot assume the structurally permissive confirmation resulting in the increased ubiquitination and proteasomal degradation. Provisional ubiquitination assays performed did suggest C/EBPαp30 ubiquitination levels do not increase in the presence of TRIB2 (data not shown). TRIB2 also exerts preferential degradation of C/EBPαp42 dimers. TRIB2 retains the ability to bind both monomeric and dimeric C/EBPαp42 however it preferentially ubiquitinates dimeric C/EBPαp42, reducing its protein half life. This suggests C/EBPα dimers are more

accessible to COP1:TRIB2 ubiquitination. TRIB2 and C/EBPα proteolytic relationship I propose is strongly influenced by steric factors such as protein dimerisation and 3D conformation in response to phosphorylation changes.

Determination of the critical lysine residue for C/EBPα ubiquitination was performed using ubpred analysis which calculated the probability score for each lysine to act as the site of ubiquitin conjugation on C/EBPα. K313 among 6 other lysines were identified with med-high probability scores. Mutation of C/EBPα-K313R abrogated TRIB2-mediated ubiquitination of C/EBPαp42, identifying K313 as the ubiquitination site on C/EBPαp42. Expression of TRIB2 did not increase the levels of C/EBPαp30 in C/EBPα-K313R expressing cells indicating that ubiquitination of C/EBPαp42 was required for the increase in C/EBPαp30. Interestingly annotation of K313 revealed the occurrence of a C/EBPα mutation in patient AML, K313dup (Carnicer et al., 2008). C/EBPα-K313dup protein displays reduced stability compared to WT-C/EBPαp42 and induces AML in murine models (Carnicer et al., 2008, Bereshchenko et al., 2009, Kato et al., 2011). K313dup mutation is associated with CD7 expression in AML patients, a phenotype observed in C/EBPαp42 excised HSCs (Wouters et al., 2007, Carnicer et al., 2008). Thus I propose K313dup mutation results in increased ubiquitination, proteasomal degradation and subsequent loss of C/EBPαp42 protein. AML is a vastly heterogeneous disease and knowledge of the molecular biology behind the genetic aberrations will further advance the treatment of the disease and help decipher targeted therapies for different causes.

Due to TRIB2-mediated ubiquitin-dependent proteasomal degradation of C/EBPαp42, proteasomal inhibition was investigated as a putative treatment strategy. Bortezomib is reported to mediate cell death by a variety of mechanisms including induction of ER stress due to the accumulation of ubiquitinated proteins triggering apoptosis (Obeng et al., 2006, Fang et al., 2012). Indeed leukaemic cells overexpressing TRIB2 were more sensitive to Bortezomib induced proteasomal inhibition mediated cell death than control cells. Ex vivo AML patient samples response further supported the increased sensitivity of high expressing TRIB2 AMLs to Bortezomib treatment. Ectopic expression of C/EBPα has also been identified to induce apoptosis and inhibit cellular proliferation in liver cancers cells, thus restoration of C/EBPα expression may also mediate Bortezomib mediated cell death (Wang et al., 2013a). Leukaemic cell sensitivity to Bortezomib induced cytotoxicity has been linked to expression of proteasomal subunits and their respective phenotypes: either immune or constitutive (Oerlemans et al., 2008, Franke et al., 2012, Fang et al., 2012, Niewerth et al., 2013). TRIB2 sensitivity to Bortezomib treatment may also be mediated by alterations in proteasomal

subunit expression levels. Bortezomib targets PSMB5 and the TRIB2 leukaemic cell may possess altered PSMB5 proteasome subunit expression (Oerlemans et al., 2008).

Aside from elevated TRIB2 AMLs, Bortezomib may serve as a targeted treatment for mutC/EBPα-K313dup AMLs, potentially restoring differentiation arrest and inducing cytotoxicity to leukaemic cells. Identification of elevated *TRIB2* expression in AML patients is associated with biphenotypic disease as they display both myeloid and lymphoid signatures (Wouters et al., 2007). Biphenotypic AMLs respond poorly to current therapeutics (Zhang et al., 2009, Matutes et al., 2011). Interestingly the subset of elevated *TRIB2* AMLs levels displayed CD7 expression, similar to K313dup AMLs potentially identifying CD7 as a biomarker for increased Bortezomib sensitivity to induced cell death and potentially improved survival for such biphenotypic patients (Wouters et al., 2007).

7.2 Future perspectives

Exploitation of the increased sensitivity of TRIB2 expressing leukaemic cells may provide opportunities for treatment of other high TRIB2 expressing malignancies. TRIB2 was identified to be elevated in 30 % of NSCLC tumours and indeed TRIB2 was identified to mediate proteasomal degradation of C/EBPα (Grandinetti et al., 2011). Bortezomib has shown efficacy in the treatment of NSCLC in both a phase I trial and in phase II trial combined with gemcitabine and carboplatin (Aghajanian et al., 2002, Davies et al., 2009). Aberrant Wnt signalling is prevalent in gastro-intestinal and liver cancers resulting in increased *TRIB2* expression, which was identified to be essential for survival and transformation of hepatocellular carcinoma cells (Wang et al., 2013a). TRIB2 oncogenicity has been linked to its negative impact of C/EBPα protein expression, and indeed TRIB2 knockdown increased C/EBPα levels revealing an inhibitory C/EBPα effect on target genes required for transformation (Wang et al., 2013a). Thus in this context Bortezomib may also provide a treatment option for the emerging role of TRIB2 or dysregulated Wnt signalling in liver cancers through facilitation of C/EBPα transformation-dependent-target gene repression. Ultimately elucidating the molecular mechanism of a disease enables the use of targeted therapy approaches. Binding dependent TRIB2-mediated K48 ubiquitin-specific proteasomal degradation of C/EBPαp42 via ubiquitin conjugation at K313, may be a relationship also conserved in different tissues and subsequent dysregulation may occur in other malignancies as mentioned above. What is learnt here in the leukaemic cell has wider implications for TRIB2 and C/EBPα molecular biology mediating malignant disease.

7.3 Proposed Model

COP1 binds TRIB2 via its C-Terminal binding site. **A**) Phosphorylation of C/EBPα at Ser21 results in a structurally favourable confirmation for TRIB2 binding through dimer separation. **B**) COP1 bound TRIB2 mediates K48 ubiquitination of C/EBPα via conjugation of polyubiquitin chain at K313 in C/EBPα C-terminus. **C**) The C/EBPα K48 polyubiquitin chain is recognised by the proteasome resulting in degradation of C/EBPαp42. **D**) Bortezomib treatment inhibits proteasomal activity resulting in accumulation of K48 polyubiquitinated C/EBPα resulting in cell death in the presence of high TRIB2 expression.

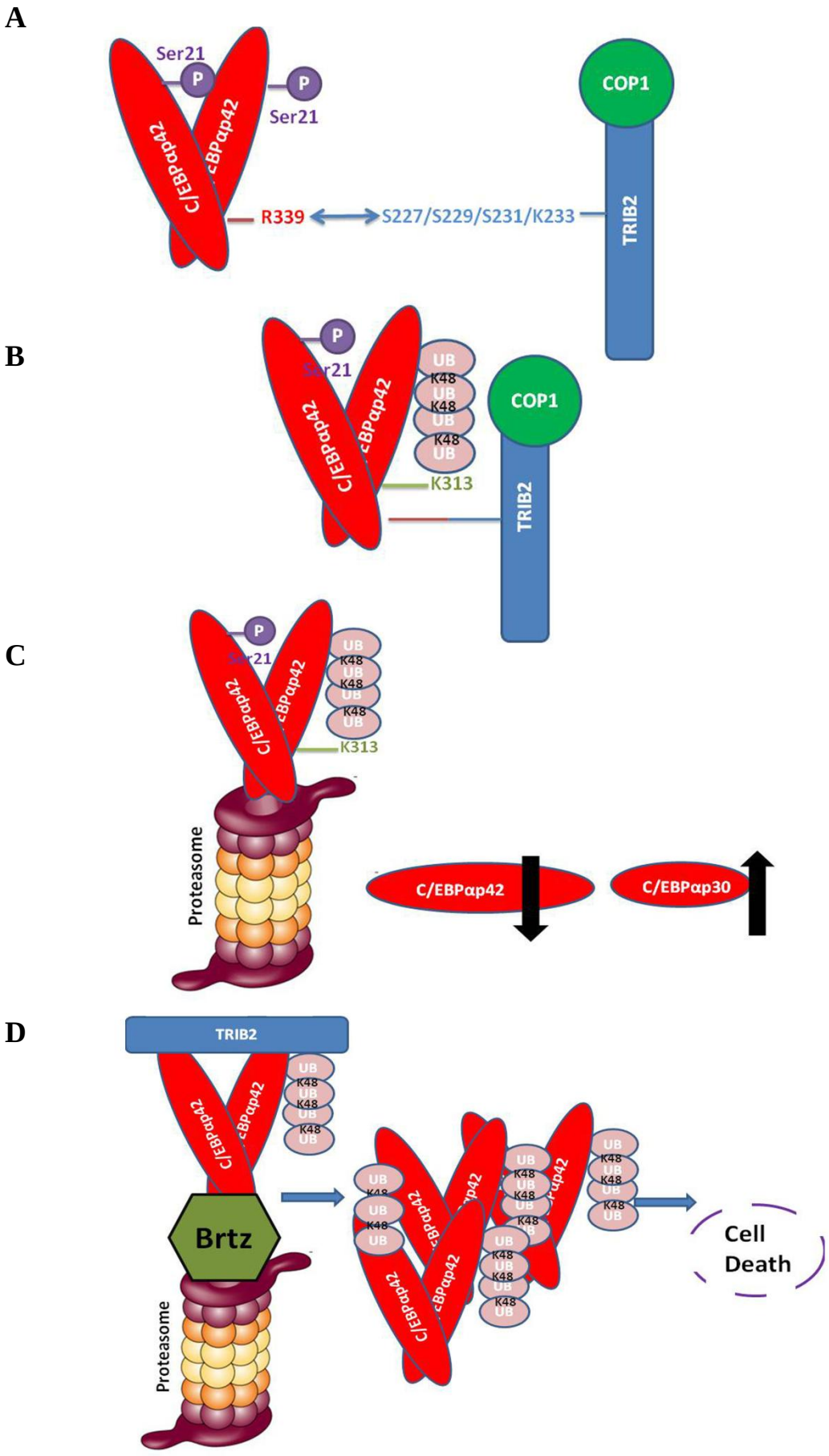
A
Ser21
P
P
Ser21
C/EBPαp42
C/EBPαp42
COP1
TRIB2
R339
S227/S229/S231/K233
B
P
Ser21
C/EBPαp42
C/EBPαp42
UB
K48
UB
K48
UB
K48
UB
K313
COP1
TRIB2
C
P
Ser21
C/EBPαp42
C/EBPαp42
UB
K48
UB
K48
UB
K48
UB
K313
Proteasome
C/EBPαp42
C/EBPαp30
D
TRIB2
C/EBPαp42
C/EBPαp42
UB
K48
UB
K48
UB
K48
UB
Brtz
Proteasome
Cell
Death

Chapter 8: Appendix

8.1.1

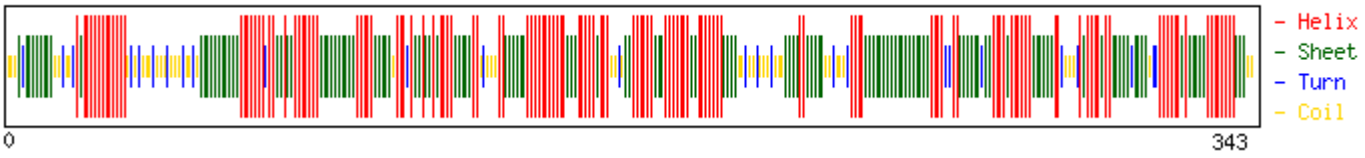

Secondary Structure:

```
                *       *       *       *       *
Query 1   MNIHRSTPITIARYGRSRNKTQDFEELSSIRSAEPSQSFSPNLGSPSPPETPNLSHCVSC 60
Helix 1                 HHHHHHHHHHHHHHH                 HHH 60
Sheet 1     EEEEEEEEEE      EEE                     EEEEEEE 60
Turns 1      T       T  T  T        T T   T   T   T  T       60

                *       *       *       *       *
Query 61  IGKYLLLEPLEGDHVFRAVHLHSGEELVCKVFDISCYQESLAPCFCLSAHSNINQITEII 120
Helix 61  HHHHHHHHHHHHHHHHHHHHHHHHHHHHHHHHHHHHHHHHHHHHHHH      HHHHHHHHHHHHHH 120
Sheet 61  EEEEEEEEE     EEEEE      EEEEEEEEEEEEEEEEEEEE      EEEEEEEE 120
Turns 61          T         TT          T         T         120

                *       *       *       *       *
Query 121 LGETKAYVFFERSYGDMHSFVRTCKKLREEEAARLFYQIASAVAHCHDGGLVLRDLKLRK 180
Helix 121 HHHHHHHHHHH     HHHHHHHHHHHHHHHHHHHHHHHHHHHHHHHHH     HHHHHHHHHH 180
Sheet 121 EEEEEEEEE      EEEEEEEEEE       EEEEEEEEEE      EEEEEEEEEE 180
Turns 121   T       T           TT             T          180

                *       *       *       *       *
Query 181 FIFKDEERTRVKLESLEDAYILRGDDDSLSDKHGCPAYVSPEILNTSGSYSGKAADVWSL 240
Helix 181 HHHHHHHHHHHHHHHHHHHHHH              HH          HHHHHHHH 240
Sheet 181 EE      EEEEEEEEEEEEE          EEEEEEEEEEE         EEEE 240
Turns 181     T T         T     T  T  T       T     T   T        240

                *       *       *       *       *
Query 241 GVMLYTMLVGRYPFHDIEPSSLFSKIRRGQFNIPETLSPKAKCLIRSILRREPSERLTSQ 300
Helix 241 HHHHHHHHH     HHHHHHHHHHHHHHHHHHHHHHHHH HHHHHHHHHHHHHHH     HHHHH 300
Sheet 241 EEEEEEEEEEEEEE      EEEEEEEEEEEEEEE      EEEEEE       EEEE 300
Turns 241               TT      TT     T  T         T   T   TT 300

                *       *       *       *
Query 301 EILDHPWFSTDFSVSNSAYGAKEVSDQLVPDVNMEENLDPFFN 343
Helix 301 HHHHHHHHHHHHH     HHHHHHHHHHHHHHHHHHHHHHH      343
Sheet 301 EEEEEEEEEEEEEE       EEEEEEEEE     EEEE   343
Turns 301     T    T     TT       T       T       343


Total Residues: H: 235   E: 197   T: 45
      Percent: H: 68.5  E: 57.4  T: 13.1
```

Fig 8.1 Chou Fasman secondary structure prediction server analysis of TRIB2 amino acid sequence. Highlighted in red are S227/S229/S231/K233 sequence and the prediction of Turns (T).

8.1.2

Amino acid	L	N	T	S	G	S	Y	S	G	K	A	A
Residue NO.	224	225	226	227	228	229	230	231	232	233	234	235
Turn	-	-	-	T	T	T	T	T	T	-	-	-

Fig 8.1.2 Net TURN P prediction of Beta Turns in proteins. Prediction of the presence of Beta turns in TRIB2 protein, output was edited for ease of represenation to analyse amino acids 224-235. S227-S331 are all expected Beta turn regions.

8.2

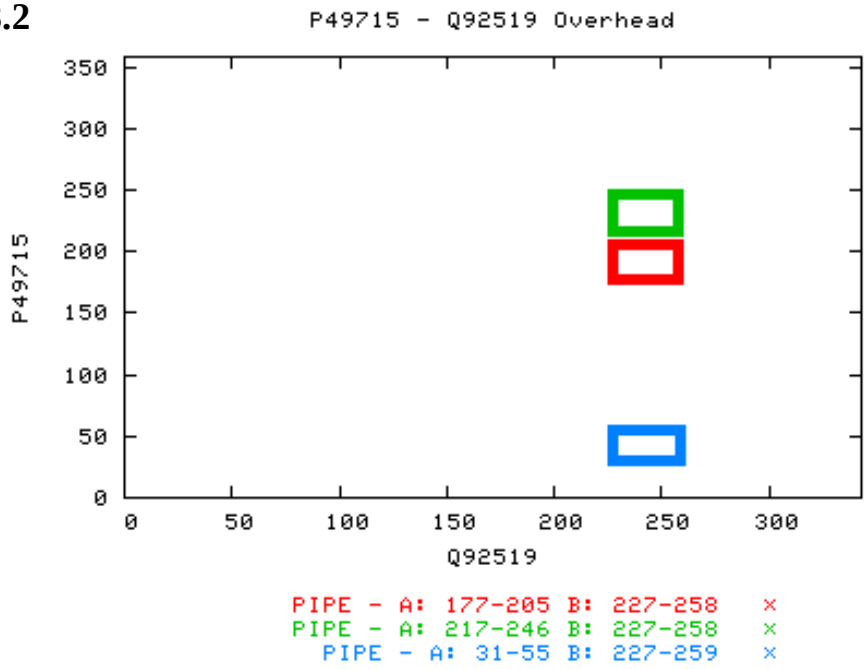

Fig 8.2 PIPE prediction of TRIB2 and C/EBPα protein interaction sites. Q92519 UnitProt accession for hTRIB2, P497515 UniProt accession for hC/EBPα

8.3

Amino acid no.	Residue	%Relative solvent accessibility	ASA (A)	Amino acid no.	Residue	%Relative solvent accessibility	ASA (A)
215	C	16	22.46	251	R	31	70.99
216	P	23	32.63	252	Y	30	64.11
217	A	20	22.04	253	P	34	48.24
218	Y	29	61.97	254	F	28	56.19
219	V	26	39.96	255	H	36	65.48
220	S	20	23.44	256	D	32	46.11
221	P	24	34.05	257	I	22	40.7
222	E	18	31.44	258	E	24	41.92
223	I	31	57.35	259	P	25	35.47
224	L	16	29.29	260	S	19	22.26
225	N	26	38.06	261	S	14	16.4
226	T	31	42.99	262	L	15	27.46
227	**S**	**33**	**38.67**	263	F	14	28.09
228	G	26	20.46	264	S	13	15.23
229	**S**	**20**	**23.44**	265	K	16	32.91
230	Y	28	59.83	266	I	21	38.85
231	**S**	**30**	**35.16**	267	R	28	64.12
232	G	29	22.82	268	R	18	41.22
233	**K**	**27**	**55.53**	269	G	33	25.97
234	A	18	19.83	270	Q	23	41.07
235	A	21	23.14	271	F	27	54.18
236	D	22	31.7	272	N	28	40.99
237	V	19	29.2	273	I	33	61.05
238	W	18	43.29	274	P	30	42.57
239	S	22	25.78	275	E	28	48.91
240	L	15	27.46	276	T	33	45.77
241	G	18	14.16	277	L	22	40.28
242	V	16	24.59	278	S	19	22.26
243	M	12	24.01	279	P	22	31.21
244	L	14	25.63	280	K	15	30.85
245	Y	8	17.09	281	A	17	18.73
246	T	24	33.28	282	K	14	28.79
247	M	23	46.02	283	C	14	19.65
248	L	23	42.11	284	L	13	23.8
249	V	20	30.74	285	I	20	37

Fig 8.3 Sarpred analysis Real Value prediction of surface accessibility of TRIB2. Prediction of solvent-accessible surface area amino acids (ASA). ASA scores of S227-39, S229-23, S231-35, K233-55.

8.4

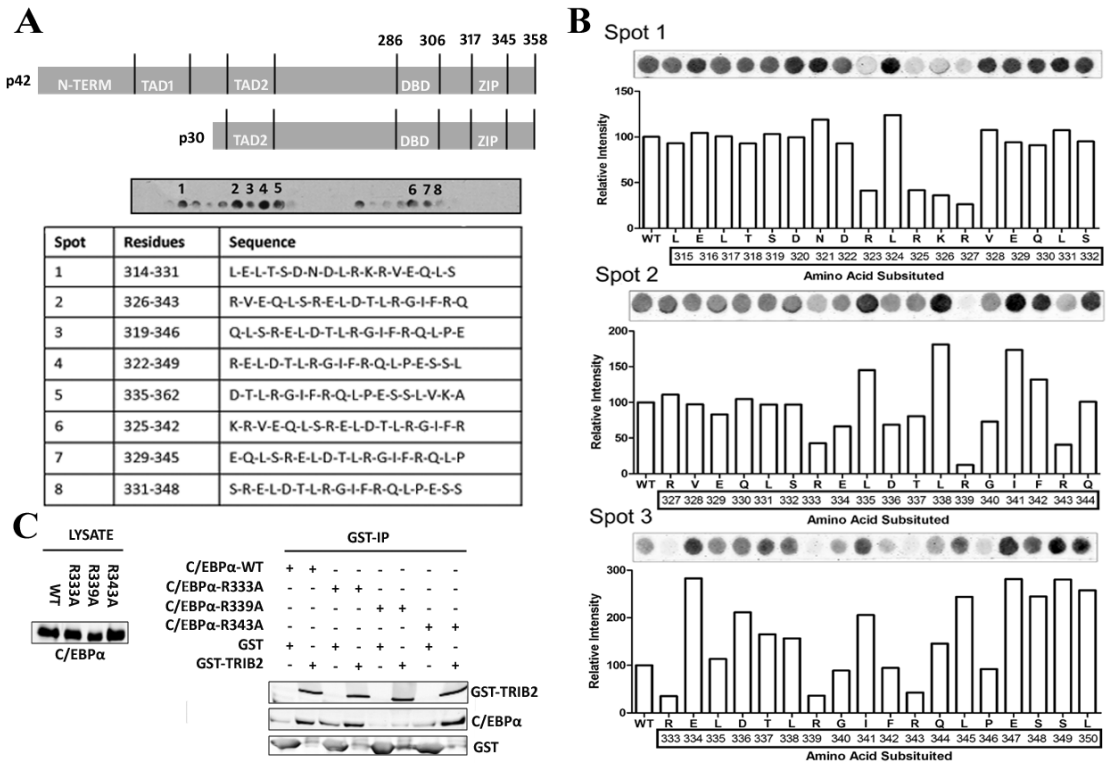

Spot	Residues	Sequence
1	314-331	L-E-L-T-S-D-N-D-L-R-K-R-V-E-Q-L-S
2	326-343	R-V-E-Q-L-S-R-E-L-D-T-L-R-G-I-F-R-Q
3	319-346	Q-L-S-R-E-L-D-T-L-R-G-I-F-R-Q-L-P-E
4	322-349	R-E-L-D-T-L-R-G-I-F-R-Q-L-P-E-S-S-L
5	335-362	D-T-L-R-G-I-F-R-Q-L-P-E-S-S-L-V-K-A
6	325-342	K-R-V-E-Q-L-S-R-E-L-D-T-L-R-G-I-F-R
7	329-345	E-Q-L-S-R-E-L-D-T-L-R-G-I-F-R-Q-L-P
8	331-348	S-R-E-L-D-T-L-R-G-I-F-R-Q-L-P-E-S-S

Fig 8.4 Identification of R339 as the TRIB2 binding site on C/EBPα. (Performed by Ciaran Forde, Dr. Karen Keeshan) (**A**) Peptide arrays of immobilized overlapping 18-mer peptides each shifted to the right by 3 amino acids encompassing C/EBPα were generated as described in Materials and Methods ***2.2.7***. Identical peptide arrays were probed with GST-TRIB2 and GST respectively. Eight binding spots unique to GST-TRIB2 were identified. The table displays the amino acid identity of these spots and reveals that GST-TRIB2 binds to amino acids within the C-Terminus of C/EBPα. This array is representative of two independent arrays. Dark spots are indicative of peptide binding. (**B**) Specific Alanine Scanning Substitution Arrays (SASSAs) on a region spanning the C-Terminus of C/EBPα were probed with GST-TRIB2. A decrease in the intensity of the spots upon alanine substitution is indicative of decreased binding of GST-TRIB2 to CEBPα. The binding of GST-TRIB2 to each alanine substituted peptide was quantified by densitometry and presented as a percentage of the control unmutated WT sequence, with an underlay identifying the amino acid which was substituted with an alanine. The intensities of spots corresponding to mutated R333, R339, and R343 show a greater than 50% reduction in intensity relative to the un-mutated peptide control spot. (**C**) Western blot analysis of HEK293t cell lysates equally expressing wild type C/EBPα and C/EBPα mutants (left panel). GST pull-down carried out using GST-TRIB2 followed by Western blot analysis for GST (right top and bottom panels) and C/EBPα (right middle panel), identify R339 as the TRIB2 binding site on C/EBPα.

8.5

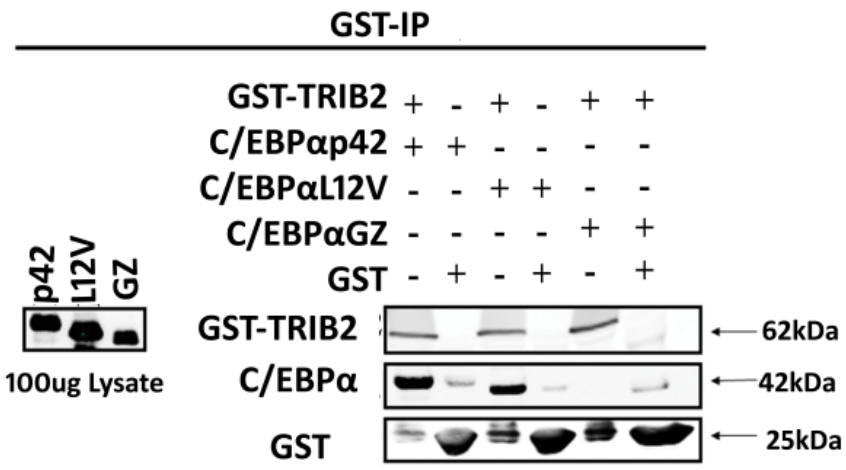

Fig 8.5 The C-Terminal LZ domain of C/EBPα is required for its interaction with TRIB2. (Performed by Ciaran Forde, Dr. Karen Keeshan). GST pull down using HEK293t lysates expressing C/EBPαp42, L12V and GZ proteins. Left panel represents Western blot for C/EBPαp30 in HEK293t cell lysates. Right panels represent IP for GST followed by western blot for GST (top and bottom panels) and C/EBPα (middle panel).

8.6

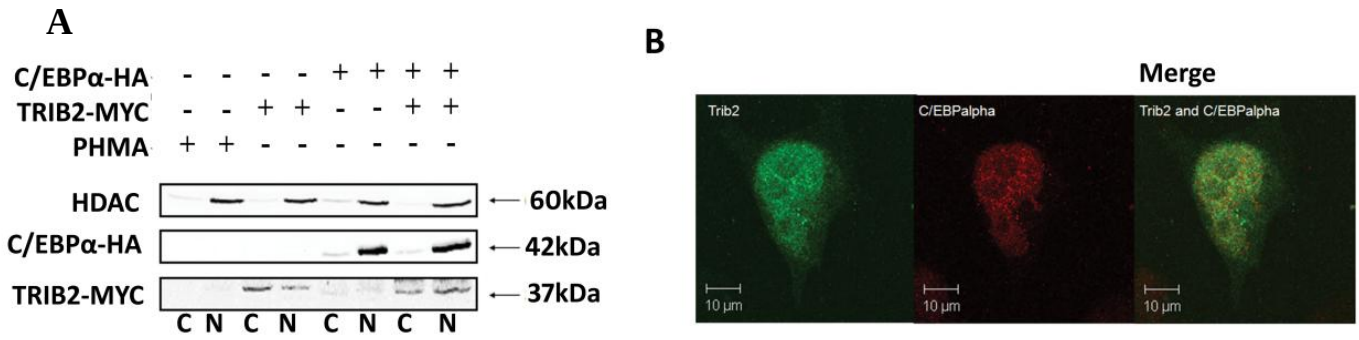

Figure 8.6: TRIB2 co-localises with C/EBPα in the nucleus. (Performed by Ciaran Forde, Dr. Karen Keeshan) (A) HeLa cells were transfected with vector only control, C/EBPα-Ha alone, TRIB2-MYC alone and C/EBPα and TRIB2-MYC together. 16 hrs post transfection cells were fractionated into cytoplasmic and soluble nuclear fractions. Protein expression of the each fraction was assessed by Western blot. TRIB2-MYC and C/EBPα were both detectable in the nuclear fraction when co-expressed. (B) HeLa cells co-expressing TRIB2-MYC (green) and C/EBPα (red) were visualised using confocal microscopy. Distinct areas of co-localisation (yellow) were seen to occur exclusively within the nucleus (arrows).

9. Bibliography

AGHAJANIAN, C., SOIGNET, S., DIZON, D. S., PIEN, C. S., ADAMS, J., ELLIOTT, P. J., SABBATINI, P., MILLER, V., HENSLEY, M. L., PEZZULLI, S., CANALES, C., DAUD, A. & SPRIGGS, D. R. 2002. A phase I trial of the novel proteasome inhibitor PS341 in advanced solid tumor malignancies. *Clin Cancer Res,* 8**,** 2505-11.

AKASAKA, , B., , R., , S., , M., , W., , K., , B., , C., , H., , G., , M.-S., , A., , B., , C., , D., , H., , H., , K., , L., , L., , M., , N.-K., , R.-W., , S., , S., , A., , W., , W., , S., , H., , S. & DYER. 2007. Five members of the CEBP transcription factor family are targeted by recurrent IGH translocations in B-cell precursor acute lymphoblastic leukemia (BCP-ALL). *Blood*.

AKASHI, K., TRAVER, D., MIYAMOTO, T. & WEISSMAN, I. L. 2000. A clonogenic common myeloid progenitor that gives rise to all myeloid lineages. *Nature,* 404**,** 193-7.

ALHARBI, R., PETTENGELL, R., PANDHA, H. & MORGAN, R. 2012. The role of HOX genes in normal hematopoiesis and acute leukemia. *Leukemia,* 27**,** 1000-1008.

ALTSCHUL, S. F., MADDEN, T. L., SCHÄFFER, A. A., ZHANG, J., ZHANG, Z., MILLER, W. & LIPMAN, D. J. 1997. Gapped BLAST and PSI-BLAST: a new generation of protein database search programs. *Nucleic Acids Research,* 25**,** 3389-3402.

ARGIROPOULOS, B., PALMQVIST, L., YUNG, E., KUCHENBAUER, F., HEUSER, M., SLY, L. M., WAN, A., KRYSTAL, G. & HUMPHRIES, R. K. 2008. Linkage of Meis1 leukemogenic activity to multiple downstream effectors including Trib2 and Ccl3. *Exp Hematol,* 36**,** 845-59.

ARGYRIOU, A. A., ICONOMOU, G. & KALOFONOS, H. P. 2008. Bortezomib-induced peripheral neuropathy in multiple myeloma: a comprehensive review of the literature.

ARKIN, M. R. & WELLS, J. A. 2004. Small-molecule inhibitors of protein-protein interactions: progressing towards the dream. *Nat Rev Drug Discov,* 3**,** 301-317.

ARNASON, T. & ELLISON, M. J. 1994. Stress resistance in Saccharomyces cerevisiae is strongly correlated with assembly of a novel type of multiubiquitin chain. *Mol Cell Biol,* 14**,** 7876-83.

ATTAR, E. C., DE ANGELO, D. J., SIRULNIK, A., WADLEIGH, M., BALLEN, K. K., MILLER, K. B., GALINSKY, I., NEUBERG, D., TREHU, E., SCHENKEIN, D., STONE, R. M. & AMREIN, P. C. 2005. Addition of Bortezomib (Velcade) to AML Induction Chemotherapy Is Well Tolerated and Results in a High Complete Remission Rate.

ATTAR, E. C., DE ANGELO, D. J., SUPKO, J. G., D'AMATO, F., ZAHRIEH, D., SIRULNIK, A., WADLEIGH, M., BALLEN, K. K., MCAFEE, S., MILLER, K. B., LEVINE, J., GALINSKY, I., TREHU, E. G., SCHENKEIN, D., NEUBERG, D., STONE, R. M. & AMREIN, P. C. 2008. Phase I and pharmacokinetic study of bortezomib in combination with idarubicin and cytarabine in patients with acute myelogenous leukemia. *Clin Cancer Res,* 14**,** 1446-54.

ATTAR, E. C., JOHNSON, J. L., AMREIN, P. C., LOZANSKI, G., WADLEIGH, M., DEANGELO, D. J., KOLITZ, J. E., POWELL, B. L., VOORHEES, P., WANG, E. S., BLUM, W., STONE, R. M., MARCUCCI, G., BLOOMFIELD, C. D., MOSER, B. & LARSON, R. A. 2013. Bortezomib added to daunorubicin and cytarabine during induction therapy and to intermediate-dose cytarabine for consolidation in patients with previously untreated acute myeloid leukemia age 60 to 75 years: CALGB (Alliance) study 10502. *J Clin Oncol,* 31**,** 923-9.

BAGGER, F. O., RAPIN, N., THEILGAARD-MONCH, K., KACZKOWSKI, B., THOREN, L. A., JENDHOLM, J., WINTHER, O. & PORSE, B. T. 2013. HemaExplorer: a database of mRNA expression profiles in normal and malignant haematopoiesis. *Nucleic Acids Res,* 41**,** D1034-9.

BEHRE, G., SINGH, S. M., LIU, H., BORTOLIN, L. T., CHRISTOPEIT, M., RADOMSKA, H. S., RANGATIA, J., HIDDEMANN, W., FRIEDMAN, A. D. & TENEN, D. G. 2002. Ras Signaling Enhances the Activity of C/EBPα to Induce Granulocytic Differentiation by Phosphorylation of Serine 248. *Journal of Biological Chemistry,* 277**,** 26293-26299.

BENGOECHEA-ALONSO, M. T. & ERICSSON, J. 2010. The ubiquitin ligase Fbxw7 controls adipocyte differentiation by targeting C/EBPα for degradation. *Proceedings of the National Academy of Sciences,* 107**,** 11817-11822.

BENNETT, J. M., CATOVSKY, D., DANIEL, M. T., FLANDRIN, G., GALTON, D. A., GRALNICK, H. R. & SULTAN, C. 1976. Proposals for the classification of the acute leukaemias. French-American-British (FAB) co-operative group. *Br J Haematol,* 33**,** 451-8.

BERESHCHENKO, O., MANCINI, E., MOORE, S., BILBAO, D., MÅNSSON, R., LUC, S., GROVER, A., JACOBSEN, S. E. W., BRYDER, D. & NERLOV, C. 2009. Hematopoietic Stem Cell

Expansion Precedes the Generation of Committed Myeloid Leukemia-Initiating Cells in C/EBP± Mutant AML. *Cancer cell,* 16**,** 390-400.

BEUTLING, U. & FRANK, R. 2010. Epitope Analysis Using Synthetic Peptide Repertoires Prepared by SPOT Synthesis Technology. *Antibody Engineering***,** 537-571.

BOGAN, A. A. & THORN, K. S. 1998. Anatomy of hot spots in protein interfaces. *J Mol Biol,* 280**,** 1-9.

BONVINI, P., ZORZI, E., BASSO, G. & ROSOLEN, A. 2007. Bortezomib-mediated 26S proteasome inhibition causes cell-cycle arrest and induces apoptosis in CD-30+ anaplastic large cell lymphoma. *Leukemia.* England.

BOUDEAU, J., MIRANDA-SAAVEDRA, D., BARTON, G. J. & ALESSI, D. R. 2006. Emerging roles of pseudokinases. *Trends in Cell Biology,* 16**,** 443-452.

BOWIE, M. B., MCKNIGHT, K. D., KENT, D. G., MCCAFFREY, L., HOODLESS, P. A. & EAVES, C. J. 2006. Hematopoietic stem cells proliferate until after birth and show a reversible phase-specific engraftment defect. *J Clin Invest,* 116**,** 2808-16.

BOYLAN, A. J. B., SHEILA, S. & JOHN, F. 2003. SKIP3, a novel Drosophila tribbles ortholog, is overexpressed in human tumors and is regulated by hypoxia. *Oncogene,* 22**,** 2823-2835.

BRYDER, D., ROSSI, D. J. & WEISSMAN, I. L. 2006. Hematopoietic Stem Cells : The Paradigmatic Tissue-Specific Stem Cell. *Am J Pathol,* 169**,** 338-46.

BUITENHUIS, M., VERHAGEN, L. P., VAN DEUTEKOM, H. W., CASTOR, A., VERPLOEGEN, S., KOENDERMAN, L., JACOBSEN, S. E. & COFFER, P. J. 2008. Protein kinase B (c-akt) regulates hematopoietic lineage choice decisions during myelopoiesis. *Blood,* 111**,** 112-21.

BURGER, J. A., GHIA, P., ROSENWALD, A. & CALIGARIS-CAPPIO, F. 2009. The microenvironment in mature B-cell malignancies: a target for new treatment strategies.

BURNETT, A., WETZLER, M. & LÖWENBERG, B. 2011. Therapeutic Advances in Acute Myeloid Leukemia.

BYRD, J. C., MROZEK, K., DODGE, R. K., CARROLL, A. J., EDWARDS, C. G., ARTHUR, D. C., PETTENATI, M. J., PATIL, S. R., RAO, K. W., WATSON, M. S., KODURU, P. R., MOORE, J. O., STONE, R. M., MAYER, R. J., FELDMAN, E. J., DAVEY, F. R., SCHIFFER, C. A., LARSON, R. A. & BLOOMFIELD, C. D. 2002. Pretreatment cytogenetic abnormalities are predictive of induction success, cumulative incidence of relapse, and overall survival in adult patients with de novo acute myeloid leukemia: results from Cancer and Leukemia Group B (CALGB 8461). *Blood,* 100**,** 4325-36.

CADWELL, K. & COSCOY, L. 2005. Ubiquitination on Nonlysine Residues by a Viral E3 Ubiquitin Ligase. *Science,* 309**,** 127-130.

CALKHOVEN, MULLER & LEUTZ 2000a. Translational control of C/EBPalpha and C/EBPbeta isoform expression. *Genes Dev,* 14**,** 1920-32.

CALKHOVEN, C. F., MULLER, C. & LEUTZ, A. 2000b. Translational control of C/EBPalpha and C/EBPbeta isoform expression. *Genes Dev,* 14**,** 1920-32.

CAMERON, S., TAYLOR, D. S., TEPAS, E. C., SPECK, N. A. & MATHEY-PREVOT, B. 1994. Identification of a critical regulatory site in the human interleukin-3 promoter by in vivo footprinting. *Blood,* 83**,** 2851-9.

CAO, Z., UMEK, R. M. & MCKNIGHT, S. L. 1991. Regulated expression of three C/EBP isoforms during adipose conversion of 3T3-L1 cells. *Genes Dev,* 5**,** 1538-52.

CARMODY, RUAN, PALMER, HILLIARD & CHEN 2007. Negative Regulation of Toll-Like Receptor Signaling by NF-κB p50 Ubiquitination Blockade. *Science*.

CARNICER, M. J., LASA, A., BUSCHBECK, M., SERRANO, E., CARRICONDO, M., BRUNET, S., AVENTIN, A., SIERRA, J., DI CROCE, L. & NOMDEDEU, J. F. 2008. K313dup is a recurrent CEBPA mutation in de novo acute myeloid leukemia (AML). *Ann Hematol,* 87**,** 819-27.

CASTAIGNE, S., CHEVRET, S., ARCHIMBAUD, E., FENAUX, P., BORDESSOULE, D., TILLY, H., DE REVEL, T., SIMON, M., DUPRIEZ, B., RENOUX, M., JANVIER, M., MICLÉA, J.-M., THOMAS, X., BASTARD, C., PREUDHOMME, C., BAUTERS, F., DEGOS, L. & DOMBRET, H. 2004. Randomized comparison of double induction and timed-sequential induction to a "3 + 7" induction in adults with AML: long-term analysis of the Acute Leukemia French Association (ALFA) 9000 study. *Blood,* 104**,** 2467-2474.

CECCARELLI, D. F., TANG, X., PELLETIER, B., ORLICKY, S., XIE, W., PLANTEVIN, V., NECULAI, D., CHOU, Y. C., OGUNJIMI, A., AL-HAKIM, A., VARELAS, X., KOSZELA, J., WASNEY, G.

A., VEDADI, M., DHE-PAGANON, S., COX, S., XU, S., LOPEZ-GIRONA, A., MERCURIO, F., WRANA, J., DUROCHER, D., MELOCHE, S., WEBB, D. R., TYERS, M. & SICHERI, F. 2011. An allosteric inhibitor of the human Cdc34 ubiquitin-conjugating enzyme. *Cell,* 145**,** 1075-87.

CHANG, J. S., SANTHANAM, R., TROTTA, R., NEVIANI, P., EIRING, A. M., BRIERCHECK, E., RONCHETTI, M., ROY, D. C., CALABRETTA, B., CALIGIURI, M. A. & PERROTTI, D. 2007. High levels of the BCR/ABL oncoprotein are required for the MAPK-hnRNP-E2 dependent suppression of C/EBPalpha-driven myeloid differentiation. *Blood,* 110**,** 994-1003.

CHAPIRO, E., RUSSELL, L., RADFORD-WEISS, I., BASTARD, C., LESSARD, M., STRUSKI, S., CAVE, H., FERT-FERRER, S., BARIN, C., MAAREK, O., DELLA-VALLE, V., STREFFORD, J. C., BERGER, R., HARRISON, C. J., BERNARD, O. A. & NGUYEN-KHAC, F. 2006. Overexpression of CEBPA resulting from the translocation t(14;19)(q32;q13) of human precursor B acute lymphoblastic leukemia. *Blood,* 108**,** 3560-3.

CHAU, V., TOBIAS, J. W., BACHMAIR, A., MARRIOTT, D., ECKER, D. J., GONDA, D. K. & VARSHAVSKY, A. 1989. A multiubiquitin chain is confined to specific lysine in a targeted short-lived protein. *Science,* 243**,** 1576-1583.

CHEN, X., CHI, Y., BLOECHER, A., AEBERSOLD, R., CLURMAN, B. E. & ROBERTS, J. M. 2004. N-Acetylation and Ubiquitin-Independent Proteasomal Degradation of p21Cip1. *Molecular cell,* 16**,** 839-847.

CHENG, J., YU, D. V., ZHOU, J.-H. & SHAPIRO, D. J. 2007. Tamoxifen Induction of CCAAT Enhancer-binding Protein α Is Required for Tamoxifen-induced Apoptosis. *Journal of Biological Chemistry,* 282**,** 30535-30543.

CHESHIER, S. H., MORRISON, S. J., LIAO, X. & WEISSMAN, I. L. 1999. In vivo proliferation and cell cycle kinetics of long-term self-renewing hematopoietic stem cells.

CHOU, P. Y. & FASMAN, G. D. 1974. Prediction of protein conformation. *Biochemistry,* 13**,** 222-245.

CHRISTENSEN, J. L. & WEISSMAN, I. L. 2001. Flk-2 is a marker in hematopoietic stem cell differentiation: a simple method to isolate long-term stem cells. *Proc Natl Acad Sci U S A,* 98**,** 14541-6.

CLEAVES, R., WANG, Q. F. & FRIEDMAN, A. D. 2004. C/EBPalphap30, a myeloid leukemia oncoprotein, limits G-CSF receptor expression but not terminal granulopoiesis via site-selective inhibition of C/EBP DNA binding. *Oncogene,* 23**,** 716-25.

COHEN, P. 2000. The regulation of protein function by multisite phosphorylation – a 25 year update. *Trends in Biochemical Sciences,* 25**,** 596-601.

COHEN, P. 2002. The origins of protein phosphorylation. *Nat Cell Biol,* 4**,** E127-E130.

COLADO, E., ALVAREZ-FERNANDEZ, S., MAISO, P., MARTIN-SANCHEZ, J., VIDRIALES, M. B., GARAYOA, M., OCIO, E. M., MONTERO, J. C., PANDIELLA, A. & SAN MIGUEL, J. F. 2008. The effect of the proteasome inhibitor bortezomib on acute myeloid leukemia cells and drug resistance associated with the CD34+ immature phenotype. *Haematologica,* 93**,** 57-66.

COMYN, S. A., CHAN, G. T. & MAYOR, T. 2014. False start: cotranslational protein ubiquitination and cytosolic protein quality control. *J Proteomics,* 100**,** 92-101.

CONWAY O'BRIEN, E., PRIDEAUX, S. & CHEVASSUT, T. 2014. The Epigenetic Landscape of Acute Myeloid Leukemia. *Advances in Hematology,* 2014**,** 15.

CORTES, J., THOMAS, D., KOLLER, C., GILES, F., ESTEY, E., FADERL, S., GARCIA-MANERO, G., MCCONKEY, D., RUIZ, S. L., GUERCIOLINI, R., WRIGHT, J. & KANTARJIAN, H. 2004. Phase I study of bortezomib in refractory or relapsed acute leukemias. *Clin Cancer Res,* 10**,** 3371-6.

CRAWFORD, L. J., CHAN, E. T., AUJAY, M., HOLYOAKE, T. L., MELO, J. V., JORGENSEN, H. G., SURESH, S., WALKER, B. & IRVINE, A. E. 2014. Synergistic effects of proteasome inhibitor carfilzomib in combination with tyrosine kinase inhibitors in imatinib-sensitive and -resistant chronic myeloid leukemia models. *Oncogenesis,* 3**,** e90.

CUMANO, A., DIETERLEN-LIEVRE, F. & GODIN, I. 1996. Lymphoid potential, probed before circulation in mouse, is restricted to caudal intraembryonic splanchnopleura. *Cell,* 86**,** 907-16.

CUMANO, A., FERRAZ, J. C., KLAINE, M., DI SANTO, J. P. & GODIN, I. 2001. Intraembryonic, but not yolk sac hematopoietic precursors, isolated before circulation, provide long-term multilineage reconstitution. *Immunity,* 15**,** 477-85.

D'ALO, F., JOHANSEN, L. M., NELSON, E. A., RADOMSKA, H. S., EVANS, E. K., ZHANG, P., NERLOV, C. & TENEN, D. G. 2003. The amino terminal and E2F interaction domains are critical

for C/EBPα-mediated induction of granulopoietic development of hematopoietic cells. *Blood,* 102**,** 3163-3171.

DANIELSEN, J. M. R., SYLVESTERSEN, K. B., BEKKER-JENSEN, S., SZKLARCZYK, D., POULSEN, J. W., HORN, H., JENSEN, L. J., MAILAND, N. & NIELSEN, M. L. 2011. Mass Spectrometric Analysis of Lysine Ubiquitylation Reveals Promiscuity at Site Level*. *Mol Cell Proteomics,* 10.

DAVIES, A. M. M., FRCPC *, CHANSKY, K. M., LARA, P. N. J. M., GUMERLOCK, P. H. P., CROWLEY, J. P., ALBAIN, K. S. M., VOGEL, S. J. M. S. & GANDARA, D. R. M. 2009. Bortezomib Plus Gemcitabine/Carboplatin as First-Line Treatment of Advanced Non-small Cell Lung Cancer: A Phase II Southwest Oncology Group Study (S0339).[Article]. *Journal of Thoracic Oncology*.

DE KLEIN, A., VAN KESSEL, A. G., GROSVELD, G., BARTRAM, C. R., HAGEMEIJER, A., BOOTSMA, D., SPURR, N. K., HEISTERKAMP, N., GROFFEN, J. & STEPHENSON, J. R. 1982. A cellular oncogene is translocated to the Philadelphia chromosome in chronic myelocytic leukaemia. *Nature,* 300**,** 765-7.

DEBELJAK, M., KITANOVSKI, L., PAJIC, T. & JAZBEC, J. 2013. Concordant acute myeloblastic leukemia in monozygotic twins with germline and shared somatic mutations in the gene for CCAAT-enhancer-binding protein ? with 13 years difference at onset. *Haematologica,* 98**,** e73-4.

DEDHIA, P. H., KEESHAN, K., ULJON, S., XU, L., VEGA, M. E., SHESTOVA, O., ZAKS-ZILBERMAN, M., ROMANY, C., BLACKLOW, S. C. & PEAR, W. S. 2010. Differential ability of Tribbles family members to promote degradation of C/EBPα and induce acute myelogenous leukemia. *Blood,* 116**,** 1321-1328.

DEGOS, L. & WANG, Z. Y. 2001. All trans retinoic acid in acute promyelocytic leukemia. *Oncogene,* 20**,** 7140-5.

DEMO, S. D., KIRK, C. J., AUJAY, M. A., BUCHHOLZ, T. J., DAJEE, M., HO, M. N., JIANG, J., LAIDIG, G. J., LEWIS, E. R., PARLATI, F., SHENK, K. D., SMYTH, M. S., SUN, C. M., VALLONE, M. K., WOO, T. M., MOLINEAUX, C. J. & BENNETT, M. K. 2007. Antitumor Activity of PR-171, a Novel Irreversible Inhibitor of the Proteasome. *Cancer Research,* 67**,** 6383-6391.

DESHAIES, R. J. & JOAZEIRO, C. A. P. 2009. RING Domain E3 Ubiquitin Ligases. *Annual Review of Biochemistry*.

DIGHIERO, G., TRAVADE, P., CHEVRET, S., FENAUX, P., CHASTANG, C. & BINET, J. L. 1991. B-cell chronic lymphocytic leukemia: present status and future directions. French Cooperative Group on CLL. *Blood,* 78**,** 1901-14.

DIJK, M., MURPHY, E., MORRELL, R., KNAPPER, S., O'DWYER, M., SAMALI, A. & SZEGEZDI, E. 2011. The Proteasome Inhibitor Bortezomib Sensitizes AML with Myelomonocytic Differentiation to TRAIL Mediated Apoptosis. *Cancers (Basel),* 3**,** 1329-50.

DOBLE, B. W. & WOODGETT, J. R. 2003. GSK-3: tricks of the trade for a multi-tasking kinase. *Journal of Cell Science,* 116**,** 1175-1186.

DOMBRET, H. 2011. Gene mutation and AML pathogenesis. *Blood,* 118**,** 5366-5367.

DOU, H., BUETOW, L., SIBBET, G. J., CAMERON, K. & HUANG, D. T. 2013. Essentiality of a non-RING element in priming donor ubiquitin for catalysis by a monomeric E3. *Nature Structural & Molecular Biology,* 20**,** 982-986.

DU, X., JIA, P. M., HE, C., DU, S. H., TONG, J. H. & ZHOU, L. 2012. [Effect of bortezomib and low concentration cytarabine on apoptosis in U937 cell line]. *Zhongguo Shi Yan Xue Ye Xue Za Zhi,* 20**,** 554-7.

DURHAM, E., DORR, B., WOETZEL, N., STARITZBICHLER, R. & MEILER, J. 2009. Solvent accessible surface area approximations for rapid and accurate protein structure prediction. *J Mol Model,* 15**,** 1093-108.

DÖHNER, H., STILGENBAUER, S., BENNER, A., LEUPOLT, E., KRÖBER, A., BULLINGER, L., DÖHNER, K., BENTZ, M. & LICHTER, P. 2000. Genomic Aberrations and Survival in Chronic Lymphocytic Leukemia. *New England Journal of Medicine,* 343**,** 1910-1916.

EMA, H. & NAKAUCHI, H. 2000. Expansion of hematopoietic stem cells in the developing liver of a mouse embryo. *Blood,* 95**,** 2284-8.

ERICKSON, R. L., HEMATI, N., ROSS, S. E. & MACDOUGALD, O. A. 2001. p300 coactivates the adipogenic transcription factor CCAAT/enhancer-binding protein alpha. *J Biol Chem,* 276**,** 16348-55.

FANG, J., RHYASEN, G., BOLANOS, L., RASCH, C., VARNEY, M., WUNDERLICH, M., GOYAMA, S., JANSEN, G., CLOOS, J., RIGOLINO, C., CORTELEZZI, A., MULLOY, J. C., OLIVA, E. N., CUZZOLA, M. & STARCZYNOWSKI, D. T. 2012. Cytotoxic effects of bortezomib in myelodysplastic syndrome/acute myeloid leukemia depend on autophagy-mediated lysosomal degradation of TRAF6 and repression of PSMA1. *Blood,* 120**,** 858-867.

FARAONI, I., LATERZA, S., ARDIRI, D., CIARDI, C., FAZI, F. & LO-COCO, F. 2012. MiR-424 and miR-155 deregulated expression in cytogenetically normal acute myeloid leukaemia: correlation with NPM1 and FLT3 mutation status. *Journal of Hematology & Oncology,* 5**,** 26.

FASAN, A., HAFERLACH, C., ALPERMANN, T., JEROMIN, S., GROSSMANN, V., EDER, C., WEISSMANN, S., DICKER, F., KOHLMANN, A., SCHINDELA, S., KERN, W., HAFERLACH, T. & SCHNITTGER, S. 2014. The role of different genetic subtypes of CEBPA mutated AML. *Leukemia,* 28**,** 794-803.

FERKOWICZ, M. J., STARR, M., XIE, X., LI, W., JOHNSON, S. A., SHELLEY, W. C., MORRISON, P. R. & YODER, M. C. 2003. CD41 expression defines the onset of primitive and definitive hematopoiesis in the murine embryo. *Development,* 130**,** 4393-403.

FERLAY, J., SOERJOMATARAM, I., ERVIK, M., DIKSHIT, R., ESER, S., MATHERS, C., REBELO, M., PARKIN, D., FORMAN, D. & BRAY, F. 2012. *GLOBOCAN 2012 v1.0, Cancer Incidence and Mortality Worldwide: IARC CancerBase No. 11* [Online]. Lyon, France: International Agency for Research on Cancer; 2013. Available: http://globocan.iarc.fr/Pages/references.aspx.

FERRARI-AMOROTTI, G., MARIANI, S. A., NOVI, C., CATTELANI, S., PECORARI, L., CORRADINI, F., SOLIERA, A. R., MANZOTTI, G., FRAGLIASSO, V., ZHANG, Y., MARTINEZ, R. V., LAM, E. W. F., GUERZONI, C. & CALABRETTA, B. 2010. The Biological Effects of C/EBPα in K562 Cells Depend on the Potency of the N-terminal Regulatory Region, Not on Specificity of the DNA Binding Domain. *Journal of Biological Chemistry,* 285**,** 30837-30850.

FRAGLIASSO, V., CHIODO, Y., FERRARI-AMOROTTI, G., SOLIERA, A. R., MANZOTTI, G., CATTELANI, S., CANDINI, O., GRISENDI, G., VERGALLI, J., MARIANI, S. A., GUERZONI, C. & CALABRETTA, B. 2012. Phosphorylation of serine 21 modulates the proliferation inhibitory more than the differentiation inducing effects of C/EBPα in K562 cells. *Journal of Cellular Biochemistry,* 113**,** 1704-1713.

FRANK, R. 2002. The SPOT-synthesis technique. Synthetic peptide arrays on membrane supports--principles and applications. *J Immunol Methods,* 267**,** 13-26.

FRANKE, N. E., NIEWERTH, D., ASSARAF, Y. G., VAN MEERLOO, J., VOJTEKOVA, K., VAN ZANTWIJK, C. H., ZWEEGMAN, S., CHAN, E. T., KIRK, C. J., GEERKE, D. P., SCHIMMER, A. D., KASPERS, G. J., JANSEN, G. & CLOOS, J. 2012. Impaired bortezomib binding to mutant beta5 subunit of the proteasome is the underlying basis for bortezomib resistance in leukemia cells. *Leukemia,* 26**,** 757-68.

FÖRSTER, F., UNVERDORBEN, P., ŚLEDŹ, P. & BAUMEISTER, W. 2013. Unveiling the Long-Held Secrets of the 26S Proteasome. *Structure,* 21**,** 1551-1562.

GARG, A., KAUR, H. & RAGHAVA, G. P. S. 2005. Real value prediction of solvent accessibility in proteins using multiple sequence alignment and secondary structure. *Proteins: Structure, Function, and Bioinformatics,* 61**,** 318-324.

GEEST, C. R., BUITENHUIS, M., LAARHOVEN, A. G., BIERINGS, M. B., BRUIN, M. C. A., VELLENGA, E. & COFFER, P. J. 2009. p38 MAP Kinase Inhibits Neutrophil Development Through Phosphorylation of C/EBPα on Serine 21. *STEM CELLS,* 27**,** 2271-2282.

GEKAS, C., DIETERLEN-LIÈVRE, F., ORKIN, S. H. & MIKKOLA, H. K. A. 2005. The Placenta Is a Niche for Hematopoietic Stem Cells. *Developmental Cell,* 8**,** 365-375.

GELETU, M., BALKHI, M., PEER ZADA, A., CHRISTOPEIT, A., PULIKKAN, J., TRIVEDI, A., D, T. & BEHRE, G. 2007. Target proteins of C/EBPαp30 in AML: C/EBPαp30 enhances sumoylation of C/EBPαp42 via up-regulation of Ubc9.

GIBSON, J., ILAND, H. J., LARSEN, S. R., BROWN, C. M. & JOSHUA, D. E. 2013. Leukaemias into the 21st century. Part 2: the chronic leukaemias. *Intern Med J,* 43**,** 484-94.

GILLILAND, G. & GRIFFIN, J. 2002. The roles of FLT3 in hematopoiesis and leukemia.

GRAHAM, J., ZHANG, L. & FRIEDMAN, A. D. 2009. M-CSF elevates c-Fos and phospho-C/EBPα(S21) via ERK whereas G-CSF stimulates SHP2 phosphorylation in marrow progenitors to contribute to myeloid lineage specification. *Blood,* 114**,** 2172-2180.

GRANDINETTI, K. B., STEVENS, T. A., HA, S., SALAMONE, R. J., WALKER, J. R., ZHANG, J., AGARWALLA, S., TENEN, D. G., PETERS, E. C. & REDDY, V. A. 2011. Overexpression of TRIB2 in human lung cancers contributes to tumorigenesis through downregulation of C/EBP[alpha]. *Oncogene,* 30**,** 3328-3335.

GRIMWADE, D., BIONDI, A., MOZZICONACCI, M. J., HAGEMEIJER, A., BERGER, R., NEAT, M., HOWE, K., DASTUGUE, N., JANSEN, J., RADFORD-WEISS, I., LO COCO, F., LESSARD, M., HERNANDEZ, J. M., DELABESSE, E., HEAD, D., LISO, V., SAINTY, D., FLANDRIN, G., SOLOMON, E., BIRG, F. & LAFAGE-POCHITALOFF, M. 2000. Characterization of acute promyelocytic leukemia cases lacking the classic t(15;17): results of the European Working Party. Groupe Francais de Cytogenetique Hematologique, Groupe de Francais d'Hematologie Cellulaire, UK Cancer Cytogenetics Group and BIOMED 1 European Community-Concerted Action "Molecular Cytogenetic Diagnosis in Haematological Malignancies". *Blood,* 96**,** 1297-308.

GROßHANS, J. & WIESCHAUS, E. 2000. A Genetic Link between Morphogenesis and Cell Division during Formation of the Ventral Furrow in Drosophila. *Cell,* 101**,** 523-531.

GUTMAN, J. & HOFFNER, B. 2012. A novel CCAAT/enhancer binding protein α germline variant in a case of acute myeloid leukemia. *http://dx.doi.org/10.3109/10428194.2011.638718*.

GUZMAN, M. L., NEERING, S. J., UPCHURCH, D., GRIMES, B., HOWARD, D. S., RIZZIERI, D. A., LUGER, S. M. & JORDAN, C. T. 2001. Nuclear factor-kappaB is constitutively activated in primitive human acute myelogenous leukemia cells. *Blood,* 98**,** 2301-7.

GUZMAN, M. L., SWIDERSKI, C. F., HOWARD, D. S., GRIMES, B. A., ROSSI, R. M., SZILVASSY, S. J. & JORDAN, C. T. 2002. Preferential induction of apoptosis for primary human leukemic stem cells. *Proc Natl Acad Sci U S A,* 99**,** 16220-5.

HALLEK, M., FISCHER, K., FINGERLE-ROWSON, G., FINK, A. M., BUSCH, R., MAYER, J., HENSEL, M., HOPFINGER, G., HESS, G., VON GRUNHAGEN, U., BERGMANN, M., CATALANO, J., ZINZANI, P. L., CALIGARIS-CAPPIO, F., SEYMOUR, J. F., BERREBI, A., JAGER, U., CAZIN, B., TRNENY, M., WESTERMANN, A., WENDTNER, C. M., EICHHORST, B. F., STAIB, P., BUHLER, A., WINKLER, D., ZENZ, T., BOTTCHER, S., RITGEN, M., MENDILA, M., KNEBA, M., DOHNER, H. & STILGENBAUER, S. 2010. Addition of rituximab to fludarabine and cyclophosphamide in patients with chronic lymphocytic leukaemia: a randomised, open-label, phase 3 trial. *Lancet,* 376**,** 1164-74.

HANKEY, W., SILVER, M., SUN, B. S., ZIBELLO, T., BERLINER, N. & KHANNA-GUPTA, A. 2011. Differential effects of sumoylation on the activities of CCAAT enhancer binding protein alpha (C/EBPalpha) p42 versus p30 may contribute in part, to aberrant C/EBPalpha activity in acute leukemias. *Hematol Rep,* 3**,** e5.

HANKS, S. K. & HUNTER, T. 1995. Protein kinases 6. The eukaryotic protein kinase superfamily: kinase (catalytic) domain structure and classification. *The FASEB Journal,* 9**,** 576-96.

HANNON, M. M., LOHAN, F., ERBILGIN, Y., SAYITOGLU, M., O'HAGAN, K., MILLS, K., OZBEK, U. & KEESHAN, K. 2012. Elevated TRIB2 with NOTCH1 activation in paediatric/adult T-ALL. *British Journal of Haematology,* 158**,** 626-634.

HASEMANN, M., SCHUSTER, M., FRANK, A., THEILGAARD-MÖNCH, K., PEDERSEN, T., NERLOV, C. & PORSE, B. 2012. Phosphorylation of Serine 248 of C/EBPα Is Dispensable for Myelopoiesis but Its Disruption Leads to a Low Penetrant Myeloid Disorder with Long Latency. *PLOS ONE,* 7.

HASEMANN, M. S., LAURIDSEN, F. K., WAAGE, J., JAKOBSEN, J. S., FRANK, A. K., SCHUSTER, M. B., RAPIN, N., BAGGER, F. O., HOPPE, P. S., SCHROEDER, T. & PORSE, B. T. 2014. C/EBPalpha Is Required for Long-Term Self-Renewal and Lineage Priming of Hematopoietic Stem Cells and for the Maintenance of Epigenetic Configurations in Multipotent Progenitors. *PLoS Genet,* 10**,** e1004079.

HATLEN, M. A., WANG, L. & NIMER, S. D. 2012. AML1-ETO driven acute leukemia: insights into pathogenesis and potential therapeutic approaches. *Front Med,* 6**,** 248-62.

HATTORI, T., OHOKA, N., INOUE, Y., HAYASHI, H. & ONOZAKI, K. 2003. C/EBP family transcription factors are degraded by the proteasome but stabilized by forming dimer. *Oncogene,* 22**,** 1273-80.

HEGEDUS, Z., CZIBULA, A. & KISS-TOTH, E. 2007. Tribbles: A family of kinase-like proteins with potent signalling regulatory function. *Cellular Signalling,* 19**,** 238-250.

HEIDENREICH, O., KRAUTER, J., RIEHLE, H., HADWIGER, P., JOHN, M., HEIL, G., VORNLOCHER, H. P. & NORDHEIM, A. 2003. AML1/MTG8 oncogene suppression by small interfering RNAs supports myeloid differentiation of t(8;21)-positive leukemic cells. *Blood,* 101**,** 3157-63.

HELBLING, D., MUELLER, B. U., TIMCHENKO, N. A., HAGEMEIJER, A., JOTTERAND, M., MEYER-MONARD, S., LISTER, A., ROWLEY, J. D., HUEGLI, B., FEY, M. F. & PABST, T. 2004. The leukemic fusion gene AML1-MDS1-EVI1 suppresses CEBPA in acute myeloid leukemia by activation of Calreticulin. *Proc Natl Acad Sci U S A,* 101**,** 13312-7.

HELBLING, D., MUELLER, B. U., TIMCHENKO, N. A., SCHARDT, J., EYER, M., BETTS, D. R., JOTTERAND, M., MEYER-MONARD, S., FEY, M. F. & PABST, T. 2005. CBFB-SMMHC is correlated with increased calreticulin expression and suppresses the granulocytic differentiation factor CEBPA in AML with inv(16). *Blood,* 106**,** 1369-75.

HEMATI, N., ROSS, S., ERICKSON, R., GROBLEWSKI, G. & MACDOUGALD, O. 1997. Signaling Pathways through Which Insulin Regulates CCAAT/Enhancer Binding Protein α (C/EBPα) Phosphorylation and Gene Expression in 3T3-L1 Adipocytes.

HERSHKO, A., CIECHANOVER, A. & VARSHAVSKY, A. 2000. Basic Medical Research Award. The ubiquitin system. *Nat Med,* 6**,** 1073-81.

HERSHKO, A., HELLER, H., ELIAS, S. & CIECHANOVER, A. 1983. Components of ubiquitin-protein ligase system. Resolution, affinity purification, and role in protein breakdown. *Journal of Biological Chemistry,* 258**,** 8206-8214.

HIRAI, H., ZHANG, P., DAYARAM, T., HETHERINGTON, C. J., MIZUNO, S., IMANISHI, J., AKASHI, K. & TENEN, D. G. 2006. C/EBPbeta is required for 'emergency' granulopoiesis. *Nat Immunol,* 7**,** 732-9.

HOWLADER, N., NOONE, A., KRAPCHO, M., GARSHELL, J., NEYMAN, N., ALTEKRUSE, S., KOSARY, C., YU, M., RUHL, J., TATALOVICH, Z., CHO, H., MARIOTTO, A., LEWIS, R., CHEN, H., FEUER, E. & CRONIN, K. 2012. *Browse the SEER Cancer Statistics Review 1975-2010* [Online]. 1975-2010, Nation cancer Insitute . Bethesda: SEER Cancer Statistics Review. Available: http://seer.cancer.gov/csr/1975_2010/browse_csr.php?sectionSEL=13&pageSEL=sect_13_table.10.html.

HOYT, M. A., ZHANG, M. & COFFINO, P. 2003. Ubiquitin-independent Mechanisms of Mouse Ornithine Decarboxylase Degradation Are Conserved between Mammalian and Fungal Cells. *Journal of Biological Chemistry,* 278**,** 12135-12143.

HSU, W., KERPPOLA, T. K., CHEN, P. L., CURRAN, T. & CHEN-KIANG, S. 1994. Fos and Jun repress transcription activation by NF-IL6 through association at the basic zipper region. *Mol Cell Biol,* 14**,** 268-76.

HUANG, D. T., HUNT, H. W., ZHUANG, M., OHI, M. D., HOLTON, J. M. & SCHULMAN, B. A. 2007. Basis for a ubiquitin-like protein thioester switch toggling E1-E2 affinity. *Nature,* 445**,** 394-8.

HUANG, G., SHIGESADA, K., ITO, K., WEE, H. J., YOKOMIZO, T. & ITO, Y. 2001. Dimerization with PEBP2? protects RUNX1/AML1 from ubiquitin-proteasome-mediated degradation. *EMBO J,* 20**,** 723-33.

HUNTER, T. 2007. The Age of Crosstalk: Phosphorylation, Ubiquitination, and Beyond. *Molecular cell,* 28**,** 730-738.

HURET, J. L., DESSEN, P. & BERNHEIM, A. 2001. An atlas of chromosomes in hematological malignancies. Example: 11q23 and MLL partners. *Leukemia,* 15**,** 987-9.

INABA, H., GREAVES, M. & MULLIGHAN, C. G. 2013. Acute lymphoblastic leukaemia. *The Lancet,* 381**,** 1943-1955.

JAGANNATH, S., BARLOGIE, B., BERENSON, J., SIEGEL, D., IRWIN, D., RICHARDSON, P. G., NIESVIZKY, R., ALEXANIAN, R., LIMENTANI, S. A., ALSINA, M., ADAMS, J., KAUFFMAN, M., ESSELTINE, D. L., SCHENKEIN, D. P. & ANDERSON, K. C. 2004. A phase 2 study of two doses of bortezomib in relapsed or refractory myeloma. *Br J Haematol,* 127**,** 165-72.

JAMES, L. C. & TAWFIK, D. S. 2003. The specificity of cross-reactivity: Promiscuous antibody binding involves specific hydrogen bonds rather than nonspecific hydrophobic stickiness. *Protein Sci,* 12**,** 2183-93.

JIN, G., YAMAZAKI, Y., TAKUWA, M., TAKAHARA, T., KANEKO, K., KUWATA, T., MIYATA, S. & NAKAMURA, T. 2007. Trib1 and Evi1 cooperate with Hoxa and Meis1 in myeloid leukemogenesis. *Blood,* 109**,** 3998-4005.

JOHANSEN, L. M., IWAMA, A., LODIE, T. A., SASAKI, K., FELSHER, D. W., GOLUB, T. R. & TENEN, D. G. 2001. c-Myc Is a Critical Target for C/EBPα in Granulopoiesis. *Molecular and Cellular Biology,* 21**,** 3789-3806.

JOHNSON, P. 2005. Molecular stop signs: regulation of cell-cycle arrest by C/EBP transcription factors.

JONES, L. C., LIN, M.-L., CHEN, S.-S., KRUG, U., HOFMANN, W.-K., LEE, S., LEE, Y.-H. & KOEFFLER, H. P. 2002. Expression of C/EBPβ from the C/ebpα gene locus is sufficient for normal hematopoiesis in vivo. *Blood,* 99**,** 2032-2036.

JONGEN-LAVRENCIC, M., SUN, S. M., DIJKSTRA, M. K., VALK, P. J. & LOWENBERG, B. 2008. MicroRNA expression profiling in relation to the genetic heterogeneity of acute myeloid leukemia. *Blood,* 111**,** 5078-85.

KAMADURAI, H., QIU, Y., DENG, A., HARRISON, J. S., MACDONALD, C., ACTIS, M., RODRIGUES, P., MILLER, D. J., SOUPHRON, J., LEWIS, S. M., KURINOV, I., FUJII, N., HAMMEL, M., PIPER, R., KUHLMAN, B., SCHULMAN, B. A. & KURIYAN, J. 2013. Mechanism of ubiquitin ligation and lysine prioritization by a HECT E3.

KANE, R. C., DAGHER, R., FARRELL, A., KO, C.-W., SRIDHARA, R., JUSTICE, R. & PAZDUR, R. 2007. Bortezomib for the Treatment of Mantle Cell Lymphoma. *Clinical Cancer Research,* 13**,** 5291-5294.

KANG, J.-W., PARK, Y. S., KIM, M. S., LEE, D. H., BAK, Y., HAM, S. Y., PARK, S. H., HONG, J. T. & YOON, D.-Y. 2013. Interleukin (IL)-32β-mediated CCAAT/Enhancer-binding Protein α (C/EBPα) Phosphorylation by Protein Kinase Cδ (PKCδ) Abrogates the Inhibitory Effect of C/EBPα on IL-10 Production. *Journal of Biological Chemistry,* 288**,** 23650-23658.

KATO, N., KITAURA, J., DOKI, N., KOMENO, Y., WATANABE-OKOCHI, N., TOGAMI, K., NAKAHARA, F., OKI, T., ENOMOTO, Y., FUKUCHI, Y., NAKAJIMA, H., HARADA, Y., HARADA, H. & KITAMURA, T. 2011. Two types of C/EBPalpha mutations play distinct but collaborative roles in leukemogenesis: lessons from clinical data and BMT models. *Blood,* 117**,** 221-33.

KAWAGOE, H., HUMPHRIES, R. K., BLAIR, A., SUTHERLAND, H. J. & HOGGE, D. E. 1999. Expression of HOX genes, HOX cofactors, and MLL in phenotypically and functionally defined subpopulations of leukemic and normal human hematopoietic cells. *Leukemia,* 13**,** 687-98.

KEESHAN, K., BAILIS, W., DEDHIA, P. H., VEGA, M. E., SHESTOVA, O., XU, L., TOSCANO, K., ULJON, S. N., BLACKLOW, S. C. & PEAR, W. S. 2010. Transformation by Tribbles homolog 2 (Trib2) requires both the Trib2 kinase domain and COP1 binding. *Blood,* 116**,** 4948-4957.

KEESHAN, K., HE, Y., WOUTERS, B. J., SHESTOVA, O., XU, L., SAI, H., RODRIGUEZ, C. G., MAILLARD, I., TOBIAS, J. W., VALK, P., CARROLL, M., ASTER, J. C., DELWEL, R. & PEAR, W. S. 2006. Tribbles homolog 2 inactivates C/EBPα and causes acute myelogenous leukemia. *Cancer Cell,* 10**,** 401-411.

KEESHAN, K., SANTILLI, G., CORRADINI, F., PERROTTI, D. & CALABRETTA, B. 2003. Transcription activation function of C/EBPα is required for induction of granulocytic differentiation. *Blood,* 102**,** 1267-1275.

KEESHAN, K., SHESTOVA, O., USSIN, L. & PEAR, W. S. 2008. Tribbles homolog 2 (Trib2) and HoxA9 cooperate to accelerate acute myelogenous leukemia. *Blood Cells, Molecules, and Diseases,* 40**,** 119-121.

KELLY, L. & GILLILAND, G. 2003. GENETICS OF MYELOID LEUKEMIAS. *http://dx.doi.org/10.1146/annurev.genom.3.032802.115046*.

KHANNA-GUPTA, A. 2008. Sumoylation and the function of CCAAT enhancer binding protein alpha (C/EBP??). *Blood Cells Mol Dis,* 41**,** 77-81.

KIM, W., BENNETT, E. J., HUTTLIN, E. L., GUO, A., LI, J., POSSEMATO, A., SOWA, M. E., RAD, R., RUSH, J., COMB, M. J., HARPER, J. W. & GYGI, S. P. 2011. Systematic and Quantitative Assessment of the Ubiquitin-Modified Proteome. *Molecular Cell,* 44**,** 325-340.

KIRSTETTER, P., SCHUSTER, M. B., BERESHCHENKO, O., MOORE, S., DVINGE, H., KURZ, E., THEILGAARD-MONCH, K., MANSSON, R., PEDERSEN, T. A., PABST, T., SCHROCK, E., PORSE, B. T., JACOBSEN, S. E., BERTONE, P., TENEN, D. G. & NERLOV, C. 2008. Modeling of C/EBPalpha mutant acute myeloid leukemia reveals a common expression signature of committed myeloid leukemia-initiating cells. *Cancer Cell,* 13**,** 299-310.

KISS-TOTH, E., BAGSTAFF, S. M., SUNG, H. Y., JOZSA, V., DEMPSEY, C., CAUNT, J. C., OXLEY, K. M., WYLLIE, D. H., POLGAR, T., HARTE, M., O'NEILL, L. A. J., QWARNSTROM, E. E. & DOWER, S. K. 2004. Human Tribbles, a Protein Family Controlling Mitogen-activated Protein Kinase Cascades. *Journal of Biological Chemistry,* 279**,** 42703-42708.

KITADA, S., ANDERSEN, J., AKAR, S., ZAPATA, J. M., TAKAYAMA, S., KRAJEWSKI, S., WANG, H. G., ZHANG, X., BULLRICH, F., CROCE, C. M., RAI, K., HINES, J. & REED, J. C. 1998. Expression of apoptosis-regulating proteins in chronic lymphocytic leukemia: correlations with In vitro and In vivo chemoresponses. *Blood,* 91**,** 3379-89.

KLEIGER, G. & MAYOR, T. 2014. Perilous journey: a tour of the ubiquitin-proteasome system. *Trends Cell Biol*.

KOEPP, D. M., SCHAEFER, L. K., YE, X., KEYOMARSI, K., CHU, C., HARPER, J. W. & ELLEDGE, S. J. 2001. Phosphorylation-dependent ubiquitination of cyclin E by the SCFFbw7 ubiquitin ligase. *Science,* 294**,** 173-7.

KOLEVA, R. I., FICARRO, S. B., RADOMSKA, H. S., CARRASCO-ALFONSO, M. J., ALBERTA, J. A., WEBBER, J. T., LUCKEY, C. J., MARCUCCI, G., TENEN, D. G. & MARTO, J. A. 2012. C/EBPα and DEK coordinately regulate myeloid differentiation. *Blood,* 119**,** 4878-4888.

KORKIN, D., DAVIS, F. P. & SALI, A. 2005. Localization of protein-binding sites within families of proteins. *Protein Sci,* 14**,** 2350-60.

KOSCHMIEDER, S., D'ALO, F., RADOMSKA, H., SCHONEICH, C., CHANG, J. S., KONOPLEVA, M., KOBAYASHI, S., LEVANTINI, E., SUH, N., DI RUSCIO, A., VOSO, M. T., WATT, J. C., SANTHANAM, R., SARGIN, B., KANTARJIAN, H., ANDREEFF, M., SPORN, M. B., PERROTTI, D., BERDEL, W. E., MULLER-TIDOW, C., SERVE, H. & TENEN, D. G. 2007. CDDO induces granulocytic differentiation of myeloid leukemic blasts through translational up-regulation of p42 CCAAT enhancer-binding protein alpha. *Blood,* 110**,** 3695-705.

KRASZEWSKA, M. D., DAWIDOWSKA, M., SZCZEPANSKI, T. & WITT, M. 2012. T-cell acute lymphoblastic leukaemia: recent molecular biology findings. *Br J Haematol,* 156**,** 303-15.

KRIVTSOV, A. V. & ARMSTRONG, S. A. 2007. MLL translocations, histone modifications and leukaemia stem-cell development. *Nat Rev Cancer,* 7**,** 823-33.

KUHN, D. J., CHEN, Q., VOORHEES, P. M., STRADER, J. S., SHENK, K. D., SUN, C. M., DEMO, S. D., BENNETT, M. K., VAN LEEUWEN, F. W. B., CHANAN-KHAN, A. A. & ORLOWSKI, R. Z. 2007. Potent activity of carfilzomib, a novel, irreversible inhibitor of the ubiquitin-proteasome pathway, against preclinical models of multiple myeloma. *Blood,* 110**,** 3281-3290.

KUMAR, C. C. 2011. Genetic Abnormalities and Challenges in the Treatment of Acute Myeloid Leukemia. *Genes Cancer,* 2**,** 95-107.

KUMARAVELU, P., HOOK, L., MORRISON, A. M., URE, J., ZHAO, S., ZUYEV, S., ANSELL, J. & MEDVINSKY, A. 2002. Quantitative developmental anatomy of definitive haematopoietic stem cells/long-term repopulating units (HSC/RUs): role of the aorta-gonad-mesonephros (AGM) region and the yolk sac in colonisation of the mouse embryonic liver. *Development,* 129**,** 4891-9.

KUMATORI, A., TANAKA, K., INAMURA, N., SONE, S., OGURA, T., MATSUMOTO, T., TACHIKAWA, T., SHIN, S. & ICHIHARA, A. 1990. Abnormally high expression of proteasomes in human leukemic cells. *Proceedings of the National Academy of Sciences,* 87**,** 7071-7075.

KUNDRANDA, M. N., TIBES, R. & MESA, R. A. 2012. Transformation of a chronic myeloproliferative neoplasm to acute myelogenous leukemia: does anything work? *Curr Hematol Malig Rep,* 7**,** 78-86.

LAIOSA, STADTFELD & GRAF 2006a. Determinants of lymphoid-myeloid lineage diversification. *Annu Rev Immunol,* 24**,** 705-38.

LAIOSA, C. V., STADTFELD, M., XIE, H., DE ANDRES-AGUAYO, L. & GRAF, T. 2006b. Reprogramming of committed T cell progenitors to macrophages and dendritic cells by C/EBP alpha and PU.1 transcription factors. *Immunity,* 25**,** 731-44.

LANDSCHULZ, W. H., JOHNSON, P. F. & MCKNIGHT, S. L. 1988. The leucine zipper: a hypothetical structure common to a new class of DNA binding proteins. *Science,* 240**,** 1759-64.

LARSON, R. A., WILLIAMS, S. F., LE BEAU, M. M., BITTER, M. A., VARDIMAN, J. W. & ROWLEY, J. D. 1986. Acute myelomonocytic leukemia with abnormal eosinophils and inv(16) or t(16;16) has a favorable prognosis. *Blood,* 68**,** 1242-9.

LAWRENCE, M. C. & COLMAN, P. M. 1993. Shape Complementarity at Protein/Protein Interfaces. *Journal of Molecular Biology,* 234**,** 946-950.

LEE, H. J., DAVER, N., KANTARJIAN, H. M., VERSTOVSEK, S. & RAVANDI, F. 2013. The Role of JAK Pathway Dysregulation in the Pathogenesis and Treatment of Acute Myeloid Leukemia.

LENGFELDER, E., GNAD, U., BUCHNER, T. & HEHLMANN, R. 2003. Treatment of relapsed acute promyelocytic leukemia. *Onkologie,* 26**,** 373-9.

LEROY, H., ROUMIER, C., HUYGHE, P., BIGGIO, V., FENAUX, P. & PREUDHOMME, C. 2005. CEBPA point mutations in hematological malignancies. *Leukemia,* 19**,** 329-334.

LEY, T. J., DING, L., WALTER, M. J., MCLELLAN, M. D., LAMPRECHT, T., LARSON, D. E., KANDOTH, C., PAYTON, J. E., BATY, J., WELCH, J., HARRIS, C. C., LICHTI, C. F., TOWNSEND, R. R., FULTON, R. S., DOOLING, D. J., KOBOLDT, D. C., SCHMIDT, H., ZHANG, Q., OSBORNE, J. R., LIN, L., O'LAUGHLIN, M., MCMICHAEL, J. F., DELEHAUNTY, K. D., MCGRATH, S. D., FULTON, L. A., MAGRINI, V. J., VICKERY, T. L., HUNDAL, J., COOK, L. L., CONYERS, J. J., SWIFT, G. W., REED, J. P., ALLDREDGE, P. A., WYLIE, T., WALKER, J., KALICKI, J., WATSON, M. A., HEATH, S., SHANNON, W. D., VARGHESE, N., NAGARAJAN, R., WESTERVELT, P., TOMASSON, M. H., LINK, D. C., GRAUBERT, T. A., DIPERSIO, J. F., MARDIS, E. R. & WILSON, R. K. 2010. DNMT3A mutations in acute myeloid leukemia. *N Engl J Med,* 363**,** 2424-33.

LI, L., KUHRT, D., DEV, A., JACHIMOWICZ, E., AKASHI, K. & WOJCHOWSKI, D. M. Trib2 Pseudokinase Marks Early CMP Progenitors, and Promotes Granulocytic Plus Erythroid Progenitor Cell Formation. 2013-11-15 2013. American Society of Hematology.

LI, W., JOHNSON, S. A., SHELLEY, W. C., FERKOWICZ, M., MORRISON, P., LI, Y. & YODER, M. C. 2003. Primary endothelial cells isolated from the yolk sac and para-aortic splanchnopleura support the expansion of adult marrow stem cells in vitro. *Blood,* 102**,** 4345-53.

LIANG, K. L., RISHI, L. & KEESHAN, K. 2013. Tribbles in acute leukemia. *Blood*.

LIN, L. & GHOSH, S. 1996. A glycine-rich region in NF-kappaB p105 functions as a processing signal for the generation of the p50 subunit. *Mol Cell Biol,* 16**,** 2248-54.

LIU, H., KEEFER, J. R., WANG, Q.-F. & FRIEDMAN, A. D. 2003. Reciprocal effects of C/EBPα and PKCδ on JunB expression and monocytic differentiation depend upon the C/EBPα basic region. *Blood,* 101**,** 3885-3892.

LIU, H.-K., PERRIER, S., LIPINA, C., FINLAY, D., MCLAUCHLAN, H., HASTIE, C., HUNDAL, H. & SUTHERLAND, C. 2006. Functional characterisation of the regulation of CAAT enhancer binding protein alpha by GSK-3 phosphorylation of Threonines 222/226. *BMC Molecular Biology,* 7**,** 14.

LIU, P., TARLE, S. A., HAJRA, A., CLAXTON, D. F., MARLTON, P., FREEDMAN, M., SICILIANO, M. J. & COLLINS, F. S. 1993. Fusion between transcription factor CBF beta/PEBP2 beta and a myosin heavy chain in acute myeloid leukemia. *Science,* 261**,** 1041-4.

LIU, P. P., HAJRA, A., WIJMENGA, C. & COLLINS, F. S. 1995. Molecular pathogenesis of the chromosome 16 inversion in the M4Eo subtype of acute myeloid leukemia. *Blood,* 85**,** 2289-302.

LIU, Y. H., TAN, K. A., MORRISON, I. W., LAMB, J. R. & ARGYLE, D. J. 2013. Macrophage migration is controlled by Tribbles 1 through the interaction between C/EBPbeta and TNF-alpha. *Vet Immunol Immunopathol,* 155**,** 67-75.

LOHAN, F. & KEESHAN, K. 2013. The functionally diverse roles of tribbles. *Biochem Soc Trans,* 41**,** 1096-100.

LOPEZ, GARCIA-SILVA, MOORE, BERESHCHENKO, MARTINEZ-CRUZ, ERMAKOVA, KURZ, PARAMIO & NERLOV 2009. C/EBP[alpha] and [beta] couple interfollicular keratinocyte proliferation arrest to commitment and terminal differentiation. *Nat Cell Biol,* 11**,** 1181-1190.

LUGO, T. G., PENDERGAST, A. M., MULLER, A. J. & WITTE, O. N. 1990. Tyrosine kinase activity and transformation potency of bcr-abl oncogene products. *Science,* 247**,** 1079-82.

MAKISHIMA, H., VISCONTE, V., SAKAGUCHI, H., JANKOWSKA, A. M., ABU KAR, S., JEREZ, A., PRZYCHODZEN, B., BUPATHI, M., GUINTA, K., AFABLE, M. G., SEKERES, M. A., PADGETT, R. A., TIU, R. V. & MACIEJEWSKI, J. P. 2012. Mutations in the spliceosome machinery, a novel and ubiquitous pathway in leukemogenesis. *Blood,* 119**,** 3203-10.

MALYUKOVA, A., DOHDA, T., VON DER LEHR, N., AKHONDI, S., CORCORAN, M., HEYMAN, M., SPRUCK, C., GRANDÉR, D., LENDAHL, U. & SANGFELT, O. 2007. The Tumor Suppressor Gene hCDC4 Is Frequently Mutated in Human T-Cell Acute Lymphoblastic Leukemia with Functional Consequences for Notch Signaling. *Cancer Research,* 67**,** 5611-5616.

MANCINI, E., SANJUAN-PLA, A., LUCIANI, L., MOORE, S., GROVER, A., ZAY, A., RASMUSSEN, K. D., LUC, S., BILBAO, D., O'CARROLL, D., JACOBSEN, S. E. & NERLOV, C. 2012. FOG-1 and GATA-1 act sequentially to specify definitive megakaryocytic and erythroid progenitors. *Embo j,* 31**,** 351-65.

MANNING, G., WHYTE, D. B., MARTINEZ, R., HUNTER, T. & SUDARSANAM, S. 2002. The Protein Kinase Complement of the Human Genome. *Science,* 298**,** 1912-1934.

MARDIS, E. R., DING, L., DOOLING, D. J., LARSON, D. E., MCLELLAN, M. D., CHEN, K., KOBOLDT, D. C., FULTON, R. S., DELEHAUNTY, K. D., MCGRATH, S. D., FULTON, L. A., LOCKE, D. P., MAGRINI, V. J., ABBOTT, R. M., VICKERY, T. L., REED, J. S., ROBINSON, J. S., WYLIE, T., SMITH, S. M., CARMICHAEL, L., ELDRED, J. M., HARRIS, C. C., WALKER, J., PECK, J. B., DU, F., DUKES, A. F., SANDERSON, G. E., BRUMMETT, A. M., CLARK, E., MCMICHAEL, J. F., MEYER, R. J., SCHINDLER, J. K., POHL, C. S., WALLIS, J. W., SHI, X., LIN, L., SCHMIDT, H., TANG, Y., HAIPEK, C., WIECHERT, M. E., IVY, J. V., KALICKI, J., ELLIOTT, G., RIES, R. E., PAYTON, J. E., WESTERVELT, P., TOMASSON, M. H., WATSON, M. A., BATY, J., HEATH, S., SHANNON, W. D., NAGARAJAN, R., LINK, D. C., WALTER, M. J., GRAUBERT, T. A., DIPERSIO, J. F., WILSON, R. K. & LEY, T. J. 2009. Recurring mutations found by sequencing an acute myeloid leukemia genome. *N Engl J Med,* 361**,** 1058-66.

MARTENS, J. H. A. & STUNNENBERG, H. G. 2010. The molecular signature of oncofusion proteins in acute myeloid leukemia. *FEBS Letters,* 584**,** 2662-2669.

MASONER, V., DAS, R., PENCE, L., ANAND, G., LAFERRIERE, H., ZARS, T., BOUYAIN, S. & DOBENS, L. L. 2013. The kinase domain of Drosophila Tribbles is required for turnover of fly C/EBP during cellmigration. *Developmental Biology,* 375**,** 33-44.

MATA, J., CURADO, S., EPHRUSSI, A. & RØRTH, P. 2000. Tribbles Coordinates Mitosis and Morphogenesis in Drosophila by Regulating String/CDC25 Proteolysis. *Cell,* 101**,** 511-522.

MATONDO, M., BOUSQUET-DUBOUCH, M.-P., GALLAY, N., UTTENWEILER-JOSEPH, S., RECHER, C., PAYRASTRE, B., MANENTI, S., MONSARRAT, B. & BURLET-SCHILTZ, O. 2010. Proteasome inhibitor-induced apoptosis in acute myeloid leukemia: A correlation with the proteasome status. *Leukemia research,* 34**,** 498-506.

MATUTES, E., PICKL, W. F., VAN'T VEER, M., MORILLA, R., SWANSBURY, J., STROBL, H., ATTARBASCHI, A., HOPFINGER, G., ASHLEY, S., BENE, M. C., PORWIT, A., ORFAO, A., LEMEZ, P., SCHABATH, R. & LUDWIG, W. D. 2011. Mixed-phenotype acute leukemia: clinical and laboratory features and outcome in 100 patients defined according to the WHO 2008 classification. *Blood,* 117**,** 3163-71.

MCCORMACK, E., BRUSERUD, O. & GJERTSEN, B. T. 2005. Animal models of acute myelogenous leukaemia - development, application and future perspectives. *Leukemia,* 19**,** 687-706.

MCGRATH, K. E. & PALIS, J. 2005. Hematopoiesis in the yolk sac: more than meets the eye. *Exp Hematol,* 33**,** 1021-8.

MCKNIGHT, S. L. 2001. McBindall--a better name for CCAAT/enhancer binding proteins? *Cell,* 107**,** 259-61.

MEDVINSKY, A. & DZIERZAK, E. 1996. Definitive hematopoiesis is autonomously initiated by the AGM region. *Cell,* 86**,** 897-906.

MESSMER, B. T., MESSMER, D., ALLEN, S. L., KOLITZ, J. E., KUDALKAR, P., CESAR, D., MURPHY, E. J., KODURU, P., FERRARINI, M., ZUPO, S., CUTRONA, G., DAMLE, R. N., WASIL, T., RAI, K. R., HELLERSTEIN, M. K. & CHIORAZZI, N. 2005. In vivo measurements document the dynamic cellular kinetics of chronic lymphocytic leukemia B cells. *J Clin Invest,* 115**,** 755-64.

MIKKOLA, H. K. A. & ORKIN, S. H. 2006. The journey of developing hematopoietic stem cells. *Development,* 133**,** 3733-3744.

MILLER, M., SHUMAN, J. D., SEBASTIAN, T., DAUTER, Z. & JOHNSON, P. F. 2003. Structural basis for DNA recognition by the basic region leucine zipper transcription factor CCAAT/enhancer-binding protein alpha. *J Biol Chem,* 278**,** 15178-84.

MITELMAN, F., JOHANSSON, B. & MERTENS, F. E. 2011. *Mitelman Database of Chromosome Aberrations and Gene Fusions in Cancer* [Online]. Available: **http://cgap.nci.nih.gov/Chromosomes/Mitelman**.

MIYAMOTO, T., IWASAKI, H., REIZIS, B., YE, M., GRAF, T., WEISSMAN, I. L. & AKASHI, K. 2002. Myeloid or lymphoid promiscuity as a critical step in hematopoietic lineage commitment. *Dev Cell,* 3**,** 137-47.

MONTELL, D. J., RORTH, P. & SPRADLING, A. C. 1992. slow border cells, a locus required for a developmentally regulated cell migration during oogenesis, encodes Drosophila C/EBP. *Cell,* 71**,** 51-62.

MOORE, A. S., KEARNS, P. R., KNAPPER, S., PEARSON, A. D. & ZWAAN, C. M. 2013. Novel therapies for children with acute myeloid leukaemia. *Leukemia,* 27**,** 1451-60.

MOORE, M. A. S., CANCER RESEARCH UNIT, W. A. E. H. I., ROYAL MELBOURNE HOSPITAL, P. O. 3052, AUSTRALIA, METCALF, D. & CANCER RESEARCH UNIT, W. A. E. H. I., ROYAL MELBOURNE HOSPITAL, P. O. 3052, AUSTRALIA 1970. Ontogeny of the Haemopoietic System: Yolk Sac Origin of In Vivo and In Vitro Colony Forming Cells in the Developing Mouse Embryo*. *British Journal of Haematology,* 18**,** 279-296.

MOORMAN, A., CHILTON, L., WILKINSON, J., ENSOR, H., BOWN, N. & PROCTOR, S. 2010. A population-based cytogenetic study of adults with acute lymphoblastic leukemia.

MORRISON, S. J., HEMMATI, H. D., WANDYCZ, A. M. & WEISSMAN, I. L. 1995. The purification and characterization of fetal liver hematopoietic stem cells. *Proc Natl Acad Sci U S A,* 92**,** 10302-6.

MUELLER, B. U. & PABST, T. 2006. C/EBPalpha and the pathophysiology of acute myeloid leukemia. *Curr Opin Hematol,* 13**,** 7-14.

MUKHOPADHYAY, D. & RIEZMAN, H. 2007. Proteasome-independent functions of ubiquitin in endocytosis and signaling. *Science,* 315**,** 201-5.

MULLER, A. M., DUQUE, J., SHIZURU, J. A. & LUBBERT, M. 2008. Complementing mutations in core binding factor leukemias: from mouse models to clinical applications. *Oncogene,* 27**,** 5759-73.

MULLER, A. M., MEDVINSKY, A., STROUBOULIS, J., GROSVELD, F. & DZIERZAK, E. 1994. Development of hematopoietic stem cell activity in the mouse embryo. *Immunity,* 1**,** 291-301.

MURAKAMI, M. 1995. Critical amino acids responsible for conferring calcium channel characteristics are located on the surface and aroundβ-turn potentials of channel proteins. *Journal of Protein Chemistry,* 14**,** 111-114.

MURAKAMI, M. & COLLEGE, M. 2014. Critical amino acids responsible for conferring calcium channel characteristics are located on the surface and aroundβ-turn potentials of channel proteins. *Journal of Protein Chemistry,* 14**,** 111-114.

MURATI, A., BRECQUEVILLE, M., DEVILLIER, R., MOZZICONACCI, M. J., GELSI-BOYER, V. & BIRNBAUM, D. 2012. Myeloid malignancies: mutations, models and management. *BMC Cancer,* 12**,** 304.

NAGEL, S., VENTURINI, L., PRZYBYLSKI, G. K., GRABARCZYK, P., SCHNEIDER, B., MEYER, C., KAUFMANN, M., SCHMIDT, C. A., SCHERR, M., DREXLER, H. G. & MACLEOD, R. A. 2011. Activation of Paired-homeobox gene PITX1 by del(5)(q31) in T-cell acute lymphoblastic leukemia. *Leuk Lymphoma,* 52**,** 1348-59.

NAIKI, T., SAIJOU, E., MIYAOKA, Y., SEKINE, K. & MIYAJIMA, A. 2007. TRB2, a Mouse Tribbles Ortholog, Suppresses Adipocyte Differentiation by Inhibiting AKT and C/EBPβ. *Journal of Biological Chemistry,* 282**,** 24075-24082.

NAKAO, M., YOKOTA, S., IWAI, T., KANEKO, H., HORIIKE, S., KASHIMA, K., SONODA, Y., FUJIMOTO, T. & MISAWA, S. 1996. Internal tandem duplication of the flt3 gene found in acute myeloid leukemia. *Leukemia,* 10**,** 1911-8.

NALEPA, G., ROLFEM & J. HARPER, W. 2006. Drug discovery in the ubiquitin|[ndash]|proteasome system. *Nature Reviews Drug Discovery,* 5**,** 596-613.

NANRI, T., UIKE, N., KAWAKITA, T., IWANAGA, E., MITSUYA, H. & ASOU, N. 2010. A family harboring a germ-line N-terminal C/EBPalpha mutation and development of acute myeloid leukemia with an additional somatic C-terminal C/EBPalpha mutation. *Genes Chromosomes Cancer,* 49**,** 237-41.

NERLOV, C. 2004. C/EBP|[alpha]| mutations in acute myeloid leukaemias. *Nature Reviews Cancer,* 4**,** 394-400.

NERLOV, C. & ZIFF, E. B. 1995. CCAAT/enhancer binding protein-alpha amino acid motifs with dual TBP and TFIIB binding ability co-operate to activate transcription in both yeast and mammalian cells. *Embo j,* 14**,** 4318-28.

NIEWERTH, D., FRANKE, N. E., JANSEN, G., ASSARAF, Y. G., VAN MEERLOO, J., KIRK, C. J., DEGENHARDT, J., ANDERL, J., SCHIMMER, A. D., ZWEEGMAN, S., DE HAAS, V., HORTON, T. M., KASPERS, G. J. & CLOOS, J. 2013. Higher ratio immune versus constitutive proteasome level as novel indicator of sensitivity of pediatric acute leukemia cells to proteasome inhibitors. *Haematologica,* 98**,** 1896-904.

NIEWERTH, D., KASPERS, G. J., ASSARAF, Y. G., VAN MEERLOO, J., KIRK, C. J., ANDERL, J., BLANK, J. L., VAN DE VEN, P. M., ZWEEGMAN, S., JANSEN, G. & CLOOS, J. 2014. Interferon-γ-induced upregulation of immunoproteasome subunit assembly overcomes bortezomib resistance in human hematological cell lines. *Journal of Hematology & Oncology,* 7**,** 7.

NIKI, M., OKADA, H., TAKANO, H., KUNO, J., TANI, K., HIBINO, H., ASANO, S., ITO, Y., SATAKE, M. & NODA, T. 1997. Hematopoiesis in the fetal liver is impaired by targeted mutagenesis of a gene encoding a non-DNA binding subunit of the transcription factor, polyomavirus enhancer binding protein 2/core binding factor. *Proc Natl Acad Sci U S A,* 94**,** 5697-702.

NOOREN, I. M. & THORNTON, J. M. 2003. NEW EMBO MEMBER'S REVIEW: Diversity of protein–protein interactions. *EMBO J,* 22**,** 3486-92.

NOVERSHTERN, N., SUBRAMANIAN, A., LAWTON, L. N., MAK, R. H., HAINING, W. N., MCCONKEY, M. E., HABIB, N., YOSEF, N., CHANG, C. Y., SHAY, T., FRAMPTON, G. M., DRAKE, A. C., LESKOV, I., NILSSON, B., PREFFER, F., DOMBKOWSKI, D., EVANS, J. W., LIEFELD, T., SMUTKO, J. S., CHEN, J., FRIEDMAN, N., YOUNG, R. A., GOLUB, T. R., REGEV, A. & EBERT, B. L. 2011. Densely interconnected transcriptional circuits control cell states in human hematopoiesis. *Cell,* 144**,** 296-309.

NOWELL, P. C. & HUNGERFORD, D. A. 1960. Chromosome studies on normal and leukemic human leukocytes. *J Natl Cancer Inst,* 25**,** 85-109.

NUCHPRAYOON, I., MEYERS, S., SCOTT, L. M., SUZOW, J., HIEBERT, S. & FRIEDMAN, A. D. 1994. PEBP2/CBF, the murine homolog of the human myeloid AML1 and PEBP2 beta/CBF beta proto-oncoproteins, regulates the murine myeloperoxidase and neutrophil elastase genes in immature myeloid cells. *Mol Cell Biol,* 14**,** 5558-68.

OBENG, E. A., CARLSON, L. M., GUTMAN, D. M., HARRINGTON, W. J., JR., LEE, K. P. & BOISE, L. H. 2006. Proteasome inhibitors induce a terminal unfolded protein response in multiple myeloma cells. *Blood,* 107**,** 4907-16.

OERLEMANS, R., FRANKE, N. E., ASSARAF, Y. G., CLOOS, J., VAN ZANTWIJK, I., BERKERS, C. R., SCHEFFER, G. L., DEBIPERSAD, K., VOJTEKOVA, K., LEMOS, C., VAN DER HEIJDEN, J. W., YLSTRA, B., PETERS, G. J., KASPERS, G. L., DIJKMANS, B. A., SCHEPER, R. J. & JANSEN, G. 2008. Molecular basis of bortezomib resistance: proteasome subunit beta5 (PSMB5) gene mutation and overexpression of PSMB5 protein. *Blood,* 112**,** 2489-99.

OFRAN, Y. & ROST, B. 2007. Protein–Protein Interaction Hotspots Carved into Sequences. *PLoS Comput Biol,* 3**,** e119.

OHLSSON, E., SIGURD HASEMANN, M., WILLER, A., LAURIDSEN, B., RAPIN, N., JENDHOLM, J. & PORSE, B. T. 2014. Initiation of MLL-rearranged AML is dependent on C/EBPα.

OHOKA, N., YOSHII, S., HATTORI, T., ONOZAKI, K. & HAYASHI, H. 2005. TRB3, a novel ER stress-inducible gene, is induced via ATF4-CHOP pathway and is involved in cell death. *EMBO J.*

OHTA, T., MICHEL, J. J., SCHOTTELIUS, A. J. & XIONG, Y. 1999. ROC1, a homolog of APC11, represents a family of cullin partners with an associated ubiquitin ligase activity. *Mol Cell,* 3**,** 535-41.

OKUDA, T., VAN DEURSEN, J., HIEBERT, S. W., GROSVELD, G. & DOWNING, J. R. 1996. AML1, the target of multiple chromosomal translocations in human leukemia, is essential for normal fetal liver hematopoiesis. *Cell,* 84**,** 321-30.

ORKIN, S. H. & ZON, L. I. 2008. Hematopoiesis: an evolving paradigm for stem cell biology. *Cell,* 132**,** 631-44.

ORLOWSKI, R. Z., VOORHEES, P. M., GARCIA, R. A., HALL, M. D., KUDRIK, F. J., ALLRED, T., JOHRI, A. R., JONES, P. E., IVANOVA, A., VAN DEVENTER, H. W., GABRIEL, D. A., SHEA, T. C., MITCHELL, B. S., ADAMS, J., ESSELTINE, D. L., TREHU, E. G., GREEN, M.,

LEHMAN, M. J., NATOLI, S., COLLINS, J. M., LINDLEY, C. M. & DEES, E. C. 2005. Phase 1 trial of the proteasome inhibitor bortezomib and pegylated liposomal doxorubicin in patients with advanced hematologic malignancies. *Blood,* 105**,** 3058-65.

OTTERSBACH, K. & DZIERZAK, E. 2005. The murine placenta contains hematopoietic stem cells within the vascular labyrinth region. *Dev Cell,* 8**,** 377-87.

PABST, T., EYHOLZER, M., HAEFLIGER, S., SCHARDT, J. & MUELLER, B. U. 2008. Somatic CEBPA mutations are a frequent second event in families with germline CEBPA mutations and familial acute myeloid leukemia. *J Clin Oncol,* 26**,** 5088-93.

PABST, T. & MUELLER, B. U. 2007. Transcriptional dysregulation during myeloid transformation in AML. *Oncogene,* 26**,** 6829-37.

PABST, T. & MUELLER, B. U. 2009. Complexity of CEBPA Dysregulation in Human Acute Myeloid Leukemia. *Clinical Cancer Research,* 15**,** 5303-5307.

PABST, T., MUELLER, B. U., HARAKAWA, N., SCHOCH, C., HAFERLACH, T., BEHRE, G., HIDDEMANN, W., ZHANG, D. E. & TENEN, D. G. 2001a. AML1-ETO downregulates the granulocytic differentiation factor C/EBPalpha in t(8;21) myeloid leukemia. *Nat Med,* 7**,** 444-51.

PABST, T., MUELLER, B. U., ZHANG, P., RADOMSKA, H. S., NARRAVULA, S., SCHNITTGER, S., BEHRE, G., HIDDEMANN, W. & TENEN, D. G. 2001b. Dominant-negative mutations of CEBPA, encoding CCAAT/enhancer binding protein-alpha (C/EBPalpha), in acute myeloid leukemia. *Nat Genet,* 27**,** 263-70.

PAL, P., LOCHAB, S., KANAUJIYA, J. K., KAPOOR, I., SANYAL, S., BEHRE, G. & TRIVEDI, A. K. 2013a. E3 Ubiquitin Ligase E6AP Negatively Regulates Adipogenesis by Downregulating Proadipogenic Factor C/EBPalpha. *PLoS One,* 8.

PAL, P., LOCHAB, S., KANAUJIYA, J. K., KAPOOR, I., SANYAL, S., BEHRE, G. & TRIVEDI, A. K. 2013b. E6AP, an E3 ubiquitin ligase negatively regulates granulopoiesis by targeting transcription factor C/EBPalpha for ubiquitin-mediated proteasome degradation. *Cell Death Dis,* 4**,** e590.

PALMA, C. A., AL SHEIKHA, D., LIM, T. K., BRYANT, A., VU, T. T., JAYASWAL, V. & MA, D. D. 2014. MicroRNA-155 as an inducer of apoptosis and cell differentiation in Acute Myeloid Leukaemia. *Mol Cancer,* 13**,** 79.

PAZ-PRIEL, I. & FRIEDMAN, A. 2011. C/EBPalpha dysregulation in AML and ALL. *Crit Rev Oncog,* 16**,** 93-102.

PEDERSEN, BERESHCHENKO, GARCIA-SILVA, ERMAKOVA., KURZ, MANDRUP, PORSE & NERLOV. 2007. Distinct C/EBPalpha motifs regulate lipogenic and gluconeogenic gene expression in vivo. *Embo j,* 26**,** 1081-93.

PEDERSEN, T., KOWENZ-LEUTZ, E., LEUTZ, A. & NERLOV, C. 2001. Cooperation between C/EBP? TBP/TFIIB and SWI/SNF recruiting domains is required for adipocyte differentiation. *Genes Dev,* 15**,** 3208-16.

PEI, X. Y., DAI, Y. & GRANT, S. 2003. The proteasome inhibitor bortezomib promotes mitochondrial injury and apoptosis induced by the small molecule Bcl-2 inhibitor HA14-1 in multiple myeloma cells. *Leukemia,* 17**,** 2036-2045.

PEREZ, A., KASTNER, P., SETHI, S., LUTZ, Y., REIBEL, C. & CHAMBON, P. 1993. PMLRAR homodimers: distinct DNA binding properties and heteromeric interactions with RXR. *Embo j,* 12**,** 3171-82.

PERROTTI, D., CESI, V., TROTTA, R., GUERZONI, C., SANTILLI, G., CAMPBELL, K., IERVOLINO, A., CONDORELLI, F., GAMBACORTI-PASSERINI, C., CALIGIURI, M. A. & CALABRETTA, B. 2002. BCR-ABL suppresses C/EBPalpha expression through inhibitory action of hnRNP E2. *Nat Genet,* 30**,** 48-58.

PETERS, J. M., CEJKA, Z., HARRIS, J. R., KLEINSCHMIDT, J. A. & BAUMEISTER, W. 1993. Structural features of the 26 S proteasome complex. *J Mol Biol,* 234**,** 932-7.

PETERSON, B., LUNDEGAARD, C. & NORDAHL-PETERSEN, T. 2010. NetTurnP – Neural Network Prediction of Beta-turns by Use of Evolutionary Information and Predicted Protein Sequence Features. *Plosone*.

PICKART, C. M. 1997. Targeting of substrates to the 26S proteasome. *The FASEB Journal,* 11**,** 1055-1066.

PIERCE, N. W., KLEIGER, G., SHAN, S. O. & DESHAIES, R. J. 2009. Detection of sequential polyubiquitylation on a millisecond timescale. *Nature,* 462**,** 615-9.

PITRE, S., DEHNE, F., CHAN, A., CHEETHAM, J., DUONG, A., EMILI, A., GEBBIA, M., GREENBLATT, J., JESSULAT, M., KROGAN, N., LUO, X. & GOLSHANI, A. 2006. PIPE: a protein-protein interaction prediction engine based on the re-occurring short polypeptide sequences between known interacting protein pairs. *BMC Bioinformatics,* 7**,** 365.

PLECHANOVOVA, A., JAFFRAY, E. G., TATHAM, M. H., NAISMITH, J. H. & HAY, R. T. 2012. Structure of a RING E3 ligase and ubiquitin-loaded E2 primed for catalysis. *Nature,* 489**,** 115-20.

PORSE, B. T., BRYDER, D., THEILGAARD-MÖNCH, K., HASEMANN, M. S., ANDERSON, K., DAMGAARD, I., JACOBSEN, S. E. W. & NERLOV, C. 2005. Loss of C/EBPα cell cycle control increases myeloid progenitor proliferation and transforms the neutrophil granulocyte lineage. *The Journal of Experimental Medicine,* 202**,** 85-96.

PORSE, B. T., PEDERSEN, T. A., HASEMANN, M. S., SCHUSTER, M. B., KIRSTETTER, P., LUEDDE, T., DAMGAARD, I., KURZ, E., SCHJERLING, C. K. & NERLOV, C. 2006. The proline-histidine-rich CDK2/CDK4 interaction region of C/EBPalpha is dispensable for C/EBPalpha-mediated growth regulation in vivo. *Mol Cell Biol,* 26**,** 1028-37.

PORSE, B. T., PEDERSEN, T. Å., XU, X., LINDBERG, B., WEWER, U. M., FRIIS-HANSEN, L. & NERLOV, C. 2001. E2F Repression by C/EBPα Is Required for Adipogenesis and Granulopoiesis In Vivo. *Cell,* 107**,** 247-258.

POULAKI, V., MITSIADES, C. S., KOTOULA, V., NEGRI, J., MCMILLIN, D., MILLER, J. W. & MITSIADES, N. 2007. The Proteasome Inhibitor Bortezomib Induces Apoptosis in Human Retinoblastoma Cell Lines In Vitro. *Investigative Ophthalmology & Visual Science,* 48**,** 4706-4719.

PRUNEDA, J. N., STOLL, K. E., BOLTON, L. J., BRZOVIC, P. S. & KLEVIT, R. E. 2011. Ubiquitin in Motion: Structural Studies of the Ubiquitin-Conjugating Enzyme∼Ubiquitin Conjugate. *Biochemistry,* 50**,** 1624-1633.

PUI, C. H., CARROLL, W. L., MESHINCHI, S. & ARCECI, R. J. 2011. Biology, risk stratification, and therapy of pediatric acute leukemias: an update. *J Clin Oncol,* 29**,** 551-65.

PUTHALAKATH, H., O'REILLY, L. A., GUNN, P., LEE, L., KELLY, P. N., HUNTINGTON, N. D., HUGHES, P. D., MICHALAK, E. M., MCKIMM-BRESCHKIN, J., MOTOYAMA, N., GOTOH, T., AKIRA, S., BOUILLET, P. & STRASSER, A. 2007. ER Stress Triggers Apoptosis by Activating BH3-Only Protein Bim. *Cell,* 129**,** 1337-1349.

QI, L., HEREDIA, J. E., ALTAREJOS, J. Y., SCREATON, R., GOEBEL, N., NIESSEN, S., MACLEOD, I. X., LIEW, C. W., KULKARNI, R. N., BAIN, J., NEWGARD, C., NELSON, M., EVANS, R. M., YATES, J. & MONTMINY, M. 2006. TRB3 Links the E3 Ubiquitin Ligase COP1 to Lipid Metabolism. *Science,* 312**,** 1763-1766.

RADIVOJAC, P., VACIC, V., HAYNES, C., COCKLIN, R. R., MOHAN, A., HEYEN, J. W., GOEBL, M. G. & IAKOUCHEVA, L. M. 2010. Identification, Analysis and Prediction of Protein Ubiquitination Sites. *Proteins,* 78**,** 365-80.

RADOMSKA, H. S., BASSÈRES, D. S., ZHENG, R., ZHANG, P., DAYARAM, T., YAMAMOTO, Y., STERNBERG, D. W., LOKKER, N., GIESE, N. A., BOHLANDER, S. K., SCHNITTGER, S., DELMOTTE, M.-H., DAVIS, R. J., SMALL, D., HIDDEMANN, W., GILLILAND, D. G. & TENEN, D. G. 2006. Block of C/EBPα function by phosphorylation in acute myeloid leukemia with FLT3 activating mutations. *The Journal of Experimental Medicine,* 203**,** 371-381.

RAMJI, D. P. & FOKA, P. 2002. CCAAT/enhancer-binding proteins: structure, function and regulation. *Biochem J.*

RECKZEH, BERESHCHENKO, MEAD, REHN, KHARAZI, JACOBSEN, NERLOV & CAMMENGA 2012a. Molecular and cellular effects of oncogene cooperation in a genetically accurate AML mouse model. *Leukemia,* 26**,** 1527-1536.

RECKZEH, K., BERESHCHENKO, O., MEAD, A., REHN, M., KHARA, S., JACOBSEN, S.-E., NERLOV, C. & J, C. 2012b. Molecular and cellular effects of oncogene cooperation in a genetically accurate AML mouse model. *Leukemia,* 26**,** 1527-1536.

RECKZEH, K. & CAMMENGA, J. 2010. Molecular mechanisms underlying deregulation of C/EBPalpha in acute myeloid leukemia. *Int J Hematol,* 91**,** 557-68.

REDAELLI, A., BOTTEMAN, M. F., STEPHENS, J. M., BRANDT, S. & PASHOS, C. L. 2004. Economic burden of acute myeloid leukemia: a literature review. *Cancer Treat Rev,* 30**,** 237-47.

RENNEVILLE, A., MIALOU, V., PHILIPPE, N., KAGIALIS-GIRARD, S., BIGGIO, V., ZABOT, M.-T., THOMAS, X., BERTRAND, Y. & PREUDHOMME, C. 2008a. Another pedigree with familial acute myeloid leukemia and germline CEBPA mutation. *Leukemia,* 23**,** 804-806.

RENNEVILLE, A., ROUMIER, C., BIGGIO, V., NIBOUREL, O., BOISSEL, N., FENAUX, P. & PREUDHOMME, C. 2008b. Cooperating gene mutations in acute myeloid leukemia: a review of the literature. *Leukemia,* 22**,** 915-31.

RENTSCH, A., LANDSBERG, D., BRODMANN, T., BULOW, L., GIRBIG, A. K. & KALESSE, M. 2013. Synthesis and pharmacology of proteasome inhibitors. *Angew Chem Int Ed Engl,* 52**,** 5450-88.

RHOADES, K. L., HETHERINGTON, C. J., ROWLEY, J. D., HIEBERT, S. W., NUCIFORA, G., TENEN, D. G. & ZHANG, D. E. 1996. Synergistic up-regulation of the myeloid-specific promoter for the macrophage colony-stimulating factor receptor by AML1 and the t(8;21) fusion protein may contribute to leukemogenesis. *Proc Natl Acad Sci U S A,* 93**,** 11895-900.

RICCIONI, R., SENESE, M., DIVERIO, D., RITI, V., BUFFOLINO, S., MARIANI, G., BOE, A., CEDRONE, M., LO-COCO, F., FOA, R., PESCHLE, C. & TESTA, U. 2007. M4 and M5 acute myeloid leukaemias display a high sensitivity to Bortezomib-mediated apoptosis. *Br J Haematol,* 139**,** 194-205.

RICHARDSON, P. G., BARLOGIE, B., BERENSON, J., SINGHAL, S., JAGANNATH, S., IRWIN, D., RAJKUMAR, S. V., SRKALOVIC, G., ALSINA, M., ALEXANIAN, R., SIEGEL, D., ORLOWSKI, R. Z., KUTER, D., LIMENTANI, S. A., LEE, S., HIDESHIMA, T., ESSELTINE, D. L., KAUFFMAN, M., ADAMS, J., SCHENKEIN, D. P. & ANDERSON, K. C. 2003. A phase 2 study of bortezomib in relapsed, refractory myeloma. *N Engl J Med,* 348**,** 2609-17.

RICHARDSON, P. G., MITSIADES, C., HIDESHIMA, T. & ANDERSON, K. C. 2006. Bortezomib: Proteasome Inhibition as an Effective Anticancer Therapy. *Annual Review of Medicine,* 57**,** 33-47.

RISHI, L., HANNON, M., SALOMÈ, M., HASEMANN, M., FRANK, A.-K., CAMPOS, J., TIMONEY, J., O'CONNOR, C., CAHILL, M. R., PORSE, B. & KEESHAN, K. 2014. Regulation of Trib2 by an E2F1-C/EBPalpha feedback loop in AML cell proliferation. *Blood*.

RODRIGUEZ, A., VIGORITO, E., CLARE, S., WARREN, M. V., COUTTET, P., SOOND, D. R., DONGEN, S. V., GROCOCK, R. J., DAS, P. P., MISKA, E. A., VETRIE, D., OKKENHAUG, K., ENRIGHT, A. J., DOUGAN, G., TURNER, M. & BRADLEY, A. 2007. Requirement of bic/microRNA-155 for Normal Immune Function.

RODRIGUEZ-UBREVA, J., CIUDAD, L., VAN OEVELEN, C., PARRA, M., GRAF, T. & BALLESTAR, E. 2014. C/EBPa-Mediated Activation of miR-34a and miR-223 Inhibits Lef1 Expression to Achieve Efficient Reprogramming into Macrophages. *Molecular and Cellular Biology*.

ROE, J. S. & VAKOC, C. R. 2014. C/EBPalpha: critical at the origin of leukemic transformation. *J Exp Med,* 211**,** 1-4.

ROSS, S. E., ERICKSON, R. L., HEMATI, N. & MACDOUGALD, O. A. 1999. Glycogen Synthase Kinase 3 Is an Insulin-Regulated C/EBP? Kinase. *Mol Cell Biol,* 19**,** 8433-41.

ROSS, S. E., RADOMSKA, H. S., WU, B., ZHANG, P., WINNAY, J. N., BAJNOK, L., WRIGHT, W. S., SCHAUFELE, F., TENEN, D. G. & MACDOUGALD, O. A. 2004. Phosphorylation of C/EBPα Inhibits Granulopoiesis. *Molecular and Cellular Biology,* 24**,** 675-686.

RÖTHLISBERGER, B., HEIZMANN, M., BARGETZI, M. J. & HUBER, A. R. 2007. TRIB1 overexpression in acute myeloid leukemia. *Cancer Genetics and Cytogenetics,* 176**,** 58-60.

RØRTH, P., SZABO, K. & TEXIDO, G. 2000. The Level of C/EBP Protein Is Critical for Cell Migration during Drosophila Oogenesis and Is Tightly Controlled by Regulated Degradation. *Molecular cell,* 6**,** 23-30.

SABIN, F. 1917. *Origin and development of the primitve vessels of the chick and of the pig,* Contrib. Embryol.

SANDA, T., LAWTON, L. N., BARRASA, M. I., FAN, Z. P., KOHLHAMMER, H., GUTIERREZ, A., MA, W., TATAREK, J., AHN, Y., KELLIHER, M. A., JAMIESON, C. H., STAUDT, L. M., YOUNG, R. A. & LOOK, A. T. 2012. Core transcriptional regulatory circuit controlled by the TAL1 complex in human T cell acute lymphoblastic leukemia. *Cancer Cell,* 22**,** 209-21.

SANDERS, M. A. & VALK, P. J. 2013. The evolving molecular genetic landscape in acute myeloid leukaemia. *Curr Opin Hematol,* 20**,** 79-85.

SARLO, C., BUCCISANO, F., MAURILLO, L., CEFALO, M., DI CAPRIO, L., CICCONI, L., DITTO, C., OTTAVIANI, L., DI VEROLI, A., DEL PRINCIPE, M. I., GRASSO, M. A., NASSO, D., DE

SANTIS, G., AMADORI, S. & VENDITTI, A. 2013. Phase II Study of Bortezomib as a Single Agent in Patients with Previously Untreated or Relapsed/Refractory Acute Myeloid Leukemia Ineligible for Intensive Therapy. *Leukemia Research and Treatment,* 2013**,** 6.

SATOH, T., KIDOYA, H., NAITO, H., YAMAMOTO, M., TAKEMURA, N., NAKAGAWA, K., YOSHIOKA, Y., MORII, E., TAKAKURA, N., TAKEUCHI, O. & AKIRA, S. 2013. Critical role of Trib1 in differentiation of tissue-resident M2-like macrophages. *Nature,* 495**,** 524-8.

SCAGLIONE, K. M., BASRUR, V., ASHRAF, N. S., KONEN, J. R., ELENITOBA-JOHNSON, K. S. J., TODI, S. V. & PAULSON, H. L. 2013. The Ubiquitin-conjugating Enzyme (E2) Ube2w Ubiquitinates the N Terminus of Substrates. *Journal of Biological Chemistry,* 288**,** 18784-18788.

SCHAUFELE, F., WANG, X., LIU, X. & DAY, R. N. 2003. Conformation of CCAAT/Enhancer-binding Protein α Dimers Varies with Intranuclear Location in Living Cells. *Journal of Biological Chemistry,* 278**,** 10578-10587.

SCHUH, A., BECQ, J., HUMPHRAY, S., ALEXA, A., BURNS, A., CLIFFORD, R., FELLER, S. M., GROCOCK, R., HENDERSON, S., KHREBTUKOVA, I., KINGSBURY, Z., LUO, S., MCBRIDE, D., MURRAY, L., MENJU, T., TIMBS, A., ROSS, M., TAYLOR, J. & BENTLEY, D. 2012. Monitoring chronic lymphocytic leukemia progression by whole genome sequencing reveals heterogeneous clonal evolution patterns. *Blood,* 120**,** 4191-6.

SCHWIEGER, M., LÖHLER, J., FISCHER, M., HERWIG, U., TENEN, D. G. & STOCKING, C. 2004. A dominant-negative mutant of C/EBPα, associated with acute myeloid leukemias, inhibits differentiation of myeloid and erythroid progenitors of man but not mouse. *Blood,* 103**,** 2744-2752.

SELLICK, G. S., SPENDLOVE, H. E., CATOVSKY, D., PRITCHARD-JONES, K. & HOULSTON, R. S. 2005. Further evidence that germline CEBPA mutations cause dominant inheritance of acute myeloid leukaemia. *Leukemia.* England.

SHIM, M. & SMART, R. C. 2003. Lithium Stabilizes the CCAAT/Enhancer-binding Protein α (C/EBPα) through a Glycogen Synthase Kinase 3 (GSK3)-independent Pathway Involving Direct Inhibition of Proteasomal Activity. *Journal of Biological Chemistry,* 278**,** 19674-19681.

SINGH, S. M., TRIVEDI, A. K. & BEHRE, G. 2008. C/EBPα S248A mutation reduces granulocytic differentiation in human leukemic K562 cells. *Biochemical and Biophysical Research Communications,* 369**,** 692-694.

SLOMIANY, B. A., D'ARIGO, K. L., KELLY, M. M. & KURTZ, D. T. 2000. C/EBP? Inhibits Cell Growth via Direct Repression of E2F-DP-Mediated Transcription. *Mol Cell Biol,* 20**,** 5986-97.

SMITH, M. L., CAVENAGH, J. D., LISTER, T. A. & FITZGIBBON, J. 2004. Mutation of CEBPA in familial acute myeloid leukemia. *N Engl J Med,* 351**,** 2403-7.

STAPNES, C., INSTITUTE OF MEDICINE, U. O. B. A. D. O. H., DEPARTMENT OF MEDICINE, HAUKELAND UNIVERSITY HOSPITAL, DØSKELAND, A. P., DIVISION FOR BIOCHEMISTRY AND MOLECULAR BIOLOGY, D. O. B., UNIVERSITY OF BERGEN, BERGEN, NORWAY, HATFIELD, K., INSTITUTE OF MEDICINE, U. O. B. A. D. O. H., DEPARTMENT OF MEDICINE, HAUKELAND UNIVERSITY HOSPITAL, ERSVÆR, E., INSTITUTE OF MEDICINE, U. O. B. A. D. O. H., DEPARTMENT OF MEDICINE, HAUKELAND UNIVERSITY HOSPITAL, RYNINGEN, A., INSTITUTE OF MEDICINE, U. O. B. A. D. O. H., DEPARTMENT OF MEDICINE, HAUKELAND UNIVERSITY HOSPITAL, LORENS, J. B., DIVISION FOR BIOCHEMISTRY AND MOLECULAR BIOLOGY, D. O. B., UNIVERSITY OF BERGEN, BERGEN, NORWAY, GJERTSEN, B. T., INSTITUTE OF MEDICINE, U. O. B. A. D. O. H., DEPARTMENT OF MEDICINE, HAUKELAND UNIVERSITY HOSPITAL, BRUSERUD, Ø. & INSTITUTE OF MEDICINE, U. O. B. A. D. O. H., DEPARTMENT OF MEDICINE, HAUKELAND UNIVERSITY HOSPITAL 2014. The proteasome inhibitors bortezomib and PR-171 have antiproliferative and proapoptotic effects on primary human acute myeloid leukaemia cells. *British Journal of Haematology,* 136**,** 814-828.

STORLAZZI, C., FIORETOS, T., , S., C, LONOCE, A., MASTRORILL, A., STRÖMBECK, B., D'ADDABBO, P., IACOVELLI, F., MINERVINI, C., AVENTIN, A., DASTUGUE, N., FONATSCH, C., HAGEMEIJER, A., JOTTERAND, M., MÜHLEMATTER, D., LAFAGE-POCHITALOFF, M., NGUYEN-KHAC, F., SCHOCH, C., SLOVAK, M. L., SMITH, A., SOLÈ, F., ROY, N. V., JOHANSSON, B. & ROCCHI, M. 2006. MYC-containing double minutes in hematologic malignancies: evidence in favor of the episome model and exclusion of MYC as the target gene.

SU, L., LI, X., GAO, S. J., YU, P., LIU, X. L., TAN, Y. H. & LIU, Y. M. 2014. Cytogenetic and genetic mutation features of de novo acute myeloid leukemia in elderly Chinese patients. *Asian Pac J Cancer Prev,* 15**,** 895-8.

SUBRAMANIAN, L., BENSON, M. & IÑIGUEZ-LLUHÍ, J. 2003. A Synergy Control Motif within the Attenuator Domain of CCAAT/Enhancer-binding Protein α Inhibits Transcriptional Synergy through Its PIASy-enhanced Modification by SUMO-1 or SUMO-3.

TASKESEN, E., BULLINGER, L., CORBACIOGLU, A., SANDERS, M. A., ERPELINCK, C. A. J., WOUTERS, B. J., VAN DER POEL-VAN DE LUYTGAARDE, S. C., DAMM, F., KRAUTER, J., GANSER, A., SCHLENK, R. F., LÖWENBERG, B., DELWEL, R., DÖHNER, H., VALK, P. J. M. & DÖHNER, K. 2011. Prognostic impact, concurrent genetic mutations, and gene expression features of AML with CEBPA mutations in a cohort of 1182 cytogenetically normal AML patients: further evidence for CEBPA double mutant AML as a distinctive disease entity. *Blood,* 117**,** 2469-2475.

THROWER, J. S., HOFFMAN, L., RECHSTEINER, M. & PICKART, C. M. 2000. Recognition of the polyubiquitin proteolytic signal. *Embo j,* 19**,** 94-102.

TIMCHENKO, N. A., HARRIS, T. E., WILDE, M., BILYEU, T. A., BURGESS-BEUSSE, B. L., FINEGOLD, M. J. & DARLINGTON, G. J. 1997. CCAAT/enhancer binding protein alpha regulates p21 protein and hepatocyte proliferation in newborn mice. *Mol Cell Biol,* 17**,** 7353-61.

TIMCHENKO, N. A., WILDE, M., NAKANISHI, M., SMITH, J. R. & DARLINGTON, G. J. 1996. CCAAT/enhancer-binding protein alpha (C/EBP alpha) inhibits cell proliferation through the p21 (WAF-1/CIP-1/SDI-1) protein. *Genes Dev,* 10**,** 804-15.

TOKGOZ, Z., SIEPMANN, T. J., STREICH, F., JR., KUMAR, B., KLEIN, J. M. & HAAS, A. L. 2012. E1-E2 interactions in ubiquitin and Nedd8 ligation pathways. *J Biol Chem,* 287**,** 311-21.

TRIVEDI, A. K., BARARIA, D., CHRISTOPEIT, M., PEERZADA, A. A., SINGH, S. M., KIESER, A., HIDDEMANN, W., BEHRE, H. M. & BEHRE, G. 2006. Proteomic identification of C//EBP-DBD multiprotein complex: JNK1 activates stem cell regulator C//EBP[alpha] by inhibiting its ubiquitination. *Oncogene,* 26**,** 1789-1801.

TWU, Y.-C., HSIEH, C.-Y., LIN, M., TZENG, C.-H., SUN, C.-F. & YU, L.-C. 2010. Phosphorylation status of transcription factor C/EBPα determines cell-surface poly-LacNAc branching (I antigen) formation in erythropoiesis and granulopoiesis. *Blood,* 115**,** 2491-2499.

TYAGI, M., SHOEMAKER, B. A., BRYANT, S. H. & PANCHENKO, A. R. 2009. Exploring functional roles of multibinding protein interfaces. *Protein Sci,* 18**,** 1674-83.

UDESHI, N. D., MERTINS, P., SVINKINA, T. & CARR, S. A. 2013. Large-scale identification of ubiquitination sites by mass spectrometry. *Nat. Protocols,* 8**,** 1950-1960.

VALK, P. J. M., VERHAAK, R. G. W., BEIJEN, M. A., ERPELINCK, C. A. J., VAN DOORN-KHOSROVANI, S. B. V. W., BOER, J. M., BEVERLOO, H. B., MOORHOUSE, M. J., VAN DER SPEK, P. J., LÖWENBERG, B. & DELWEL, R. 2004. Prognostically Useful Gene-Expression Profiles in Acute Myeloid Leukemia. *New England Journal of Medicine,* 350**,** 1617-1628.

VARDIMAN, J. W., THIELE, J., ARBER, D. A., BRUNNING, R. D., BOROWITZ, M. J., PORWIT, A., HARRIS, N. L., LE BEAU, M. M., HELLSTROM-LINDBERG, E., TEFFERI, A. & BLOOMFIELD, C. D. 2009. The 2008 revision of the World Health Organization (WHO) classification of myeloid neoplasms and acute leukemia: rationale and important changes. *Blood,* 114**,** 937-51.

VERMA, R., PETERS, N. R., D'ONOFRIO, M., TOCHTROP, G. P., SAKAMOTO, K. M., VARADAN, R., ZHANG, M., COFFINO, P., FUSHMAN, D., DESHAIES, R. J. & KING, R. W. 2004. Ubistatins inhibit proteasome-dependent degradation by binding the ubiquitin chain. *Science,* 306**,** 117-20.

VILLAR, H. O. & KAUVAR, L. M. 1994. Amino acid preferences at protein binding sites. *FEBS Lett,* 349**,** 125-30.

VINSON, C. R., SIGLER, P. B. & MCKNIGHT, S. L. 1989. Scissors-Grip Model for DNA Recognition by a Family of Leucine Zipper Proteins. *Science,* 246**,** 911-916.

WANG, D., D'COSTA, J., CIVIN, C. I. & FRIEDMAN, A. D. 2006a. C/EBPα directs monocytic commitment of primary myeloid progenitors. *Blood,* 108**,** 1223-9.

WANG, G., SHI, X., HAEFLIGER, S., JIN, J., MAJOR, A., IAKOVA, P., FINEGOLD, M. & TIMCHENKO, N. A. 2010. Elimination of C/EBPα through the ubiquitin-proteasome system promotes the development of liver cancer in mice.

WANG, G.-L., IAKOVA, P., WILDE, M., AWAD, S. & TIMCHENKO, N. A. 2004. Liver tumors escape negative control of proliferation via PI3K/Akt-mediated block of C/EBPα growth inhibitory activity. *Genes & Development,* 18**,** 912-925.

WANG, G. L., SHI, X., SALISBURY, E., SUN, Y., ALBRECHT, J. H., SMITH, R. G. & TIMCHENKO, N. A. 2006b. Cyclin D3 maintains growth-inhibitory activity of C/EBPalpha by stabilizing C/EBPalpha-cdk2 and C/EBPalpha-Brm complexes. *Mol Cell Biol,* 26**,** 2570-82.

WANG, H., GOODE, T., IAKOVA, P., ALBRECHT, J. H. & TIMCHENKO, N. A. 2002. C/EBPalpha triggers proteasome-dependent degradation of cdk4 during growth arrest. *Embo j,* 21**,** 930-41.

WANG, H., IAKOVA, P., WILDE, M., WELM, A., GOODE, T., ROESLER, W. J. & TIMCHENKO, N. A. 2001. C/EBP± Arrests Cell Proliferation through Direct Inhibition of Cdk2 and Cdk4. *Molecular cell,* 8**,** 817-828.

WANG, H., WANG, X., LI, Y., LIAO, A., FU, B., PAN, H., LIU, Z. & YANG, W. 2012. The proteasome inhibitor bortezomib reverses P-glycoprotein-mediated leukemia multi-drug resistance through the NF-κB pathway.

WANG, H. H., LI, Y. C., LIAO, A. J., FU, B. B., YANG, W., LIU, Z. G. & WANG, X. B. 2011. Reversion of Multidrug-Resistance by Proteasome Inhibitor Bortezomib in K562/DNR Cell Line. *Chin J Cancer Res,* 23**,** 69-73.

WANG, J., PARK, J.-S., WEI, Y., RAJURKAR, M., COTTON, JENNIFER L., FAN, Q., LEWIS, BRIAN C., JI, H. & MAO, J. 2013a. TRIB2 Acts Downstream of Wnt/TCF in Liver Cancer Cells to Regulate YAP and C/EBPα Function. *Molecular Cell,* 51**,** 211-225.

WANG, J., ZHANG, Y., WENG, W., QIAO, Y., MA, L., XIAO, W., YU, Y., PAN, Q. & SUN, F. 2013b. Impaired phosphorylation and ubiquitination by P70 S6 kinase (P70S6K) and Smad ubiquitination regulatory factor 1 (Smurf1) promotes Tribbles homolog 2 (TRIB2) stability and carcinogenic property in liver cancer. *Journal of Biological Chemistry*.

WANG, N. D., FINEGOLD, M. J., BRADLEY, A., OU, C. N., ABDELSAYED, S. V., WILDE, M. D., TAYLOR, L. R., WILSON, D. R. & DARLINGTON, G. J. 1995. Impaired energy homeostasis in C/EBP alpha knockout mice. *Science,* 269**,** 1108-12.

WANG, Q.-F., CLEAVES, R., KUMMALUE, T., NERLOV, C. & FRIEDMAN, A. D. 2003. Cell cycle inhibition mediated by the outer surface of the C//EBP[alpha] basic region is required but not sufficient for granulopoiesis. *Oncogene,* 22**,** 2548-2557.

WEI, S.-C., ROSENBERG, I. M., CAO, Z., HUETT, A. S., XAVIER, R. J. & PODOLSKY, D. K. 2012. Tribbles 2 (Trib2) is a novel regulator of toll-like receptor 5 signaling. *Inflammatory Bowel Diseases,* 18**,** 877-888 10.1002/ibd.22883.

WEI, W., JIN, J., SCHLISIO, S., HARPER, J. W. & KAELIN, W. G. 2005. The v-Jun point mutation allows c-Jun to escape GSK3-dependent recognition and destruction by the Fbw7 ubiquitin ligase. *Cancer cell,* 8**,** 25-33.

WEISSMAN, I. L., ANDERSON, D. J. & GAGE, F. 2001. Stem and progenitor cells: origins, phenotypes, lineage commitments, and transdifferentiations. *Annu Rev Cell Dev Biol,* 17**,** 387-403.

WELCKER, M. & CLURMAN, B. E. 2008. FBW7 ubiquitin ligase: a tumour suppressor at the crossroads of cell division, growth and differentiation. *Nat Rev Cancer,* 8**,** 83-93.

WENG, A., FERRANDO, A. A., LEE, W., IV, J. P. M., SILVERMAN, L. B., SANCHEZ-IRIZARRY, C., BLACKLOW, S. C., LOOK, A. T. & ASTER, J. C. 2004. Activating Mutations of NOTCH1 in Human T Cell Acute Lymphoblastic Leukemia.

WILKIN, F., SUAREZ-HUERTA, N., ROBAYE, B., PEETERMANS, J., LIBERT, F., DUMONT, J. E. & MAENHAUT, C. 1997. Characterization of a Phosphoprotein whose mRNA is Regulated by the Mitogenic Pathways in Dog Thyroid Cells. *European Journal of Biochemistry,* 248**,** 660-668.

WILLIAMS, S. C., CANTWELL, C. A. & JOHNSON, P. F. 1991. A family of C/EBP-related proteins capable of forming covalently linked leucine zipper dimers in vitro. *Genes & Development,* 5**,** 1553-1567.

WILLIS & DYER 2000. The role of immunoglobulin translocations in the pathogenesis of B-cell malignancies. *Blood*.

WILSON, A. & TRUMPP, A. 2006. Bone-marrow haematopoietic-stem-cell niches. *Nature Reviews Immunology,* 6**,** 93-106.

WOUTERS, B. J., JORDÀ, M. A., KEESHAN, K., LOUWERS, I., ERPELINCK-VERSCHUEREN, C. A. J., TIELEMANS, D., LANGERAK, A. W., HE, Y., YASHIRO-OHTANI, Y., ZHANG, P., HETHERINGTON, C. J., VERHAAK, R. G. W., VALK, P. J. M., LÖWENBERG, B., TENEN, D. G., PEAR, W. S. & DELWEL, R. 2007. Distinct gene expression profiles of acute myeloid/T-lymphoid leukemia with silenced CEBPA and mutations in NOTCH1. *Blood,* 110**,** 3706-3714.

WOUTERS, B. J., LOWENBERG, B., ERPELINCK-VERSCHUEREN, C. A., VAN PUTTEN, W. L., VALK, P. J. & DELWEL, R. 2009. Double CEBPA mutations, but not single CEBPA mutations, define a subgroup of acute myeloid leukemia with a distinctive gene expression profile that is uniquely associated with a favorable outcome. *Blood,* 113**,** 3088-91.

WU, Z.-X., ZHAO, M., XIA, L., YU, Y., SHEN, S.-M., HAN, S.-F., LI, H., WANG, T.-D., CHEN, G.-Q. & WANG, L.-S. 2013. PKCδ enhances C/EBPα degradation via inducing its phosphorylation and cytoplasmic translocation. *Biochemical and Biophysical Research Communications,* 433**,** 220-225.

XIE, H., YE, M., FENG, R. & GRAF, T. 2004. Stepwise Reprogramming of B Cells into Macrophages. *Cell,* 117**,** 663-676.

XIN, J. X., YUE, Z., ZHANG, S., JIANG, Z. H., WANG, P. Y., LI, Y. J., PANG, M. & XIE, S. Y. 2013. miR-99 inhibits cervical carcinoma cell proliferation by targeting TRIB2. *Oncol Lett,* 6**,** 1025-1030.

YAMASAKI, H., ERA, T., ASOU, N., SANADA, I., MATUTES, E., YAMAGUCHI, K. & TAKATSUKI, K. 1995. High degree of myeloid differentiation and granulocytosis is associated with t(8;21) smoldering leukemia. *Leukemia,* 9**,** 1147-53.

YANG, Y., KITAGAKI, J., DAI, R.-M., TSAI, Y. C., LORICK, K. L., LUDWIG, R. L., PIERRE, S. A., JENSEN, J. P., DAVYDOV, I. V., OBEROI, P., LI, C.-C. H., KENTEN, J. H., BEUTLER, J. A., VOUSDEN, K. H. & WEISSMAN, A. M. 2007. Inhibitors of Ubiquitin-Activating Enzyme (E1), a New Class of Potential Cancer Therapeutics. *Cancer Research,* 67**,** 9472-9481.

YE, M., ZHANG, H., AMABILE, G., YANG, H., STABER, P. B., ZHANG, P., LEVANTINI, E., ALBERICH-JORDÀ, M., ZHANG, J., KAWASAKI, A. & TENEN, D. G. 2013. C/EBPa controls acquisition and maintenance of adult haematopoietic stem cell quiescence. *Nat Cell Biol,* 15**,** 385-394.

YOKOYAMA, T., KANNO, Y., YAMAZAKI, Y., TAKAHARA, T., MIYATA, S. & NAKAMURA, T. 2010. Trib1 links the MEK1/ERK pathway in myeloid leukemogenesis. *Blood,* 116**,** 2768-2775.

YOKOYAMA, T., TOKI, T., AOKI, Y., KANEZAKI, R., PARK, M.-J., KANNO, Y., TAKAHARA, T., YAMAZAKI, Y., ITO, E., HAYASHI, Y. & NAKAMURA, T. 2012. Identification of TRIB1 R107L gain-of-function mutation in human acute megakaryocytic leukemia. *Blood,* 119**,** 2608-2611.

YOSHIDA, A., KATO, J. Y., NAKAMAE, I. & YONEDA-KATO, N. 2013. COP1 targets C/EBPalpha for degradation and induces acute myeloid leukemia via Trib1. *Blood,* 122**,** 1750-60.

YOSHIDA, K., SANADA, M., SHIRAISHI, Y., NOWAK, D., NAGATA, Y., YAMAMOTO, R., SATO, Y., SATO-OTSUBO, A., KON, A., NAGASAKI, M., CHALKIDIS, G., SUZUKI, Y., SHIOSAKA, M., KAWAHATA, R., YAMAGUCHI, T., OTSU, M., OBARA, N., SAKATA-YANAGIMOTO, M., ISHIYAMA, K., MORI, H., NOLTE, F., HOFMANN, W.-K., MIYAWAKI, S., SUGANO, S., HAFERLACH, C., KOEFFLER, H. P., SHIH, L.-Y., HAFERLACH, T., CHIBA, S., NAKAUCHI, H., MIYANO, S. & OGAWA, S. 2011. Frequent pathway mutations of splicing machinery in myelodysplasia. *Nature,* 478**,** 64-69.

ZEISIG, B. B., KWOK, C., ZELENT, A., SHANKARANARAYANAN, P., GRONEMEYER, H., DONG, S. & SO, C. W. 2007. Recruitment of RXR by homotetrameric RARalpha fusion proteins is essential for transformation. *Cancer Cell,* 12**,** 36-51.

ZHANG, CHI, WANG, WANG, ZHANG, DENG, LV & XIE 2012a. miR-511 and miR-1297 inhibit human lung adenocarcinoma cell proliferation by targeting oncogene TRIB2. *PLoS One,* 7**,** e46090.

ZHANG, C., CHI, Y. L., WANG, P. Y., WANG, Y. Q., ZHANG, Y. X., DENG, J., LV, C. J. & XIE, S. Y. 2012b. miR-511 and miR-1297 inhibit human lung adenocarcinoma cell proliferation by targeting oncogene TRIB2. *PLoS One,* 7**,** e46090.

ZHANG, D. E., ZHANG, P., WANG, N. D., HETHERINGTON, C. J., DARLINGTON, G. J. & TENEN, D. G. 1997. Absence of granulocyte colony-stimulating factor signaling and neutrophil development in CCAAT enhancer binding protein alpha-deficient mice. *Proc Natl Acad Sci U S A,* 94**,** 569-74.

ZHANG, J., MI, Y. C., WANG, Y., LIN, D., LI, W., SUN, X. M., ZHOU, K., BIAN, S. G. & WANG, J. X. 2009. [Study on the clinical characteristics of adult biphenotypic acute leukaemia]. *Zhonghua Xue Ye Xue Za Zhi,* 30**,** 18-21.

ZHANG, P., IWAMA, A., DATTA, M. W., DARLINGTON, G. J., LINK, D. C. & TENEN, D. G. 1998. Upregulation of interleukin 6 and granulocyte colony-stimulating factor receptors by transcription factor CCAAT enhancer binding protein alpha (C/EBP alpha) is critical for granulopoiesis. *J Exp Med,* 188**,** 1173-84.

ZHANG, P., IWASAKI-ARAI, J., IWASAKI, H., FENYUS, M. L., DAYARAM, T., OWENS, B. M., SHIGEMATSU, H., LEVANTINI, E., HUETTNER, C. S., LEKSTROM-HIMES, J. A., AKASHI, K. & TENEN, D. G. 2004. Enhancement of hematopoietic stem cell repopulating capacity and self-renewal in the absence of the transcription factor C/EBP alpha. *Immunity,* 21**,** 853-63.

ZHANG, S. & KIPPS, T. 2013. The Pathogenesis of Chronic Lymphocytic Leukemia. *Annual Review of Pathology: Mechanisms of Disease,* 9**,** 103-118.

ZHANG, W. & SIDHU, S. S. 2014. Development of inhibitors in the ubiquitination cascade. *FEBS Letters,* 588**,** 356-367.

ZHANG, Y. & MA, X. 2010. Triptolide Inhibits IL-12/IL-23 Expression in APCs via CCAAT/Enhancer-Binding Protein ? *J Immunol,* 184**,** 3866-77.

ZHAO, M., DUAN, X. F., ZHAO, X. Y., ZHANG, B., LU, Y., LIU, W., CHENG, J. K. & CHEN, G. Q. 2009. Protein kinase Cdelta stimulates proteasome-dependent degradation of C/EBPalpha during apoptosis induction of leukemic cells. *PLoS One,* 4**,** e6552.

ZHENG, Y. S., ZHANG, H., ZHANG, X. J., FENG, D. D., LUO, X. Q., ZENG, C. W., LIN, K. Y., ZHOU, H., QU, L. H., ZHANG, P. & CHEN, Y. Q. 2012. MiR-100 regulates cell differentiation and survival by targeting RBSP3, a phosphatase-like tumor suppressor in acute myeloid leukemia. *Oncogene,* 31**,** 80-92.

ZHOU, S. & DEWILLE, J. W. 2007. Proteasome-mediated CCAAT/enhancer-binding protein delta (C/EBPdelta) degradation is ubiquitin-independent. *Biochem J,* 405**,** 341-9.

ZHOU, Y., LIU, S., SONG, J. & ZHANG, Z. 2013. Structural Propensities of Human Ubiquitination Sites: Accessibility, Centrality and Local Conformation. *PLoS One,* 8.

10. Publications